BLACK CARBON IN MARINE SEDIMENTS: QUANTIFICATION AND IMPLICATIONS FOR THE SORPTION OF POLYCYCLIC AROMATIC HYDROCARBONS

By

AmyMarie Accardi-Dey

B.S. Chemistry, B.S. Geology, Rensselaer Polytechnic Institute, 1998

Submitted in partial fulfillment of the requirements for the degree of

Doctor of Philosophy

at the

MASSACHUSETTS INSTITUTE OF TECHNOLOGY

and the

WOODS HOLE OCEANOGRAPHIC INSTITUTION

June 2003

Signature of Author

Joint Program in Oceanography/Applied Ocean Science and Engineering
Massachusetts Institute of Technology
and Woods Hole Oceanographic Institution
June 2003

Certified by

Philip M. Gschwend
Professor of Civil and Environmental Engineering
Thesis Supervisor

Accepted by

Oral Buyukozturk
Chairman, Departmental Committee on Graduate Studies
Massachusetts Institute of Technology

Accepted by

Philip M. Gschwend
Chair, Joint Committee for Chemical Oceanography
Woods Hole Oceanographic Institution

BLACK CARBON IN MARINE SEDIMENTS: QUANTIFICATION AND IMPLICATIONS FOR THE SORPTION OF POLYCYCLIC AROMATIC HYDROCARBONS

by

AmyMarie Accardi-Dey

Submitted to the MIT/WHOI Joint Program in Oceanography on May 7, 2003, in partial fulfillment of the requirements for the degree of Doctor of Philosophy in the field of Chemical Oceanography and Environmental Engineering

THESIS ABSTRACT

Sorption is a key factor in determining the fate of polycyclic aromatic hydrocarbons (PAHs) in the environment. Here, PAH sorption is proposed as the sum of two mechanisms: absorption into a biogenic, organic carbon (OC) fraction and adsorption onto a combustion-derived, black carbon (BC) fraction. To study BC adsorption, a 375°C thermal oxidation method was employed to remove OC and isolate the BC fraction. Test studies showed that nitrogen-containing macromolecules charred during this pretreatment causing a positive bias to the BC measurement. Meanwhile, the oxidation of relatively small BC particles underestimated the total BC content in non-charring samples. Models based on carbon oxidation were then proposed to estimate reasonably the total BC and OC contents of sediment samples.

The adsorption of pyrene onto isolated BC particles was then studied by constructing a nonlinear isotherm, which was characterized with a BC-normalized distribution coefficient and a Freundlich exponent. Pyrene sorption to Boston Harbor sediment was then modeled as the sum of OC absorption and BC adsorption using the measured adsorption parameters and literature absorption values. Finally, literature reports of high PAH distribution coefficients from the field and nonlinear PAH isotherms from the laboratory were re-explained by considering BC adsorption.

Thesis advisor: Philip M. Gschwend

Title: Professor of Civil and Environmental Engineering

ACKNOWLEDGMENTS

To my family, to whom I graciously dedicate my doctoral thesis and all my hard work - this thesis would not be possible without your love and continuous support. Your prayers, letters, and telephone calls have kept me laughing and smiling for the past five years. You all have contributed to my success and helped me fulfill my goal of earning a Doctor of Philosophy in Chemical Oceanography & Environmental Engineering from Massachusetts Institute of Technology and Woods Hole Oceanographic Institution. I thank you all: the Accardi Family, the Hildebrandt Family, the Giusto Family, the Link Family, the Kowinsky Family, the Koehler Family, the Quinn Family, the Kraft Family, the Giordano Family, and the Dey Family.

To my husband, Mark - words can not describe how much I appreciate your endless and devoted support. Thank you for always being there for me, listening to me, offering suggestions, and taking care of me. You have always been by my side whether I was screaming in excitement or crying my heart out, whether I were laughing together in the middle of the day or supporting each other in the middle of the night. Your love is immeasurable, thank you.

To my Mom, my first teacher, and my Dad, my loving fisherman - thank you for showing me the ocean and inspiring me to pursue a challenging career in chemistry. From Sycamore Elementary, to Connetquot High School, to Rensselaer Polytechnic Institute, to Washington DC, to Cape Cod, to Boston, I have been through it all. I want to thank you for seeing me through my thesis – love from a devoted family can make impossible dreams come true.

I would also like to acknowledge technical support at Perkin Elmer - Michael Mentzer, Kenneth R. Uliano, and Charles H. Beine. Without your help, I would never have been able to keep the 2400 CHN Elemental Analyzer (Series #1) alive and functional. Over 6,000 runs and counting!

Special thanks to my advisor, Philip Gschwend, for guiding me through my publications, and my thesis committee, Jean Whelan, Christopher Reddy, and Tim Eglinton, for many helpful discussions and suggestions. I also thank Sheila Frankel and John MacFarlane for their help in the Parsons Laboratory and keeping me sane over the past several years. To John Farrington for chairing my thesis. To Julia Westwater, and Marsha Bissonette, thank you for all your time and friendly discussions. Without all your help, I would never have made it through the graduate school gauntlet.

To my devoted friends and companions: Sara Gaetano Dudley, Ana Lucia Lima, Erin Sweeney, Linda Kalnejais, Emily Slaby, Peter Oates, J. Sam Arey, Nicholas Drenzek, Bernedette Proskoczilo Minnella, Helen White, Sarah Marsh, Bridget Bergquist, and Dr. Richard Bopp. Thank you for always listening to me and inspiring me to finish my thesis.

Happy reading, and if anyone is looking for me, I will be sittin' on the dock of the bay, enjoying my well-deserved vacation.

Sittin in the morning sun,
I'll be sittin' when the evening comes,
Watching the ships roll in,
And I'll watch 'em roll away again, yeah,

I'm sittin' on the dock of the bay,
Watching the tide roll away, ooh,
I'm just sittin' on the dock of the bay,
Wasting time
...
Sittin' here resting my bones,
And this loneliness won't leave me alone, yes,
Two thousand miles I roam
Just to make this dock my home

Now I'm just go sit at the dock of the bay
Watching the tide roll away, ooh
Sittin' on the dock of the bay
Wasting time

Written by Otis Redding and Steve Cropper
© 1967 Otis Redding

This work was supported by National Science Foundation Grant No BES-9800485 and OCE-00223441. The project, number RC-70, was also funded (in part) by the MIT Sea Grant College Program under a federal grant number NA86RG0074 from the National Sea Grant College Program, National Oceanic and Atmospheric Administration, US Department of Commerce.

TABLE OF CONTENTS

TABLE OF FIGURES

CHAPTER 2

CHAPTER 3

CHAPTER 4

CHAPTER 5

CHAPTER 6

CHAPTER 7

APPENDIX A6.3

TABLE OF TABLES

CHAPTER 2

CHAPTER 3

CHAPTER 4

CHAPTER 5

CHAPTER 1: GENERAL INTRODUCTION

1.1 JUSTIFICATION FOR THESIS

An accidental or intentional release of anthropogenic chemicals into the marine environment can cause numerous health and environmental problems [1, 2, 3] as these chemicals distribute themselves among the water, the sediment, and the biota via partitioning [4, 5]. Recent work by O'Connor, who compiled a decade of data from the National Oceanic and Atmospheric Administration (NOAA) Mussel Watch Program [6], revealed a positive correlation between anthropogenic chemicals assimilated in mollusk tissue and human population growth. Although this correlation does not prove cause and effect, O'Connor suggests that human activity is significantly altering the concentration of trace metals and organic chemicals, including polycyclic aromatic hydrocarbons (PAHs), in sediment beds and pore waters to near toxic levels for the inhabiting mollusks. Moreover, despite regulation designed to curb the release of PAHs into the environment, bioaccumulated PAH concentrations in mollusks have not decreased during the years of 1965-1993 [7, 8]. With the enduring threat of "urban sprawl" [9] and increased PAH exposure [10], oceanographers continue to study the bioavailability and bioaccumulation of organic chemicals in the marine environment [11].

Non-biodegradable toxic chemicals persisting in sediments and pore waters tend to bioaccumulate in the benthic biota, and eventually infiltrate the food web [12]. In an effort to monitor bioaccumulation, biologists established the Biota-Sediment Accumulation Factor (BSAFs, units of $(\mu g/g_{\text{lipid}})/(\mu g/g_{\text{total organic carbon}})$) as a method to quantify pollutants in benthic organisms. (Note that the lipid content and the total organic carbon content in the BSAF term are used to normalize the chemical concentration in the organism and sediment, respectively, since hydrophobic chemicals will preferentially partition into these phases.) Previous work by Tracey and Hansen showed that regardless of feeding type or habitat of benthic organisms, all species were equally exposed to a given chemical class as noted by the same BSAF value [13]. However, BSAF values varied for different chemical classes – indicating unequal

bioavailability of each chemical class. For example, for a suite of benthic organisms and a group of pesticides with log K_{ow} values ranging from 2.8-7.0 and a group of PCBs with log K_{ow} values ranging from 5.1-8.0, the corresponding average BSAFs were 1.4 and 1.0, respectively. However, for the same benthic species and a group of PAHs with similar log K_{ow} values (3.4-6.7), the average BSAF value was 0.34, indicating that for a given gram of contaminated sediment, PAHs were less bioavailable than either PCBs or pesticides to the benthic community. Similar results were observed by Krauss *et al.*, who observed less bioavailability of PAHs to earthworms in soils relative to PCBs [14]. The limited bioavailability of sorbed PAHs may be due to the presence of black carbon (BC) in sediment beds [15] since PAHs are hypothesized to bond more strongly to BC than biogenic, organic carbon (OC) [16].

As a key note, BC is a collective term that encompasses all thermally altered carbonaceous material including soots and chars; however, BC is operationally defined throughout this thesis as the carbon content remaining after a 375°C thermal oxidation method [16]. (Note, experiments discussed in Chapter 3 show that the 375°C-isolated BC content may underestimate the "true" total BC content in the sample due to oxidation of relatively small BC particles.) The carbon that is oxidized during the 375°C pretreatment (or the "non-BC" fraction) is operationally defined as the organic carbon (OC) content. In the sorption field, the OC content of a sediment or soil sample represents a labile/biogenic absorption media and is typically used as a metric of the organic matter content in a sample. The sum of the BC and OC contents is then operationally defined throughout this thesis as the total organic carbon (TOC) content of a sediment or soil sample. The TOC terminology is used in this thesis to denote that BC and OC are resistant to an acid treatment to remove inorganic carbon. As an aside, although the terminology in this thesis is consistent, other referenced authors may define their OC and BC fractions differently. For example, Karickhoff *et al.*, Chiou *et al.*, and Means *et al.* unknowingly included BC in their f_{oc} term [17, 18, 19]. These differences in terminology are highlighted in the text where appropriate.

Throughout this thesis, an elemental analyzer is used to quantify these three terms (TOC, BC, and OC). First, a sediment or soil sample is dried, ground, and acidified with sulfurous acid to remove the inorganic carbon fraction. The TOC content is then measured with an elemental analyzer (see Appendix 3.6) and expressed as a carbon weight percentage. To measure the BC fraction (or f_{BC} in units of $kg_{sediment}/kg_{black\ carbon}$), a sediment/soil subsample is combusted for 24 hours at 375°C under air in a muffle furnace to remove the labile OC. The carbon content in the combusted sediment expressed as a weight percentage is operationally defined as the BC fraction, and the OC fraction (or f_{oc} in units of $kg_{sediment}/kg_{organic\ carbon}$) is then calculated as the difference between the measured TOC and BC weight percentages.

Several researchers have hypothesized that this close association between PAHs and BC may be linked to the planar PAH structure and the aromatic makeup of BC [16, 20]. Nonetheless, the intense sorption strength of BC prohibits, or substantially hinders, desorption of PAHs into the pore water, and thus limits the bioavailability of PAHs to the biota [21, 22]. For example, Talley *et al.* observed that for a sediment sample from a Milwaukee disposal site, coal particles and wood char accounted for 5% of the sediment by mass, but contained more than 60% of the total sorbed PAHs concentration. Moreover, these authors noted that PAHs sorbed onto this coal-derived fraction were unavailable to earthworms and microorganisms because the PAHs did not desorb readily from these BC particles [23].

An understanding of BC in marine sediments is critical to understanding the fate of PAHs and the bioavailability of sorbed PAHs in the marine environment. Unfortunately, no universally accepted method exists to measure the BC content in marine sediments. For example, Currie *et al.* with the National Institute of Standards and Technology (NIST) recently orchestrated an intercomparison study of 13 published BC methods [24]. Their results showed that for the same standard reference material (1649a, urban dust from Washington D.C. collected in 1976-1977), the measured BC content varied by a factor of 10 among these 13 BC methods. This intercomparison study illustrates the importance of instituting a universal method for measuring BC in marine

sediments. Furthermore, the sorption strength between PAHs and BC in the environment is relatively unknown. On one hand, researchers hypothesize that PAHs will partition into BC particles with a BC-normalized distribution coefficient similar to PAHs sorbing to activated carbon [16, 25]. On the other hand, researchers have proposed that PAHs may actually adsorb onto BC particles [26, 27], thus accounting for observed nonlinear isotherms of PAHs and other hydrophobic chemicals. However, prior to this thesis no work has been done to construct a PAH/BC isotherm on BC isolated from environmental samples.

1.2 THESIS OUTLINE

This thesis contributes to the oceanography and engineering fields by exploring a method to quantify the BC content in marine sediments and by examining the sorption properties of PAHs to BC. An accurate BC method will help researchers quantify BC fluxes and reservoirs in the environments, which will have a tremendous impact on understanding the global carbon cycle, since BC may trap anthropogenic CO_2 in a long-term carbon pool [28]. In addition, the ability to quantify PAH/BC interactions will assist other researchers in predicting pore water and sorbed PAH concentrations as well as predicting the bioavailability of contaminants in the marine environment. A general outline of this thesis is as follows. Chapter 2 opens with an extensive literature review of BC, covering the physical and chemical properties of BC, the BC cycle including estimated global fluxes (from land to atmosphere), and ends with a comparison of current BC methods. Chapter 3 explores the accuracy and precision of measuring the BC content in marine sediments using the established 375°C thermal oxidation method. This methods chapter shows that (1) samples with a high total nitrogen content have a greater potential of charring (i.e., creating a BC artifact), (2) oxygen accessibility is the key factor in determining what material will survive a 375°C pretreatment; therefore, the 375°C only isolates relatively large BC particles, and (3) by modeling the carbon oxidation in a sediment sample, the BC content in a sample is reasonably estimated.

Chapter 4 continues with a literature review that introduces sorption, the possible roles that BC may play, and evidence that BC is contributing to observed nonlinear isotherms. In Chapter 5, a BC sample is isolated in sediments from Boston Harbor, and pyrene (a representative PAH) spiking experiments are performed to measure the BC-normalized distribution coefficient and corresponding Freundlich exponent that describes the adsorption of pyrene onto BC. In Chapter 6, literature sorption data is re-interpreted considering both an OC absorbent and a BC adsorbent. Finally, Chapter 7 concludes the thesis by summarizing the results of the work and suggesting future research directions. The work presented in this thesis supports the contentions that BC is the dominant sorbent of PAHs in marine sediments, and BC adsorption can account for the observed nonlinear isotherms (assuming that adsorption to mineral surfaces is negligible [29]) and large distribution coefficients in the field. Furthermore, this thesis shows that the 375°C thermal method can isolate BC from marine sediment with minimal effects from charring; however, the method may underestimate the total BC content by preferentially oxidizing relatively small BC particles.

1.3 REFERENCES

1. Ketchum, B. H. *Mar. Technol. Soc. J.* **1973**, *7,* 8-15.
2. Boudreau, P.; Barth, H. *Wat. Sci. Tech.* **1986**, *18,* 1-14.
3. Giroult, E. *Wat. Sci. Tech.* **1995**, *32,* 11-16.
4. Shea, D. *Environ. Sci. Technol.* **1988**, *22,* 1256-1261.
5. DiToro, D. M.; Zarba, C. S.; Hansen, D. J.; Berry, W. J.; Swartz, R. C.; Cowan, C. E.; Pavlou, S. P.; Allen, H. E.; Thomas, N. A.; Paquin, P. R. *Environ. Toxicol. Chem.* **1991**, *10,* 1541-1583.
6. O'Connor, T. P. *Mar. Environ. Res.* **2002**, *53,* 117-143.
7. O'Connor, T. P. *Mar. Pollut. Bull.* **1998**, *37,* 14-19.
8. Lauenstein, G. G.; Daskalakis, K. D. *Mar. Pollut. Bull.* **1998**, *37,* 6-13.
9. Metre, P. C. V.; Mahler, B. J.; Furlong, E. T. *Environ. Sci. Technol.* **2000**, *34,* 4064-4070.
10. Lima, A. L. C.; Eglinton, T. I.; Reddy, C. M. *Environ. Sci. Technol.* **2003**, *37,* 53-61.
11. Hellou, J.; Steller, S.; Zitko, V.; Leonard, J.; King, T.; Milligan, T. G.; Yeats, P. *Mar. Environ. Res.* **2002**, *53,* 357-379.

12. Thomann, R. V.; Connolly, J. P.; Parkerton, T. F. *Environ. Toxicol. Chem.* **1992**, *11,* 615-629.
13. Tracey, G. A.; Hansen, D. J. *Arch. Environ. Contam. Toxicol.* **1996**, *30,* 467-475.
14. Krauss, M.; Wilcke, W.; Zech, W. *Environ. Sci. Technol.* **2000**, *34,* 4335-4340.
15. Levine, R. H. *MS: Model of PAH and PCB Bioaccumulation in Mya arenaria and Application for Site Assessment in Conjunction with Sediment Quality Screening Criteria.* **1999**, Massachusetts Institute of Technology: Cambridge. 1-108.
16. Gustafsson, Ö.; Haghseta, F.; Chan, C.; MacFarlane, J.; Gschwend, P. M. *Environ. Sci. Technol.* **1997**, *31,* 203-209.
17. Karickhoff, S. W.; Brown, D. S.; Scott, T. A. *Water Res.* **1979**, *13,* 241-248.
18. Chiou, C. T.; Peters, L. J.; Freed, V. H. *Science* **1979**, *206,* 831-832.
19. Means, J. C.; Wood, S. G.; Hassett, J. J.; Banwart, W. L. *Environ. Sci. Technol.* **1980**, *14,* 1524-1528.
20. Kubicki, J. D.; Apitz, S. E. *Org. Geochem.* **1999**, *30,* 911-927.
21. Chapman, P. M.; Downie, J.; Maynard, A.; Taylor, L. A. *Environ. Toxicol. Chem.* **1996**, *15,* 638-642.
22. Lamoureux, E. M.; Brownawell, B. J. *Environ. Toxicol. Chem.* **1999**, *18,* 1733-1741.
23. Talley, J. W.; Ghosh, U.; Tucker, S. G.; Furey, J. S.; Luthy, R. G. *Environ. Sci. Technol.* **2002**, *36,* 477-483.
24. Currie, L. A.; Benner, B. A.; Kessler, J. D.; Klinedinst, D. B.; Klouda, G. A.; Marolf, J. V.; Slater, J. F.; Wise, S. A.; Cachier, H.; Cary, R.; Chow, J. C.; Watson, J.; Druffel, E. R. M.; Masiello, C. A.; Eglinton, T. I.; Pearson, A.; Reddy, C. M.; Gustafsson, O.; Quinn, J. G.; Hartmann, P. C.; Hedges, J. I.; Prentice, K. M.; Kirchstetter, T. W.; Novakov, T.; Puxbaum, H.; Schmid, H. *J. Res. Natl. Inst. Stan.* **2002**, *107,* 279-298.
25. Bucheli, T. D.; Gustafsson, Ö. *Environ. Sci. Technol.* **2000**, *34,* 5144-5151.
26. Chiou, C. T.; Kile, D. E. *Environ. Sci. Technol.* **1998**, *32,* 338-343.
27. Xia, G. S.; Ball, W. P. *Environ. Sci. Technol.* **1999**, *33,* 262-269.
28. Kuhlbusch, T. A. J.; Crutzen, P. J. *Global Biogeochem. Cy.* **1995**, *9,* 491-501.
29. Mader, B. T.; Uwe-Goss, K.; Eisenreich, S. J. *Environ. Sci. Technol.* **1997**, *31,* 1079-1086.

CHAPTER 2: LITERATURE REVIEW: BLACK CARBON IN THE ENVIRONMENT

2.1 ABSTRACT

Black carbon (BC) is a collective term that encompasses all thermally altered carbonaceous material generated from fossil fuels burning and biomass burning. These particles are subdivided into two classes: soot and char, based on their physical and chemical properties. Teragrams of BC are emitted annually from combustion sources and are disseminated by aeolian transport and runoff into the environment. Because of its light absorbing properties and recalcitrant nature, BC can influence atmospheric processes and the global carbon cycling. Once deposited, BC may account for a certain percentage of the total organic carbon (TOC) content in sediments and soils. Numerous analytical methods have been designed to quantify the amount of BC in environmental samples. In general, these methods involve a chemical digestion or a thermal oxidation of the labile organic carbon (OC) and operationally defining the remaining carbon as BC. However, a comparison of these various BC methods reveals discrepancies in these measurements because of incomplete removal of OC or loss of BC particles. Here, after an extensive literature review of BC, a variety of BC methods designed to quantify BC are explored. Specific attention is then given to the 375°C thermal oxidation method, which is used throughout this thesis to measure BC in sediment samples.

2.2 INTRODUCTION

Black carbon (BC) is a collective term that encompasses all thermally altered carbonaceous material. Since most combustion reactions are incomplete, BC is emitted into the environment from an array of combustion sources [1]. For example, BC is emitted from: boilers, car and truck engines, fireplaces, natural gas burners, cigarettes, wear of brakes and tires, biomass burning, and tar pots [2]. Due to the various BC sources, BC encompasses a wide spectrum of carbonaceous particles; however, each BC particle possesses distinct chemical and physical properties that depend on reaction time and combustion temperature [3].

Over time, researchers have coined commonplace names to typically studied BC particles in order to identify them and their properties. For example, "activated carbon" is industrially formed from wood char that combusts in a steam or carbon dioxide atmosphere at temperatures between 800-1,000°C. These combustion conditions create a carbonaceous material with a high surface area (>2,500 m^2/g) possessing a wide range of chemical functional groups and adsorptive capacity [1]. Another BC example is "carbon black," which is used to improve tire rubber quality and is an important component in toners, roofing, paints, and plastics. This carbonaceous material is produced from a petroleum-based feedstock under anoxic conditions with temperatures ranging from 1,320-1,540°C [1, 4]. Yet, another BC is "fly ash," a byproduct of coal combustion, generated at electrical power plants. Fly ash typically has a rather low carbon content (26 wt % C; [4]) and a high metal content (like Si, Al, Fe, K, Mg, and Ca) due to the condensation of metal volatiles during combustion [1, 4]. In addition to these terms, the literature contains a suite of other names describing various BC particles, such as: elemental carbon, lampblack, charcoal, coke, soot, aciniform, cenosphere, carbonaceous microgel, acetylene black, or graphitic carbon.

2.3 SOOTS VERSUS CHARS

Here, the BC spectrum is subdivided into two regimes, "soots" and "chars," based on terminology proposed by E.D. Goldberg in his book *Black Carbon in the Environment*

[1]. The division between the two BC particles is based on particle size [5] and formation conditions [1, 6] (Table 1). Soots are submicron particles formed from the condensation of hydrocarbon radicals at high temperatures >600°C [4, 7]. These radical hydrocarbons may include acetylene or PAHs. The "particle inception" process of soot [7] is poorly understood but follows a logical sequence of collisions and growth. Lahaye characterized soot formation in a three-step process (Figure 1). First, a large number of PAH macromolecules are formed (on the order of 1,000 molecular weight [8]) from the condensation of hydrocarbons. Some scientists argue that acetylene radicals are the precursors to these PAH macromolecules [9]. These macromolecules then collide to produce larger spheroids (10-30 nm diameter spheroids [3, 10]), which are characterized by concentric, aromatic layers [11, 12]. These spheroids finally aggregate, yielding grape like clusters that ultimately form submicron soot particles.

Interestingly, only 10% of the total soot mass forms during soot formation whereas the remaining soot mass forms during "soot growth" [7]. Soot growth can occur either on the individual spherical particles or the aggregates [13]; nonetheless, soot growth stabilizes the soot by linking particles together. An ongoing debate focuses on whether acetylene or PAHs precursors are the dominant chemical species responsible for soot growth. For example, Harris and Weiner explained that acetylene radicals were the main hydrocarbon responsible for soot growth since the concentration of PAHs in the flame was too low to make a significant contribution to soot growth [14, 15]. Similar results were reported by Smedley *et al.*[8] who showed that the PAH concentration in a flame was depleted after the soot inception process, and acetylene radicals were then responsible for growth. In contrast, Benish *et al.* argued that the acetylene-soot collision frequency was less efficient than the PAH-soot collision frequency; therefore, PAHs were the dominant chemical species for soot growth [9]. Yet, Kazakov and Frenklach argued against the findings of Benish *et al.* commenting that hydrogen abstraction from the aromatic soot surface and the assimilation of acetylene was the dominant mechanism for soot growth [13], and PAHs do not contribute to soot growth [16]. On the contrary, Macadam *et al.* suggested that both PAH and acetylene precursors contributed to soot

Table 1: Characterization of soots and chars based on physical and chemical properties (references are italicized).

Property	Soot	Char
Diameter	<1 μm *Medalia and Rivin, 1982* *Lahaye, 1990*	1-100 μm *Medalia and Rivin, 1982* *Lim and Cachier, 1996*
Formation Temperature	>600°C *Lim and Cachier, 1990*	<600°C *Lim and Cachier, 1990*
Morphology	Grape clusters *Medalia and Rivin, 1982* *Gustafsson et al., 2001*	Unburned fragments *Griffin and Goldberg, 1979*
Surface Area	≈ 100 m^2/g *Rockne et al., 2000* *NIST Certificate of Analysis*	≈ 10 m^2/g *Medalia and Rivin, 1982* *Kleineidam et al., 1999*
Bulk Density	0.1 g/cm^3 *Rockne et al., 2000*	0.6 g/cm^3 *Rockne et al., 2000*
C/H molar ratio	4-7 *Akhter et al., 1985* *Rockne et al., 2000*	0.3-4 *Goldberg, 1982* *Kuhlbusch, 1995*

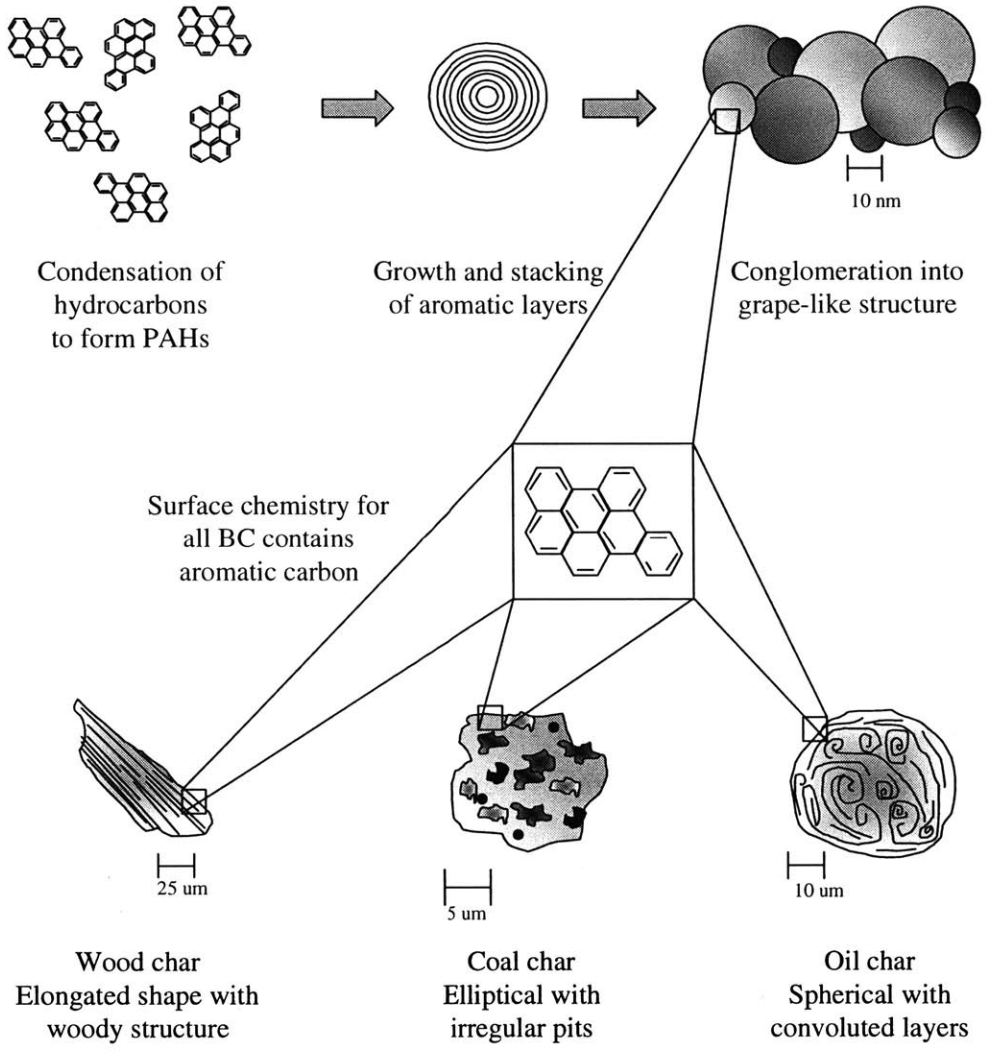

Figure 1: Schematic of BC particles (based on electron microscope images in Griffin *et al.* (1981), Gustafsson *et al.* (2001), and Kralovec *et al.* (2002)). Soots are submicron particles formed from the condensation of gaseous hydrocarbon. Aromatic layers stack and grow to form spheroids, which in turn conglomerate into grape-like structures. Chars are larger particles that form when source materials are not fully destroyed, thus leaving behind partially burnt fragments, or when liquid drops carbonize. Unlike soots, chars retain the morphology of their source material. All BC particles have similar aromatic carbon surface chemistry.

growth, and the dominant species depended on both flame conditions and the residence time of the precursors in the flame [17].

Chars, in contrast, form at lower temperatures (<600°C; Table 1) when source materials are not fully destroyed, thus leaving behind partially burnt fragments, or when liquid drops carbonize [4, 6, 18, 19, 20]. Unlike soots that form submicron, grape-like clusters, chars retain the morphology of their source material with diameters ranging from 1-100 μm (Figure 1; [19, 20]). While the morphology of char particles differ from soots, the chemical properties on the surface of a char particle resemble the surface properties of soot (i.e., condensed, aromatic carbon, Figure 1). Venkataraman and Friedlander noted that the main sources of char particles are emissions from coal, wood, or oil-fired heaters [21]. Based on morphology and surface texture, Griffin and Goldberg identified certain physical features of chars to characterize their BC source [19, 22]. For example, chars generated from oil burning were characterized by spherical, convoluted structures known as "cenospheres." Coal combustion generated chars that were spherical with a pitted surface while wood burning generated elongated chars that retained a woody tissue structure. In general though, since a combustion source can emit an array of particles, both soots and chars can originate from the same combustion source.

In addition to morphology, other chemical and physical differences distinguish soots from chars (Table 1). Rockne *et al.* observed that soots generated in the laboratory from a dodecane flame had a higher surface area and were more porous than representative chars were [23]. In addition, they observed that soots had a higher carbon content and higher C/H molar ratio. For example, Rockne *et al.* measured a surface area of 85.3 m^2/g for soot, which is about a factor of 60 greater than the surface area measured for chars generated from bus exhaust, wood burning, and an oil furnace [23]. Similarly, Kleineidam *et al.* measured the surface area of coal from Quaternary sand as 7.6 m^2/g [24] while Medalia and Rivin measured the surface area of domestic chimney char as 12 m^2/g [4]. These surface areas for char are 10 times less than the NIST certified surface area for diesel particulate matter (soot, SRM 1650a) of 102 m^2/g [25]. Because of the large surface area of soots, Rockne *et al.* proposed that soots are more porous than chars

are. This porosity difference is reflected in the lower bulk density values for soot relative to char. For example, Rockne *et al.* measured a bulk density of 0.1 g/cm^3 for soot compared to a bulk density of 0.6 g/cm^3 for char particles generated from marine diesel exhaust, wood burning, and an oil furnace [23]. Although these bulk density values are not representative of all BC particles, they are much less than the specific density of crystalline graphite of 2 g/cm^3 [1, 26].

Lastly, since soots form from condensation, they have a larger carbon content than char with weight percent carbon exceeding 87 wt % for laboratory soots [23, 27, 28] and exceeding 77 wt % C for NIST diesel particulate matter [10, 25]. These high carbon contents are reflected in high C/H molar ratios for soots, and give some indication of the degree of condensation in these carbonaceous materials (Table 1). For example, Akhter *et al.* estimated a C/H molar ratio of 4-6 [27] for soot generated from a hexane flame while Rockne *et al.* estimated a C/H molar ratio of 7 for soot generated in a dodecane flame [23]. In contrast, the C/H molar ratio for chars generated from oil furnaces and diesel ranged from 0.7-2 [23]. Similarly, low ratios ranging from 0.8-4 were observed for charcoals ([1] references therein) while even lower C/H molar ratios of 0.3-0.7 were measured for activated charcoal and savanna grass ash [29].

One can infer from the C/H molar ratio that soots are primarily composed of aromatic carbon. However, other analyses suggest that BC contains other components besides aromatic carbon including inorganic oxides, salts, metals, absorbed liquids and gases, and resins [4]. Other researchers have also measured traces of potassium, nitrogen, and sulfur in BC samples [1, 3, 30]. For example, Medalia and Rivin measured the nitrogen content in an assortment of domestic chimney BC with weight percents ranging from 0.8-5 wt % [4]. Likewise, Akhter *et al.* measured the oxygen content of 6-11 wt % for soots generated in a hexane flame [27]. Akhter *et al.* proposed that soot contained oxygen moieties, such as anhydrides, carbonyls, alkyl ketones, and aryl ether linkages that covered over 50% of the soot surface. Later work by Kulhbusch showed that these oxygen moieties could survive intense heating implying that BC does contain oxygen as well as carbon [29]. In addition to possessing oxygen moieties, Akhter *et al.*

proposed that soots contained an alkyl component with a 9:1 ratio of aromatic carbon to aliphatic carbon [27]. The presence of an alkyl component in addition to an unsaturated carbon signal in NIST diesel particulate matter was later confirmed by Gelinas *et al.* using cross-polarization ^{13}C NMR [31]. However, this alkyl carbon contribution was not stable at higher temperatures [1, 31] implying that NIST diesel particulate matter and other BC particles may contain a BC core with some sort of amorphous-oily coating [10] (diesel derived; SRM 1650a contains $20.2 \pm 0.4\%$ extractable mass using Soxhlet extraction with dichloromethane [25]). This coating was probably added onto the BC particle before it was emitted to the environment.

2.4 ENVIRONMENTAL IMPACT OF BLACK CARBON

Once emitted into the atmosphere, BC is disseminated by aeolian transport and water runoff becoming ubiquitous in the environment (Figure 2; [26, 32]). Investigators have detected BC in aerosols in the Norwegian Arctic [33] and across the Atlantic Ocean [30, 34, 35] as well as in rain droplets [36]. BC was also measured in ice cores [37], alpine lacustrine sediments [38], marine sediments [39, 40, 41, 42], soils [43, 44, 45], and riverine suspended particles [46]. The widespread occurrence of BC has created new concerns in the geochemistry field as investigators hypothesize how BC is impacting the environment.

BC may play in important role in atmospheric chemistry. Novakov *et al.* hypothesized that BC may catalyze the oxidation of sulfur dioxide to sulfate in polluted atmospheres [47]. BC may also affect climate either by directly absorbing radiation [48, 49, 50] or indirectly by affecting cloud processes [3, 36, 51]. For example, recent work by Jacobson hypothesized that BC aerosols can contribute a positive 0.55 W/m^2 forcing factor that could severely offset the anticipated cooling effects of sulfate aerosols [52]. On the contrary, Liu *et al.* argued that BC concentrations (except near BC point sources) are not high enough to modify light scattering or absorption; hence, BC should have minimal effects on climate [49]. Other health concerns focus on the pollutants that are transported with BC, such as polycyclic aromatic hydrocarbons (PAHs; [53]). Many

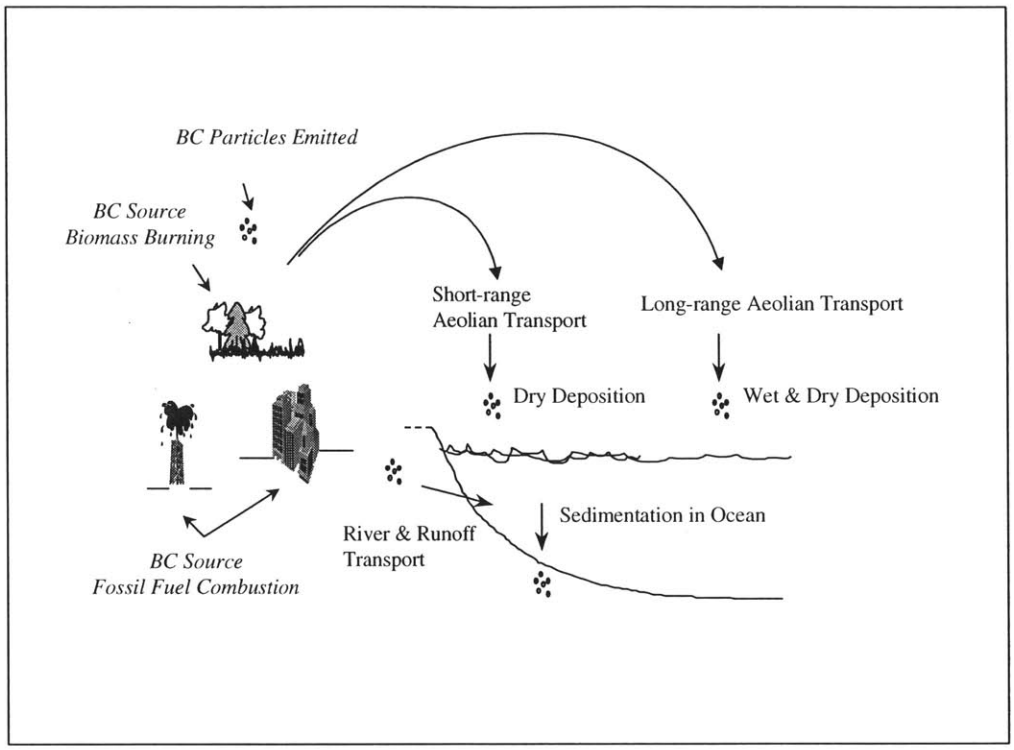

Figure 2: Schematic of the BC cycle. BC particles are predominantly emitted from two combustion sources: biomass burning and fossil fuel combustion. BC particles are disseminated throughout the environment by aeolian transport and riverine/runoff transport. Larger char particles tend to settle out of the atmosphere close to their source. Smaller soot particles are dispersed throughout the environment by long-range aeolian transport. Eventually these soot particles wash out of the atmosphere, or they coagulate and settle out by dry deposition. Once in the ocean, BC particles will eventually settle into sediment beds where they are preserved in the sediment record. (Based on Kuhlbusch (1998) Science)

PAHs form with BC during combustion, while other planar organic compounds (including other PAHs) condense onto the BC after combustion [1, 21, 54].

BC may also have a substantial impact on the global oxygen cycle [32, 55, 56] and/or the global carbon cycle [57, 58, 59]. As organic carbon (OC) burns and converts to BC, carbon moves from a short-term, labile OC pool to a long-term, recalcitrant BC pool. (As noted in Chapter 1, BC is a collective term representing thermally altered carbonaceous material. The term OC (or the "non-BC fraction") represents the biogenic/diagenetic carbonaceous material. The sum of these two carbon fractions represents the total organic carbon (TOC) content of a sample.) Since BC is recalcitrant and slowly decomposes relative to natural organic matter [1, 41, 56], a percentage of the total carbon becomes sequestered, thus representing a possible carbon sink that may offset the rising anthropogenic CO_2 levels [57, 58, 59]. In addition, new BC measurements suggest that previous calculations of global carbon primary productivity were erroneously high [60]. For these calculations, researchers historically used the total organic carbon (TOC) content of marine sediments, which is now known to contain both combustion-derived BC and biogenic/diagenetic OC [40, 61]. Moreover, Gustafsson and Gschwend proposed that 10-20% of the TOC in New England coastal sediments is BC [40]. Recent work by Middelburg *et al.* suggests that the BC/TOC ratio may be as high as 30% in marine sediments from an intertidal zone near The Netherlands, the Iberian Margin in the Atlantic Ocean (water depth of 766-4,909 meters), North Sea (water depth of 5-30 meters), and the Eastern Mediterranean (water depth of 2,539 meters) [41]. Masiello and Druffel also proposed that the deep oceanic DOC pool might contain 4-22% BC [62]. BC may also contribute a significant fraction to the aromatic nature of humic acids in soils [63].

2.5 BLACK CARBON TRANSPORT, DEPOSITION, AND GLOBAL FLUX

2.5.1 BC Transport. The two major sources of BC are biomass burning and fossil fuel combustion (Figure 2; [1]). Models by Cooke and Wilson predict that the highest concentrations of BC from biomass burning occur in the Southern Hemisphere (80%

occurring in the intertropical zone [3]) while the highest BC emissions from fossil fuel are focused in the Northern Hemisphere [64]. Aeolian transport and runoff disseminate BC in the environment. Since BC consists of relatively large char particles and small soot particles, chars will settle close to their source by dry deposition whereas soots will remain airborne until being washed out of the atmosphere by wet deposition [51, 54, 65]. Windsor and Hites and other researchers projected with Stoke's Settling Law that char particles (>10 μm) will settle out of the atmosphere within 10 km of their source while soots (<1 μm) will travel over 1,000 km with an atmospheric residence time on the order of days before being washed out [51, 64, 66]. In addition to wet deposition, organic coatings and electrolytes may build up on the soot during long-range transport, changing the surface reactivity of soot causing aggregation, accumulation, and dry deposition [3, 52]. Consequently, aeolian transport of soot is the most important source of BC to the open ocean. In contrast, BC in the coastal waters consists of soot and char particles transported by river runoff and surface runoff; char particles transported by short-range deposition from coastal sources; and soot particles transported by long-range deposition from inland sources.

Due to its exclusively landbased origin, BC concentrations in air masses are greater over continents than over oceans. Therefore, since more land mass exists in the Northern Hemisphere than the Southern Hemisphere, BC concentrations are higher in the North than the South [3]. For example, Andreae noted in his work that continental air masses from Europe contained 1,000 ng BC/m^3 from fossil fuel combustion and continental air masses from Central Africa contained 200 ng BC/m^3 from biomass burning of savanna grasslands. Both of these continental BC concentrations were 10 to 50 times higher than the BC concentration in marine air masses from the Southern or Northern Atlantic Oceans (20 ng BC/m^3; [30]). Similar results were observed by Cooke *et al.* who observed BC concentration in clean marine air masses blowing off the North Atlantic Ocean equal to 14 ng BC/m^3 that were 15 times less polluted than continental air masses originating from the European continent [34].

While BC concentrations are greatest near industrialized nations, the long-range transport of BC has a measurable impact on remote locations. For example, Kaneyasuo and Murayama observed BC concentrations that were >150 ng BC/m^3 in the Western Pacific Ocean – 4,300 km from its coal source on the Asian continent [67]. Bodhaine also observed BC pollution in remote polar areas due to long-range transport of BC (termed "Arctic Haze" [68]). This researcher measured seasonal BC concentrations in the South Pole that varied by 5 orders of magnitude (0.01-100 ng BC/m^3). Similar seasonal trends were also measured in the Arctic with BC concentrations varying from 0.8-200 ng BC/m^3 [68].

2.5.2 BC Deposition. Goldberg as well as Kulhbusch and Crutzen have estimated that 80% of the BC released into the environment is deposited on land due to dry deposition [1, 59]; hence runoff and rivers can deposit a substantial amount of BC into coastal waters. The Mississippi River is estimated to deposit about 500 Gg BC (Gg = 10^9 grams) annually into the Gulf of Mexico [46] while the Santa Clara River is estimated to deposit about 50 Gg BC/yr [69]. The focused input of BC into coastal waters (both riverine and atmospheric deposition) is reflected in the higher BC sedimentary fluxes measured on the coast relative to the open ocean (Table 2). For example, Lim and Cachier estimated a sedimentary flux of 120 μg BC/cm^2/yr in the Mediterranean Sea [6], and Gustafsson and Gschwend recently estimated a sedimentary flux of 90-200 μg BC/cm^2/yr for the Gulf of Maine Proper [40]. Griffin and Goldberg estimated similar coastal sedimentary fluxes off western Canada and America as 30-70 μg BC/cm^2/yr [70]. These coastal sedimentary fluxes are 1,000 fold greater than oceanic sedimentary fluxes estimated by Smith *et al.* (0.002-0.2 μg BC/cm^2/yr) and Herring (0.001-3.6 μg BC/cm^2/yr) for the Central Pacific Ocean [18, 56]. Once deposited, the BC reservoir may range from 2,000-5,000 Pg (Pg = 10^{15} grams) in coastal sediments and 400-1,000 Pg in open ocean sediments [26, 32] (estimates based on a chemical/thermal BC method by Kuhlbusch), which may account for 20-50% of the sedimentary organic carbon content [32].

Table 2: Reported BC fluxes (μg BC/cm^2/yr) to sediment beds in coastal and open oceans along with comments on the BC methodology employed to calculate given flux.

Location **Research group**	**BC Flux** **(μg BC** **/cm^2/yr)**	**Comments on BC methodology**
Mediterranean Sea Lim and Cachier (1996)	120	***Dichromate/sulfuric acid oxidation; coulometric titration*** may overestimate BC due to incomplete removal of OC
Gulf of Maine Proper Gustafsson and Gschwend (1998)	90-200	***375 ℃ thermal oxidation; elemental analysis*** may underestimate BC due to oxidizing small BC particles
Canadian and American Coast Griffin and Goldberg (1975)	30-70	***Peroxide/base & acid digestion; infrared analysis*** may underestimate BC due to loss material and infrared artifacts
Central Pacific Ocean Smith *et al* (1973) & Herring (1985)	0.001- 3.6	***Peroxide/base & acid digestion; infrared analysis*** may underestimate BC due to loss material and infrared artifacts

However, these reported fluxes and reservoirs might misrepresent the true BC value because each value was calculated with a different method, which isolated a different percentage of the total BC particles in the sample (Table 2). For example, the dichromate/sulfuric acid method developed by Wolbach *et al.* [71] may overestimate the BC content of sediments because of the possible incomplete removal of OC; thus, the sedimentary flux calculated by Lim and Cachier may be too high [6]. The 375°C thermal oxidation method, on the contrary, may underestimate the BC content because of oxidation of small BC particles (discussed in Chapter 3). Likewise, an infrared analysis may underestimate the BC concentration in environmental matrices because the analysis indirectly measures BC with a carbonyl stretching frequency, which is actually an artifact of the method [72]. Thus, the sedimentary fluxes calculated by Gustafsson and Gschwend [40], Griffin *et al.* [70], Smith *et al.* [18], and Herring *et al.* [56] may be too low.

When considering these factors and the reported fluxes above (i.e., Lim and Cachier's value is probably too high, Gustafsson and Gschwend's value is probably too low, Table 2), the BC sedimentary flux is estimated here as ≈100 μg BC/cm^2/yr to coastal sediments and ≈1 μg BC/cm^2/yr to the open ocean. These estimated sedimentary fluxes then correspond to an estimated BC reservoir of 3,600 Tg BC (Tg = 10^{12} grams) in coastal sediments and 300 Tg BC in the open ocean (assuming the same BC flux over the past 100 years). These calculated BC reservoirs are a 1,000 times less than the BC reservoirs reported above by Kuhlbusch [32]. Either a different length of time for deposition or different BC sedimentary fluxes may account for the discrepancies between the two BC reservoirs. For example, if the same BC sedimentary fluxes to the coastal and open oceans applied for the past 100,000 years (instead of 100 years), then the BC reservoir would equal 3,600 Pg BC in the coastal sediments and the 300 Pg BC in the open ocean sediments, which correlates well with the BC reservoirs calculated previously by Kulhbusch [32].

Nonetheless, once deposited in sediment beds, a BC record is preserved in the sediment because BC is resistant to degradation relative to labile, organic matter. For

example, Griffin, Goldberg and coworkers reported in a series of papers the preservation of BC in Lake Michigan [22, 73, 74]. They noted that their BC profile (BC particles >38 μm) reflected the onset of the American industrialization, and using the morphology of the BC particles, they observed the change from wood burning to coal and oil combustion [22, 73, 74]. Similar BC profiles were also reported in other Great Lakes, showing the preservation of micron size BC particles over the past century [20, 75].

On a longer time scale, Bird and Cali reported the preservation of char from biomass burning (isolated with a modified Wolbach-chemical method) in a sediment core on the Sierra Leone Rise (ODP-668B), recording fires on the savanna for the past million years (dated using oxygen isotopes and glacial stages) [76]. Likewise, Herring observed a continuous record of BC to the Lower Cretaceous period. The author noted no trend in particle size down core implying little degradation of the BC over time [56]. Similar results were observed by Middelburg *et al.* who showed the preferential preservation of BC relative to other forms of organic carbon in a 140 kyr-old turbidite that was exposed to oxygen under pelagic conditions for 10-20 kyr [41]. An intense soot signal is also preserved at the KT boundary referring to the global fires that occurred 65 million years ago [77, 78]. Likewise, charcoalified plant fragments, coined "fusinite," are observed in many post-Devonian sedimentary beds [55] dating back 350 million years ago. Lastly, several researchers over the past two decades illustrated that BC is more resistant to chemical oxidation (dichromate and sulfuric acid) than kerogen (on the time scale of 2,000 hours of chemical digestion) [6, 71, 79].

2.5.3 Global BC Flux. The amount of BC released into the environment during combustion depends on the temperature of the reaction, the oxygen supply, and the exposed carbon surface area. For example, smoldering fires occurring at low temperatures that are poorly ventilated will produce more BC than flaming, high temperature fires [80, 81]. BC emissions also depend on the type of fuel burned. For example, coal, lignite, diesel, and coke release >1 g C/kg fuel while natural gases, kerosene, and gasoline emit <1 g C/kg fuel [3]. Therefore, although passenger cars

(powered by gasoline) outnumber diesel trucks on the road (2:1 in industrial nations), diesel engines emit about 50 times as much BC per kg of fuel as car engines do [1, 82] (i.e. 1,440 μg BC/kg diesel versus 30 μg BC/kg gasoline [83]). Based on a 1973 energy budget for Los Angeles, Cass *et al.* estimated that tire wear and diesel exhaust from trucks and railroads accounted for 75% of the BC released in that area. However, diesel consumed <5% of the total fuel burned in their study [84]. In addition to diesel combustion, new work by Streets *et al.* as well as Kaneyasu and Murayama suggest that the combustion of coals in residential sectors on the Asian continent may contribute to the global impact of anthropogenic BC [67, 81]. Cooke *et al.* further proposed that one-quarter of the global anthropogenic BC might originate from China from the burning of coal and biofuels [85].

To quantify the impact of BC in the environment, numerous investigators have attempted to estimate the global flux of BC (i.e., BC emitted from land to atmosphere). In general, investigators hypothesize that the annual global production of BC is on the order of teragrams BC per year (Tg = 10^{12} g), which is comparable to the flux of OC annually buried in sediment beds [26, 32]. However, similar to the sedimentary BC fluxes noted above, estimated global BC fluxes vary by a factor of 1,000 because of various "best guess" estimates for emission factors and different methods used to assess reliable BC concentrations (Table 3).

Earlier work by Seiler and Crutzen projected that the annual BC flux (from the land to atmosphere) was 500-1,700 Tg BC/yr [57] with biomass burning dwarfing fossil fuel-derived BC. This estimate was later revised by Crutzen and Andreae to 200-600 Tg BC/yr (from the land to atmosphere) [58] and further revised by Kulhbush and Crutzen to 50-270 Tg BC/yr (from the land to atmosphere) [59] by applying different emission factors. Kuhlbusch and Crutzen then proposed that shifting agriculture and permanent deforestation alone accounted for 50% of the annual global BC formation [59]. Their proposal was supported by work done by Penner *et al.* who hypothesized that fossil fuel combustion only emitted 13-24 Tg BC/yr (from land to atmosphere) [86, 87]; thus, suggesting that biomass burning was the dominant contributor to global BC production.

Table 3: Reported global BC fluxes (Tg BC/yr) and corresponding BC methodology employed to calculate given fluxes.

Research Group	Global BC Flux (Tg BC/yr)	BC methodology
Seiler and Crutzen (1980)	500-1,700 (*flux from land to atmosphere*)	BC emitted from biomass burning 1. Assume that BC is 20-30% of total unburned carbon (estimated at 1.8-5.0 Pg C/yr), 2. Assume that BC is 40% of particulate matter (estimated at 200-450 Tg/yr) in smoke, and 3. Sum values
Crutzen and Andreae (1990)	200-600 (*flux from land to atmosphere*)	BC emitted from biomass burning 1. Estimate the amount of global biomass burning (1.8-4.7 Pg C/yr), 2. Estimate BC/(carbon exposed to fire) emission ratios, and 3. Multiply values
Kulhbush and Crutzen (1995)	50-270 (*flux from land to atmosphere*)	BC emitted from biomass burning 1. Estimate a BC/CO_2 emission factor for various biomass burning, 2. Estimate the total CO_2 released (2.6-5.1 Pg C/yr), 3. Multiply values, and 4. Combine with BC/(carbon exposed to fire) data
Penner *et al.* (1993)	13-24 (*flux from land to atmosphere*)	BC emitted from fossil fuel burning 1. Estimate the amount of SO_2 emitted from different fossil fuel usage, 2. Estimate BC/SO_2 emission factor, and 3. Multiply values
Cooke and Wilson (1996)	14 ±2 (*flux from land to atmosphere*)	BC emitted from biomass & fossil fuel burning 1. Estimate the biomass density, fraction of biomass burning, and an emission factor, 2. Estimate fuel usage and emission factor, 3. Model to determine BC emissions globally
Liousse *et al.* (1996)	13 ±2 (*flux from land to atmosphere*)	BC emitted from biomass & fossil fuel burning Compilation of literature BC emission factors
Suman *et al.* (1994)	7 ±3 (*flux from atmosphere to land*)	BC Deposition 1. Use atmospheric BC concentration (ng/m^3) modeled from Cooke and Wilson (1996), 2. Estimated wet/dry deposition rates, and 3. Calculate BC deposition

These previous global approximations, however, far exceeded work by Suman *et al.* [88] who estimated that the annual BC flux (from atmosphere to land) was 7 ±3 Tg BC/yr. Moreover, Liousse *et al.* proposed that fossil fuel burning generated more BC than biomass burning [89], which contradicts the Kuhlbusch and Crutzen hypothesis that biomass burning was the major contributor to global BC. For example, they estimated that biomass burning emitted 6 Tg BC/yr (from land to atmosphere) whereas fossil fuels emitted 7 Tg BC/yr (from land to atmosphere) [89]. Modeling done by Cooke and Wilson also suggested that fossil fuels (8 Tg BC/yr) produced more BC annually than biomass burning (6 Tg BC/yr [64]), thus suggesting that 14 Tg BC/yr were emitted annually from the land to the atmosphere.

This diverse set of global BC fluxes as well as sedimentary BC fluxes exist because each approximation is dependent on the methodology of measuring BC and estimating emission factors (Table 3). For example, Kuhlbusch and Crutzen defined BC in their samples as the fraction of total carbon surviving a chemical and thermal oxidation pretreatment [59], whereas Cooke *et al.* calculated BC from measurements of light attenuation through a filter [64]. Since no universal BC method exists, each researcher is characterizing a different component of the BC spectrum with their method – hence, calculating different emission factors, different global BC fluxes, and different BC reservoirs. The development of an accurate BC method that is universally applied to estimate the BC content in sediments and soils may reduce the uncertainty in present estimates of BC fluxes and BC reservoirs. Moreover, the ability to calculate an accurate global BC flux and sedimentary BC flux will allow proper estimation of the BC reservoir compared to the OC reservoirs in sediments and soils.

2.6 A REVIEW OF BLACK CARBON METHODS

BC is a collective term encompassing a spectrum of carbonaceous materials, and therefore, it is difficult (maybe impossible) to design a BC method that will not only isolate all the BC particles, but will also be applicable for different sample matrices (i.e., aerosols and sediments). Typically, a given method will retain only a certain percentage

of the total BC particles. For example, Muhlbaier and Williams showed with thermograms (ramp rate of 25°C/min from 100-1,000°C) that BC generated from a fireplace oxidized at 450°C in air. In contrast, BC from a diesel engine oxidizes at 650°C while BC from an oil furnace will oxidize at 750°C [82]. Hence, given a sample containing BC particles originating from a fireplace, diesel engine, and oil furnace, a thermal oxidation method operating at 750°C would isolate a smaller BC fraction (only the oil furnace BC particles) than a method operating at 450°C. Nonetheless, the essence of each BC method is to remove the labile OC from the environmental matrix and then measure the residual BC carbon.

The three dominant methods for removing labile OC are chemical extraction or oxidation, thermal oxidation, or a combination of both procedures ([26, 90] and references therein). The residual carbon is then measured by optical detection (reflectance, absorbance, or transmittance), IR spectroscopy, microscopic (including SEM and counting), coulometric titration, or CO_2 analysis (i.e. elemental analysis). Other indirect methods employed include mass balance, mass loss, ^{13}C-NMR, or biomarkers. Thus, variations between these methods and detectors will result in the isolation of different BC fractions. Instead of reviewing each BC method independently, a suite of intercomparison studies is presented (Table 4) to illustrate the advantages and disadvantages of a variety of BC methods.

2.6.1 Cadle and Groblicki Review. Early work by Cadle and Groblicki [91] compared several methods for isolating BC from atmospheric particles on glass fiber filters: chemical extraction, chemical oxidation, thermal oxidation, and an optical technique (Table 4, 1A). The first method involved extracting OC with a solvent of 4:1 benzene-ethanol in a Soxhlet extraction apparatus. The second method removed OC with a 6 N nitric acid digestion at 110°C for 2 hours. This nitric acid method is similar to later work by Verardo who removed OC with a 6 N nitric acid digestion at 50°C for 30 minutes [60]. In both instances, the OC and BC contents were determined by total

Table 4: Summary of BC methods reviewed (#1 to #4) along with a description of pretreatment to remove organic carbon and the BC method recommended by authors (noted by asterisk; if applicable)

Inter-comparison		BC Method	Description of Pretreatment to remove Organic Carbon
1A		Chemical Extraction	Soxhlet extract OC with a 4:1 benzene-ethanol solvent
		Chemical Oxidation	6 N nitric acid digestion at 110°C for 2 hours
	*	Thermal Method	Pyrolyzed OC in helium at 650°C
		Optical Method	Integrated plate technique calculates BC based on light transmission
1B		Optical Method	Aethalometer calculates BC based light attenuation
		Thermal Oxidation	Oxidize OC in pure oxygen at 340°C for 42 minutes
1C		Optical Method	Integrated sphere technique calculates BC based light reflection
		Thermal-Optical	Pyrolyzed OC in a helium atmosphere at 900°C
2A		Optical Method	Integrated plate technique calculates BC based on light transmission
		Optical Method	Integrated sphere technique calculates BC based light reflection
		Optical Method	Integrated sandwich technique calculates BC based light adsorption
2B		Optical Method	Aethalometer calculates BC based light attenuation
		Optical Method	Integrated sphere technique calculates BC based light reflection
	*	Thermal-Optical	Pyrolyzed OC in a helium atmosphere at 900°C
		Thermal Oxidation	Oxidize OC in pure oxygen at 340°C for 2 hours
3A		Chemical Oxidation	6 N nitric acid digestion at 50°C for 30 minutes
	*	Thermal Oxidation	Oxidize OC in air at 375°C for 14 hours
3B	*	Chemical Oxidation	0.1 M dichromate / 2 M sulfuric acid at 55°C for 2 hours
		Thermal Oxidation	Oxidize OC in pure oxygen at 340°C for 5 hours
4A		Thermal Oxidation	Oxidize OC in air at 375°C for 24 hours
	*	Chemical/Thermal	HCl/HF/TFA acid digestion / 375°C oxidation in air for 24 hours
		Chemical/Thermal	$NaOH/HNO_3/HCl/H_2O_2$ extraction / 340°C oxidation in oxygen for 2 hours
		Chemical/Thermal	$NaOH/HNO_3/HCl/H_2O_2$/ HF digestion / 340°C oxidation in oxygen for 2 hours
		Indirect Method	Chemical extraction of benzenecarboxylic acid as a biomarker
		Indirect Method	UV treatment and calibrating ^{13}C NMR signals to a BC concentration

carbon analysis with an elemental analyzer before and after treatment. In addition to these two methods, Cadle and Groblicki also compared a thermal technique, which pyrolyzed OC in a helium atmosphere at 650°C and then oxidized BC in air at <800°C to produce thermograms. This method is similar to later work done by Chow *et al.* who performed pyrolysis in helium at 550°C followed by oxidation in oxygen at 800°C [92, 93]. Lastly, the BC content of atmospheric particles was determined with an integrated plate technique [94] that correlated the amount of light absorbed to the BC content (no pretreatment necessary to remove OC; Figure 3).

Cadle and Groblicki first observed in their work that chemical oxidation removed more OC than organic solvent extractions. Secondly, they noticed that the OC remaining after an acid digestion was removable with pyrolysis in helium. Thus, BC measurements obtained using either chemical extraction or chemical oxidation probably were biased too high due to the non-extracted OC in the BC fraction. The pyrolysis-oxidation method was recommended by the authors as the best method to measure BC, but they cautioned of the potential effects of charring. They noted in their work that the BC fraction was the carbon resistant to pyrolysis in helium but oxidized in air at temperatures greater than a 340°C threshold temperature (similar to work by Cachier *et al.* [95]).

In addition, Cadle and Groblicki asserted that although optical measurements were hindered by (1) proper absorptivity coefficients, (2) corrections for light penetration into the filter, and (3) light-absorbing organic matter, optical observations gave comparable BC measurements to the pyrolysis-oxidation technique. Interestingly, Lavanchy *et al.* also reported comparable BC measurements between an optical technique (aethalometer that measures the attenuation of light transmitted through the filter) and a thermal method (combust in pure oxygen at 340°C for 42 minutes; Table 4, 1B). This measurement assumes that the authors isolated the same BC fraction with both methods. For example, the BC concentration in an ice core ranged from 7-128 μg BC/L melt water with the optical method while the thermal method measured 5-130 μg BC/L melt water with a correlation $R^2 = 0.81$ for the two methods [37]. In addition, Hitzenberger *et al.*

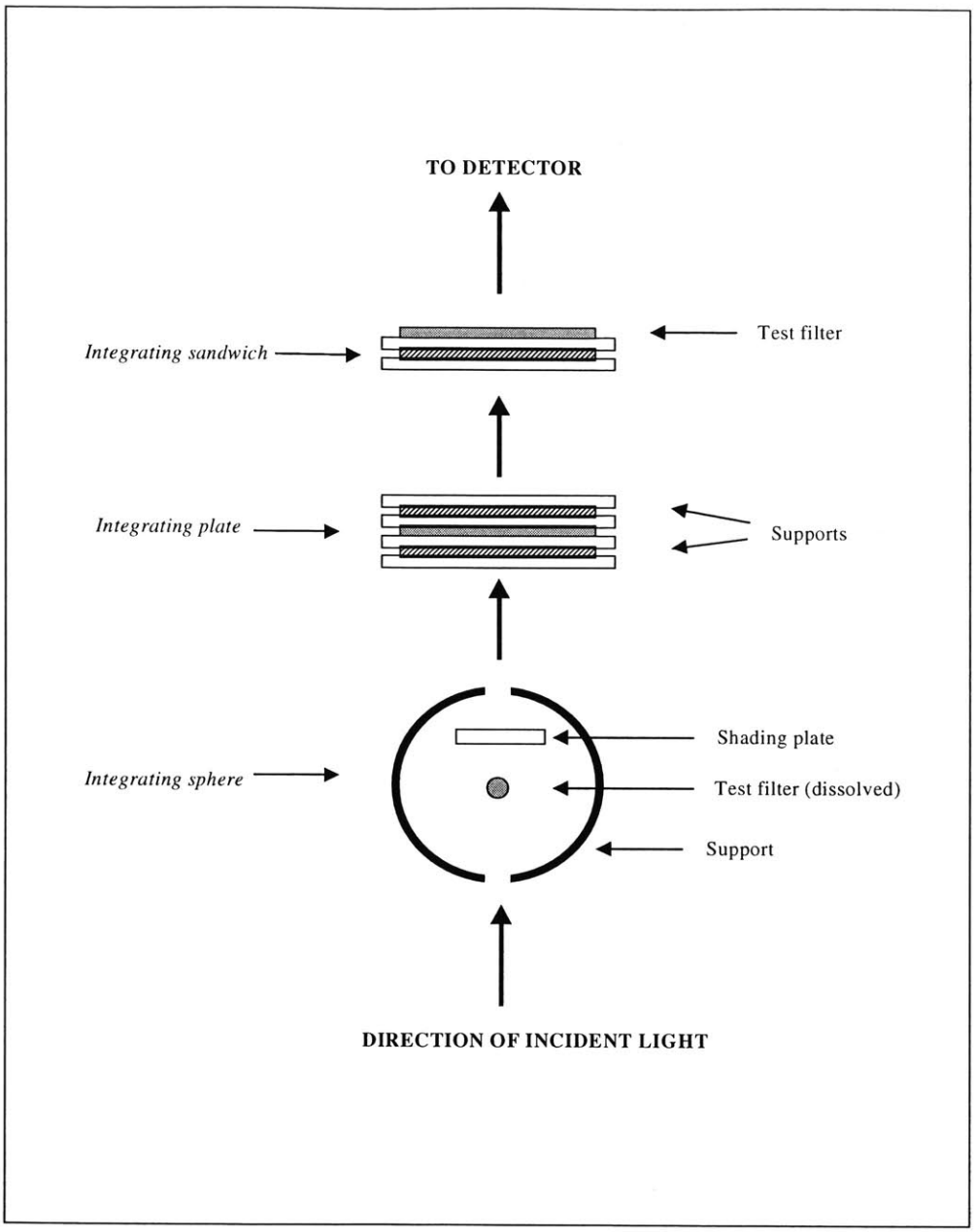

Figure 3: Schematics of three optical techniques: integrating plate, integrating sandwich, and integrating sphere (adapted from Clarke *et al.* (1987) Atmos. Environ.). In the integrating plate method, the transmission of light is measured before and after the collection of aerosols. The change in light transmission relates to absorption and BC concentration by Beer's law. The integrating plate operates with one set of light-diffusing supports and tends to overestimate BC concentration due to light scattering. In the integrating sandwich technique, a second set of light-diffusing supports is added, which amplifies the net absorption by the aerosols. Although nonlinear, the response allows for rapid sample collection at low aerosol concentration. In the integrating sphere method, a sphere is illuminated through a small hole, and the incoming light strikes the sample (dissolve filter) suspended in the center of the sphere. The detector compares the relative intensity of the incoming light and the light reflected off the inside walls of the sphere.

reported that their BC measurements agreed within 5% for an integrated sphere technique (Figure 3) and a thermal-optical method [96] (Table 4, 1C). This thermal-optical reflectance method developed by Birch and Cary is similar to the method studied by Cadle and Groblicki and involves pyrolyzing in a helium atmosphere while monitoring charring with light transmission. The remaining carbon is then oxidized in an oxygen-helium atmosphere. Hence, a thermal or optical method may provide a more effective method for measuring BC than a chemical oxidation or extraction procedure.

2.6.2 Review of optical methods. While the thermal and optical methods appear compatible, other researchers have reported discrepancies in their BC measurements for various optical techniques. Clarke *et al.* noted that:

> *Apart from instrument calibration and measurement uncertainties, a given mass of [BC aerosol] can yield significantly different optical properties depending upon such things as the geometric mass mean diameter and shape of the size distribution, the morphology of the particles, the complex refractive index, and the presence of particle coatings or condensates [65].*

In addition, optical measurements are dependent on loading of the collection surface and light absorbing organic matter and crustal dust [3, 36, 65]. A previous intercomparison study by Clarke *et al.* investigated three optical techniques used to measure BC (Table 4, 2A and Figure 3): integrated plate [94], integrated sphere [97], and integrated sandwich [98]. They noted that the conversion factor (units of m^2/g) for converting light attenuation to BC concentration varied by about 40% (including all the data) among the three methods. Moreover, the conversion factor had an uncertainty of about 25% for each given method over a range of BC standards [65]. However, the conversion coefficient is assumed a constant. Variations in the conversion coefficient can significantly affect the calibration of different optical methods, resulting in unacceptable uncertainty in BC measurements [99].

In another optical intercomparison study, Hitzenberger *et al.* reported discrepancies between BC measurements in aerosols on filters using different optical and thermal methods [99] (Table 4, 2B). First, they reported that two optical methods did not give comparable BC measurements. For example, the aethalometer [33] consistently underestimated the BC content by 30% relative to the integrated sphere technique [99]. Interestingly, Hitzenberger *et al.* noted that since the inaccuracy in the aethalometer method is directly dependent on the conversion factor, then comparable BC values could be achieved between the two optical methods by simply adjusting the conversion factor. They continued to report that neither optical technique gave comparable BC measurements to a thermal method [95, 96]. For example, the integrated sphere technique consistently overestimated the BC content by 21% relative to the Cachier-thermal method [95].

2.6.3 Middelburg *et al.* and Lim and Cachier Review. Similar to the study by Cadle and Groblicki, Middelburg *et al.* [41] compared the nitric acid digestion of Verardo [60] with thermal oxidation method developed by Gustafsson *et al.* [10, 61] (Table 4, 3A). The latter involved oxidizing OC at 375°C for 24 hours in air, removing inorganic carbon by acidification with HCl, and then operationally defining the remaining carbon as BC with an elemental analyzer. (Note that Middelburg *et al.* combusted sediment for 14 hours instead of 24 hours.) The first observation of this intercomparison was that the thermal oxidation method removed more carbon in sediment samples than the nitric acid method. For example, the carbon remaining after nitric acid digestion always accounted for >50% of the TOC, whereas the carbon fraction remaining after the 375°C thermal method ranged from 15-30%. The authors then noted that the nitric acid method could not remove any residual carbon following thermal oxidation at 375°C. Middelburg *et al.* also speculated that the nitric acid method did not remove all the OC since the isotopic signature of the sediment ($\delta\ ^{13}C = -22$ to $-21‰$) did not reflect an intense terrestrial "charcoal signature" of $\delta\ ^{13}C = -27$ to $-26‰$ [41].

Contrary to the work of Cadle and Groblicki plus Middelburg *et al.*, a recent investigation by Lim and Cachier suggested that a chemical oxidation was a better approach to isolating BC than a thermal oxidation [6] (Table 4, 3B). A chemical oxidation method developed by Wolbach *et al.* (0.1 M dichromate / 2 M sulfuric acid at 55°C for 2 hours [71]) was compared with a 340°C thermal oxidation method that operated under oxygen for 4 hours [95]. For both methods, sediments were pretreated with a 10 M HF / 1 M HCl solution to remove silicates and inorganic carbon to ensure that BC particles were not occluded, and the BC fraction was defined as the residual carbon after chemical or thermal oxidation. Their work showed that for the same sample the 340°C thermal oxidation method gave rather erratic results with weight percents varying from 0.15-0.40 wt % C (almost a factor of 3 variability). Meanwhile, the chemical oxidation method gave a lower more consistent BC content of 0.080 ±0.003 wt % BC for the same sample. They hypothesized that the variability in the BC abundance observed in the thermal treatment was due to charring of OC. However, their total carbon analysis yielded errors as large as 35%, and the pretreatment with HF (to demineralize) may have affected accurate gravimetric determination and calculation of carbon weight percentage, thus contributing to the observed variability.

2.6.4 Schmidt *et al.* Review. Another intercomparison investigation was conducted by Schmidt *et al.* and involved six different BC methods from five international laboratories [43] (Table 4, 4A). The methods compared were (1) a 375°C thermal oxidation for 24 hours under air *without* acidification [61], (2) a chemical extraction with HCl/HF/TFA followed by the 375°C thermal oxidation method [31], (3) a chemical extraction with $NaOH/HNO_3/HCl/H_2O_2$ followed by the 340°C thermal oxidation for 2 hours under oxygen [59], (4) a modification to the Kuhlbusch method [59] with the addition of a HF acidification step, (5) an indirect method involving the hydrolysis of BC to yield of benzenepolycarboxylic acids and using these chemicals as biomarkers for BC [100], and (6) an indirect method involving UV treatment and calibrating ^{13}C NMR signals to a BC concentration [101]. The work by Schmidt *et al.* presents several interesting

interpretations of BC methodology. The authors noted that no systematic offset existed between the six different BC methods. Hence, they could not recommend an appropriate method for measuring BC in soil or sediment matrices. They did observe, however that for a few samples, BC weight percents decreased from the Gustafsson method to the Kulhbusch method to the Gelinas method. Thus, Schmidt *et al.* inferred that BC methods employing a combination of chemical and thermal oxidation measured the most resistant BC fraction [43].

Another interpretation of the data suggests that Schmidt *et al.* overlooked some important observations. First, the UV oxidation / ^{13}C NMR analysis reported the largest BC values compared to the other methods in 75% of the cases studied. These high BC values are probably associated with the uncertainties in quantifying ^{13}C NMR signals since lignin/tannin structures that are present in soils give the same aromatic ^{13}C signal as BC [101]. Secondly, the intense chemical oxidation method developed by Gelinas *et al.* reported the lowest BC values in all instances. For the five soil samples analyzed, BC weight percents ranged from <0.005-0.02 wt % C with BC/TOC ratio approximately 0.1%. These results (approximately equal to zero) suggest that the Gelinas method erred too low. A closer analysis of their method reveals that samples were centrifuged and filtered more than 10 times [31], which can encourage the loss of BC either during filtration or removal of BC suspended in the acidic supernatants [6].

Of the three remaining methods, the Kuhlbusch method consistently reports lower BC values than the Gustafsson method; however, the modified Gustafsson method employed in this study was the only method that did not include acidification to remove inorganic carbon. Hence, no conclusion can be established on the more appropriate method of the two. Finally, the Glaser method, which employs biomarkers to determine the BC fraction, was comparable within a factor of 1.5 to the Gustafsson method. However, this Glaser-method is still questionable because it uses an estimated 2.27 conversion factor to convert the amount of extracted benzenepolycarboxylic acids to BC content in soils [100]. This conversion factor may be skewed because the number was derived from the mean results of three commercial charcoals and does not consider the

other forms of BC that exist in the environment. Plus, Glaser *et al.* showed that their method to extract benzenepolycarboxylic acids was dependent on their acid digestion period with the yield of benzenepolycarboxylic acids varying between a factor of 5 and 10 [100] (no error bars are reported in their original work). The dependency on the acid digestion period suggests that BC values may not be reproducible between different runs or different laboratories.

2.6.5 Currie *et al.* Review. All the studies above describe several comparable and non-comparable BC methods (Table 4). In summary, work by Cadle and Groblicki as well as Middelburg *et al.* showed that thermal oxidation methods removed OC more effectively than a chemical method. Secondly, while several researchers noted that thermal and optical methods can yield comparable BC measurements [37, 91, 99], other researchers have reported large discrepancies between various optical methods. Finally, work by Schmidt *et al.* suggest that indirect BC methods tend to overestimate the BC content while extensive chemical manipulations tend to underestimate the BC content. These studies also illustrate that all BC methods are plagued by internal error (i.e. accuracy). For example, lengthy manipulations and inefficient OC removal procedures hinder chemical methods. Thermal oxidation methods are challenged by charring and by defined temperature cutoff points, while optical methods are affected by proper calibration of their conversion factor and corrections for additional absorption or scattering.

The National Institute of Standards and Technology orchestrated the last intercomparison study presented here [90] (Figure 4). They reported the BC content of NIST SRM 1649a (urban dust from Washington D.C. collected in 1976-1977) measured from 13 different BC methods (8 methods were already introduced above) practiced in 15 international laboratories. Unlike the comparisons previously discussed, this NIST study is unique because all the laboratories measured the BC content for the same standard reference material. Interestingly for this aerosol matrix, the BC content varied from 1.2

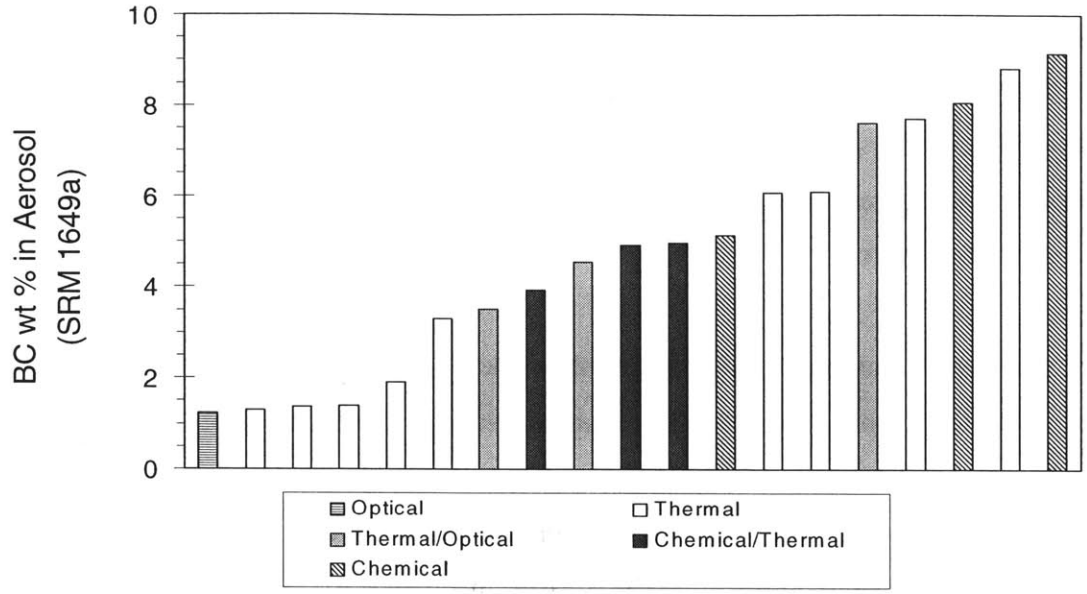

Figure 4: Nineteen independent measurements of the BC content (wt % C) in a standard reference material (NIST SRM 1649a; Certificate of Analysis) using 13 different BC methods. These methods are grouped into five categories: optical (horizontal hashed bars), thermal (unfilled bars), combination of thermal and optical (gray filled bars), combination of chemical and thermal (black filled bars), and chemical (diagonally hashed bars). Description of each method is reported in Currie *et al.* (2002) J. Res. Natl. Inst. Stan.

wt % C to 9.2 wt % C for 19 independent measurements (Figure 4). This factor of 8 difference among the various BC methods (optical, thermal, thermal/optical, chemical/thermal, and chemical) underlines the need for a standard BC method.

The results gathered by Currie *et al.* both support and contradict the findings reported in the comparisons explored above. The NIST study showed that thermal oxidation methods (unfilled bars; Figure 4) isolated a smaller carbon fraction than chemical methods (diagonally hashed bars; Figure 4). Consequently, thermal methods measure a smaller BC fraction. Currie *et al.* indicated that because BC covers a spectrum of material, thermal oxidation methods isolate the most resistant fraction notably soots, while gentler chemical methods routinely isolate a more labile char fraction [90]. This work confirms previous work done by Cadle and Groblicki as well as Middelburg *et al.* who showed that the Gustafsson-375°C thermal method and the Chow-O_2/ He thermal method were more aggressive than the Verardo-nitric acid chemical method in isolating BC [41, 90, 91]. Currie *et al.* also observed in their study that the 375°C-thermal method consistently reproduced one of the lowest BC values (1.3 wt % BC) second only to the aethalometer method (1.2 wt % BC; [90]). The comparable BC measurements for the 375°C-thermal oxidation and the aethalometer may support work by Cadle and Groblicki, Lavanchy *et al.*, and Hitzenberger *et al.* who all observed comparable BC measurements between their various thermal and optical methods [37, 91, 99]. Finally, the NIST study confirms observations by Gustafsson *et al.* [10, 61] that the 375°C-thermal method isolates a more resistant BC fraction than the Cachier 340-thermal method (6.1 wt % BC; [90]).

2.7 INCORPORATION OF THESIS WORK

2.7.1 375°C Thermal Oxidation Method. Based on the studies reviewed thus far, especially the results of the NIST intercomparison, the 375°C-thermal oxidation method was used in the following thesis work to measure the BC content in sediments and soils. Gustafsson and colleagues developed the 375°C-thermal oxidation method by systematically increasing the oxidation temperature to define an optimal temperature that

isolates BC from an organic complex [61]. They created a thermogram with Aldrich humic acid and NIST diesel particulate matter (SRM 1650) that represents the carbon mass remaining after oxidation. Their work showed that 95% of the NIST material survived oxidation at 375°C after 24 hours under air while 99.8% of the Aldrich humic acid was removed. In later work, Gustafsson *et al.* re-confirmed the 375°C benchmark by showing that 99.9% of the carbon mass for a medium-grade coal (ANL Coal #6) was oxidized after the 375°C pretreatment [10]. This method was further tested with representative samples of organic matter, such as: acetanilide, polystyrene, polyethylene, oak wood, fuel oil, crude oil and kerogen (green river shale and kimberlite). All these labile compounds were oxidized with <0.01% of the total carbon mass remaining.

Unlike the labile OC, a certain percentage of more recalcitrant carbon material, like high-rank coals (or thermally mature coals), carbon black, and activated carbon, survived the 375°C treatment. Similar results were observed by Gelinas *et al.* who showed that >93% of the total carbon mass for graphite powder and acetylene soot survived the 375°C treatment while essentially no carbon from bituminous coal (low-rank coal) survived the oxidation [31]. Gelinas *et al.* did note that for the same diesel particulate matter (SRM 1650) studied by Gustafsson *et al.* approximately 40% of the carbon mass was lost after the 375°C treatment, suggesting that the standard contained a more volatile organic fraction than previously measured. This observation was later confirmed by Gustafsson *et al.* who also measured a 38% loss of carbon mass with the diesel particulate matter [10] and attributed this loss to an oily coating on the diesel particles. Nonetheless, all three laboratories noted the potential of isolating a BC fraction from an organic matrix with the 375°C-thermal oxidation method.

2.7.2 Charring Potential of Organic Carbon. A common criticism of the 375°C-thermal oxidation method is that OC creates a BC artifact during oxidation. Reviewers tend to compare the 375°C-thermal method to other methods that employ an optical technique to monitor potential charring [93, 96]. Moreover, critics hypothesize that charring will result in a strong correlation between the TOC and the resulting BC

measurements. For example, Schmidt *et al.* observed a strong correlation of $R^2 = 0.98$ (Population size (Z) = 5) between TOC and BC for soil samples; thus implying that the thermal oxidation method had the potential of charring [43]. However, the authors ignored other reasonable TOC-BC correlations that existed for the same sample set. For example, the Glaser-biomarker method gave a correlation coefficient of 0.84 (Z = 8) while a modified Kulhbusch, thermal-chemical method resulted in a correlation of $R^2 =$ 0.79 (Z = 8) for the same soils [43]. These results suggest that correlation coefficients are inappropriate indicators of charring, especially since a thermal method and a biomarker method gave reasonable TOC-BC correlations. Gelinas *et al.* also asserted that the 375°C-thermal oxidation created BC, and noted a strong correlation of 0.92 (Z = 9) for sediment samples in the Gulf of Maine ([31, 40]; Figure 5). However, the authors neglected to include the entire sample set of 17 data points, which corresponded to a rather low correlation coefficient of 0.59 (Z = 17) [61]. Interestingly, a low TOC-BC correlation ($R^2 = 0.35$, Z = 17) was also measured within the Gelinas *et al.* data set after the authors took into account acidification to remove inorganic carbon [31].

Nonetheless, some literature results that do suggest a linear correlation between TOC and BC cannot be ignored. For example, Middelburg *et al.* measured the BC content of 33 sediment samples using the 375°C-thermal oxidation method, and they calculated a R^2 value of 0.90 between TOC and BC. Meanwhile, they measured a similar correlation coefficient of 0.95 for the same sediment samples using the Verardo-chemical method [41, 60]. The authors concluded that since the Verardo method gave a similar TOC-BC correlation as the 375°C-thermal method, then charring could not be significantly affecting measurements. Instead, they hypothesized that depositional factors and hydrodynamic sorting caused the strong correlation between OC and BC. Here, in this thesis, a strong TOC-BC correlation ($R^2 = 0.87$, Z = 7) for sediments from north Quincy Bay (Boston Harbor, MA) was observed (Table 5). Similar to conclusions by Middelburg *et al.*, deposition and hydrodynamic sorting may explain the BC sample set better than charring of OC. For example, sediment samples with a larger OC content

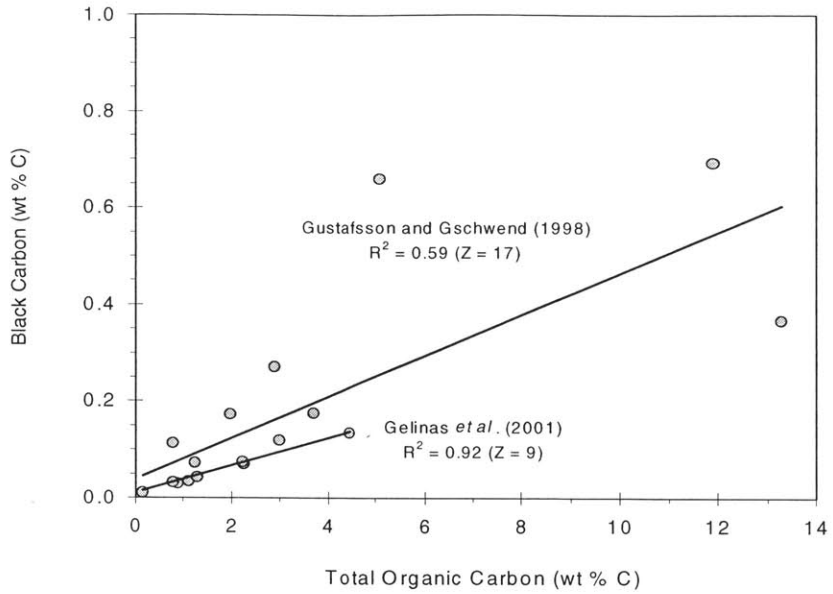

Figure 5: Black carbon content (wt % C) and total organic content (wt % C) for 17 coastal sediment samples measured by Gustafsson and Gschwend (1998) Geochim. Cosmochim. Acta using the 375°C thermal oxidation method. The correlation coefficient for the entire set of data is 0.59 (Z = 17). Note that the correlation coefficient reported by Gelinas *et al.* (2001) Environ. Sci. Tech. only includes a selected sub-set of the sediment samples (Z = 9).

Table 5: Five sediment samples from north Quincy Bay, MA along with their percent of solid mass removed through a 40 mesh sieve, the measured total OC content (wt % C, mean ±1σ) and the measured BC content (wt % C, mean ±1σ).

% Removal by 40 mesh	TOC wt %	BC wt %
2	7.2 ±0.22	0.92 ±0.11
28	0.37 ±0.11	0.03 ±0.01
30	1.3 ±0.13	0.13 ±0.02
34	1.7 ±0.25	0.16 ±0.02
44	2.5 ±0.27	0.55 ±0.10

and a larger BC content in general corresponded to shallow sites, and exhibited a higher percentage of mass removed through a 40 mesh sieve (425 μm aperture). On the contrary, lower OC and BC contents corresponded to sediments located offshore as noted by a smaller loss of mass through the same sieve (Table 5).

Recent radiocarbon work by Reddy *et al.* showed that the 375°C-thermal oxidation method could isolate BC without interference from charring [102]. In their work, individual PAH compounds were extracted from sediment and aerosol standards (NIST SRM 1941a, 1944, and 1649a). The low ^{14}C abundance in these isolated PAHs (excluding perylene) was consistent with a fossil fuel combustion source (f_m = 0.01-0.09). The BC fraction in these same standards was then isolated with the 375°C thermal method. Similar to the extracted PAH compounds, the ^{14}C abundance of the BC fractions was low (f_m = 0.02-0.06), and >90% of the BC in these sediment and aerosol standards was derived from a fossil fuel combustion source. If the organic matter in these matrices were charring, then the ^{14}C measurements in the BC fraction would appear artificially high (or more "modern") relative to the PAHs. However, since the ^{14}C abundance in the PAH and the BC were similar, and these ^{14}C measurements were different from the ^{14}C abundance of the TOC, charring probably did not occur during the 375°C pretreatment.

During the NIST intercomparison study, the BC isolated by the 375°C-thermal method gave a fraction modern of 0.065 ±0.003 while another thermal method gave a similar BC fraction modern of 0.038 ±0.012 [90]. In contrast, the chemical method developed by Wolbach [71] gave a fraction modern of their BC isolate of 0.153 ±0.002 [90]. The higher fraction modern from the chemical method as opposed to the two thermal methods suggest that the chemical method was not efficient in removing all the OC, thus increasing the fraction modern by a factor of 3. Nonetheless, Masiello *et al.* continue to contend that the high fraction modern value was acceptable based on a prior study that attempted to isolate PAHs and the aromatic fraction from SRM 1649a [79]. However, this prior study was plagued by analytical errors because earlier methods could not separate PAHs from the organic, unresolved complex mixture [102, 103].

2.7.3 Objectives of thesis work. While some evidence exists to support the hypothesis that charring is not occurring, reviewers raised legitimate concerns that the 375°C-thermal oxidation method may result in charring of OC. For example, Gelinas *et al.* noted that a fresh plankton tow from Dabob Bay (WA) had a BC/TOC ratio of 65%. If it is assumed that the referenced tow material contained no BC, then the reported BC/TOC ratio suggests that the biopolymers charred [31]. Similarly Gustafsson *et al.* also observed in their studies that in addition to fresh phytoplankton, other complex organic matrices like pollens and nitrogen-containing macromolecules had a tendency to char [10, 61]. Although steps are necessary to reduce charring, a method that involves a multitude of manipulations and transfers to demineralize and chemically oxidize OC is probably too extensive and risks the potential of BC loss. In addition, Gelinas *et al.* noted that their extensive chemical method removes between 95-98% of the total sample mass [31], raising doubt as to the reliability of the method to provide an accurate elemental analysis of their samples.

In this thesis, the accuracy and precision of the 375°C method is explored in detail. In general, the incomplete combustion of organic matter can lead to an overestimation of the BC content while the oxidation of small BC particles at 375°C can cause an underestimation of the BC content. Through a series of internal additions of organic compounds, the work presented in Chapter 3 shows that oxygen accessibility is the key ingredient in determining what carbon material will survive the 375°C pretreatment.

2.8 REFERENCES

1. Goldberg, E. D. *Black Carbon in the Environment: Properties and Distribution.* **1985**, A Wiley-Interscience Publication, John Wiley & Sons: New York. 1-198.
2. Hildemann, L. M.; Markowski, G. R.; Cass, G. R. *Environ. Sci. Technol.* **1991**, *25,* 744-759.
3. Cachier, H. *Carbonaceous combustion aerosols* in *Atmospheric Particles.* R. M. Harrison; R. V. Grieken. **1998**, John Wiley & Sons: New York. 295-348.
4. Medalia, A. I.; Rivin, D. *Carbon* **1982**, *20,* 481-492.

5. Whitby, K. T.; Charlson, R. E.; Wilson, W. E.; Stevens, R. K. *Science* **1974**, *183,* 1098-1099.
6. Lim, B.; Cachier, H. *Chem. Geol.* **1996**, *131,* 143-154.
7. Lahaye, J. *Polym. Degrad. Stabil.* **1990**, *30,* 111-121.
8. Smedley, J. M.; Williams, A.; Bartle, K. D. *Combust. Flame* **1992**, *91,* 71-82.
9. Benish, T. G.; Lafeur, A. L.; Taghizadeh, K.; Howard, J. B. *C2H2 and PAH as Soot Growth Reactants in Premixed C2H4 Air Flames* in *Twenty-sixth Symposium (International) on Combustion.* **1996**, The Combustion Institute: Pittsburg. 2319-2326.
10. Gustafsson, Ö.; Bucheli, T. D.; Kukulska, Z.; Anderson, M.; Largeau, C.; Rouzaud, J. N.; Reddy, C. M.; Eglinton, T. E. *Global Biogeochem. Cy.* **2001**, *15,* 881-890.
11. Rainey, L. C.; Palotas, A. B.; Bolsaitis, P.; VanderSande, J. B.; Sarofim, A. F. *Appl. Occup. Environ. Hyg.* **1996**, *11,* 777-781.
12. Palotas, A. B.; Rainey, L. C.; Sarofim, A. F.; VanderSande, A. B.; Flagan, R. C. *Chemtech* **1998**, *28,* 24-30.
13. Frenklach, M. *On surface growth mechanism of soot particles* in *Twenty-sixth Symposium (International) on Combustion.* **1996**, The Combustion Institute: Pittsburgh. 2285-2293.
14. Harris, S. J.; Weine, A. M. *Combust. Sci. Technol.* **1983**, *31,* 155-167.
15. Harris, S. J. *Combust. Sci. Technol.* **1990**, *72,* 67-77.
16. Kazakov, A.; Frenklach, M. *Combust. Flame* **1998**, *112,* 270-274.
17. Macadam, S.; Beer, J. M.; Sarofim, A. F. *Soot surface growth by PAH and acetlyene additions* in *Twenty-sixth symposium (International) on Combustion.* **1996**, The Combustion Institute: Pittsburg. 2295-2302.
18. Smith, D. M.; Griffin, J. J.; Goldberg, E. D. *Nature* **1973**, *241,* 268-270.
19. Griffin, J. J.; Goldberg, E. D. *Geochim. Cosmochim. Acta* **1981**, *45,* 763-769.
20. Kralovec, A. C.; Christensen, E. R.; Camp, R. P. V. *Environ. Sci. Technol.* **2002**, *36,* 1405-1413.
21. Venkataraman, C.; Friedlander, S. K. *Environ. Sci. Technol.* **1994**, *28,* 563-572.
22. Griffin, J. J.; Goldberg, E. D. *Science* **1979**, *206,* 563-565.
23. Rockne, K. J.; Taghon, G. L.; Kosson, D. S. *Chemosphere* **2000**, *41,* 1125-1135.
24. Kleineidam, S.; Rugner, H.; Ligouis, B.; Grathwohl, P. *Environ. Sci. Technol.* **1999**, *33,* 1637-1644.
25. NIST *Certificate of Analysis for SRM 1650a Diesel Particulate Matter.* **2001**, National Institute of Standards and Technology: Gaithersburg. 1-9.
26. Schmidt, M. W. I.; Noack, A. G. *Global Biogeochem. Cy.* **2000**, *14,* 777-793.
27. Akhter, M. S.; Chughtal, A. R.; Smith, D. M. *Appl. Spectrosc.* **1985**, *39,* 143-153.
28. Akhter, M. S.; Chughtal, A. R.; Smith, D. M. *Appl. Spectrosc.* **1985**, *39,* 154-167.
29. Kuhlbusch, T. A. J. *Environ. Sci. Technol.* **1995**, *29,* 2695-2702.
30. Andreae, M. O. *Science* **1983**, *220,* 1148-1151.
31. Gelinas, Y.; Prentice, K. M.; Baldock, J. A.; Hedges, J. I. *Environ. Sci. Technol.* **2001**, *35,* 3519-3525.
32. Kuhlbusch, T. A. J. *Science* **1998**, *280,* 1903-1904.

33. Hansen, A. D. A.; Rosen, H.; Novakov, T. *Sci. Total Environ.* **1984**, *36,* 191-196.
34. Cooke, W. F.; Jennings, S. G.; Spain, T. G. *J. Geophys. Res.* **1997**, *102,* 25339-25346.
35. Eglinton, T. I.; Eglinton, G.; Dupont, L.; Sholkovitz, E. R.; Montlucon, D.; Reddy, C. M. *Geochem. Geophy. Gosy.* **2002**, *3,* U1-U27.
36. Chylek, P.; Kou, L.; Johnson, B.; Boudala, F.; Lesins, G. *Atmos. Environ.* **1999**, *33,* 2269-2277.
37. Lavanchy, V. M. H.; Gaggeler, H. W.; Schotterer, U.; Schwikowski, M.; Baltensperger, U. *J. Geophys. Res.* **1999**, *104,* 21,227-221,236.
38. Muri, G.; Cermelj, B.; Faganeli, J.; Brancelj, A. *Chemosphere* **2002**, *46,* 1225-1234.
39. Gustafsson, Ö.; Gschwend, P. M. *Soot as a strong partition medium of polycyclic aromatic hydrocarbons in aquatic systems* in *Molecular Markers in Environmental Geochemistry*. R. P. Eganhouse. **1997**, ACS Symposium Series: Washington DC. *671,* 365-381.
40. Gustafsson, Ö.; Gschwend, P. M. *Geochim. Cosmochim. Acta* **1998**, *62,* 465-472.
41. Middelburg, J. J.; Nieuwenhuize, J.; Breugel, P. V. *Mar. Chem.* **1999**, *65,* 245-252.
42. Accardi-Dey, A.; Gschwend, P. M. *Environ. Sci. Technol.* **2002**, *36,* 21-29.
43. Schmidt, M. W. I.; Skjemstad, J. O.; Czimczik, C. I.; Glaser, B.; Prentice, K. M.; Gelinas, Y.; Kuhlbusch, T. A. J. *Global Biogeochem. Cy.* **2001**, *15,* 163-167.
44. Elias, V. O.; Simoneit, B. R. T.; Cordeiro, R. C.; Turcq, B. *Geochim. Cosmochim. Acta* **2001**, *65,* 267-272.
45. Accardi-Dey, A.; Gschwend, P. M. *Environ. Sci. Technol.* **2003**, *37,* 99-106.
46. Mitra, S.; Bianchi, T. S.; McKee, B. A.; Sutula, M. *Environ. Sci. Technol.* **2002**, *36,* 2296-2302.
47. Novakov, T.; Chang, S. G.; Harker, A. B. *Science* **1974**, *186,* 259-261.
48. Kirkevag, A.; Iversen, T.; Dahlback, A. *Atmos. Environ.* **1999**, *33,* 2621-2635.
49. Liu, L.; Mishchenko, M. I.; Menon, S.; Macke, A.; Lacis, A. A. *J. Quant. Spectrosc. Ra.* **2002**, *74,* 195-204.
50. Menon, S.; Hansen, J.; Nazarenko, L.; Luo, Y. *Science* **2002**, *297,* 2250-2253.
51. Charlson, R. J.; Orgen, J. A. *The atmospheric cycle of elemental carbon* in *Particulate Carbon: Atmospheric Life Cylces*. G. T. Wolff; R. L. Klimisch. **1982**, Plenum Press: New York. 3-16.
52. Jacobson, M. Z. *Nature* **2001**, *409,* 695-697.
53. Swartz, R. C. *Environ. Toxicol. Chem.* **1999**, *18,* 780-787.
54. Allen, J. O.; Dookeran, N. M.; Smith, K. A.; Sarofim, A. F.; Taghizadeh, K.; Lafleur, A. L. *Environ. Sci. Technol.* **1996**, *30,* 1023-1031.
55. Cope, M. J.; Chaloner, W. G. *Nature* **1980**, *283,* 647-649.
56. Herring, J. R. *Charcoal fluxes into sediments of the North Pacific Ocean: The Cenozoic record of burning* in *The Carbon Cycle and Atmospheric CO2: Natural Variations Archean to Present*. E. T. Sundquist; W. S. Broecker. **1985**, American Geophysical Union: Washington D.C., 419-442.
57. Seiler, W.; Crutzen, P. J. *Climatic Change* **1980**, *2,* 207-247.

58. Crutzen, P. J.; Andreae, M. O. *Science* **1990**, *250,* 1669-1678.
59. Kuhlbusch, T. A. J.; Crutzen, P. J. *Global Biogeochem. Cy.* **1995**, *9,* 491-501.
60. Verardo, D. J. *Limnol. Oceanogr.* **1997**, *42,* 192-197.
61. Gustafsson, Ö.; Haghseta, F.; Chan, C.; MacFarlane, J.; Gschwend, P. M. *Environ. Sci. Technol.* **1997**, *31,* 203-209.
62. Masiello, C. A.; Druffel, E. R. M. *Science* **1998**, *280,* 1911-1913.
63. Haumaier, L.; Zech, W. *Org. Geochem.* **1995**, *23,* 191-196.
64. Cooke, W. F.; Wilson, J. N. *J. Geophys. Res.* **1996**, *101,* 19395-19409.
65. Clarke, A. D.; Noone, K. J.; Heintzenberg, J.; Warren, S. G.; Covert, D. S. *Atmos. Environ.* **1987**, *21,* 1455-1465.
66. Windsor, J. G.; Hites, R. A. *Geochim. Cosmochim. Acta* **1978**, *43,* 27-33.
67. Kaneyasu, N.; Murayama, S. *J. Geophys. Res.* **2000**, *105,* 19881-19890.
68. Bodhaine, B. A. *J. Geophys. Res.* **1995**, *100,* 8967-8975.
69. Masiello, C. A.; Druffel, E. R. M. *Global Biogeochem. Cy.* **2001**, *15,* 407-416.
70. Griffin, J. J.; Goldberg, E. D. *Limnol. Oceanogr.* **1975**, *20,* 456-463.
71. Wolbach, W. S.; Anders, E. *Geochim. Cosmochim. Acta* **1989**, *53,* 1637-1647.
72. Smith, D. M.; Griffin, J. J.; Goldberg, E. D. *Anal. Chem.* **1975**, *47,* 233-238.
73. Goldberg, E. D.; Hodge, V. F.; Griffin, J. J.; Kiode, M. *Environ. Sci. Technol.* **1981**, *15,* 466-471.
74. Griffin, J. J.; Goldberg, E. D. *Environ. Sci. Technol.* **1983**, *17,* 244-245.
75. Karls, J. F.; Christensen, E. R. *Environ. Sci. Technol.* **1998**, *32,* 225-231.
76. Bird, M. I.; Cali, J. A. *Nature* **1998**, *394,* 767-769.
77. Wolbach, W. S.; Lewis, R. S.; Anders, E. *Science* **1985**, *230,* 167-170.
78. Wolbach, W. S.; Gilmour, I.; Anders, E.; Orth, C. J.; Brooks, R. R. *Nature* **1988**, *334,* 665-669.
79. Masiello, C. A.; Druffel, E. R. M.; Currie, L. A. *Geochim. Cosmochim. Acta* **2002**, *66,* 1025-1036.
80. Cachier, H.; Bremond, M. P.; Buat-Menard, P. *Nature* **1989**, *340,* 371-373.
81. Streets, D. G.; Gupta, S.; Waldhoff, S. T.; Wang, M. Q.; Bond, T. C.; Yiyum, B. *Atmos. Environ.* **2001**, *35,* 4281-4296.
82. Muhlbaier, J. L.; Williams, R. L. *Fireplaces, furnaces, and vehicles as emission sources of particulate carbon* in *Particulate Carbon: Atmospheric Life Cylces*. G. T. Wolff; R. L. Klimisch. **1982**, Plenum Press: New York. 185-198.
83. Miguel, A. H.; Kirchstetter, T. W.; Harley, R. A. *Environ. Sci. Technol.* **1998**, *32,* 450-455.
84. Cass, G. R.; Boone, P. M.; Macias, E. S. *Emissions and air quality relationships for atmospheric carbon particles in Los Angeles* in *Particulate Carbon: Atmospheric Life Cylces*. G. T. Wolff; R. L. Klimisch. **1982**, Plenum Press: New York. 207-225.
85. Cooke, W. F.; Liousse, C.; Cachier, H. *J. Geophys. Res.* **1999**, *104,* 22137-22162.
86. Penner, J. E.; Eddleman, H.; Novakov, T. *Atmos. Environ.* **1993**, *27,* 1277-1295.
87. Penner, J. E. *Carbonaceous aerosols influencing atmospheric radiation: Black and organic carbon* in *Aerosol Forcing of Climate*. R. J. Charlson; J. Heintzenberg. **1995**, John Wiley & Sons: New York. 91-108.

88. Sumam, D. O.; Kulbusch, T. A. J.; Lim, B. *Marine sediments: A reservoir for black carbon and their use as spacial and temporal records of combustion* in *Sediment Records of Biomass Burning and Global Change.* J. S. Clark. **1994**, NATO ASI Series: *51*, 271-293.
89. Liousse, C.; Penner, J. E.; Chuang, C.; Walton, J. J.; Eddleman, H.; Cachier, H. *J. Geophys. Res.* **1996**, *101,* 19411-19432.
90. Currie, L. A.; Benner, B. A.; Kessler, J. D.; Klinedinst, D. B.; Klouda, G. A.; Marolf, J. V.; Slater, J. F.; Wise, S. A.; Cachier, H.; Cary, R.; Chow, J. C.; Watson, J.; Druffel, E. R. M.; Masiello, C. A.; Eglinton, T. I.; Pearson, A.; Reddy, C. M.; Gustafsson, O.; Quinn, J. G.; Hartmann, P. C.; Hedges, J. I.; Prentice, K. M.; Kirchstetter, T. W.; Novakov, T.; Puxbaum, H.; Schmid, H. *J. Res. Natl. Inst. Stan.* **2002**, *107,* 279-298.
91. Cadle, S. H.; Groblicki, P. J. *An evaluation of methods for the determination of organic and elemental carbon in particulate samples* in *Particulate Carbon: Atmospheric Life Cylces.* G. T. Wolff; R. L. Klimisch. **1982**, Plenum Press: New York. 89-108.
92. NIOSH *5040 Elemental Carbon (Diesel particulate).* **1999**, National Institute for Occupational Safety and Health: Washington D.C., 1-9.
93. Chow, J. C.; Watson, J. G.; Crow, D.; Lowenthal, D. H.; Merrifield, T. *Aerosol Sci. Tech.* **2001**, *34,* 23-34.
94. Lin, C. I.; Baker, M.; Charlson, R. J. *Appl. Optics* **1973**, *12,* 1356-1363.
95. Cachier, H.; Bremond, M. P.; Buat-Menard, P. *Tellus* **1989**, *41B,* 379-390.
96. Birch, M. E.; Cary, R. A. *Aerosol Sci. Tech.* **1996**, *25,* 221-241.
97. Heintzenberg, J. *Atmos. Environ.* **1982**, *16,* 2461-2469.
98. Clarke, A. D. *Appl. Optics* **1982**, *21,* 3011-3020.
99. Hitzenberger, R.; Jennings, S. G.; Larson, S. M.; Dillner, A.; Cachier, H.; Galambos, Z.; Rouc, A.; Spain, T. G. *Atmos. Environ.* **1999**, *33,* 2823-2833.
100. Glaser, B.; Haumaier, L.; Guggenberger, G.; Zech, W. *Org. Geochem.* **1998**, *29,* 811-819.
101. Skjemstad, J. O.; Clarke, P.; Taylor, J. A.; Oades, J. M.; McClure, S. G. *Aust. J. Soil Res.* **1996**, *34,* 251-271.
102. Reddy, C. M.; Pearson, A.; Xu, L.; McNichol, A. P.; Benner, B. A.; Wise, S. A.; Klouda, G. A.; Currie, L. A.; Eglinton, T. I. *Environ. Sci. Technol.* **2002**, *36,* 1774-1782.
103. Currie, L. A.; Eglinton, T. I.; Benner, B. A.; Pearson, A. *Nucl. Instrum. Meth. B* **1997**, *123,* 475-486.

CHAPTER 3: THE PRECISION AND ACCURACY OF QUANTIFYING BLACK CARBON IN SEDIMENT USING A THERMAL OXIDATION METHOD

3.1 ABSTRACT

The 375°C thermal oxidation method is re-examined to determine the accuracy and precision of the method in oxidizing labile organic carbon (OC) and isolating black carbon (BC) in sediments samples. Experiments were designed to address concerns of organic matter charring (i.e. creating artifact BC) and the potential oxidation of BC particles. Through additions of natural compounds (such as bovine serum albumin, cellulose, phytoplankton), charring was typically observed in samples containing a high total nitrogen content. A direct correlation between observed charring and a measurable nitrogen residue in the combusted sample suggests that N-containing macromolecules (and the associated carbon) are surviving the 375°C pretreatment by converting to BC. Further studies revealed that charring was significantly minimized by increasing the oxygen accessibility to the carbon surface by either physically grinding the sample to smaller sizes, or chemically dispersing the sample. In general, the 375°C method will underestimate the total BC content of a sediment sample (assuming no charring has occurred) by isolating only a fraction of the large BC particles in a sample and almost none of the relatively small BC particles. To constrain the BC content, a computational model was tested to provide another reasonable estimate of the BC content in sediments by using a combination of endmember thermograms to represent OC and BC oxidation. Overall, the Boltzmann model was able to extract reasonable values (BC/TOC <30%) for the OC and BC contents in several marine sediment samples; however, the model was unable to differentiate between similar carbon fractions, such as fresh OC and degraded OC. Finally, a second model was proposed (but not tested) based on kinetics to discriminate between the different carbon fractions in a sample by varying combustion time and temperature. Although future work is necessary, the models presented here are able to estimate the BC content within 10-30% of the total carbon content for the sediment samples tested.

3.2 INTRODUCTION

Approximately, 10 Tg (Tg = 10^{12} grams) of black carbon (BC; commonly known as soot or char) are emitted annually from fossil fuel combustion and biomass burning [1, 2, 3] and are disseminated by continental runoff and aeolian transport [4]. Because BC is a recalcitrant material [5, 6, 7], these combustion particles will not significantly degrade or oxidize in the water column [8]. Ultimately, this amount of BC will settle into marine sediment beds. Meanwhile, phytoplankton in surface waters produce approximately 50 Pg BC (Pg = 10^{15} grams) of labile organic carbon (OC) annually [9, 10]. Although the majority of this OC is recycled in the upper water column, a small percentage (<0.1%) escapes oxidation and is preserved in marine sediments [9]. Hence, sediment beds act as a passive collector for both BC and OC particles settling through the water column [11, 12, 13].

BC deposited in the oceans may constitute a certain percentage of the total carbon that is measured in marine sediments and particulate organic matter [13]. For example, if 0.1% of the OC produced annually in surface waters were ultimately buried (equaling ≈50 Tg/yr) and if 10 Tg of BC [1, 2, 3] were emitted and buried annually, then BC will comprise about 15% of the total organic carbon (TOC) in marine sediment beds. This estimate is supported by recent reports yielding BC/TOC ratios of 10-20% in marine sediments [14, 15]. (As noted in Chapter 1, BC is a collective term representing thermally altered carbonaceous material. The term OC (or the "non-BC fraction") represents the biogenic/diagenetic carbonaceous material. The sum of these two carbon fractions represents the total organic carbon (TOC) content of a sample.) In addition, Masiello and Druffel proposed in recent work that BC may also constitute 4-22% of the dissolved organic carbon (DOC) pool [16], since DOC is isolated by physical size (<1 μm) not chemical properties during filtration [17]. If sediments include OC and BC, then any bulk carbon measurements, such as C/N molar ratio, TOC weight percentage, or radiocarbon, will have a bias due to the presence of BC. Hence, previous geochemical interpretations of organic matter preservation in sediments (bulk TOC weight percents

used; [9]) and "old" surficial sediment (bulk ^{14}C values used [18]) may possibly be skewed by unknown amounts of BC in their samples.

Accurate BC measurements can correct these bulk carbon measurements by assuming that the labile OC is the difference between TOC and BC – unfortunately, no universally accepted BC method exists. Common BC methods involve removing the labile OC by chemical digestion or thermal oxidation, and then operationally defining the remaining carbon in the sample as BC [7]. However, the inefficient removal of OC can cause an overestimation of the total BC content, while any loss of BC material during a method that involves many manipulations can cause an underestimation of the true BC content. Recently, NIST orchestrated an intercomparison study among 15 international laboratories to measure the BC content in an aerosol standard (NIST SRM 1649a; [19]). Surprisingly, the measured BC weight percentages for this standard varied by almost a factor of 10 with thermal methods giving generally lower BC values than chemical methods. Among the various thermal methods studied, the 375°C thermal oxidation method, which was designed to oxidize labile OC under air within 24 hours [20, 21], consistently yielded the lowest values for the abundance of BC. The results from the NIST intercomparison study suggest that the 375°C thermal oxidation method may be among the best methods for quantifying BC in sediment/soil samples, especially since recent radiocarbon work by Reddy *et al.* has shown that the 375°C thermal method can isolate BC without any apparent interference from OC [22]. However, critics of the 375°C thermal method argue that the method is flawed because the incomplete oxidation of organic matter (i.e., "charring") [23] or the oxidation of some BC particles [24] will affect the measured BC values.

On one hand, "charring" of organic matter, which includes the incomplete removal of TOC and the condensation of TOC to form a resistant carbon material (i.e., Browning reaction), may cause the measured BC values to be too high. For example, Gelinas *et al.* argues that the linear correlation ($R^2 = 0.90$) reported by Middelburg *et al.* [6] for a suite of sediment samples is evidence that the 375°C thermal method is charring (i.e., the more TOC in a sample, the more BC measured) [23]. During a careful

inspection of reported BC data (isolated with the 375°C method), high BC values were consistently observed for sediments, or soils, that contained high total nitrogen (TN). This discovery suggests that N-containing organic material may have a higher potential for charring. For example, the BC content for alpine lacustrine sediments (>10 wt % TOC and >1 wt % TN) ranged from 0.4-0.8 wt % BC, which is exceedingly high for sediment horizons dating back to the turn of the century [25]. Moreover, for the same lacustrine sediment, the patterns in the down core BC profiles mimicked the same patterns observed in the accompanying TN profile [25]. Measured BC values (0.4-0.6 wt % BC) for soils from Australia that were also loaded with organic nitrogen (SS6 contained ≈6 wt % TN; SS7 contained ≈7 wt % TN; [23, 26]) are also suspicious. These high BC values may in fact represent charring of N-containing organic matter.

On the other hand, new work submitted by Nguyen *et al.* suggests that the 375°C thermal oxidation method may actually underestimate the total BC content in samples [24]. They observed that both diesel soots and wood chars (with high H/C molar ratios) are not stable in an oxidizing environment at 375°C over time. Thus, Nguyen *et al.* proposed that the 375°C thermal method would only isolate robust particles, possessing small surface areas and a high degree of carbonization (with low H/C molar ratio). Also, the 375°C method tends to discriminate between BC particles of different sizes. For example, in the work by Jonker and Koelmans, micron-size BC samples were oxidized almost completely at 375°C whereas 70% of a larger 30 μm graphite particle survived the 375°C pretreatment [27]. Hence, while charring of organic matter may overestimate the total BC content, oxidation of small or less robust BC particles may underestimate the total BC content.

Here, the 375°C thermal oxidation method is re-examined to determine the accuracy and precision of the pretreatment to oxidize labile OC and to isolate BC in sediments. To investigate the incomplete combustion of organic matter, charring was encouraged in sediment samples by the addition of various organic compounds. The results suggest that samples amended with large particles, or particles that tend to self-aggregate, will char because of limited oxygen accessibility. However, in the absence of

charring, the 375°C thermal oxidation method will actually underestimate the total BC content of a sediment sample by only isolating a fraction of the large BC particles and none of the relatively small BC particles. As a second approach to estimating the BC content of sediment, a model containing two Boltzmann sigmoidal functions was introduced to describe the oxidation of OC and BC and to extract the total OC content and total BC content of four sediment samples. In general, the Boltzmann model and the 375°C method together provide an estimate of the BC content in a sample assuming no charring.

3.3 METHODS

3.3.1 Black Carbon Measurements. BC is operationally defined here as the reduced carbon content remaining in a sediment sample (g C/g $_{sediment}$) after a 375°C thermal pretreatment. (Descriptions of sediment sites are provided below.) Following this method, less than 200 mg of sediment were spread into pre-combusted ceramic crucibles and were heated at 375°C ±5°C for 24 hours under air in either a Sybron F-A1730 Thermolyne muffle furnace (Dubuque, IA), or a F47915 Barnstead Thermolyne bench top muffle furnace (Dubuque, IA). Samples were also combusted at Woods Hole Oceanographic Institution in a programmable oven (Fisher Scientific IsoTemp) for 24 hours under air at 375°C. The temperature program for this oven included a ramp at 15°C/min to 300°C, hold for 5 min, a second ramp at 5°C/min to 375°C, and a final hold at 375°C for 24 hours. (This temperature program was chosen to minimize the temperature overshoot as the oven approached its targeted temperature.)

3.3.2 Elemental Analysis. The masses (μg) of carbon and nitrogen in both the uncombusted and 375°C-combusted sediment samples were measured with a Perkin Elmer 2400, Series #1 CHN elemental analyzer (Norwalk, CT), and are reported here as weight percentages (wt %). (A further discussion on the CHN elemental analyzer is provided in Appendix A3.1.) Before analysis, sediments were placed in silver capsules (8 x 5 mm; Elemental Microanalysis Limited, MA), were wetted with 50 μL of low-

carbon water (Aries Vaponic, MA), and were acidified with 50 μL sulfurous acid (Fisher Scientific, 6% assay) to remove inorganic carbon. The signal-to-noise ratio was >2:1 for all samples, except nitrogen in the combusted sediment. The instrument detection limit of the CHN analyzer throughout the experiments ranged from 1.6-2.3 μg C and 6.7-7.7 μg N [28]. Instrumental blanks were run after each sample to verify that previous samples were completely combusted. All reported weight percents represent the mean ±1 standard deviation for a given population size (Z).

Elemental abundance (expressed as weight percentages) for carbon and nitrogen were accepted only when standard acetanilide samples were within ±0.3 wt % of the known acetanilide values. The instrument was also calibrated with NIST sediment standards (SRM 1944, NY/NJ Waterway Sediment and SRM 1941a, Marine Organic Sediment) and benzoic acid standard (C_7H_6O). The measured TOC content for SRM 1944 was 4.9 ±0.27 wt % C (Z = 4), which was within error of the accepted mean value of 4.4 ±0.3 wt % C. The measured TOC for SRM 1941a was 4.7 ±0.16 wt % C (Z = 4), which was also within error of the accepted mean value of 4.8 ±1.2 wt % C. (Note that NIST does not provide certified total nitrogen (TN) values for these samples.) The measured weight percents for benzoic acid were 68.86 ±0.08 wt % C, 5.00 ±0.15 wt % H and 0.00 ±0.01 wt % N (Z = 3), which compared well to the theoretical values of 68.85 wt % C, 4.95 wt % H, and 0.00 wt % N. The ability of the CHN to measure no nitrogen in a standard (relative to the blank, i.e., 40 ±3 electronic counts) implies that a sample with a small but reproducible nitrogen signal (i.e., 70 ±5 electronic counts) is different from the blank even though the signal-to-noise ratio is <2:1.

3.3.3 Sediment Samples. Grab samples of surface sediment were collected from Boston Harbor, MA in December 1999 and kept frozen until needed. A sediment core was also retrieved from the Pettaquamscutt River, RI in 1999 (core described elsewhere [29]), and subsamples from five core horizons were generously donated by A. L. Lima, C. M. Reddy, and T. I. Eglinton. Archived sediment samples from Massachusetts Bay (42° 22' 00" N, 70°54' 00" W; collected May 1994) and Wilkinson Basin (42° 38' 00" N 69° 36'

26" W; collected July 1996) were gathered and were defrosted [14]. Lastly, a subsample of Boston Blue Clay was collected from a monitoring well (core section 15-17 feet depth) drilled by Carr-Dee Corporation (Medford, MA). A 5 gram sample from each site was dried overnight at 100°C. The dried sediment samples were then ground with a mortar and pestle to break up sediment clumps and were stored in clean, pre-combusted vials until needed.

3.3.4 Internal Addition Experiments. The TOC and TN contents of the Boston Harbor sediment were increased by more than a factor of 10 with a series of additions with representative organic compounds. After the sediment and organic compounds were manually mixed with a spatula, they were ground together with a mortar and pestle until the added organic matter could no longer be distinguished among the sediment grains. A subsample of the mixture was taken to measure the new TOC and TN contents. The remaining sample was combusted at 375°C for 24 hours to isolate the BC fraction. All correlation coefficients (R^2) and standard deviations ($\pm 1\ \sigma$) for the internal addition experiments were calculated with Microsoft Excel 97.

The following carbonaceous compounds were added to separate aliquots of Boston Harbor sediment: cellulose powder from spruce (Fluka BioChemika, 20-150 μm length fibers), anhydrous D-glucose (Mallinckrodt Analytical), bovine serum albumin (BSA; Fluka BioChemika; MW = 67,000 g/mol), pelletized organic matter from a phytoplankton culture (described below), L-histidine (Avocado Research Chemicals), L-leucine (Avocado Research Chemicals), L-tryptophan (Aldrich Chemical Company), D,L-methionine (Aldrich Chemical Company), L-glutamine (Fluka BioChemika), polyethyleneimine (Alfa Aesar; linear polymer, MW = 25,000 g/mol), and polyglycine (Aldrich Chemical Company; linear polymer, MW = 2,000-5,000 g/mol). Figure 1 provides the chemical structure of the five amino acids and the two polymers tested. For the phytoplankton addition, a stationary-phase *Prochlorococcus* culture was centrifuged for 15 min at 1,325 *g*. (Note that *Prochlorococcus* are a type of cyanobacteria containing photosynthetic pigments.) The organic matter that pelletized in the centrifuge tube was

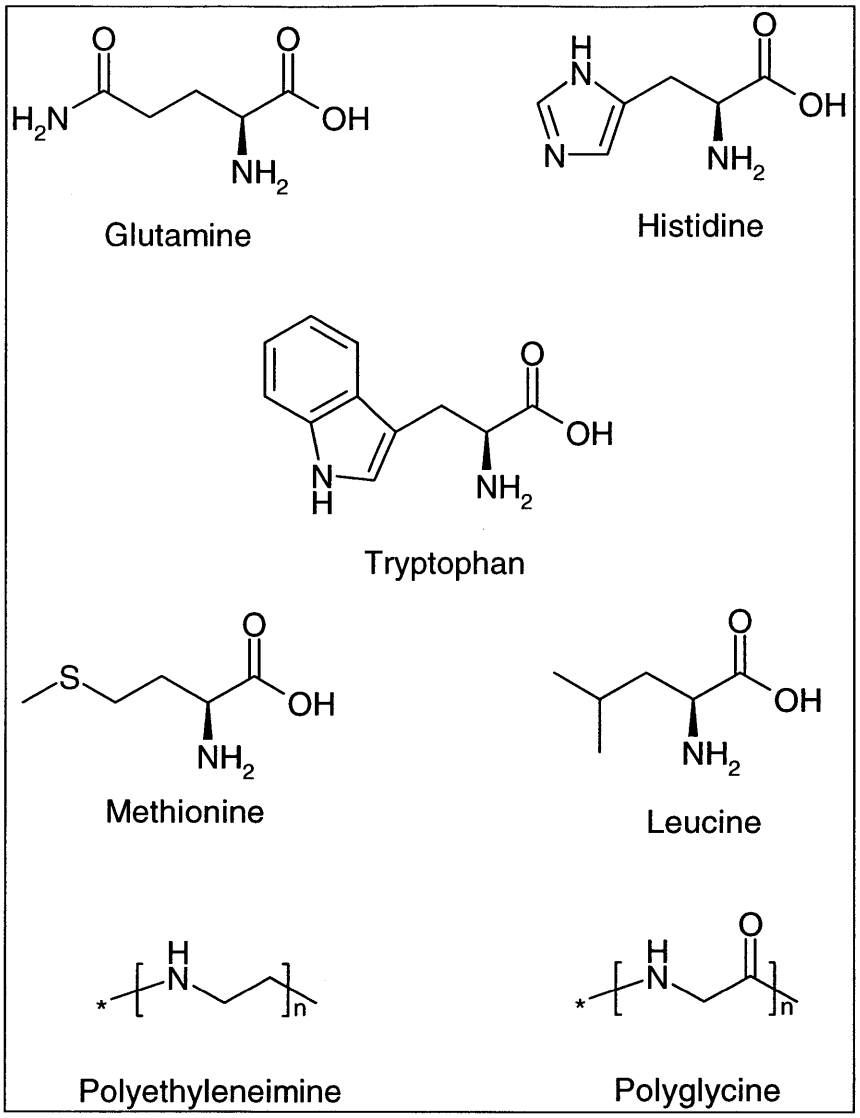

Figure 1: Chemical structure of the five amino acids and two linear polymers added to Boston Harbor sediment.

transferred to an aliquot of Boston Harbor sediment with a pipette. The sample was allowed to dry at room temperature with occasional mixing with a spatula. Then, the mixture was ground with a mortar and pestle.

3.3.4.1 Particle Size. To further investigate the effects of particle size, sodium citrate dihydrate ($Na_3C_6H_5O_7 \cdot 2\ H_2O$; Mallinckrodt Analytical) was ground and sieved through a series of mesh sizes ranging from 40 mesh (425 μm aperture) to 400 mesh (38 μm aperture). A known mass, retained on a given sieve, was mixed with a known mass of Boston Harbor sediment to create a series of internal additions with approximately the same citrate carbon weight percent (TOC = 4.2 ±0.7 wt % C) but varying crystal sizes. This series of additions was then subdivided. One set was combusted at 375°C for 24 hours; another set was wetted with 100 μL of water. After mixing the slurry, the samples were dried at 100°C, samples were ground again with a mortar and pestle, and then combusted at 375°C for BC analysis.

Similar to the sodium citrate experiments other chemicals were sieved and added to separate aliquots of Boston Harbor sediments; the following details explain the variations among the different experiments. (1) Bovine serum albumin (BSA) was ground and sieved through a series of mesh sizes ranging from 120 mesh (125 μm aperture) to 400 mesh (38 μm aperture). A known mass, retained on a given sieve, was mixed with a known mass of Boston Harbor sediment to create a series of additions. The series was subdivided. One set was combusted at 375°C with no manipulations. The second set was wetted with 10 μL of water, dried at room temperature under a N_2 gas stream, ground with a mortar and pestle, and then combusted at 375°C. (2) Unsieved polyethyleneimine, unsieved polyglycine, and unsieved BSA were added to separate aliquots of Boston Harbor sediment. After the samples were divided, the polyethyleneimine was wetted with 10 μL of methanol, polyglycine was wetted with 10 μL hydrochloric acid (12N), and BSA was wetted with 10 μL of water. Mixtures were dried at room temperature under a N_2 gas stream, were ground with a mortar and pestle, and were combusted at 375°C. Note in regards to the polyglycine experiments, technical

support at Sigma Aldrich Company confirmed that at room temperature hydrochloric acid will not hydrolyze the polyglycine. To verify that the acid did not attack other organic material in the sediment, a control experiment (Boston Harbor sediment no additions) was run concurrently. (3) Anthracite coal from the laboratory and metallurgical coke donated from Mid-continent Coal & Coke Company (Cleveland, OH) were sieved through a series of mesh sizes ranging from 40 mesh (425 μm aperture) to 200 mesh (75 μm aperture). A known mass, retained on a given sieve, was mixed with a known mass of Boston Harbor sediment to create a series of additions. The mixtures were not wetted.

3.3.5 Thermograms. Separate aliquots of pre-combusted glass beads (50-70μm diameter) were coated (methods described below) with Aldrich humic acid (H1675-2), pelletized phytoplankton material, or NIST 1650 diesel particulate matter to create a "stock material." Test samples analyzed in the CHN elemental analyzer indicated that the total carbon and nitrogen contents of these stocks were relatively uniform and varied <5%. Other stocks that were created included NIST 1650 mixed with Boston Harbor sediment and chemically extracted Boston Harbor sediment (extraction method discussed below). Subsamples of these stocks as well as sediment samples from Boston Harbor (no additions), Massachusetts Bay, Wilkinson Basin, and Boston Blue Clay were then combusted at a range of temperatures from 100°C to 400°C for 24 hours under air. Combusted samples were then analyzed on the CHN analyzer – results are reported for all samples as the mass of carbon remaining relative to the total carbon content of the stock. For the phytoplankton thermogram, the mass of nitrogen remaining was also reported. To confirm that the added material was dispersed among the glass beads and to approximate the thickness of the material covering the glass beads, subsamples were viewed with a scanning electron microscope (XL30 ESEM FEG; FEI and Philips, OR). The SEM operated with a gaseous secondary electron detector using 5 kV of energy in a depressurized chamber.

To coat the glass beads with humic acid, 48 mg of humic acid were dissolved in 10 mL of a 0.1M potassium hydroxide solution (Mallinckrodt Analytical reagent) in a

glass centrifuge tube. Approximately, 300 mg of glass beads were added to the tube, and the solution was acidified with 10 mL of 6N hydrochloric acid (J. T. Baker Ultra-pure Reagent, NJ) to a pH = 1.5. The precipitating humic material was shaken, and then the tube was centrifuged at 1,430 *g* for 20 minutes. Afterwards, the supernatant (dark yellow indicating the presence of fulvic acids) was removed with a pipette. The humic acid/glass bead mixture was stirred and dried under a N_2 gas stream at room temperature and then was ground with a mortar and pestle to break up clumps. This process created visibly brown beads with a TOC content of 1.1 ±0.1 wt % C.

To coat the glass beads with phytoplankton, a stationary-phase *Prochlorococcus* culture was centrifuged for 20 min at 2,060 *g* in polypropylene centrifuge tubes (Corning Inc., NY). After the supernatant was decanted, the organic matter that pelletized in each centrifuge tube (approximately 1 mL by volume total) was transferred with a pipette to a ceramic crucible containing 300 mg of glass beads. The phytoplankton/glass bead mixture was stirred, dried under a N_2 gas stream at room temperature, and then was ground with a mortar and pestle to break up clumps. This process created visibly green beads with a TOC content of 2.0 ±0.1 wt % C and a TN content of 0.36 ±0.02 wt % N.

To coat the beads with NIST diesel particulate matter, an unknown amount of standard reference material was suspended in ethyl acetate (EM Science, HPLC Grade), and then a 1-mL aliquot of this suspension was transferred to a ceramic crucible containing 300 mg of glass beads. The beads were occasionally mixed as the solvent evaporated off at room temperature in a fume hood. Then, the beads were ground with a mortar and pestle to break up clumps. This process created visibly black beads. The first set of beads had a TOC content of 0.61 ±0.03 wt % C, and a second set had a TOC content of 0.69 ±0.02 wt % C.

To create a thermogram of "BC with sediment," an aliquot of Boston Harbor sediment was mixed with an unknown amount of BC (NIST 1650; diesel particulate matter). This mixture was manually stirred with a spatula and was ground with a mortar and pestle until all the BC clumps were broken and the sediment became visibly black in color. The thermogram for the native sediment (representing only native carbon) was

then subtracted from the thermogram of the BC-added sediment (representing added BC and native carbon). The resulting thermogram represents the oxidation of the added BC.

To create a thermogram of marine organic matter, Boston Harbor sediment was chemically extracted with a mixture of base and hydrogen peroxide [30]. At room temperature, 201 mg of Boston Harbor sediment were mixed with a 10 mL of 4 M potassium hydroxide solution (Mallinckrodt Analytical Reagent) and 2 mL of hydrogen peroxide (EM Science, Assay 30%; Gibbstown, NJ). The mixture was occasionally stirred with a spatula and allowed to react for 1 hour until the hydrogen peroxide bubbling ceased. Afterwards, another 2 mL of hydrogen peroxide were added to the sediment mixture and allowed to react again for ½ hour until the peroxide bubbling ceased. Next, 40 mL of water was added to the centrifuge tube and the mixture was capped and shaken by hand. (The tube was filled with water to prevent sediment from sticking to the sides of the tube.) After centrifuging the sediment (20 minutes at 1,100 *g*), the supernatant was discarded. Again, the tube was filled with 40 mL of water, shaken by hand, and centrifuged. After removing the supernatant, the wet sediment was finally dried in a bench top oven at 100°C overnight. The thermogram for the extracted sediment (representing mostly BC) was then subtracted from the thermogram of the non-extracted sediment (representing BC and OC). The difference represents the thermogram for the oxidation of marine organic matter.

3.3.5.1 Data Analysis. For the constructed thermograms, a Boltzmann sigmoidal function was fitted through the data (e.g. phytoplankton material on beads, humic acid on beads, extracted marine organic, BC on beads, and BC with sediment). The parameters of the Boltzmann function were fitted with SigmaPlot (version 4, Scientific Graphing Software, SPSS Inc.). All reported values represent the best-fit value, ±1 standard deviation error, and the corresponding correlation coefficient (R^2). A model was then constructed using the humic acid thermogram and the BC with sediment thermogram. The model estimated the total OC content and the total BC content from sediment samples using a "preconditioned conjugate gradient" function with MATLAB (version 6.1.0.450 R12.1, The MathWorks, Inc., Natick, MA). All reported values represent the

best-fit value ±1 standard deviation error. (Appendix A3.2 contains the MATLAB code for the model used.) The difference between the model line and the observed thermogram are reported as residuals, which equals the sum of the differences squared.

3.3.6 Kinetic Experiment. An isothermal experiment was conducted at 350°C for incubation times ranging from 15 minutes to 14 hours. Approximately 200 mg of BC-coated beads (0.69 ±0.03 wt % TOC) were spread in eight crucibles, and all eight crucibles were combusted in the Sybron F-A1730 Thermolyne muffle furnace. At a given time, one crucible was removed from the oven, and the carbon content was measured on the CHN analyzer. The surface area was measured on five samples by Porous Materials, Inc. using multi-point Brunauer-Emmett-Teller (BET) analysis with krypton gas (model BET-201A; Porous Materials, Inc. Ithaca, NY). The measured surface area measurements are reported in units of m^2/g_{mass}, and then converted to units of m^2/g_{carbon} with the measured carbon weight percentage. All surface area measurements have a corresponding error of 5%. All kinetics data (rate constant, activation energy, and frequency factor) were calculated with SigmaPlot and are reported as the mean ±1 standard deviation with the corresponding correlation coefficient (R^2).

3.4 RESULTS AND DISCUSSION – PART I: OVERESTIMATING BLACK CARBON CONTENT

3.4.1 BC Measurements in Boston Harbor Sediment. Boston Harbor sediment was combusted with no internal additions (1.3 ±0.1 wt % TOC and 0.10 ±0.01 wt % TN) in the muffle furnace to assess the precision of the 375°C thermal oxidation method. The resulting BC content formed a Gaussian distribution spanning from 0.08 wt % C to 0.17 wt % C with a mean and standard deviation of 0.12 ±0.02 wt % C (Z = 27; Figure 2). A BC/TOC ratio of 9% for this Boston Harbor sediment compared well to other reported BC/TOC ratios (3-15%) for coastal sediments in this region where the same method was used to quantify BC [14].

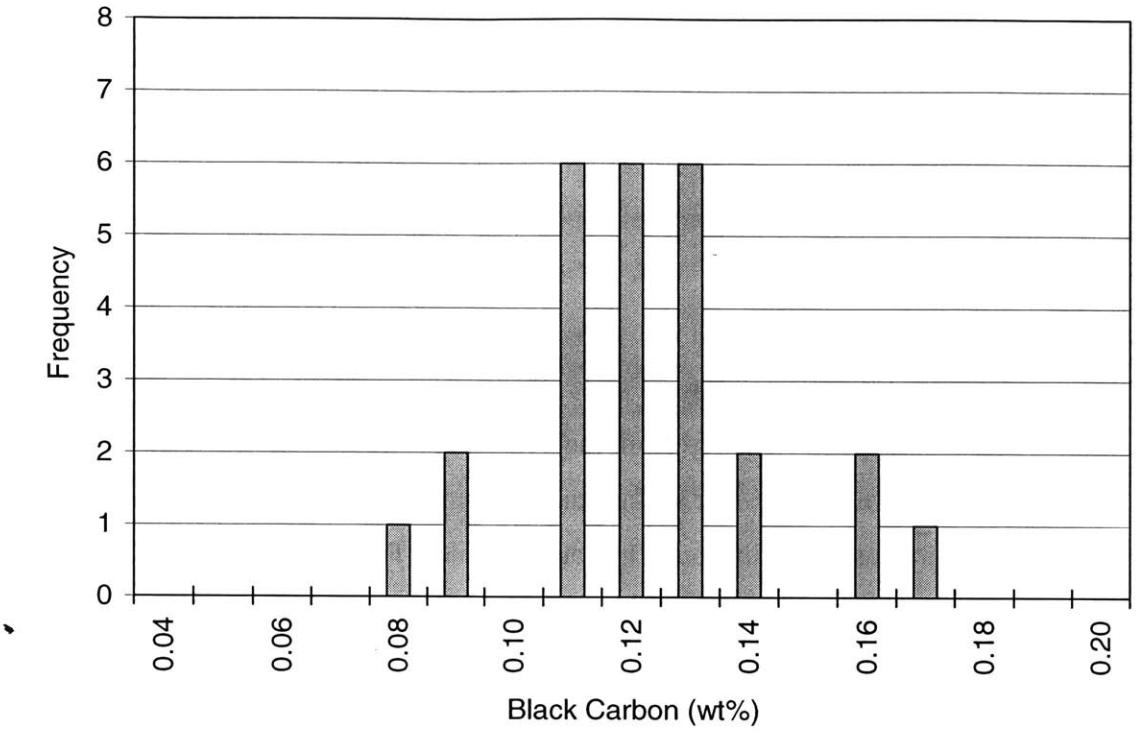

Figure 2: Distribution of measured black carbon (BC) weight percentages (wt %) for 375°C combusted (24 hours) Boston Harbor sediment (no internal additions). Mean value (±1 standard deviation) equals 0.12 ±0.02 wt % C for a population size of 27.

Meanwhile, approximately 20% of the native TN remained after the 375°C thermal oxidation pretreatment with a nitrogen residue in the combusted sediment equaling 0.02 ±0.01 wt % N (Z = 27). This nitrogen residue may represent either the incomplete combustion of organic matter or the nitrogen content of the BC. Although BC materials usually contain nitrogen, a C/N molar ratio of 7 for this Boston Harbor BC is unusually low. For comparison, NIST 1650 diesel particulate matter has a reported C/N molar ratio of 60 ±3 [31], anthracite coal has a measured C/N molar ratio of 81 ±6 (Z = 3), and wood soot has a measured C/N molar ratio of 14 ±4 (Z = 3). However, KOH-H_2O_2-treated Boston Harbor sediment, which should contain non-hydrolyzable organic matter and BC, had a TOC content of 0.58 ±0.07 (Z = 5) and a TN content of 0.02 ±0.01 (Z = 5). Since this residual nitrogen can survive a chemical treatment as well as a 375°C thermal pretreatment, the material could be part of the BC fraction. Therefore, the organic nitrogen content of Boston Harbor sediment is 0.08 ±0.01 wt % N, which corresponds to a C/N molar ratio of 15 ±2, a typical value for degraded organic matter, or a mixture of marine and terrestrial matter [32, 33].

The distribution of BC values for Boston Harbor sample (50% error over ±3 standard deviation) reflects sediment heterogeneity and/or temperature variability in the muffle furnace. Since the Sybron Thermolyne muffle furnace operates with a slow-response thermocouple, the temperature inside the oven varied over a range of 10°C [31]. To confine the variability of the muffle furnace, Boston Harbor sediments (no internal additions) were also combusted in a programmable oven at 375°C. The resulting carbon and nitrogen contents in this combusted sample were 0.13 ±0.01 wt % C (Z = 3) and 0.02 ±0.01 wt % N (Z = 3), respectively, which compared well to the mean values obtained with the muffle furnace.

3.4.2 Potential of Charring Natural Compounds. Tests were conducted with the Boston Harbor sediment to address the concerns that macromolecules may have the potential of charring and may cause a positive bias to the BC measurement. Charring

was encouraged in the Boston Harbor sediment with internal additions of two types of organic compounds: glucose or cellulose and BSA (Figure 3A). One set of sediment samples was amended with carbohydrates and had a low TN content (<0.8 wt % TN); the other set of samples was amended with protein and had a high TN content (>0.8 wt % TN). If combustion were *complete*, then no correlation between the TOC added and the measured BC weight percentage (relative to the native BC concentration of 0.12 ±0.02 wt % C) would be expected. If combustion were *incomplete* (or the condensation of TOC occurred), then BC weight percentages would be expected to be greater than the native BC concentration and to be correlated with the amount of TOC added.

The first set of sediment samples was amended with substantial amounts of glucose or cellulose fibers and minimal amounts of protein (BSA). After a 375°C pretreatment, no correlation ($R^2 = 0.02$) between the added TOC and the measured BC for these samples was observed (filled circles, Figure 3A) with a regression slope statistically equal to zero (0.001 ±0.001). Low correlation coefficients between TOC and BC were also reported in the literature for a suite of standard EPA soil and sediment samples ($R^2 = 0.08$, Z = 12 [15]) and sediments off New England ($R^2 = 0.25$, Z = 15 [14]), which had similar TOC and TN contents as the Boston Harbor sediment. The average BC weight percent for samples having a low TN content (filled circles) equaled 0.13 ±0.03 (Z = 91), which is statistically indistinguishable from the BC content for sediment with no internal addition.

The nitrogen residue was <0.04 wt % N for all the carbohydrate-loaded samples, implying that <3% of the added TN remained after the pre-treatment. Also, test samples containing only cellulose (13 wt % TOC, 0.05 wt % TN) did not char and had a BC content equal to 0.11 ±0.02 (Z = 3; Table 1). Similar results were observed by Gustafsson *et al.* [20] and Nguyen *et al.* [24] who observed that oak wood and natural or synthetic wood chars (with a high H/C molar ratio) were completely oxidized at 375°C. Hence, within the limitations of the analytical techniques, charring in samples with a low TN content cannot be detected, and neither glucose nor cellulose fibers char when ground and mixed with sediment.

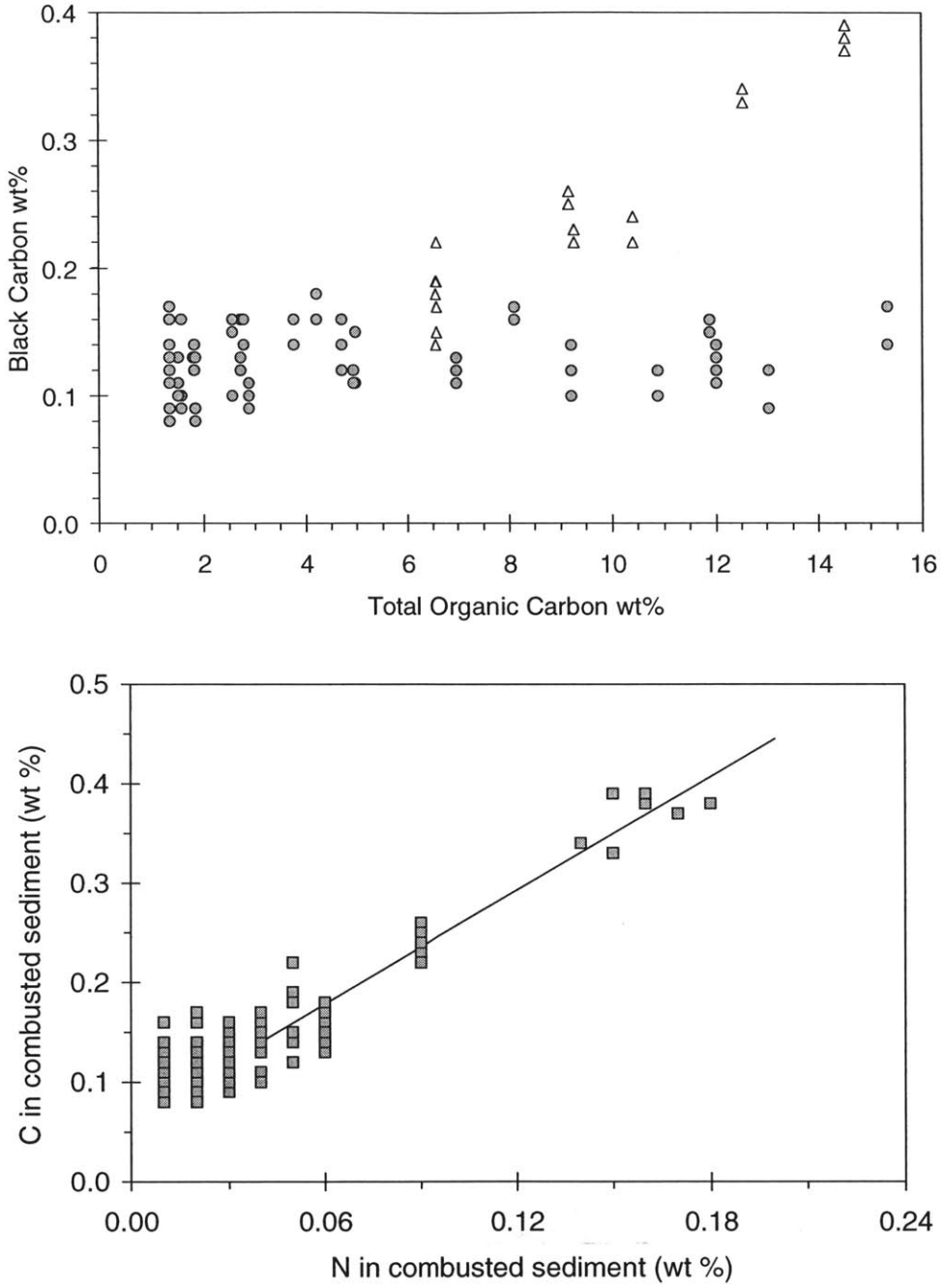

Figure 3: Elemental analysis of combusted mixtures of cellulose or glucose and bovine serum albumin with Boston Harbor sediment (population size = 117). (a) The measured black carbon weight percentage (BC wt %) in 375°C combusted samples versus the total organic carbon weight percentage (TOC wt %). Filled circles represent samples with a low total nitrogen content (<0.8 wt % TN) and open triangles represent samples with a high total nitrogen content (>0.8 wt % TN). (b) Data re-plotted as the carbon content in the combusted samples (wt %) versus the nitrogen residue in the combusted sample (wt %). The regression line ($y = 1.904\ x + 0.0643$) is fitted at the point where the nitrogen residue is >0.04 wt % N.

Table 1: Carbon and nitrogen elemental analysis (reported as weight percent; mean ±1 standard deviation) for mixtures of organic compounds with Boston Harbor sediment both before and after a 375°C thermal oxidation. [a]

Sample	Dry Powder / Combust		Dissolve / Combust	
	C wt %	N wt %	C wt %	N wt %
Control – no additions 1.3 wt % TOC, 0.10 wt % TN	0.13 ±0.01	0.02 ±0.01	0.12 ±0.01	0.02 ±0.01
Cellulose 13 wt % TOC, 0.05 wt % TN	0.11 ±0.02	0.01 ±0.01	N/A	N/A
Cellulose & Bovine serum albumin 10 wt % TOC, 1.1 wt % TN	0.23 +0.01	0.09 +0.01	N/A	N/A
Cellulose & Bovine serum albumin 11 wt % TOC, 0.29 wt % TN	0.11 +0.11	0.03 +0.01	N/A	N/A
Bovine serum albumin, Test #1 6.4 wt % TOC, 1.7 wt % TN	0.37 ±0.02	0.15 ±0.01	0.13 ±0.02	0.02 ±0.01
Bovine serum albumin, Test #2 6.4 wt % TOC, 1.7 wt % TN	0.32 ±0.03	0.16 ±0.01	0.11 ±0.02	0.04 ±0.01
Phytoplankton 9.9 wt % TOC, 1.9 wt % TN	1.05 ±0.05	0.25 ±0.01	0.59 ±0.03 *	0.18 ±0.01 *
Polyethyleneimine 8.3 wt % TOC, 3.8 wt % TN	0.13 ±0.00	0.04 ±0.01	0.14 ±0.01	0.03 ±0.01
Polyethyleneimine 7.5 wt % TOC, 3.3 wt % TN	0.14 ±0.00	0.04 ±0.01	0.11 ±0.00	0.03 ±0.00
Polyethyleneimine 5.2 wt % TOC, 2.1 wt % TN	0.14 ±0.01	0.06 ± 0.01		
Polyglycine 5.4 wt % TOC, 2.3 wt % TN	0.47 ±0.01	0.28 ±0.01	N/A	N/A
Polyglycine 3.5 wt % TOC, 1.3 wt % TN	0.28 ±0.01	0.14 ±0.01	N/A	N/A
Polyglycine 2.4 wt % TOC, 0.7 wt % TN	0.19 ±0.02	0.10 ±0.01	0.12 ±0.00	0.06 ±0.01

a: Column 1 provides the measured total organic carbon (TOC wt %) and total nitrogen (TN wt %) contents (approximately 5% error on TOC and TN values) of the uncombusted sample. Column 2 provides the carbon and nitrogen contents for the powder/sediment mixtures after being combusted at 375°C for 24 hours under air. Column 3 provides the carbon and nitrogen content for samples that were first dissolved, dried at room temperature, and then combusted at 375°C for 24 hours under air.

The second set of sediment samples had the opposite configuration of organic compounds, containing minimal amounts of carbohydrates, but substantial amounts of protein as denoted by their high TN content. Unlike previous experiments, samples with a high TN content had a strong correlation ($R^2 = 0.93$) between the TOC added and the BC measured (open triangles, Figure 3A). Among the various samples tested, the most intense charring occurred for a cellulose/BSA sample containing 15 wt % TOC and 1.6 wt % TN. After combustion, this sample had a BC content of 0.38 ±0.03 wt % C, which was 3 times greater than the BC content in the control. Gelinas *et al.* also observed that a mixture of BSA and glucose (no sediment carrier) charred, yielding a BC/TOC ratio of 5% [23].

Upon closer inspection of the data, the incomplete combustion of carbon was correlated with the incomplete combustion of nitrogen, suggesting that BSA, not the carbohydrates, was surviving the 375°C pretreatment. For example, it was observed that for a given pair of experiments with similar TOC content (Table 1), the sample with the higher TN content charred. The nitrogen residue in this charred sample was 3 times greater than the residue in the corresponding paired sample that had a lower TN content. Residues of nitrogen in the combusted sediments were observed for all samples with high TN content relative to the control (Figure 3B; further discussed below). This nitrogen residue may represent either the remnants of BSA, or a melanoidin that formed from the condensation of carbohydrates and protein at high temperatures. However, Gustafsson *et al.* reported that <1% of their synthetic melanoidin remained after the 375°C pretreatment [21]. In addition, since the experiments did not involve acid and further experimentation revealed that the combustion of BSA alone led to charring (Table 1), the nitrogen residue probably does not represent a melanoidin, but some form of condensed BSA remnants.

The same charring phenomenon (a correlation between high BC values and samples that had a high TN content) was also observed with the addition of pelletized organic matter from phytoplankton to Boston Harbor sediment. For example, a phytoplankton/sediment mixture containing 9.9 wt % TOC and 1.9 wt % TN charred significantly with 11% of the added carbon remaining after the pretreatment (Table 1).

Both Gelinas *et al.* [23] and Gustafsson *et al.* [21] also observed that phytoplankton charred, and they reported BC/TOC ratios for their phytoplankton residues as 7% and 20%, respectively. In the combustion residues from the phytoplankton-amended samples, the BC content was 9 times larger than the control with no internal addition, and the nitrogen residue was 12 times larger than the control, corresponding to the survival of 14% of the added TN. The detection of nitrogen in the combusted samples not only signals charring, but also implies that other N-containing macromolecules besides BSA will char. Interestingly, phytoplankton tended to char more than the BSA/carbohydrate mixtures. For example, the above phytoplankton mixture can be compared with a BSA/carbohydrate mixture containing 10 wt % TOC and 1.1 wt % TN (Table 1). Although the two mixtures have a similar elemental composition before combustion, the phytoplankton mixture charred 5 times as much as the BSA/carbohydrate mixture and the residue contained 3 times more nitrogen.

A substantial nitrogen residue was also detected in the combusted sediment samples from the Pettaquamscutt River [29], suggesting that the measured BC values may overestimate the true BC content in these samples. For example, the average nitrogen residue in the combusted sediment from Pettaquamscutt was 0.11 ±0.02 wt % N (Z = 10) down core (Figure 4A). Moreover, uniformly high BC values (0.62 ±0.10 wt % C, Z = 10) that do not co-vary with the reported PAH profile [28], especially in sediment horizons dating to the pre-industrial era [29], suggest that the organic matter in the Pettaquamscutt sediment charred (Figure 4B). Although, high BC values for sediments were reported for alpine lacustrine sediments [25], these BC values may reflect, as noted before, the charring of N-containing macromolecules. Hence, (1) samples with high TN content have a strong potential of charring, and (2) the presence of a nitrogen residue in combusted samples may serve as a useful indicator of the incomplete combustion of N-containing macromolecules.

3.4.3 Why Do Proteins Char? The existence of nitrogen in the residues from combustion at 375°C implies that N-containing macromolecules, such as BSA, are

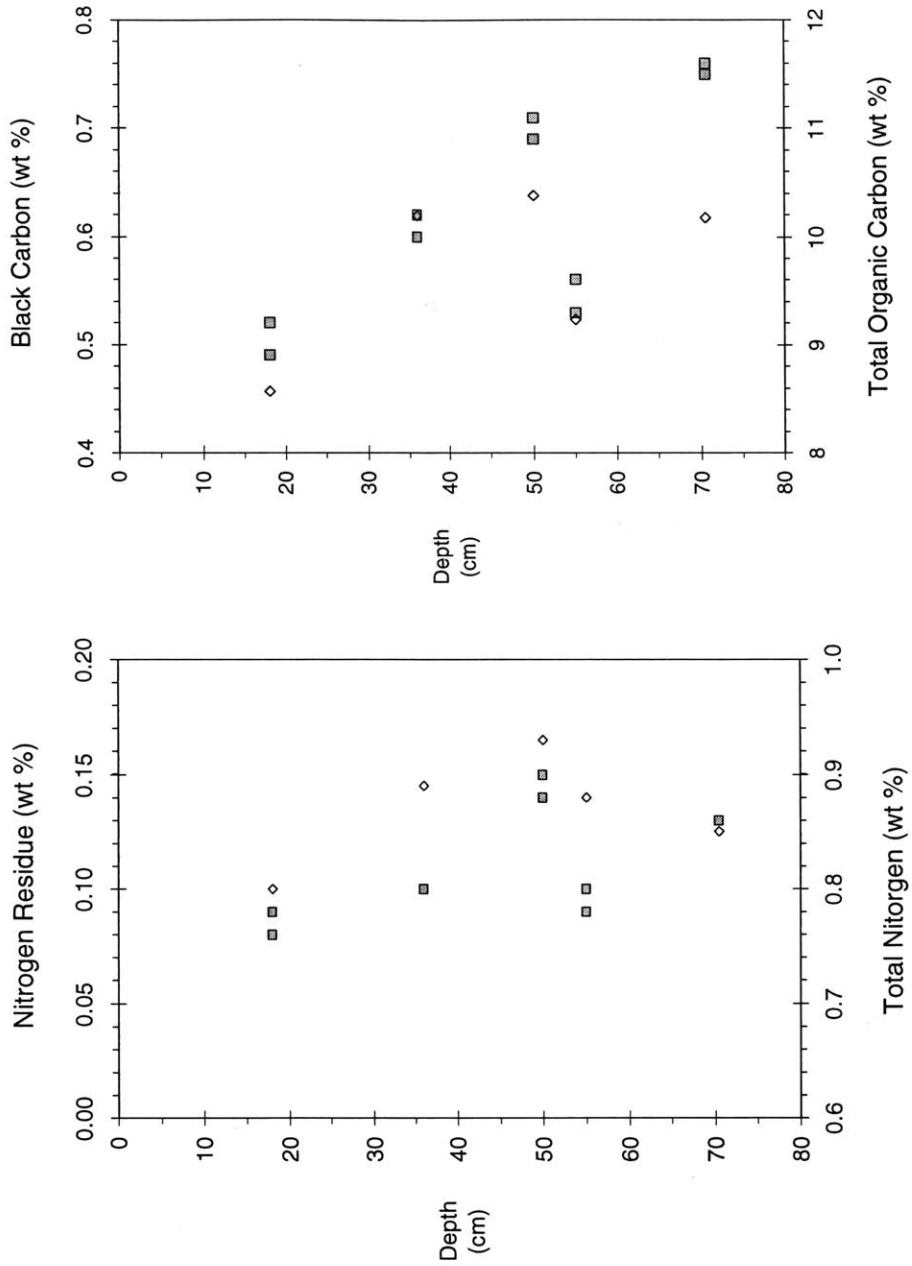

Figure 4: Depth profiles of elemental analysis for a core from the Pettaquamscutt River, RI. (a) The measured total organic carbon content (TOC wt %; open diamonds) and measured black carbon content (BC wt %; filled squares) in the 375°C combusted samples versus depth (cm). (b) The measured total nitrogen content (TN wt %; open diamonds) and measured nitrogen residues (N wt %; filled squares) in the 375°C combusted samples versus depth (cm).

remaining after this thermal pretreatment. Two explanations for the persistence of protein over cellulose in the samples are: (1) organic nitrogen may not be susceptible to oxidation at 375°C and/or (2) the structure of protein (either the size or packaging) may restrict oxygen access causing the incomplete combustion or condensation of organic matter.

3.4.3.1 Chemical Perspective. In proteins, nitrogen (and the associated carbon) can originate from the functional R-side groups of amino acids or from the backbone of the polypeptide (i.e., amide bond). Work in pyrolysis mass spectrometry has already shown that R-side groups form the dominant fragments during protein cracking [34, 35]. If the nitrogen-containing side groups can survive pyrolysis, then these fragments may survive a 375°C pretreatment and cause a bias to the BC measurement. To test the first hypothesis that the nitrogen residue reflected the survival of N-containing side groups, tryptophan, histidine, and glutamine (Figure 1) were tested. In addition, the charring potential of leucine, which is known to re-arrange and form stable dimers, and methionine, which is known to form methanethiol during pyrolysis [34, 35], were investigated. Interestingly, the internal addition experiments for these five amino acids indicated no charring relative to the control (Table 2). For example, the BC content for these five amino acids mixtures was 0.13 ±0.03 wt % C (Z = 34). No nitrogen in the combusted samples (0.03 ±0.01 wt % N, Z = 34) relative to Boston Harbor sediment also implies that N-containing side groups were susceptible to the 375°C thermal oxidation.

The second hypothesis was that the nitrogen residue in combusted sediments originated from the amide bonds in the polypeptide backbone. Johnson *et al.* previously proposed that polypeptides could survive pyrolysis by radical crosslinking or enolization/dehydration reactions. They even reported the presence of amide linkages in polypeptide residues using infrared spectroscopy [36]. To begin addressing the hypothesis that the polypeptide backbone was surviving the 375°C method, the data presented in Figure 3A was re-arranged and the nitrogen residue in the combusted sediment was plotted versus the BC content (Figure 3B). A regression line was fit at the point (0.04 wt % N) where the nitrogen residue became greater than the nitrogen content

Table 2: Carbon and nitrogen elemental analysis (reported as weight percent; mean ±1 standard deviation) for mixtures of amino acids and cellulose with Boston Harbor sediment both before and after a 375°C thermal oxidation. [a]

Sample	Uncombusted Sample		Combusted Sample	
	TOC wt %	TN wt %	C wt %	N wt %
Glutamine	3.6 ±0.2	1.2 ±0.06	0.13 ±0.02	0.02 ±0.01
	7.3 ±0.4	2.9 ±0.15	0.10 ±0.02	0.03 ±0.01
Tryptophan	6.0 ±0.3	1.0 ±0.05	0.14 ±0.02	0.02 ±0.00
	18 ±0.9	3.7 ±0.19	0.14 ±0.01	0.03 ±0.00
Methionine	4.1 ±0.2	0.74 ±0.04	0.14 ±0.01	0.02 ±0.01
	13 ±0.7	2.8 ±0.14	0.11 ±0.00	0.02 ±0.01
Histidine & Cellulose	13 ±0.7	1.8 ±0.09	0.12 ±0.01	0.02 ±0.01
	11 ±0.6	5.6 ±0.28	0.13 ±0.00	0.05 ±0.00
Leucine & Cellulose	10 ±0.5	1.8 ±0.09	0.13 ±0.01	0.02 ±0.01
	16 ±0.8	1.4 ±0.07	0.11 ±0.01	0.03 ±0.01

a: Column 2 provides the total organic carbon (TOC wt %) and the total nitrogen (TN wt %) contents of the uncombusted mixtures (added amino acids were not sieved). Column 3 provides the carbon and nitrogen contents of the mixtures after a 375°C combustion for 24 hours under air.

of combusted Boston Harbor sediment (no internal additions). Remarkably, the slope of this regression line had a C/N molar ratio of 2.2 ±0.1 (R^2 = 0.92) – suggesting the 2:1 carbon:nitrogen sequence in the polypeptide backbone.

To investigate further the possible survival of the polypeptide backbone, mixtures of polyglycine and polyethyleneimine with Boston Harbor sediment were prepared. Both polymers are linear and contain the same 2:1 carbon:nitrogen backbone as BSA; however, polyglycine contains amide bonds while polyethyleneimine does not (Figure 1). Unlike BSA, no charring was observed with polyethyleneimine additions to the Boston Harbor sediment (Table 1). The BC content in the combusted polyethyleneimine samples ranged from 0.13-0.15 wt % BC (Z = 4), which compared well to the control experiments that contained no internal additions. However, trace amounts of nitrogen residue (<0.06 wt % N) were detected in the combusted samples and remain a concern that charring is still occurring (discussion continues below). On the contrary, the polyglycine additions did char and combusted samples contained measurable amount nitrogen residue (Table 1). For example, approximately 10% of both the added carbon and nitrogen remained after the 375°C pretreatment for a polyglycine/sediment mixture that originally contained 5.4 wt % TOC and 2.3 wt % TN. Moreover, similar to the BSA experiments, the C/N molar ratio in the combusted polyglycine samples was 1.8 ±0.2 (R^2 = 0.99, Z = 3) – suggesting that the amide bonds continued to preserve the 2:1 carbon:nitrogen sequence during the 375°C thermal oxidation.

The evidence presented here strongly suggests that the amide bonds in BSA and polyglycine could explain why these two compounds char. However, while polyglycine is a linear polymer, the compound was received from the chemical company as tight, globular balls as opposed to a dissolved solution. Not only were these polyglycine balls difficult to grind, they were insoluble in water and many organic solvents including: acetonitrile:methanol (60:40 v/v), methanol, acetone, ethyl acetate, dichloromethane, hexane, and acetic acid. These observations introduces the possibility that polyglycine was charring not because of the chemical integrity of the amide bond, but because of the physical packaging of the polymer. The amide bond may contribute to this packaging by

causing the protein to coil in a particular fashion that isolates the polar groups from the nonpolar groups, thus hindering oxygen accessibility. The same physical phenomena could explain the charring of BSA. Furthermore, Gelinas *et al.* argues that polypeptide can survive oxidation because oxygen cannot access the organic matter embedded in mineral pores causing incomplete combustion [23]. Although the added BSA is not embedded in pores, oxygen accessibility (not availability) is still an issue since BSA exists as an aggregated powder. The restrictive packaging of BSA and polyglycine can easily restrict oxygen inside these polypeptides and cause charring.

3.4.3.2 Physical Perspective. To further address oxygen accessibility, sodium citrate, a nitrogen free organic salt, was used. The sodium citrate experiments were unique because the total amount of citrate carbon in the pre-combusted sample was the same in each experiment; the only variable was crystal size. If oxygen accessibility is contributing to charring, then relatively smaller citrate particles should be more susceptible to oxidation than larger citrate particles. Consequently, more carbon surviving the 375°C pretreatment should be observed for relatively large particles. As predicted, the percentage of added citrate carbon remaining after the pretreatment decreased with decreasing crystal size (Figure 5A). (See Appendix A3.3 for a complete listing of elemental data.) For example, 37% of the added citrate carbon remained for the 425-250 μm crystals while 2% remained for the 53-38 μm crystals. Moreover, no charring was detected in samples containing crystals <38 μm, suggesting that oxygen was more accessible to these smaller crystals, and citrate was completely oxidized.

Similar trends were observed after sieving the BSA powder and mixing the different size fractions with Boston Harbor sediment. As the size of the BSA decreased from >125 μm to <38 μm, the percentage of added carbon and nitrogen that survived 375°C decreased (Figure 5B). For example, the amount of carbon remaining after the 375°C treatment decreased from 13% to 4% in the size range tested while the nitrogen decreased from 25% to 8% in the size range tested. Unlike the sodium citrate experiments, however, the charring of BSA was not eliminated at particle sizes <38 μm. The greater persistence of nitrogen over carbon at all size ranges indicates that for a given

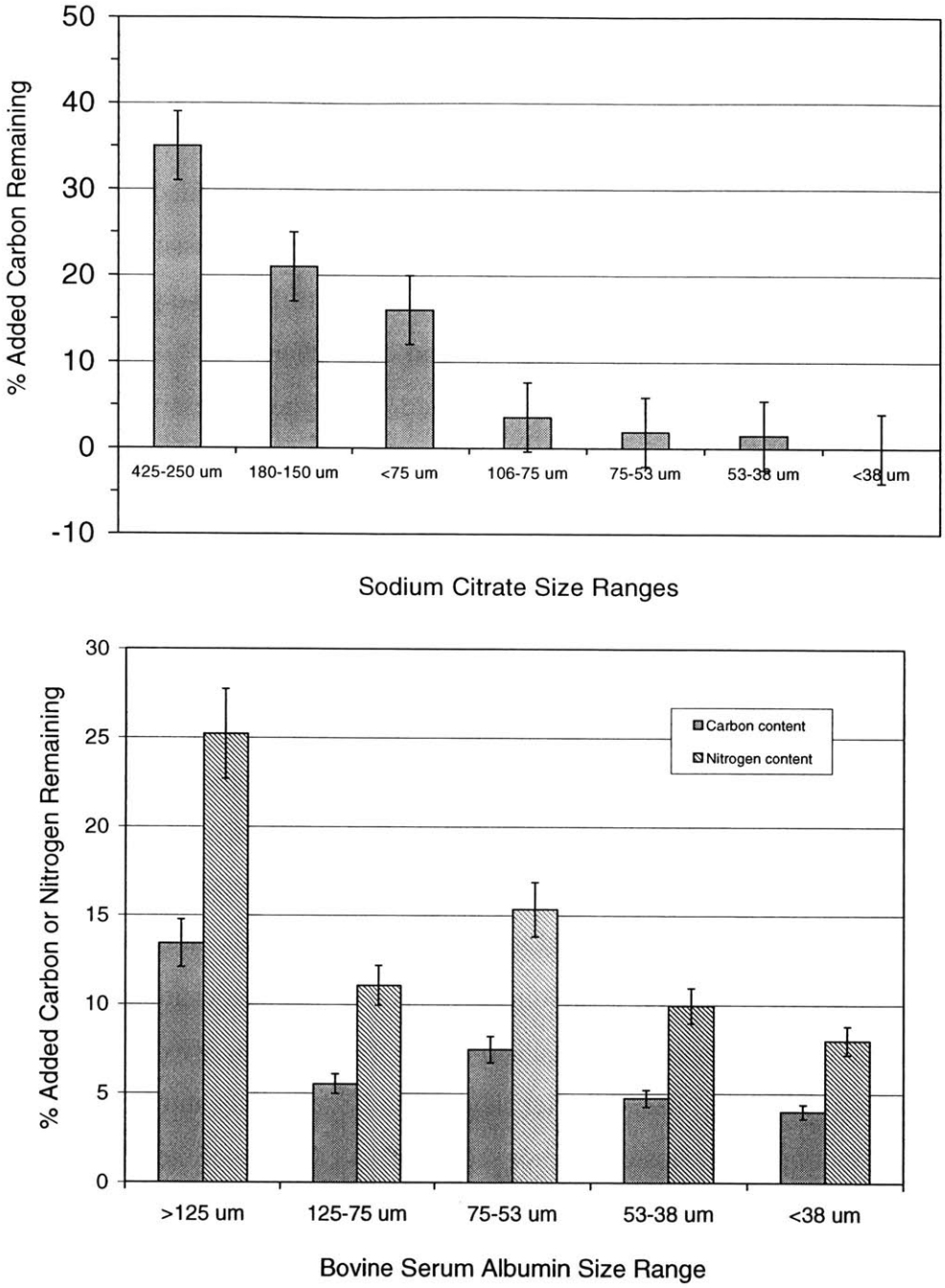

Figure 5: (a) The percent of added carbon remaining after a 375°C thermal oxidation versus particle size (>425 μm to <38 μm) for mixtures of sodium citrate crystals and Boston Harbor sediment. (b) Percent of added carbon and added nitrogen remaining after a 375°C thermal oxidation versus particle size (>125 μm to <38 μm) for mixtures of bovine serum albumin powder and Boston Harbor sediment. (Data corresponds to Appendix A3.3).

particle size, nitrogen is less susceptible to oxidation than carbon. This observation is not unexpected since nitrogen oxide formation is less favorable than carbon dioxide formation, especially at low combustion temperatures [37]. For example, the free energies of formation for nitric oxide and nitrogen dioxide at 600K (or 327°C) are +82.8 kJ/mol and +70.2 kJ/mol, respectively, while the free energy of formation for carbon dioxide at 600K is -395.1 kJ/mol [38]. In other words, the presence of an amine bond opposed to a methyl bond will make the combustion of N-containing compound less favorable. For example, the complete combustion of propanic acid (CH_3CH_2COOH) to carbon dioxide at 600K generates 1,366 kJ/mol. However, the combustion of glycine (NH_2CH_2COOH; note the replacement of one methyl bond with an amine bond) to carbon dioxide and nitric oxide releases only 927 kJ/mol – a difference of 439 kJ/mol ([39] and personal communication with Jeffrey Dick at University of California at Berkeley).

In an effort to decrease the BSA size further in order to eliminate charring, BSA was dissolved in water at room temperature, allowing the organic compound to disperse among the mineral grains and organic matter of the Boston Harbor sediment. If oxygen accessibility is the key in determining what material can survive the 375°C thermal method, then dispersing the organic matter should reduce charring. Remarkably, this simple dissolution step eliminated charring in the BSA samples! For example, a BSA/sediment mixture (6.4 wt % TOC and 1.7 wt % TN) was originally reported to char by a factor of 3 due to the 375°C combustion (Table 1). However, once the BSA was dispersed among the sediment grains, no charring was detected in the combusted sample, with an average BC content equal to 0.12 ±0.02 wt % C and a nitrogen residue ≤0.04 wt % N (Table 1). As an aside, it was observed that these dissolution experiments were not successful if the volume of water were greater than the volume of solids. These observations suggest that as the water evaporates, the BSA will re-aggregate at the air-water interface. On the contrary, if the water volume is less than the solids, then the BSA probably disperses among the sediment grains before re-aggregating.

Similarly, for the sodium citrate experiment discussed previously, charring was eliminated by first dissolving the sodium citrate in water and then proceeding to combust the samples. Even the 250 μm citrate crystals that charred previously (37% of added carbon remaining) showed little evidence of charring after dissolving the sodium citrate crystals (0.15 ±0.05 wt % BC). (See Appendix A3.3 for complete data tables of dissolution experiment.) Furthermore, the nitrogen residue that persisted in the combusted polyethyleneimine samples was minimized by first dissolving the polymer in methanol and dispersing the polymer among the sediment grains (Table 1). In addition, the charring in the polyglycine sample (2.4 wt % TOC and 0.7 wt % TN) was reduced when the polymer was first dissolved in hydrochloric acid at room temperature. However, trace amounts of nitrogen (≤0.06 wt % N) persisted in the combusted sample (Table 1), which could possibly reflect the continuing difficulty of oxidizing nitrogen over carbon.

Limited oxygen accessibility may explain literature reports of waxy corn pollen charring (BC/TOC of 28-82% [20]) as well as vitamin B1 charring (BC/TOC = 3.7% [21]) since vitamin B1 is typically sold as an organic salt (thiamine hydrochloride; Sigma Aldrich, MO). Although not tested, other problematic matrices may include sediments containing reduced solids and sulfur-rich sediments. The precipitation of authigenic minerals and/or reduced solids in sediment beds may magnify charring because these minerals may encapsulate organic matter and further restrict oxygen accessibility [23, 40]. Vulcanization (the incorporation of sulfur into organic matter to produce a refractory biomacromolecule [41, 42, 43]) and aromatization (the transformation of saturated bonds to unsaturated bonds in the presence of sulfur [44, 45, 46]) processes may also contribute to charring in sulfur-rich sediments. Refractory organic matter containing sulfur-linkages may be resistant to the 375°C pretreatment. The incomplete combustion of sulfur-containing organic matter may cause an overestimation in the measured BC content. In addition, elemental sulfur present in sediments during the 375°C pretreatment may also react with steroid hydrocarbons in the sediment and may produce aromatic macromolecules. This aromatic macromolecules could then survive the pretreatment and

cause a positive bias in the BC measurement. For example, Abbott *et al.* observed that the aromatization of a steroid hydrocarbon (mixed with sediment) increased (from monoaromatic to triaromatic) in the presence of elemental sulfur when heated to temperatures >250°C [44]. Although sulfur-rich sediments may char, Middelburg *et al.* did not observed any unusually high BC contents (measured with the 375°C method) in sediment from an anaerobic, sulfide-rich basin of the Black Sea [6]. For example, the BC/TOC ratio for these sulfur-rich sediment was 15-18% (Z = 5), which were among the lowest values measured in their study (BC/TOC ratios ranged from 13-61% (Z = 33), average ratio = 27% ±12%[6]).

3.5 RESULTS AND DISCUSSION – PART II: UNDERESTIMATING BLACK CARBON CONTENT

3.5.1 Potential Black Carbon Oxidation. Since oxygen accessibility appears to be the key ingredient in determining what material can survive the 375°C thermal method, BC particles could be susceptible to our pretreatment if oxygen becomes more accessible to the carbon surface. In other words, similar to our sodium citrate experiments, smaller BC particles could potentially oxidize while larger BC particles could potentially survive the 375°C pretreatment. Under these conditions, the 375°C method may underestimate the total BC content of a sample by only quantifying the larger BC particles. For example, in this work, small metallurgical coke and anthracite coal particles were more susceptible to oxidation than larger particles (Figure 6). Although 85 ±12% of the total carbon for >425 μm anthracite coal particles survived the 375°C oxidation, only 31 ±5% of the total carbon remained for the <75 μm anthracite particles. Similar results were observed by Nguyen *et al.* with activated carbon particles (Aldrich Chemical Company). Compared to the larger activated carbon particles (1,700-4,750 μm) where 36 ±6.7% of the total carbon survived a 375°C oxidation, only 21 ±0.6% of the total carbon remained for the smaller 38-75 μm particles [24].

Furthermore, as noted by Nguyen *et al.* [24], BC particles with a higher degree of

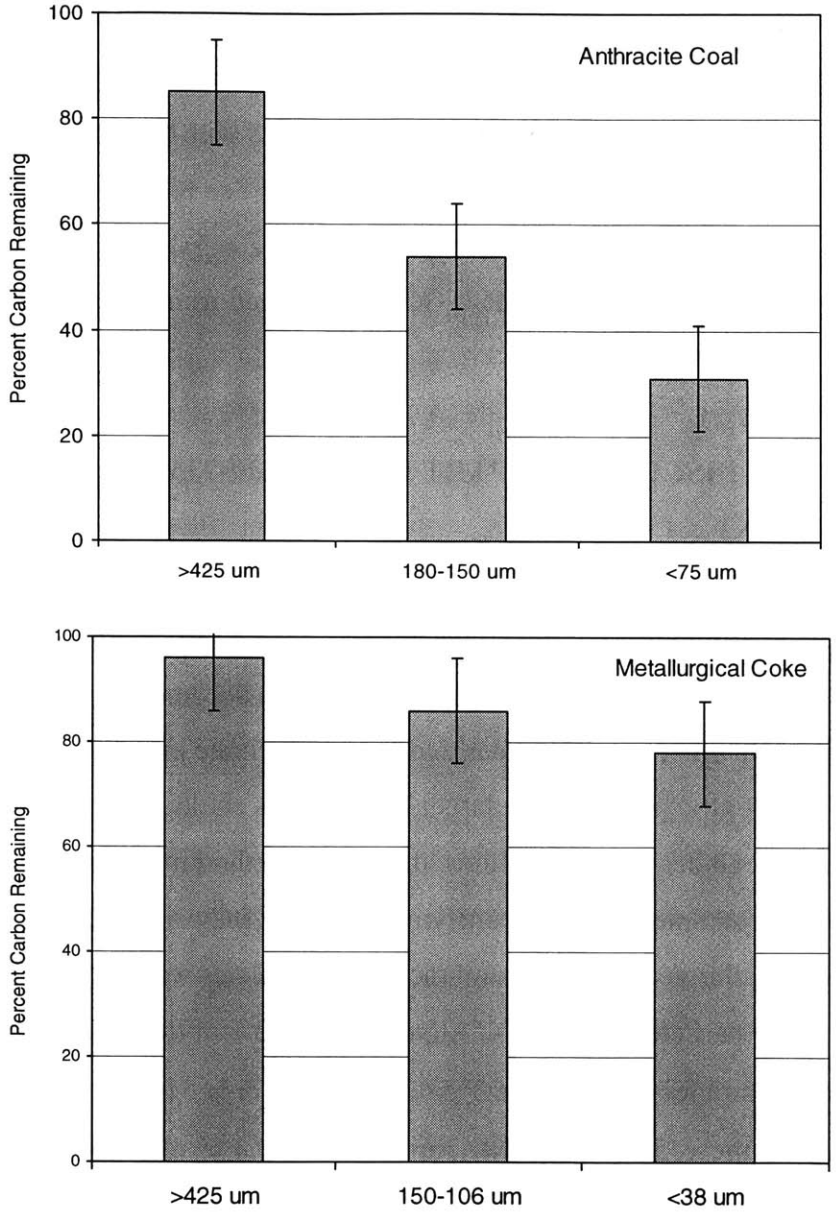

Figure 6: (a) The percent of added carbon remaining after a 375°C thermal oxidation versus particle size (>425 μm to <57 μm) for mixtures of anthracite coal particles and Boston Harbor sediment. (b) Percent of added carbon remaining after a 375°C thermal oxidation versus particle size (>425 μm to <38 μm) for mixtures of metallurgical coke and Boston Harbor sediment.

carbonization (or a lower H/C molar ratio) have a higher potential of surviving a 375°C pretreatment than less carbonized BC particles. For example, metallurgical coke with a H/C molar ratio of 0.29 ±0.06 was observed to be more resistant to oxidation than anthracite coal with a H/C molar ratio of 0.50 ±0.10 (Figure 6). These results are expected since "metallurgical coke" is a high-grade fuel obtained by partially burning coal to produce a solid that burns at a higher temperature than coal (personal communication with D. Joyce Jr., Mid-Continent Coal and Coke Company, Cleveland, OH). Although 31 ±5% of the total anthracite carbon survived our 375°C pretreatment (<75 μm particles), 78 ±11% of the total coke carbon remained (<38 μm particles), suggesting that both particle size and the degree of carbonization will determine which BC particles will survive the 375°C thermal method.

To further explore the oxidation potential of relatively small BC particles, we began to research the oxidative potential of diesel particulate matter (SRM 1650). This BC material is the same reference material used earlier by Gustafsson *et al.* to establish the 375°C thermal method [20]. Although diesel soot is initially formed as a sub-micron particle, soot particles tend to coagulate into clumps on the order of millimeter size. These clumps may hinder carbon oxidation by restricting oxygen diffusion. As a method check, the BC standard was first combusted with no manipulations, resulting in 53-62% of the BC surviving the thermal pretreatment. Similar results were observed in other laboratories that used the same 375°C method and the same BC reference material. Jonker and Koelmans [27] reported a 48% survival of this soot standard, Gelinas *et al.* [23] reported a 50% survival, Nguyen *et al.* [24] reported a 59% survival, and Bucheli and Gustafsson [47] reported a 62% survival. Previously, researchers attributed the observed loss of carbon (40-50% of the total carbon content) to the oxidation of an oily coating on the soot [21, 23].

If oxygen accessibility is the key in determining what material can survive the 375°C thermal method, then a smaller percentage of BC material should survive the 375°C method once the clumps of soot are broken down to yield smaller particles. As suspected, when the BC standard was manually mixed with Boston Harbor sediment

(thus breaking the millimeter clumps to micrometer size), only 22 ±2% of the added BC survived the 375°C oxidation, which is significantly less than previously reported recoveries (black squares, Figure 7). Although an oily coating might exist on this BC standard, which may contribute to some loss of carbon during oxidation, a more likely scenario is that BC oxidation is restricted when soot exists in clumps or packed in capsules. Under these restrictive conditions, only the outer carbon materials will oxidize, allowing the rest of the BC material to survive the 375°C pretreatment. In the experiments presented here, the BC is spread out among the sediment grains, allowing more oxygen accessibility to the BC surface and thus more carbon oxidation.

3.5.2 Thermograms for Black Carbon and Organic Carbon. The percentage of BC remaining after a 24-hour oxidation was tested for a range of temperatures using our BC/sediment mixture (black squares, Figure 7; Appendix A3.4). For temperatures between 250°C and 400°C, a smaller percentage of the added BC standard survived the pretreatment than observed by Gustafsson *et al.* (open squares, Figure 7). These results continue to support the hypothesis that oxygen accessibility is key in determining what material can survive a 24-hour pretreatment. In an effort to characterize these thermograms better, a Boltzmann sigmoidal function was fitted through the data (Eq. 1).

$$Percent\_Carbon\_Remaining = Bottom + \frac{Top - Bottom}{1 + \exp\left(\frac{T - V}{Spread}\right)} \qquad (1)$$

In this Boltzmann function, "*Bottom*" and "*Top*" represents the bottom and top boundaries of the thermogram (values typically equal 0% and 100%, respectively). The parameter, *V*, equals the half-temperature (units °C), and the parameter, "*Spread*," represents the spread of temperatures (units °C). Each carbon material has specific values for the Boltzmann parameters – all parameters are listed in Table 3. Lastly, the variable, *T*, equals the temperature of combustion (units °C). A Boltzmann function (Eq. 1) fitted through the BC/sediment data (solid line, Figure 7 and Table 3) determined that

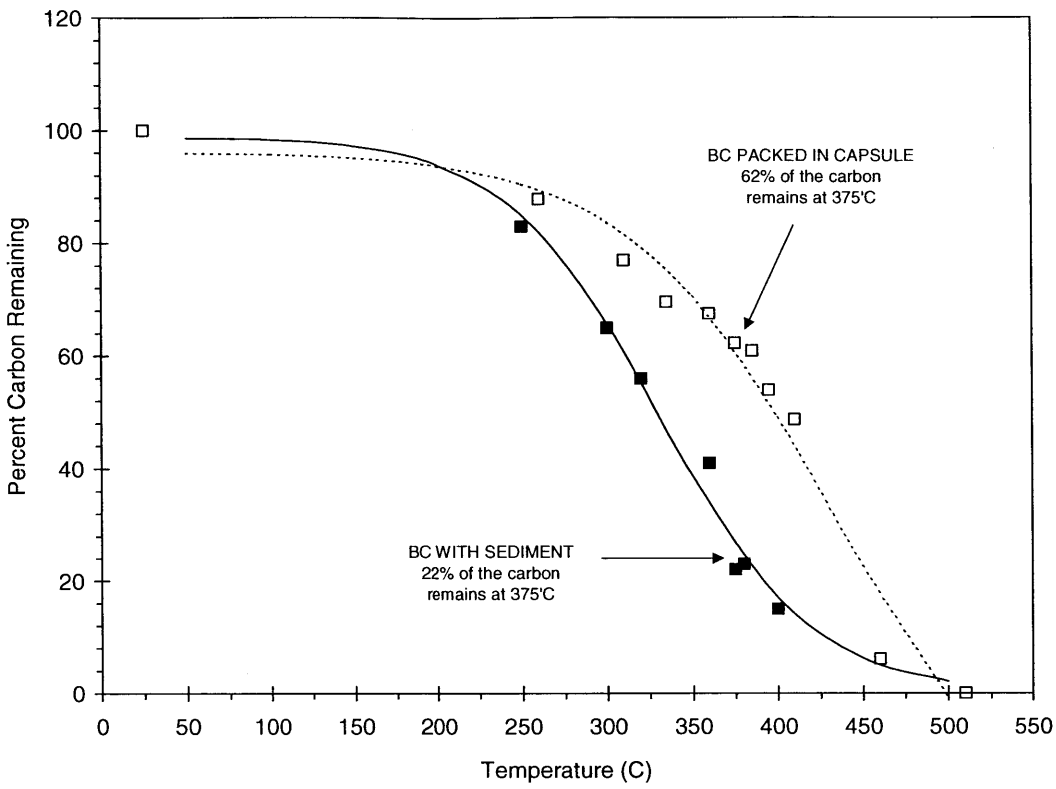

Figure 7: Thermogram (representing the percent carbon remaining after a 24-hour combustion at a given temperature (°C)) for BC mixed with sediment (black squares) and BC packed in capsules (open squares; Gustafsson *et al.* (2001) Global Biogeochem. Cy.) along with best-fit Boltzmann sigmoidal functions (Eq. 1). Thermogram data are listed in Appendix A3.4 and Boltzmann parameters are listed in Table 3.

Table 3: Best-fit Boltzmann sigmoidal parameters (±1 σ) for the observed thermograms (parameters also corresponding to Equation 1 and Equation 2-based model). To constrain the function ("Constr."), the bottom boundary was forced as ≥0 and the top boundary was forced as ≤1 ("Unconstr." corresponds to a function not constrained).

Sample	Bottom Boundary		Top Boundary		Half Temperature		Spread of Temperature	
	Constr.	Not Constr.	Constr.	Not Constr.	Constr.	Not Constr.	Constr.	Not Constr.
BC with sediment	0.00 ±19.1	-41.3 ±62.5	98.9 ±4.72	101 ±4.73	331 ±20.5	371 ±56.1	-44.3 ±13.6	-62.7 ±21.6
BC on beads	0.00 ±9.10	-14.5 ±14.0	98.2 ±5.80	101 ±5.19	263 ±12.8	277 ±16.3	-43.6 ±11.3	-56.9 ±13.4
Humic acid on beads	0.998 ±3.15	0.476 ±3.08	100 ±1.89	97.0 ±1.59	239 ±2.78	238 ±2.84	-23.2 ±2.42	-24.4 ±2.41
Marine Organic	1.69 ±1.95	1.36 ±1.85	100 ±2.53	102 ±2.41	257 ±2.62	257 ±2.46	-23.8 ±2.36	-24.8 ±2.24
Phytoplankton [a]	-6.25 ±8.96	NA	100	NA	207 ±12.8	NA	-53.9 ±9.62	NA

a: The phytoplankton thermogram represents a theoretical thermogram with no charring (dotted line in Figure 13a and 14a). NA equals not available.

half of the carbon in SRM 1650 would survive a 24-hour oxidation at 331 ±21°C. This half-temperature is much less than the half-temperature of 432 ±30°C that was calculated by fitting a Boltzmann sigmoidal function (unconstrained parameters) through the BC data measured by Gustafsson *et al.* ([21]; dotted line, Figure 7).

To challenge the hypothesis further that small BC particles are more susceptible to oxidation, the BC standard (SRM 1650) was dispersed onto glass beads to mimic small BC particles adhered to sediment grains. Scanning electron microscope images revealed that the BC coated the glass beads in a speckled pattern (0.61 ±0.03 wt % C, Figure 8) with BC patches typically ranging from 10-30 μm in size and approximately 5 μm thick (Figure 8d). After combusting these BC-coated beads at 375°C for 24 hours, only 3 ±0.2% of the total BC survived the oxidation (filled squares, Figure 9; Appendix A3.4). Hence, as the BC particles were manipulated to smaller sizes, they become more susceptible to oxidation. In summary, ≈62% of the BC can survive a 375°C pretreatment when the particles are packed in silver capsules [21], ≈22% of the BC can survive when the particles are mixed with the sediment grains, and ≈3% of the BC survives when the carbon is dispersed on glass beads. Likewise, the calculated half-temperature for BC-coated glass beads was 263 ±13°C (solid line, Figure 9 and Table 3), which is distinctly less than the half-temperature for BC with sediment of 331 ±21°C (dotted line, Figure 9). It would appear then that the 375°C method will underestimate the total BC content of sediment by isolating only a fraction of the large BC particles and none of the small BC particles.

Although a lower pretreatment temperature could isolate a higher percentage of BC particles, the incomplete combustion of OC could interfere with the BC measurements. To investigate the oxidative potential of OC, Aldrich humic acid was dispersed on glass beads to mimic organic matter coating sediment grains. The scanning electron microscope showed the humic acids lightly coated more than 50% of the glass bead surface area (1.1 ±0.1 wt % C, Figure 10). Note that the humic material did not create the speckled pattern observed when the NIST BC standard was dispersed on the glass beads (Figure 8). Compared to small and large BC particles, the humic material

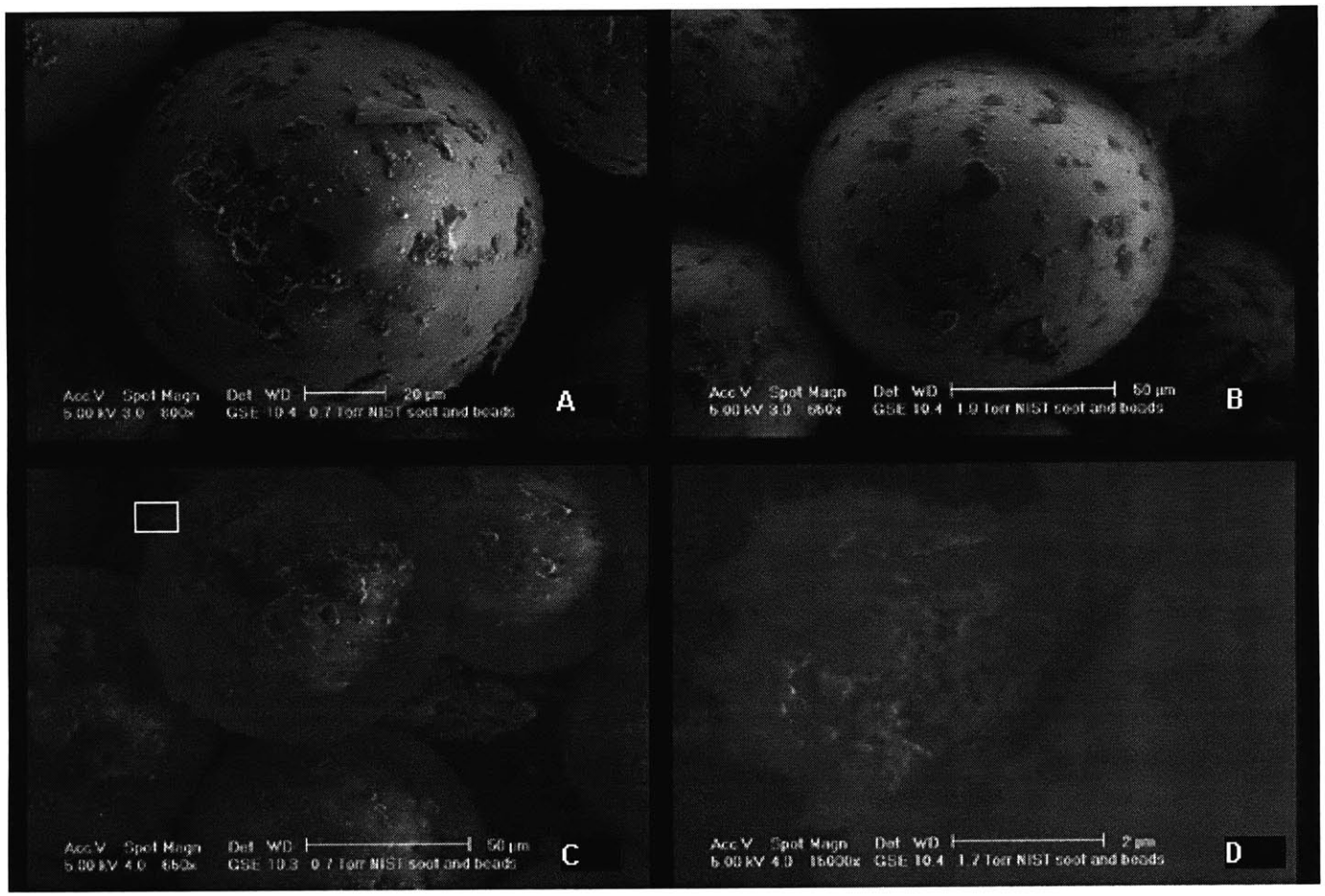

Figure 8: Scanning electron microscope images of BC (NIST 1650) on glass beads (note that specific operating parameters and relevant scale (μm) are provided in each panel). Panels A-C show various beads from the same BC stock (0.61 ±0.03 wt % C). Panel D is an enlargement of the box in panel C.

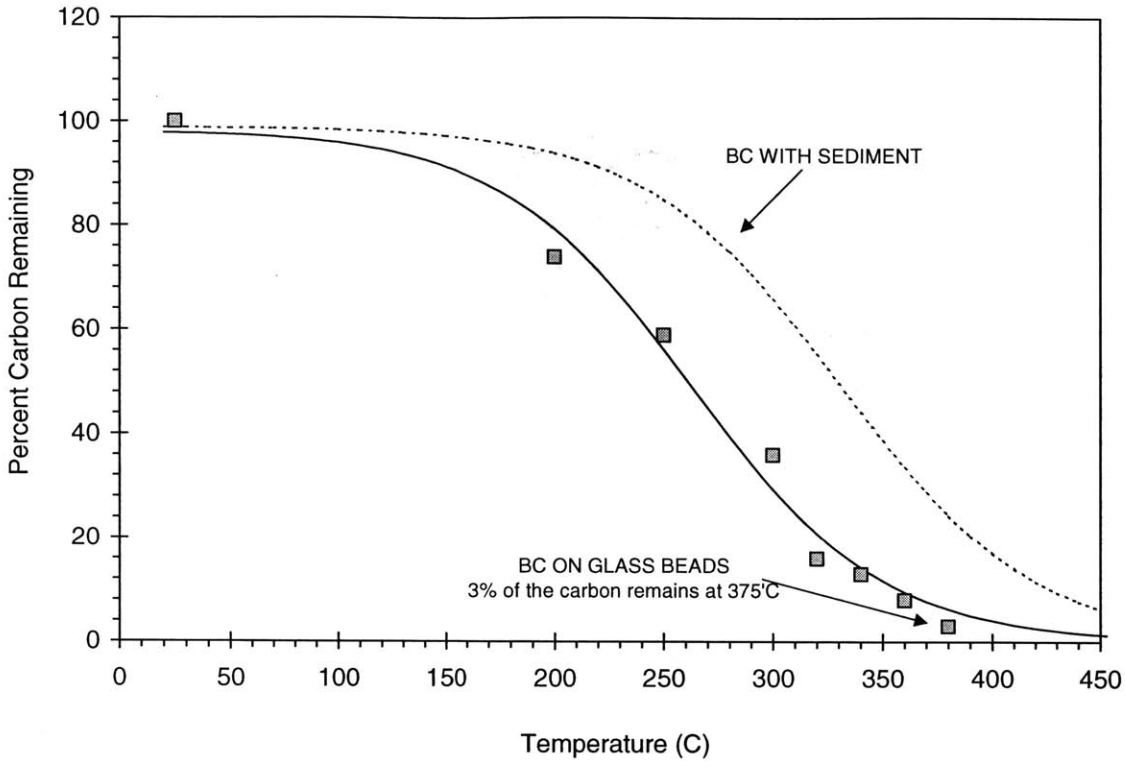

Figure 9: Thermogram (representing the percent carbon remaining after a 24-hour combustion at a given temperature (°C)) for BC on glass beads (filled squares) along with best-fit Boltzmann sigmoidal function (solid line). The dotted line represents the Boltzmann sigmoidal function for the BC mixed with sediment (corresponds to black squares in Figure 7). Thermogram data are listed in Appendix A3.4 and Boltzmann parameters (Eq. 1) are listed in Table 3.

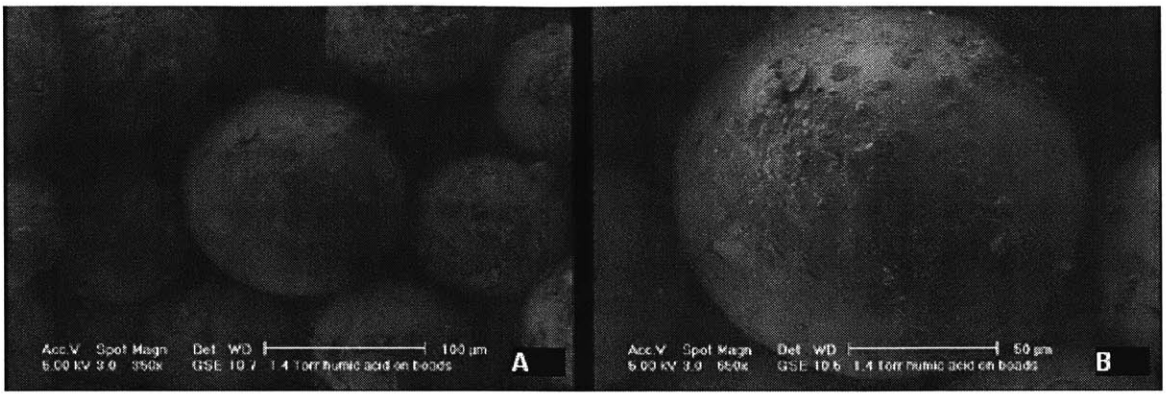

Figure 10: Scanning electron microscope images of Aldrich humic acid on glass beads (note that specific operating parameters and relevant scale (μm) are provided in each panel). Panels A and B show various beads from the same humic acid stock (1.1 ±0.1 wt % C).

had a distinctly lower half-temperature of 238 ±3°C (solid line and black circles, Figure 11; Table 3 and Appendix A3.4). Moreover, unlike the BC particles that had a large thermogram spread (ΔT >40°C, Table 3), the humic acids had a narrow temperature spread (ΔT = 24.4 ±2.4 °C), resulting in a steep thermogram slope. In a thermodynamic sense, a Boltzmann temperature spread reflects the heterogeneity of the reactive sites on the carbon surface. Thus, the narrow temperature spread displayed by humic acid reflects a more homogeneous set of reactive sites than the BC samples, and in turn, this narrow temperature spread reflects a uniform set of activation energies for carbon oxidation.

Marine organic matter also reacted over a narrow temperature range (ΔT = 23.8 ±2.0°C) with a low half-temperature of 257 ±2°C (dotted line and open circles, Figure 11; Table 3). The marine organic matter half-temperature was slightly higher than the half-temperature for humic acid by 18 ±4°C. This offset in half-temperatures may reflect the different composition of terrestrial and marine organic carbon. However, unlike the humic acid thermogram where the data were measured directly, the marine organic thermogram was measured indirectly as the difference between untreated and extracted sediment (Appendix A3.5). Therefore, if the extraction of organic matter were incomplete, then the true marine organic thermogram would lie to the right of the modeled line. On the other hand, if the peroxide/base extraction were too harsh, oxidizing both organic matter and small BC, then the true marine organic thermogram would exist to the left of the modeled line. Nevertheless, OC does persist at low temperatures with approximately 20-50% of the total OC remaining after pretreatment for temperatures ranging from 250-300°C, indicating that small BC cannot be isolated at low temperatures because of the interference from OC.

In addition to investigating the oxidation of humic acid and marine organic matter, the oxidation potential of fresh organic matter was explored by spreading phytoplankton material on glass beads. Images from the scanning electron microscopy revealed that the phytoplankton material formed thick clumps on the glass beads, roughly 10 μm thick, and tended to coagulate two or three beads together (2.0 ±0.4 wt % C, Figure 12). In general, the phytoplankton material was labile, losing 20% of the carbon

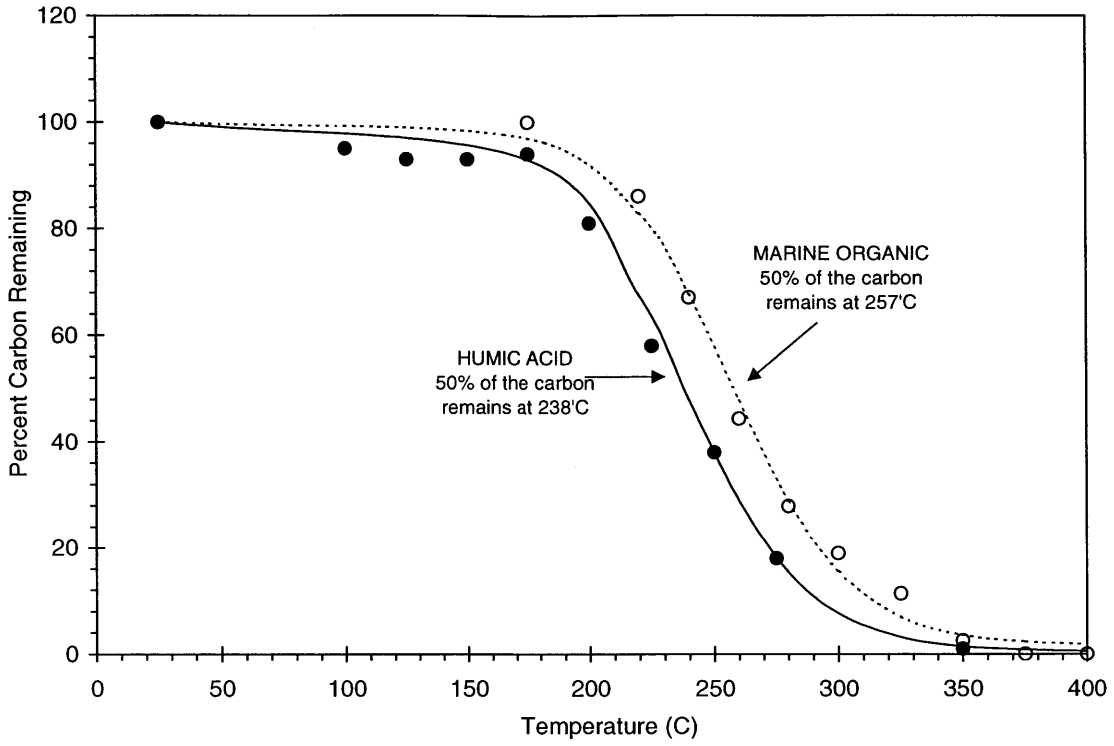

Figure 11: Thermogram (representing the percent carbon remaining after a 24-hour combustion at a given temperature (°C)) for humic acid on beads (black circles) and extracted marine organic matter (open circles) along with best-fit Boltzmann sigmoidal functions. Thermogram data are listed in Appendix A3.4 and Appendix A3.5 and Boltzmann parameters (Eq. 1) are listed in Table 3.

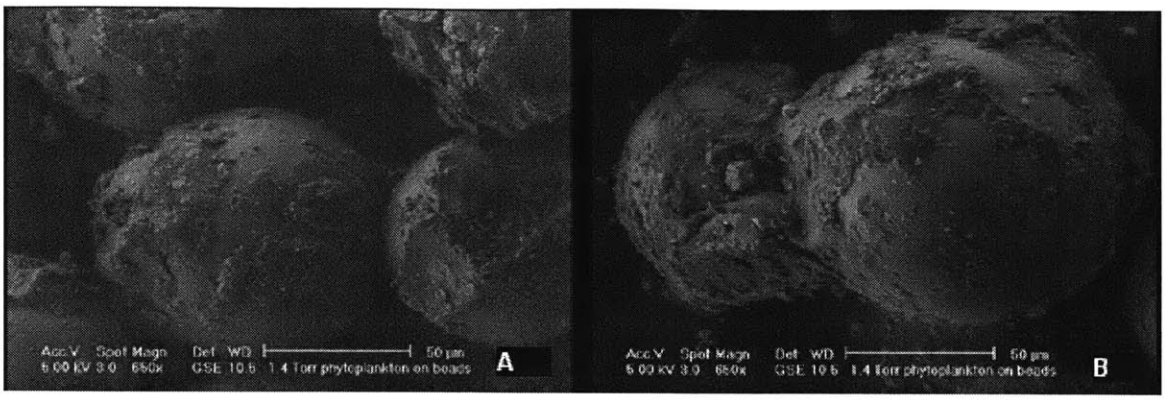

Figure 12: Scanning electron microscope images of phytoplankton material on glass beads (note that specific operating parameters and relevant scale (µm) are provided in each panel). Panels A and B show various beads from the same phytoplankton stock (2.0 ±0.1 wt % TOC and 0.36 ±0.02 wt % TN).

at 150°C and 50% of the carbon at 207 ±13°C (filled triangles, Figure 13a; Table 3 and Appendix A3.6). The half-temperature for phytoplankton is 32 ±13°C less than the half-temperature for humic acid and 50 ±13°C less than the half-temperature for marine organic matter. These results suggest that during the course of diagenesis (fresh organic matter transitioning to degraded organic matter), organic matter matures and becomes more resistant to oxidation, thus leading higher half-temperatures.

Similarly, the pyrolysis and combustion of coals was also observed to be a function of coal maturity (28°C/min from 350-700°C in helium [48]; 25°C/min from 300-550°C in helium [49]; 4°C/min in argon [50]; 30°C/min to 900°C in helium then 30°C/min to 700°C in helium/oxygen [51]). Instead of measuring carbon oxidation with weight percentages in the form of a thermogram, other techniques monitor the evolution of carbon dioxide as a function of temperature. Burnham *et al.* observed that the temperature of maximum carbon dioxide evolution (T_{max}) increased as the coal maturity increased (measured as a function of C weight percent) for a suite of Argonne Premium Coal Standards [50, 52]. For example, T_{max} for subbituminous coal (Wyodak-Anderson; 75 wt % C; C/H molar ratio of 0.85) was 400°C, the T_{max} for high-volatile bituminous coal (Illinois #6; 78 wt % C; C/H molar ratio of 0.77) was 410°C, and the T_{max} for low-volatile bituminous coal (Pocahontas; 91 wt % C; C/H molar ratio of 0.58) was 483°C. These results were later confirmed by Solomon *et al.* [51]. Other researchers have observed similar trends and have correlated coal maturity, or the vintrinite reflectance value, with T_{max} [48, 49]. The increase in T_{max} values with coal is similar to the increase in half-temperatures of the thermograms, indicating that more mature carbonaceous material oxidizes at higher temperatures.

3.5.2.1 Phytoplankton Charring. During the construction of the phytoplankton thermogram, we observed that beads pretreated at temperatures <150°C remained visibly green while beads pretreated at temperature <275°C were visibly brown in color. Unlike the humic acid and marine organic matter thermograms, the percentage of carbon surviving a 24-hour oxidation reached a distinct plateau at ≈20% the initial carbon

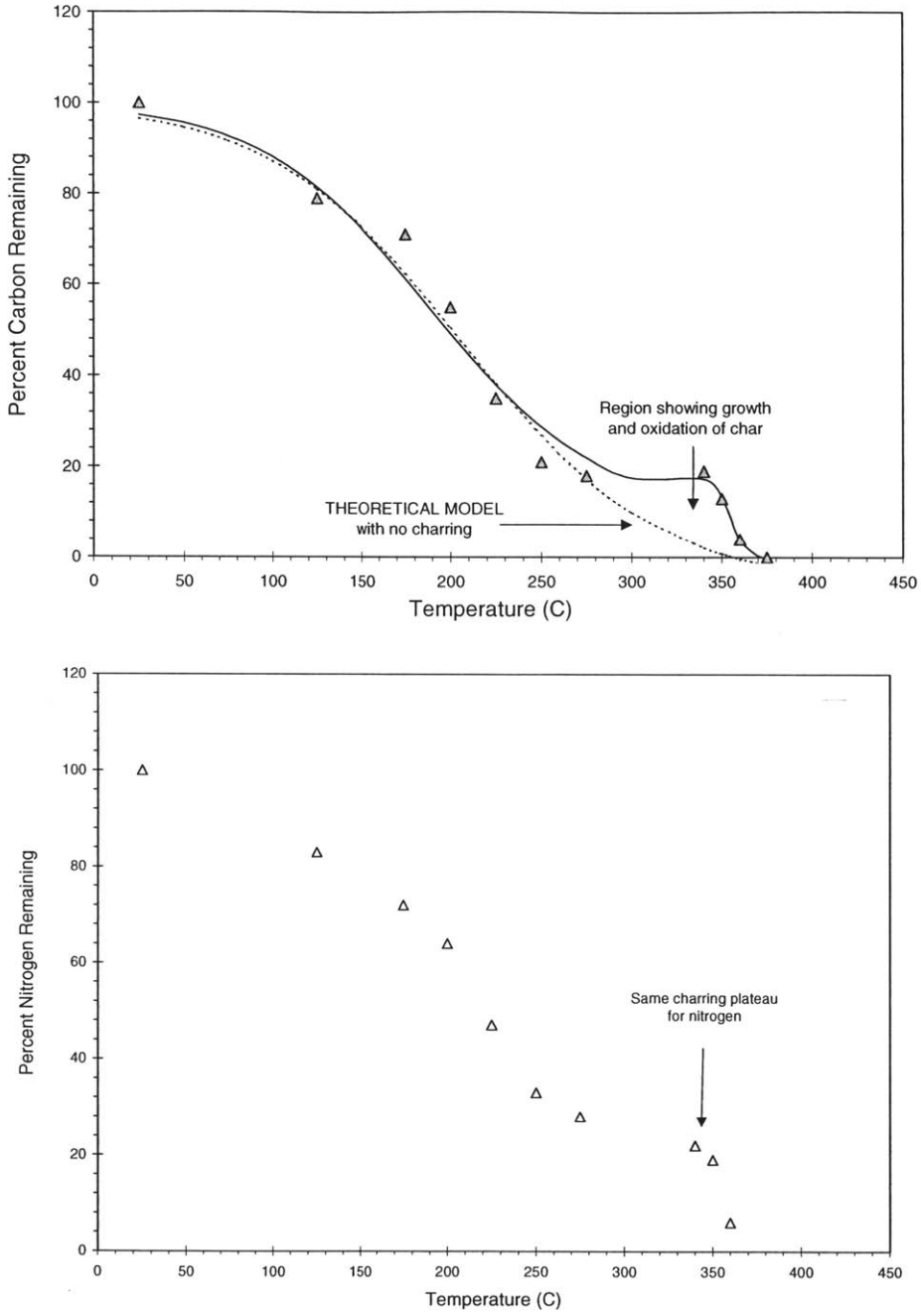

Figure 13: Thermogram representing the percent carbon remaining (Panel A; filled triangles) and percent nitrogen remaining (Panel B; open triangles) after a 24-hour combustion at a given temperature (°C) for phytoplankton material on beads. The dotted line represents a theoretical Boltzmann sigmoidal assuming no phytoplankton charring. The solid line represents the summation of two Boltzmann sigmoidal functions to capture the observed charring of the phytoplankton. Thermogram data are listed in Appendix A3.6 and Boltzmann parameters (Eq. 1) for the theoretical function are listed in Table 3.

content, producing visibly black beads. This plateau reflects the charring of phytoplankton material. A similar pattern was also observed for the nitrogen content of the phytoplankton (Figure 13b, Appendix A3.6). The percentage of total nitrogen decreased from 100% to 30% over the temperature range of 25°C to 275°C. The nitrogen content then reached a plateau of 20% for temperatures ranging from 275°C to 350°C. Interestingly, above 350°C both carbon and nitrogen began to decrease steadily until no carbon remained at temperatures >375°C.

To model the observed phytoplankton data, two Boltzmann sigmoidal functions were fitted through the data. The first curve begins at 100% carbon and ends at 20% carbon, representing the steady loss of carbon due to oxidation. The second curve begins at 20% carbon and ends at 0% carbon, representing the persistence of the recalcitrant char and the subsequent oxidation (solid line, Figure 13a). In addition, a theoretical Boltzmann sigmoidal was fitted through the data, assuming that the phytoplankton did not char (dotted line, Figure 13a; Table 3). The difference between these two curves reflects then the growth and oxidation of char. Hence, samples containing a low TN content probably do char, but the created char will oxidize at temperatures <375°C, and therefore, not interfere with the BC measurements (note that phytoplankton on glass beads contained 0.36 ±0.02 wt % TN). On the contrary, samples containing a high TN content char to such a high degree that residual char persists at 375°C, and this char does interfere with BC measurements.

Initially, it seemed beneficial to model the extent of phytoplankton charring in order to provide a tool for back-calculating the true BC content from a charred sample. However, simple calculations revealed that different N-containing compounds char to a different extent, so a universal "charring correction" is not possible. For example, the charring potential of bovine serum albumin (BSA) was illustrated previously in Figure 3B. If all N-containing macromolecules did char to the same extent, then the plotted regression line ($y = 1.904\ x + 0.0643$, Figure 3B where y = carbon content in the combusted sediment and x = nitrogen content in the combusted sediment) through the BSA data could be used to back-calculate the true BC content in any charred sediment

sample. In the first test, a mixture of BSA and Boston Harbor sediment charred with a measured BC content of 0.39 ±0.03 wt % C (Z = 3) and a nitrogen residue of 0.18 ±0.01 wt % N (Z = 3). By correcting for the char using the regression line given above and the measured nitrogen residue, the true BC content is back-calculated as 0.11 ±0.03 (which equals the BC content of Boston Harbor sediment with no additions). Hence, correcting a BSA charred sample with the BSA regression line works well. In contrast, in the next test, the correction does not work. In this example, a mixture of phytoplankton and Boston Harbor sediment charred with a measured BC content of 1.05 ±0.05 wt % C (Z = 4) and a nitrogen residue of 0.25 ±0.02 (Z = 3). A back-calculation using the regression line above and the measured nitrogen residue gives a true BC content of 0.23 ±0.04, which is two times greater than the expect value of 0.12 ±0.02 for Boston Harbor sediment with no addition. Thus, in this scenario, a phytoplankton charred sample cannot be corrected with a BSA regression line. Likewise, the charred samples in the Pettaquamscutt core could not be corrected because the extent of charring for degraded N-containing organic matter is unknown.

3.5.3 Model BC and OC Contents of Sediment with Thermograms. Since the 375°C method determines a lower limit of the total BC content in a sediment sample, a new computational model was developed to provide another reasonable estimate of the BC content. With the collection of thermograms discussed above, a model containing two functions – an OC thermogram and a BC thermogram – may be able to estimate the OC and BC contents of a sediment sample assuming that the shape of the thermograms remain constant as the carbon concentration changes. In this model, the measured carbon weight percentage for a sediment sample (C wt $\%_{\text{temperature}}$) will equal the fractions of OC and BC that survived a 24-hour combustion as a function of temperature (Eq. 2).

$$\text{C wt }\%_{\text{temperature}} = \text{OC wt \% (fraction OC surviving)} + \text{BC wt \% (fraction BC surviving)} \quad (2)$$

Here, "OC wt %" and "BC wt %" represent the total organic carbon content and the total black carbon content of the sediment sample as a weight percentage, respectively. The terms "fraction OC surviving" and "fraction BC surviving" represent the fractions of the total OC and total BC contents that will survive a 24-hour combustion at a given temperature as defined by the Boltzmann sigmoidal function (Eq. 1, re-defined here).

$$fraction\_surviving = Bottom + \frac{Top - Bottom}{1 + \exp\left(\frac{T - V}{Spread}\right)} \quad (1)$$

Note that the Boltzmann function re-defined here is the same function as defined in Eq. 1 except the "*Bottom*" and "*Top*" boundaries of the thermogram now equal 0 and 1, respectively, instead of a carbon percentage. The parameter, *V*, equals the half-temperature (units °C), and the parameter, "*Spread*," represents the spread of temperatures (units °C). Each carbon material has specific values for the Boltzmann parameters – all parameters are listed in Table 3. Lastly, the variable, *T*, equals the temperature of combustion (units °C).

In an ideal situation, this Eq. 2-based model would be able to extract not only the total OC content, but also the percentage of fresh organic matter and degraded organic matter using the phytoplankton thermogram and the marine organic matter thermogram as end-members. Likewise, the model would be able to extract the fraction of small BC and large BC in the sediment. However, because the Boltzmann sigmoidal functions are limited by only two parameters (the inflection point, or half-temperature, and the spread of temperatures), a model with multiple thermograms is undetermined and cannot distinguish between similar carbon fractions. For example, the half-temperatures between the humic acid thermogram and the marine organic thermogram only differ by 18 ±4°C while their spread of temperatures only differ by 0.6 ±3°C (Table 3). Hence, the model is restricted to having one thermogram representing the total OC content and one thermogram representing the total BC content (Eq. 2).

3.5.3.1 Test the Combined OC/BC Model (Eq. 2) To test the Eq. 2-based model, samples from Boston Harbor, Massachusetts Bay, and Wilkinson Basin were selected to

measure the BC content in this off-shore transect. Boston Blue Clay was also tested because this buried glacial-meltwater deposit of fine sediment grains (≈14,000 years old) was assumed not to contain contemporary BC particles. To establish a lower limit for the BC content in these samples, the sediments were combusted at 375°C for 24 hours under air. Combusted sediment from Massachusetts Bay (MB) had a BC content of 0.01 ±0.00 wt % C (Z = 3, Table 4) corresponding to a BC/TOC ratio of 9%. The low nitrogen residue of 0.01 ±0.01 wt % N (Z = 3) indicated that charring of N-containing organic matter did not occur. The BC content for combusted sediment from Wilkinson Basin (WB) was 0.21 ±0.01 wt % C (Z = 3, Table 4), which also corresponded to a BC/TOC ratio of 9%; however, the presence of a notable nitrogen residue (0.06 ±0.01 wt % N, Z = 3) suggests that charring may have occurred in the sample. Although the TN content of WB was small (0.29 ±0.01 wt % TN, Z = 3), it is suspected that this N-containing material is well packaged since the majority of organic matter deposited in WB (≈300 m depth) may be in the form of pellets. For example, approximately 55% of the total nitrogen content remained after a combustion at 240°C, 24% of the nitrogen remained at 350°C, and 10% of the native nitrogen remained at 400°C, suggesting that the N-containing organic matter in WB is recalcitrant, or it charred. Lastly, combusted Boston Blue Clay (BBC) had a BC content of 0.06 ±0.02 wt % C (Z = 3, Table 4) for a lower limit, corresponding to a BC/TOC ratio of 12%. A negligible amount of nitrogen in the combusted sediment (0.02 ±0.01 wt % N, Z = 3) suggests that charring was not an issue in the BBC; however, because of the low TN content of the sediment, this nitrogen residue represents 33% of the nitrogen in the sample.

As a second approximation of the BC content in these samples, a thermogram for each sediment sample was constructed (thermogram data are listed in Appendix A3.7). Endmember thermograms were selected to represent the oxidation of OC and BC. In the Boston Harbor sample, three thermograms could possibly represent the oxidation of OC: the phytoplankton on glass beads (the theoretical model with no charring), the humic acid on glass beads, or the extracted marine organic carbon thermogram (Figure 14a). For

Table 4: Two estimates for the BC and OC contents for various sediment samples (mean ±1 σ) (a) measured BC content with a 375°C thermal oxidation and calculated OC content as difference between the measured TOC wt % and the 375°C-measured BC wt % (b) modeled BC content and the modeled OC content using Eq. 2-based model.

Sample	Measured 375°C-BC Content	Calculated OC Content	Eq.2-based BC Content	Eq. 2-based OC Content
Boston Harbor sediment	0.12 ±0.02	1.3 ±0.1	0.46 ±0.08	0.95 ±0.10
Massachusetts Bay sediment	0.01 ±0.00	0.10 ±0.01	0.04 ±0.01	0.07 ±0.01
Wilkinson Basin sediment	0.21 ±0.01	2.07 ±0.03	0.80 ±0.09	1.30 ±0.12
Boston Blue Clay	0.06 ±0.01	0.46 ±0.05	0.12 ±0.04	0.33 ±0.05

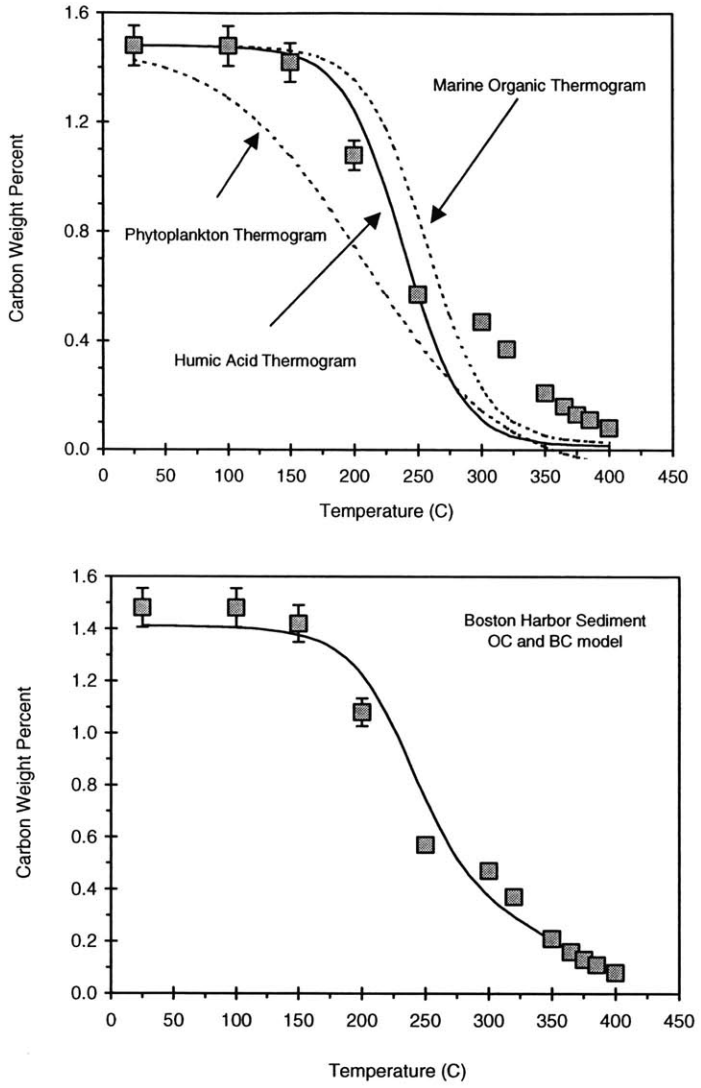

Figure 14: Thermogram (representing the measured carbon weight percentage after a 24-hour combustion at a given temperature (°C)) for Boston Harbor sediment (filled squares). (a) Possible models (marine organic thermogram, the humic acid thermogram, and the phytoplankton thermogram) to represent the oxidation of OC (b) the best-fit, Eq. 2-based OC/BC model (using the humic acid thermogram and the "BC with sediment thermogram"). Thermogram data are listed in Appendix A3.7 and Boltzmann parameters (Eq. 1) are listed in Table 3.

temperatures <250°C, the phytoplankton thermogram underestimated the observed carbon oxidation while the marine organic thermogram overestimated the data. The underestimation of the phytoplankton thermogram is not surprising since the sediment in Boston Harbor has been reworked, and the fraction of fresh organic matter is probably minimal. The overestimation of the marine organic thermograms was unexpected, especially since the extracted material was extracted from the Boston Harbor sediment. These results suggest that the peroxide/base extraction method was too harsh, and some BC was probably lost in the process, thus shifting the thermogram to the right.

Overall, the humic acid thermogram was the best-fit of the three thermograms to model the initial carbon oxidation (T <250°C) in the Boston Harbor sediment. For example, for temperatures ranging from 25°C to 250°C, the humic acid thermogram has the smallest residual (defined as the sum of the differences squared) of 0.029 compared to the residual of 0.163 for the marine organic thermogram, or the residual of 0.297 for the phytoplankton thermogram. By using the humic acid thermogram to characterize the oxidation of OC, the initial loss of carbon (T<250°C) was well modeled for all the sediment samples analyzed (i.e., MB in Figure 15a, WB in Figure 16a, and BBC in Figure 17a). As suspected, a model containing only OC oxidation could not describe the sediment thermograms alone. At temperatures >250°C, the humic acid thermogram consistently underestimated the observed data, indicating that another carbon fraction, such as BC (either native or created by charring), was present in the sediment. (Note currently no one carbon material is known to display a thermogram similar to the observed sediment thermograms.)

Either the thermogram for "BC with sediment" (representing large BC particles) or the thermogram for "BC on beads" (representing small BC particles) could describe the BC oxidation in the sediment samples. However, since the thermogram for "BC on beads" overlaps with the humic acid thermogram at low temperatures and the half-temperatures for these two thermograms only differ by 24 ±13°C, the "BC with sediment" thermogram provided a more distinct function for characterizing BC oxidation. By using the humic acid thermogram and the "BC with sediment" thermogram together,

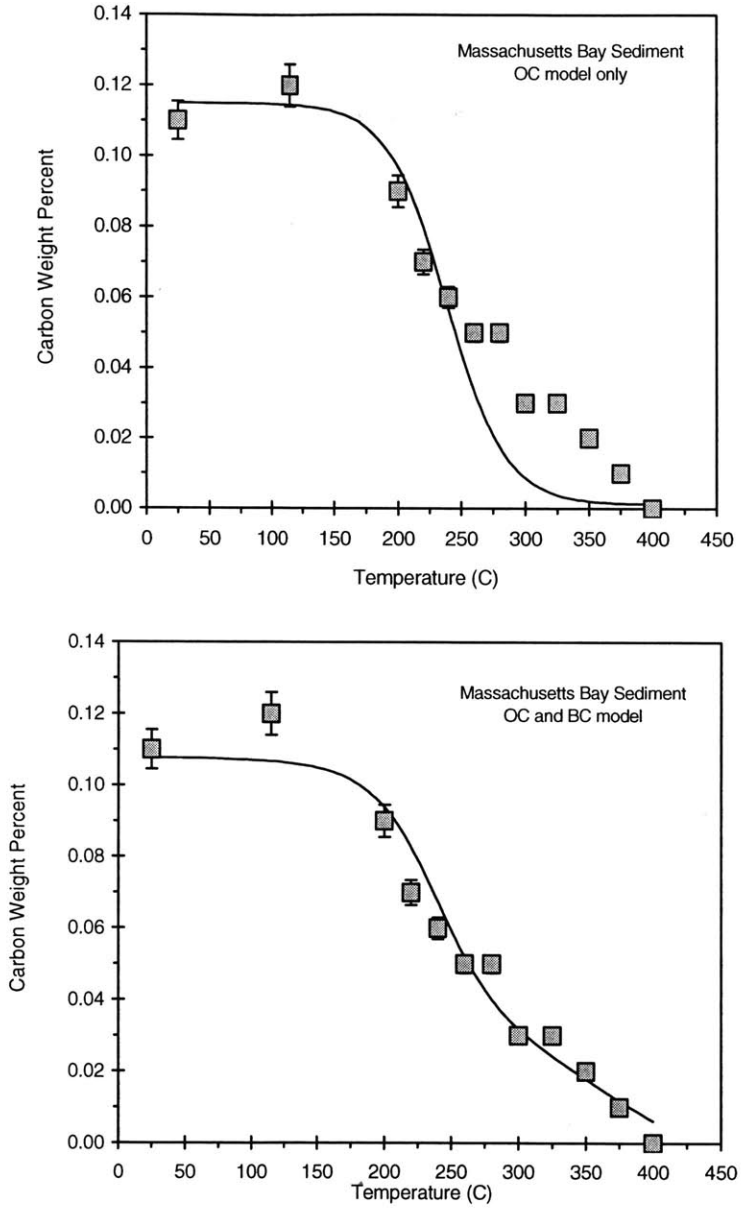

Figure 15: Thermogram (representing the measured carbon weight percentage after a 24-hour combustion at a given temperature (°C)) for Massachusetts Bay sediment (filled squares) along with (a) the best-fit OC model and (b) the best-fit, Eq. 2-based OC/BC model. Thermogram data are listed in Appendix A3.7 and Boltzmann parameters (Eq. 1) are listed in Table 3.

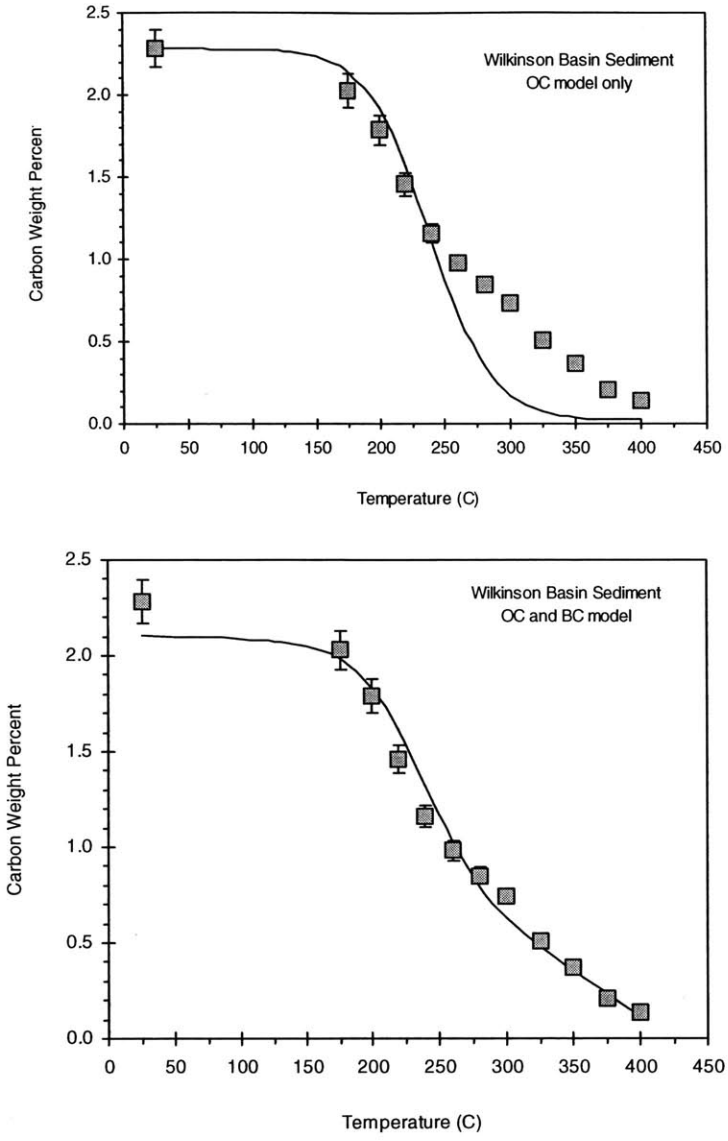

Figure 16: Thermogram (representing the measured carbon weight percentage after a 24-hour combustion at a given temperature (°C)) for Wilkinson Basin sediment (filled squares) along with (a) the best-fit OC model and (b) the best-fit, Eq. 2-based OC/BC model. Thermogram data are listed in Appendix A3.7 and Boltzmann parameters (Eq. 1) are listed in Table 3.

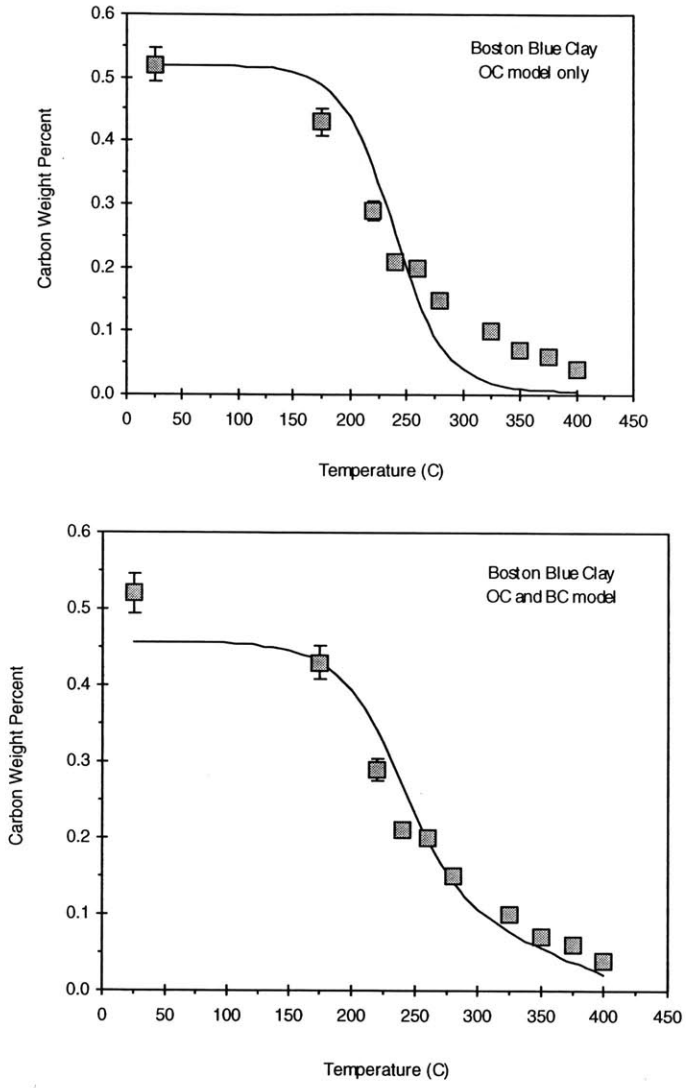

Figure 17: Thermogram (representing the measured carbon weight percentage after a 24-hour combustion at a given temperature (°C)) for Boston Blue clay (filled squares) along with (a) the best-fit OC model and (b) the best-fit, Eq. 2-based OC/BC model. Thermogram data are listed in Appendix A3.7 and Boltzmann parameters (Eq. 1) are listed in Table 3.

the combined OC/BC model (Eq. 2) was able to predict the observed thermograms for all four sediment samples by optimizing the OC and BC contents (Figure 14b, 15b, 16b, and 17b). The better fit of the combined OC/BC model (Eq. 2) over the OC model is reflected in a smaller residual for the combined model. For example in the Boston Harbor sediment, the residual equaled 0.333 for a model that only included OC oxidation; however, the residual decreased to 0.079 by incorporating OC and BC oxidation in the model. Likewise, the residual for MB sediment decreased from 3.07×10^{-3} to 0.599×10^{-3}, the residual for WB sediment decreased from 1.06 to 0.106, and the residual for BBC decreased from 0.032 to 0.012 by incorporating BC oxidation in the model. These results indicate that these four sediment samples contain both OC and BC.

In general, the BC content estimated from the Eq. 2-based model accounted for 27-38% of the total carbon in the sample (Table 4). While the combined model fits the observed data well, the modeled BC values may not represent the true BC content of the sample, especially since earlier work has shown that two different types of carbon may share similar Boltzmann parameters. Hence, the model cannot distinguish between two similar carbon materials. For example, just as the thermograms for the two BC have the same spread (approximately 44°C, Table 3), another carbon material, such as kerogen, may overlap these BC thermograms. Therefore, the reported BC content may overestimate the BC content in sediments by representing more than one type of carbon in the sediment. Yet, the 375°C thermal method and the combined model (Eq. 2) together allow for a reasonable estimate of the BC and OC contents in these four various sediment samples. The Boston Harbor sample contains 0.1-0.4 wt % BC and ≈1 wt % OC, the Massachusetts Bay sample contains 0.01-0.04 wt % BC and 0.07-0.1 wt % OC, the Wilkinson Basin sample contains 0.2-0.8 wt % BC and 1-2 wt % OC (as a reminder, this site may have charred), and the Boston Blue Clay sample contains ≈0.1 wt % BC and 0.3-0.5 wt % OC (Table 4).

3.6 RESULTS AND DISCUSSION – PART III: EXPLORATION OF THE USE OF KINETICS FOR CARBON OXIDATION TO OPTIMIZE BLACK CARBON DETERMINATION

3.6.1 New Model Based on Carbon Oxidation. Although the Boltzmann sigmoidal function can describe endmember thermograms in terms of a half-temperature and a spread of temperatures, the combined OC/BC model (Eq. 2), which combines two endmember thermograms, cannot accurately estimate the true OC and BC contents in sediment. Hence, another approach is necessary. Interestingly, the thermograms discussed above do provide additional information on the rate of carbon oxidation. For example, for a given 24-hour reaction, as the temperature increases, the rate of oxidation increases, and less carbon material survives the pretreatment. If the reaction rate for carbon oxidation follows first-order kinetics, then the rate constant (k) will depend on temperature (T, units of Kelvin) and follow an Arrenhius Equation (Eq. 3).

$$k = Ae^{\frac{-E_a}{RT}} \tag{3}$$

Hence, an activation energy (E_a, units of kJ/mol) and a frequency factor (A, units of 1/hour) can characterize each carbon material as well as a Boltzmann half-temperature and a temperature spread. Therefore, in the Boltzmann-based model, instead of defining the "fraction surviving" with a Boltzmann sigmoidal function, the fraction surviving for either OC or BC could be determined by first-order kinetics (Eq. 4):

$$fraction\_surviving = \frac{[C]_{time}}{[C]_{initial}} = \exp(-kt) \tag{4}$$

where $[C]_{time}$ equals the measured carbon weight percentage after a given combustion period, $[C]_{initial}$ equals the initial measured carbon weight percentage, and t equals time. Substituting the Arrenhius Equation (Eq. 3) into Eq. 4, the fraction of OC or BC surviving a thermal pretreatment is dependent on the activation energy and frequency factor of either OC or BC and the combustion time (Eq. 5).

$$fraction\_surviving = \exp\left(-A\exp\left(\frac{-E_a}{RT}\right)t\right) \tag{5}$$

For example, during the NIST intercomparison study, an urban dust sample (SRM 1649a) was combusted at 375°C for 24 hours and 12 hours, and each combustion time yielded a different percentage of carbon surviving [19]. By calculating an activation energy (41 kJ/mol) and frequency factor ($\ln A = 5.5$) from the thermogram reported by Gustafsson *et al.* (assuming first-order kinetics; [21]), the fraction of carbon surviving a given combustion time was estimated. Remarkably, the percentage of carbon surviving a 12-hour combustion was calculated as 20% with Eq. 5 and compared well to the observed value of 19% by Currie *et al.* [19]. Furthermore, Eq. 5 implies that instead of distinguishing between OC and BC with one cut off temperature and one cut-off time, such as 375°C for 24 hours, it may be possible to discriminate between the two fractions by setting two combustion temperatures, each with a certain combustion time. However, before this model can be applied, initial work needs to be done to determine if carbon oxidation follows first-order kinetics, and values for activation energy and frequency factor are necessary.

3.6.2 First-Order Kinetics for Carbon Oxidation. Previous work by Smith showed that the oxidation of several sub-bituminous coal particles display an apparent first-order reaction rate [53]. In other words, the rate of carbon oxidation (dC/dt) is directly proportional by the rate constant (k) to the amount of carbon remaining (first-order in terms of carbon) but independent of the oxygen concentration (zero-order in terms of oxygen; [54]) (Eq. 6).

$$rate = \frac{dC}{dt} = -k[O_2]^0[C]^1 \qquad \text{(Eq. 6)}$$

Investigators have suggested that during oxidation, oxygen molecules saturate the reactive surface sites, forming carbon-oxygen activated complexes. The rate-limiting step then becomes desorption of this carbon-oxygen complex from the surface to form carbon monoxide [55, 56, 57]. Although first-order kinetics (having one activation energy and one frequency factor) have been proposed to describe the oxidation of BC, it should be noted here that other models have suggested a distribution of activation

energies with one frequency factor to reflect the various chemical and physical reactions are occurring in parallel or in series [50]. For example, Burnham *et al.* observed that a distribution of activation energies (ranging from 160-280 kJ/mol) characterized the oxidation of each Argonne Premium Coal standard studied [52].

To investigate the rate order for oxidation of BC on glass beads, an isothermal kinetic experiment was conducted at 350°C for times varying from 15 minutes to 14 hours. By integrating the first-order kinetics expression (Eq. 6), the rate constant (k) for the oxidation of BC on glass beads equals 0.23 ±0.0044 1/hours with a strong correlation coefficient (R^2) of 0.999 (Figure 18). The goodness of fit of this kinetic data strongly suggests that BC oxidation follows first-order kinetics. Similar exponential decay curves are reported in the literature for the oxidation of carbon black [58] and the oxidation of diesel soot [59].

Several literature reports have suggested that first-order kinetics are characteristic of "regime #1 burning" where oxygen can diffuse into a BC particle and oxidize the entire particle at the same time [53, 60]. This type of burning is distinctly different from "regime #3 burning" where oxygen diffusion is limited, and carbon oxidation only occurs on the outer layers [61, 62]. As a particle burns from the outside inwards, the diameter of the porous soot particle will decrease while the surface area remains virtually the same. (Note that "regime #2 burning" is an intermediate burn between the two extremes.) On the contrary, if oxygen can diffuse into the soot particle (during regime #1 burning), oxidation can open occluded pores or create new pores, thus increasing surface area [57, 60, 63]. Interestingly, Ishiguro *et al.* were able to capture the changed microstructure of diesel soot particles during combustion with a high-resolution scanning electron microscope [64]. They also reported that during combustion as the surface area of diesel soot increased by a factor of 5, the diameter of the soot particles remained virtually the same (28-35 nm; [64]).

If the BC on glass beads were following first-order kinetics, then the carbon-specific surface area (m^2/g_{carbon}) should also increase with burn-off. As suspected, the surface area was observed to increase by a factor of 5 (Table 5). For example, the carbon

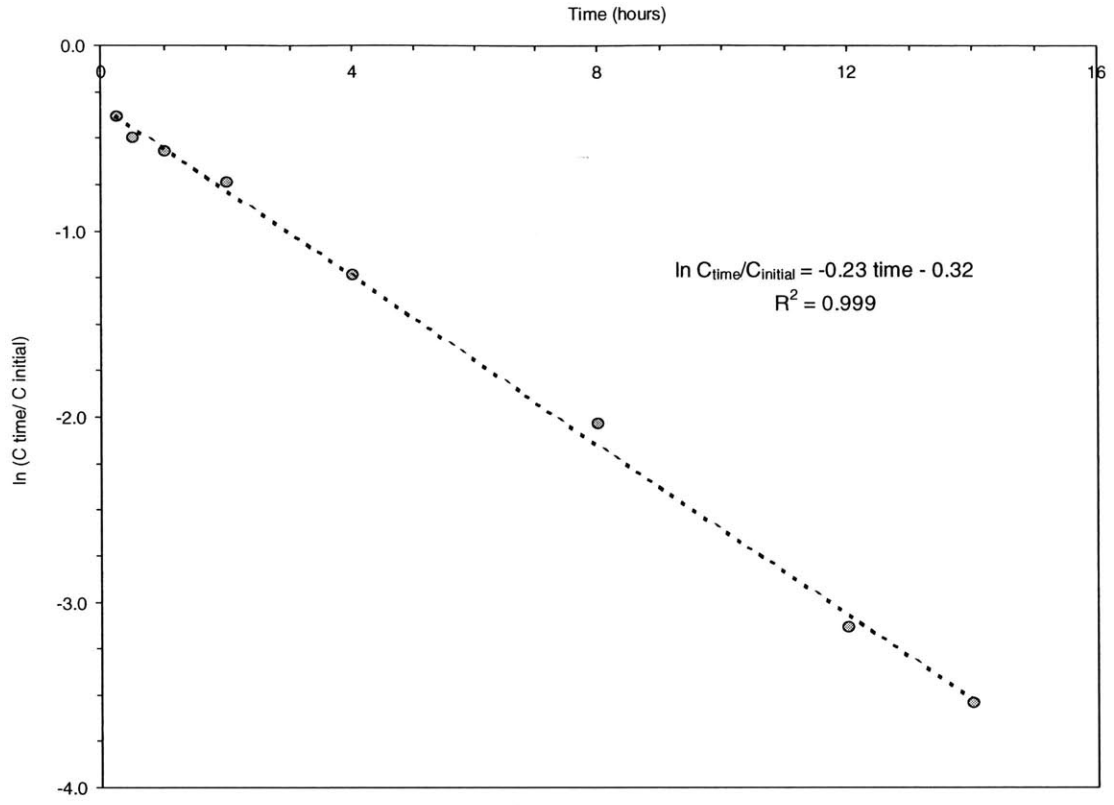

Figure 18: Kinetic data for the carbon oxidation of BC on glass beads. Regression line represents the integrated form of Eq. 6 where the slope equals the first-order rate constant.

Table 5: Surface area measurements for the kinetic data (isothermal combustion at 350°C for varying time).

Sample (Time Data)	Measured [a] Surface Area m^2/g_{mass}	Measured [b] C wt %	Calculated [c] Surface Area m^2/g_{carbon}	Percent Burn-off
0 hours	0.436	0.69 ±0.02	59 ±3.4	0%
15 minutes	0.399	0.47 ±0.01	79 ±4.3	32%
½ hours	0.739	0.42 ±0.01	170 ±9.3	39%
2 hours	0.481	0.33 ±0.04	140 ±18	52%
8 hours	0.295	0.09 ±0.02	290 ±67	87%
Glass beads	0.0296	0.01 ±0.01		

a: Measured surface area by Porous Materials, Inc. using a multi-point BET analysis with krypton gas. All values are reported to three significant figures and have a 5% error.

b: Measured carbon weight percentage on CHN analyzer (mean ±1 σ).

c: Calculated carbon-based surface area (mean ±1 σ) determined by subtracting the glass bead control from the BC-coated beads and then normalizing to the measured carbon weight percentage. Values rounded to two significant figures.

surface area before combustion was 59 ±4 m^2/g_{carbon} and increased to 290 ±21 m^2/g_{carbon} after 87% carbon conversion (Table 5). Similar results were observed by Gilot *et al.* [65], who reported a factor of 2 increase in surface area during carbon conversion, and by Floess *et al.* [66], who reported a factor of 3 increase in surface area. Hence, the increase in surface area over time (corresponding to more burn-off) plus the exponential decay curve for carbon oxidation suggests that BC on glass beads is displaying first-order kinetics.

3.6.2.1 Activation Energy and Frequency Factors. Assuming that all the carbon materials (phytoplankton on glass beads, humic acid on beads, extracted marine organic, and BC with sediment) display first-order kinetics similar to BC on glass beads, a 24-hour rate constant can be calculated at different temperatures from the thermograms constructed above (Eq. 7).

$$k_{24hours} = \frac{\left(\ln \frac{[C]_{24hours}}{[C]_{initial}}\right)}{-24} \tag{7}$$

Here, $[C]_{24hours}$ represents the measured carbon weight percent after a 24 hour combustion, and $[C]_{initial}$ represents the total carbon weight percent before combustion. Then, the values for the activation energy and frequency factor for each type of carbon material can be derived from a natural logarithm form of the Arrenhius Equation (Eq. 8):

$$\ln k = \ln A - \frac{E_a}{R}\left(\frac{1}{T}\right) \tag{8}$$

where k is the calculated 24-hour rate constant (Eq. 7) and R is the universal gas constant (units of J/K/mol).

In general, the measured activation energies ranged from 35-70 kJ/mol and the measured frequency factor ($\ln A$) ranged from 4-13 1/hours (Figure 19, Table 6). Unfortunately, no activation energies or frequency factors for phytoplankton and humic acid oxidation under air at elevated temperatures exist in the literature for comparison. In general though, the highest activation energies corresponded to the carbon materials with

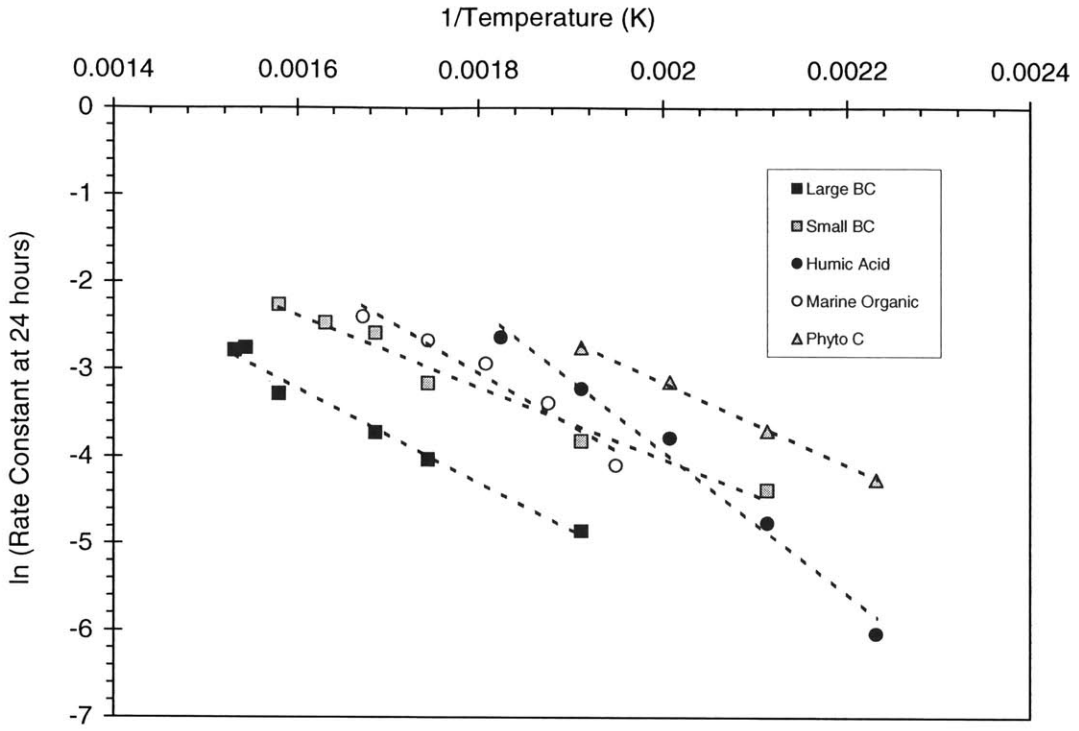

Figure 19: Natural logarithm of the 24-hour rate constant (1/hours) for carbon oxidation versus temperature (1/K). Data corresponds to the thermograms presented in Figure 7 (black squares, BC with sediment), Figure 9 (filled squares, BC on beads), Figure 11 (black circles, humic acid; open circles, marine organic), and Figure 13 (filled triangles, phytoplankton). Activation energies and frequency factors for each regression line are listed in Table 6.

Table 6: SigmaPlot calculated activation energies and frequency factors (mean ±1 σ) with corresponding correlation coefficient for constructed thermograms. Values correspond to Figure 19 and Equation 8.

Samples	Activation Energy (E_a, kJ/mol)	Frequency Factor (ln A, 1/hr)	Correlation Coefficient (R^2)
BC with sediment	45 ±3	5.5 ±0.63	0.981
BC on beads	34 ±3	4.2 ±0.61	0.973
Marine organic	50 ±6	7.8 ±1.4	0.954
Humic acid on beads	69 ±5	13 ±1.2	0.984
Phytoplankton [a]	40 ±1	6.4 ±0.30	0.998

a: The phytoplankton thermogram represents a theoretical thermogram with no charring (dotted line in Figure 13a and 14a).

the smallest Boltzmann spread. For example, humic acid and marine organic had activation energies >50 kJ/mol and thermogram spreads of ≈24°C (Tables 3 and 6).

For the BC samples, the activation energies ranged 34-45 kJ/mol. These measured activation energies are substantially less than literature reports of activation energies ranging from 136-168 kJ/mol for the oxidation of diesel soot [54, 59, 62] and from 100-300 kJ/mol for kerogen decomposition to petroleum ([67] and references therein; 25°C/min in helium [68]; isothermal heating in water [69]). Although some researchers have reported low activation energies (20 kJ/mol for carbon black oxidation [65, 70] and 70-90 kJ/mol for coal oxidation [53]), the data presented here may not be comparable to that from chemical engineering and geochemical studies. For example, chemical engineers focused heavily on oxidizing soot packed on filters in engines. They tended to use a less oxidizing atmosphere (10% oxygen in argon), employ a fast ramp (1-50°C per minute), combust at high temperatures (>400°C) with a short incubation time (<1 hour), and pack BC into pellets (weighing 20-300 mg) to mimic filters. Meanwhile, geochemists tended to pyrolyze samples at high pressures (10-100 MPa) in order to model geological conditions during oil expulsion from fine-grain sediments [69]. In contrast, the BC presented here is dispersed on glass beads with micrometer dimensions and is combusted in an oxidizing atmosphere (21% oxygen). The difference in experimental setup is also reflected in radically different frequency factors. For example, Neeft *et al.* reported a frequency factor (ln A, units of 1/hour) of 25 ±0.5 for carbon black oxidation in a flow-reactor, and Quigley *et al.* reported a frequency factor of 38-39 1/hr for the decomposition of kerogens [68]. These frequency factors are significantly greater than the observed frequency factors of 4-13 1/hours (Table 6).

3.6.3 Discriminating between OC and BC Using Temperature and Time. With the information discussed above, a new model may be proposed that uses different combinations of combustion temperature and time to discriminate between OC and BC. In a series of temperature steps, a model could be envisioned to include long combustion times at low temperatures to remove labile, fresh organic matter (i.e. phytoplankton) and

short combustion times at high temperatures to remove degraded organic matter (i.e. humic acids). Further studies constraining the oxidation of kerogen could also help the model distinguish BC from the other carbon material in a sediment sample.

This envisioned model would operate by using the activation energy, frequency factor, and combustion time in Eq. 5 to calculate the fraction of carbon surviving. An optimal recipe would then be established by varying time and temperature to isolate BC from the OC fraction. For example, the 375°C/24 hour recipe results in the isolation of 25% of the large BC particles and none of the small BC particles or OC (Table 7). However, a recipe designed to combust for 4 hours at 500°C will isolate a larger percentage of large BC particles (41%), 26% of the small BC particles, and approximately the same amount of total OC (3%) as the current 375°C method. Another possible recipe includes a 24-hour combustion at 250°C followed by a 1-hour, 500°C combustion, which would isolate 66% of the large BC particles and 38% of the small BC particles, but include 19% of the marine organic matter and 7% of the phytoplankton material. Interestingly, similar results are obtained by combusting at 350°C for 4 hours followed by a 4-hour combustion at 450°C (Table 7). Preliminary estimates of possible combustion recipes revealed that the most difficult step is discriminating between small BC and marine organic matter. Because these two carbon materials have similar thermodynamic properties, the small BC will oxidize at the same rate as the marine organic matter. Therefore, a recipe designed to remove all the OC will underestimate the total BC by oxidizing the small BC as well.

3.7 SUMMARY

In summary, the work presented here re-examines the 375°C thermal oxidation method to determine the accuracy and precision of the method in oxidizing labile OC and isolating BC sediments samples. Recent work by Gelinas *et al.* [23] suggests that N-containing macromolecules will cause an overestimation of the BC measurement due to charring at 375°C. On the contrary, Nguyen *et al.* [24] hypothesizes that the 375°C will underestimate the total BC content of a sample because small, less robust BC particles

Table 7: Percent carbon surviving (calculated from Eq. 5) a thermal combustion under air for the given recipes (temperature, °C/time, hour)

Sample	Percent Carbon Surviving for a Given Recipe			
	375°C / 24 hr	500°C / 4 hr	250 °C / 24 hr 500°C / 1 hr	350°C / 4 hr 450°C / 4 hr
Large BC	25%	41%	66%	62%
Small BC	6%	26%	38%	37%
Marine Organic	0%	2%	20%	15%
Humic Acid	0%	0%	0%	0%
Phytoplankton [a]	0%	1%	7%	5%

a: Assuming no phytoplankton charring

are susceptible to oxidation. Thus, experiments were designed and conducted to address the concerns of organic matter charring (i.e. creating a BC artifact) and the potential oxidation of BC particles.

Through additions of natural compounds, charring was observed in samples containing a high total nitrogen content; moreover, charring was always accompanied by a nitrogen residue in the combusted sample. These results suggest that N-containing macromolecules (such as bovine serum albumin, phytoplankton, and degraded N-containing organic matter) are surviving the thermal pretreatment. Further studies revealed that charring in sodium citrate and bovine serum albumin could be minimized by physically grinding the sample to <38 μm size or dissolving the sample with water to disperse the compound among the sediment. Hence, oxygen accessibility is the key ingredient in determining what material will survive a 375°C thermal oxidation. In general, the 375°C method will underestimate the total BC content of a sediment sample (assuming no charring has occurred) by isolating only a fraction of the large BC particles in a sample and almost none of the small BC particles. By using a combination of endmember thermograms (humic acid and "BC with sediment"), a model (Eq. 2) was proposed to provide another reasonable estimate of the BC content in sediments. Overall, the Eq. 2-based model was able to extract reasonable values (BC/TOC <30%) for the OC and BC contents in several marine sediment samples; however, the model was unable to differentiate between similar carbon fractions. Finally, a second model (Eq. 5) was proposed (but not tested) based on kinetics to discriminate between the different carbon fractions in a sample by varying combustion time and temperature. Although future work is necessary, the models presented here are able to estimate reasonably the BC content.

3.8 ACKNOWLEDGMENTS

This work was supported by NSF Grant No BES-9800485 and OCE-00223441. The project, number RC-70, was also funded (in part) by the MIT Sea Grant College Program under a federal grant number NA86RG0074 from the National Sea Grant College Program, National Oceanic and Atmospheric Administration, US Department of

Commerce. Special thanks to Professor Sallie W. Chisholm and her laboratory for donating the stationary-phase *Prochlorococcus* culture, Ana Lucia C. Lima for generously providing sediment samples from the Pettaquamscutt River, RI, and Don Joyce Jr. Vice President of the Mid-continent Coal and Coke Company (Cleveland, OH) for donating the metallurgical coke sample. Thank you to Patrick Boisvert and Anthony Garratt-Reed of the MIT Center for Material Science and Engineering for the scanning electron microscope images (FEI/Philips XL30 FEG SEM); Krishna Gump and Heath Reimers of Porous Materials, Inc. for measuring surface area; Peter M. Oates for help with modeling on MATLAB; and Jeffrey Dick at University of California at Berkeley for providing thermodynamic data.

3.9 REFERENCES

1. Liousse, C.; Cachier, H. *Environ. Tech.* **1992**, *13,* 959-967.
2. Sumam, D. O.; Kulbusch, T. A. J.; Lim, B. *Marine sediments: A reservoir for black carbon and their use as spacial and temporal records of combustion* in *Sediment Records of Biomass Burning and Global Change.* J. S. Clark. **1994**, NATO ASI Series: *51,* 271-293.
3. Cooke, W. F.; Liousse, C.; Cachier, H. *J. Geophys. Res.* **1999**, *104,* 22137-22162.
4. Windsor, J. G.; Hites, R. A. *Geochim. Cosmochim. Acta* **1979**, *43,* 27-33.
5. Herring, J. R. *Charcoal fluxes into sediments of the North Pacific Ocean: The Cenozoic record of burning* in *The Carbon Cycle and Atmospheric CO2: Natural Variations Archean to Present.* E. T. Sundquist; W. S. Broecker. **1985**, American Geophysical Union: Washington D.C., 419-442.
6. Middelburg, J. J.; Nieuwenhuize, J.; Breugel, P. V. *Mar. Chem.* **1999**, *65,* 245-252.
7. Schmidt, M. W. I.; Noack, A. G. *Global Biogeochem. Cy.* **2000**, *14,* 777-793.
8. Goldberg, E. D. *Black Carbon in the Environment: Properties and Distribution.* **1985**, A Wiley-Interscience Publication, John Wiley & Sons: New York. 1-198.
9. Hedges, J. I.; Keil, R. G. *Mar. Chem.* **1995**, *49,* 81-115.
10. Falkowski, P.; Scholes, R. J.; Boyle, E.; Canadell, J.; Canfield, D.; Elser, J.; Gruber, N.; Hibbard, K.; Hogberg, P.; Linder, S.; Mackenzie, F. T.; Moore, B.; Pedersen, T.; Rosenthal, Y.; Seitzinger, S.; Smetacek, V.; Steffen, W. *Science* **2000**, *290,* 291-296.
11. Griffin, J. J.; Goldberg, E. D. *Geochim. Cosmochim. Acta* **1981**, *45,* 763-769.
12. Verardo, D. J. *Limnol. Oceanogr.* **1997**, *42,* 192-197.

13. Hedges, J. I.; Eglinton, G.; Hatcher, P. G.; Kirchman, D. L.; Arnosti, C.; Derenne, S.; Evershed, R. P.; Kogel-Knabner, I.; Leeuw, J. W. d.; littke, R.; Michaelis, W.; Rullkotter, J. *Org. Geochem.* **2000**, *31,* 945-958.
14. Gustafsson, Ö.; Gschwend, P. M. *Geochim. Cosmochim. Acta* **1998**, *62,* 465-472.
15. Accardi-Dey, A.; Gschwend, P. M. *Environ. Sci. Technol.* **2003**, *37,* 99-106.
16. Masiello, C. A.; Druffel, E. R. M. *Science* **1998**, *280,* 1911-1913.
17. Williams, P. M.; Druffel, E. R. M. *Nature* **1987**, *330,* 246-248.
18. Raymond, P. A.; Bauer, J. E. *Org. Geochem.* **2001**, *32,* 469-485.
19. Currie, L. A.; Benner, B. A.; Kessler, J. D.; Klinedinst, D. B.; Klouda, G. A.; Marolf, J. V.; Slater, J. F.; Wise, S. A.; Cachier, H.; Cary, R.; Chow, J. C.; Watson, J.; Druffel, E. R. M.; Masiello, C. A.; Eglinton, T. I.; Pearson, A.; Reddy, C. M.; Gustafsson, O.; Quinn, J. G.; Hartmann, P. C.; Hedges, J. I.; Prentice, K. M.; Kirchstetter, T. W.; Novakov, T.; Puxbaum, H.; Schmid, H. *J. Res. Natl. Inst. Stan.* **2002**, *107,* 279-298.
20. Gustafsson, Ö.; Haghseta, F.; Chan, C.; MacFarlane, J.; Gschwend, P. M. *Environ. Sci. Technol.* **1997**, *31,* 203-209.
21. Gustafsson, Ö.; Bucheli, T. D.; Kukulska, Z.; Anderson, M.; Largeau, C.; Rouzaud, J. N.; Reddy, C. M.; Eglinton, T. E. *Global Biogeochem. Cy.* **2001**, *15,* 881-890.
22. Reddy, C. M.; Pearson, A.; Xu, L.; McNichol, A. P.; Benner, B. A.; Wise, S. A.; Klouda, G. A.; Currie, L. A.; Eglinton, T. I. *Environ. Sci. Technol.* **2002**, *36,* 1774-1782.
23. Gelinas, Y.; Prentice, K. M.; Baldock, J. A.; Hedges, J. I. *Environ. Sci. Technol.* **2001**, *35,* 3519-3525.
24. Nguyen, T. H.; Brown, R. A.; Ball, W. P. *Org. Geochem.* ***submitted.***
25. Muri, G.; Cermelj, B.; Faganeli, J.; Brancelj, A. *Chemosphere* **2002**, *46,* 1225-1234.
26. Schmidt, M. W. I.; Skjemstad, J. O.; Czimczik, C. I.; Glaser, B.; Prentice, K. M.; Gelinas, Y.; Kuhlbusch, T. A. J. *Global Biogeochem. Cy.* **2001**, *15,* 163-167.
27. Jonker, M. T. O.; Koelmans, A. A. *Environ. Sci. Technol.* **2002**, *36,* 3725-3734.
28. Glaser, J. A.; Foerst, D. L.; McKee, G. D.; Quave, S. A.; Budde, W. L. *Environ. Sci Technol.* **1981**, *15,* 1426-1435.
29. Lima, A. L. C.; Eglinton, T. I.; Reddy, C. M. *Environ. Sci. Technol.* **2003**, *37,* 53-61.
30. Griffin, J. J.; Goldberg, E. D. *Limnol. Oceanogr.* **1975**, *20,* 456-463.
31. Accardi-Dey, A.; Gschwend, P. M. *Environ. Sci. Technol.* **2002**, *36,* 21-29.
32. Muller, P. J. *Geochim. Cosmochim. Acta.* **1977**, *41,* 765-776.
33. Ruttenberg, K. C.; Goni, M. A. *Mar. Geol.* **1997**, *139,* 123-145.
34. Meuzelaar, H. L. C.; Haverkamp, J.; Hileman, F. D. *Pyrolysis Mass Spectrometry of Recent and Fossil Biomaterial.* **1982**, Elsevier Scientific Publishing Company: Amsterdam, The Netherlands. *3*, 1-281.
35. Eglinton, T. I.; Boon, J. J.; Minor, E. C.; Olson, R. J. *Marine Chem.* **1996**, *52,* 27-54.
36. Johnson, W. R.; Nedlock, J. W.; Hale, R. W. *Tobacco Sci.* **1973**, *17,* 89-92.

37. Turco, R. P. *Earth Under Siege: From Air Pollution to Global Change.* **1997**, Oxford University Press: New York. 1-527.
38. Barin, I. *Thermochemical Data of Pure Substances.* **1993**, V.C.H. Verlagsgesellschaft: Germany. *Part 1 & 2*
39. Helgeson, H. C.; Owens, C. E.; Knox, A. M.; Richard, L. *Geochim. Cosmochim. Acta* **1998**, *62,* 985-1081.
40. Holmen, B. A.; Gschwend, P. M. *Environ. Sci. Technol.* **1997**, *31,* 105-113.
41. Brassell, S. C.; Lewis, C. A.; Deleeuw, J. W.; Delange, F.; Damste, J. S. S. *Nature* **1986**, *320,* 160-162.
42. Damste, J. S. S.; Tenhaven, H. L.; Deleeuw, J. W.; Schenck, P. A. *Org. Geochem.* **1986**, *10,* 791-805.
43. Kohnen, M. E.; Damste, J. S. S.; Deleeuw, J. W. *Nature* **1991**, *349,* 775-778.
44. Abbott, G. D.; Lewis, C. A.; Maxwell, J. R. *Nature* **1985**, *318,* 651-653.
45. Schmid, J. C.; Connan, J.; Albrecht, P. *Nature* **1987**, *329,* 54-56.
46. McCollom, T. N.; Simoneit, B. R. T.; Shock, E. L. *Energ. Fuel* **1999**, *13,* 401-410.
47. Bucheli, T. D.; Gustafsson, Ö. *Environ. Sci. Technol.* **2000**, *34,* 5144-5151.
48. Dembicki, H.; Horsfield, B.; Ho, T. *AAPG Bull.* **1983**, *67,* 1094-1103.
49. Peters, K. E. *AAPG Bull.* **1986**, *70,* 318-329.
50. Burnham, A. K.; Oh, M. S.; Crawford, R. W.; Samoun, A. M. *Energ. Fuel* **1989**, *3,* 42-55.
51. Solomon, P. R.; Serio, M. A.; Carangelo, R. M. *J. Anal. Appl. Pyrol.* **1991**, *19,* 1-14.
52. Vorres, K. S. *Users Handbook for the Argonne Premium Coal Sample Program.* **1990**, Argonne National Laboratory: Argonne, IL.
53. Smith, I. W. *The combustion rates of coal chars: A review* in *Nineteenth Symposium (International) on Combustion.* **1982**, The Combustion Institute: Philadelphia. *19,* 1045-1065.
54. Peterson, R. C. *The oxidation rate of diesel particulate which contains lead* in *International Congress and Exposition.* **1987**, Society of Automotive Engineers, Inc.: Detroit, Michigan. *870628,* 1-20.
55. Wicke, B. G.; Wong, C.; Grady, K. A. *Combust. Flame* **1986**, *66,* 37-46.
56. Adschiri, T.; Nozaki, T.; Furusawa, T.; Zi-bin, Z. *AIChE Journal* **1991**, *37,* 897-904.
57. Zhuang, Q. L.; Kyotani, T.; Tomita, A. *Energ. Fuel* **1994**, *8.*
58. Neeft, J. P. A.; Makkee, M.; Moulijn, J. A. *Fuel* **1998**, *77,* 111-119.
59. Otto, K.; Sieg, M. H.; Zinbo, M. *The oxidation of soot deposits from diesel engines.* **1980**, Society of Automotive Engineers, Inc.: Warrendale, PA. *800336,* 277-289.
60. Stanmore, B. R.; Brihac, J. F.; Gilot, P. *Carbon* **2001**, *39,* 2247-2268.
61. Kapteijn, F.; Moulijn, J. A. *Kinetics of catalyzed and uncatalyzed coal gasification* in *Carbon and Coal Gasification.* J. L. Figueiredo; J. A. Moulijn. **1986**, Martinus Nijhoff Publishers: Dordrecht, The Netherlands. *NATO ASI Series (Series E: Applied Science),* 291-360.

62. Neeft, J. P. A.; Nijhuis, T. X.; Smakman, E.; Makkee, M.; Noulijn, J. A. *Fuel* **1997**, *76,* 1129-1136.
63. Bhatia, S. K.; Perlmutter, D. D. *AIChE Journal* **1980**, *26,* 379-385.
64. Ishiguro, T.; Suzuki, N.; Fujitani, Y.; Morimoto, H. *Combust. Flame* **1991**, *85,* 1-6.
65. Gilot, P.; Bonnefoy, F.; marcuccilli, F.; Prado, G. *Combust. Flame* **1993**, *95,* 87-100.
66. Floess, J. K.; Longwell, J. P.; Sarofim, A. F. *Energ. Fuel* **1988**, *2,* 18-26.
67. Wood, D. A. *AAPG Bull.* **1988**, *72,* 115-134.
68. Quigley, T. M.; Mackenzie, A. S. *Nature* **1988**, *333,* 549-552.
69. Lewan, M. D.; Ruble, T. E. *Org. Geochem.* **2002**, *33,* 1457-1475.
70. Marcuccilli, F.; Gilot, P.; Stanmore, B.; Prado, G. *Experimental and theoretical study of diesel soot reactivity* in *Twenty-fifth Symposium (International) on Combustion.* **1994**, The Combustion Institute: Philadelphia. *25*, 619-626.

CHAPTER 4: LITERATURE REVIEW: SORPTION OF POLYCYCLIC AROMATIC HYDROCARBONS TO SEDIMENTS AND SOILS

4.1 ABSTRACT

Historical advancements in the sorption field were made in the late 1970s when Karickhoff *et al.* and Chiou *et al.* proposed that the organic carbon content in sediments and soils controlled the sorption of hydrophobic chemicals by acting as a partitioning medium. Based on this model, sorbates display linear isotherms, do not compete with other hydrophobic sorbates, and exhibit reversible exchanges. Moreover, the partitioning model (f_{oc} K_{oc} where f_{oc} equals the organic carbon fraction and K_{oc} is the organic carbon-normalized distribution coefficient (L/kg)) assumes that all organic carbon in sediments and soils possesses the same affinity for a given sorbate. However, new research has shown that geologically older material ("hard carbon") sorbs hydrophobic chemicals more strongly than younger material ("soft carbon"), which contains a larger aliphatic carbon content and more polar groups. To account for these two carbon groups, Weber *et al.* proposed that sorption of hydrophobic chemicals is the sum of two mechanisms: absorption and adsorption. Here, after an extensive literature review of sorption, black carbon (BC) in the environment is proposed to act as a strong adsorbent of hydrophobic chemicals, such as PAHs.

4.2 INTRODUCTION: ORGANIC CARBON AS A PARTITIONING MEDIUM

The idea that organic matter could behave like an organic solvent for partitioning sorbate was pioneered in the early 1960s by Lambert *et al.* [1]. Similar to an octanol-water system, nonpolar organic compounds would distribute themselves between the aqueous phase and an organic sorbent due to the incompatibility of the sorbate with the aqueous phase [2, 3]. Based on this concept, Karickhoff *et al.* and Chiou *et al.* proposed that the organic carbon (OC) in soils and sediment beds should govern the sorption of hydrophobic organic compounds in the environment [4, 5]. (Note that in the OC definition used here, the OC fraction unknowingly contained black carbon.) Moreover, if chemicals were partitioning between the aqueous phase and the solid phase, then the system should display linear isotherms, reversible desorption, and no competition with other sorbates. Competition is absent in a partitioning system since the sorbates are not competing for specific sorption sites but rather absorbing into the media. The slope of the isotherm (with a zero intercept), or the solid-water distribution coefficient (K_d, L/kg), equals then the ratio between the sorbed concentration (Cs, μg/kg) and the dissolved concentration (C_w, μg/L; Eq. 1).

$$K_d = \frac{C_s}{C_w} \qquad \text{(Eq. 1)}$$

To illustrate that the isotherms were linear and not Langmuirian, sorption experiments by Karickhoff *et al.* were conducted at high sorbate concentrations, typically 10-50% of the sorbate solubility [4]. In addition, experiments were incubated for 1 day, and isotherms were constructed with only 4-5 data points (Figure 1). Although current researchers understand that these experimental conditions emphasized sorbate partitioning [6, 7], the work by Karickhoff *et al.* advanced the sorption field by emphasizing the potential that organic matter can act as a partitioning medium. Concurrent work by Chiou *et al.* [2, 8] and Means *et al.* [9] also reported linear isotherms for an array of hydrophobic compounds, thus disproving that adsorption to mineral surfaces was the dominant sorption mechanism in sediments containing organic matter. Meanwhile, Chiou *et al.* [8] showed that their single-solute isotherms remained linear in a

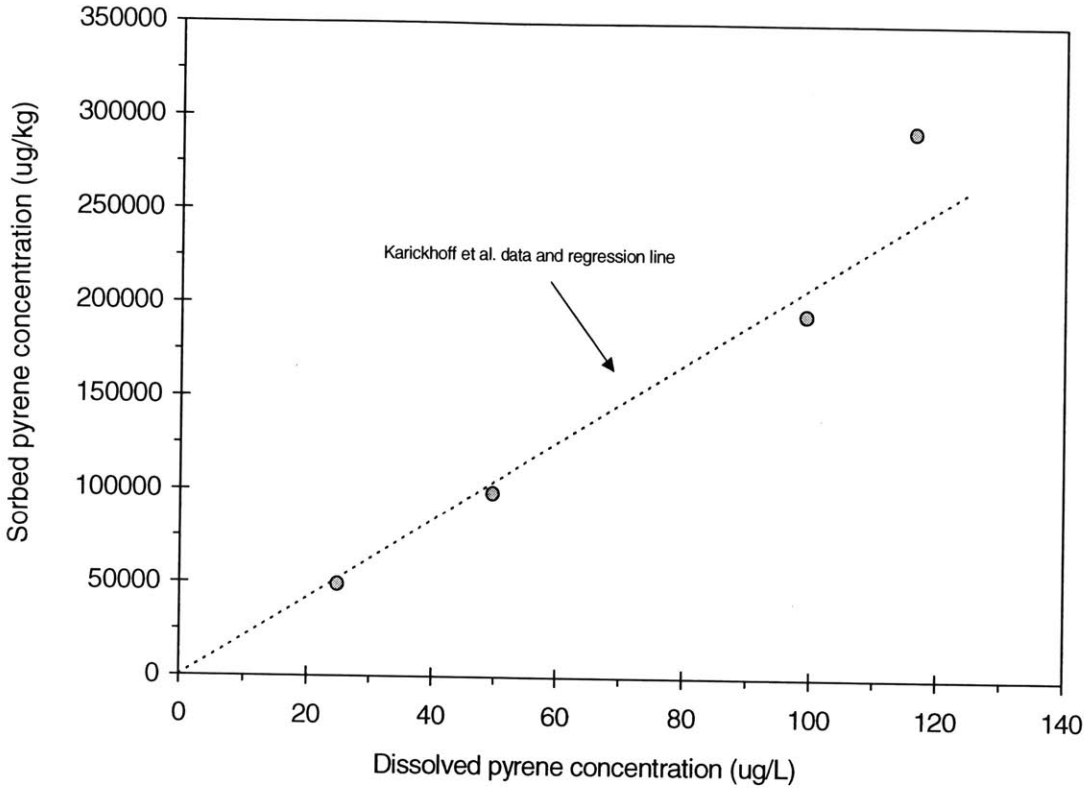

Figure 1: Reported pyrene sorption data (filled circles) by Karickhoff *et al.* (1979) Water Res. and corresponding regression line (K_d = 2,100 L/kg). Sorption experiments incubated for 1 day.

binary (nonpolar chemical) system, indicating that competition between the solutes was absent – a key component in the partitioning theory. Future work by Huang and Weber reported that phenanthrene sorption into Chelsea humic acid was linear and displayed no desorption hysteresis, providing more evidence that sorbates are partitioning into organic matter [10].

In addition to reporting linear isotherms, scientists discovered that their distribution coefficients were a function of the OC content, regardless of the other physical properties of the sorbent. For example, a clear correlation ($R^2 = 0.84$, [9]; Figure 2) exists between the pyrene distribution coefficient and the total OC content for a suite of EPA sediment/soil samples that possessed a range of surface areas (49-269 m^2/g [11]) and mineral compositions (0.01-0.25 Al wt % [12]). Further work by Mader *et al.*, who explored PAH sorption onto aluminum and iron oxides, showed that when the OC content was >0.01 wt % the contribution from PAH partitioning into the OC fraction was more significant (>90%) than adsorption to mineral surfaces [13]. If the OC content is controlling sorption, then Karickhoff *et al.* proposed that the distribution coefficient should be normalized to the OC fraction (f_{oc}, kg_{oc}/kg_{solid}) to define a new variable, K_{oc} (L/kg_{oc}), which reflects the affinity of hydrophobic chemicals to an organic medium (Eq 2; [3, 4, 5]).

$$\frac{K_d}{f_{oc}} = K_{oc} = \frac{\gamma_w V_w}{\gamma_{oc} V_{oc} \rho_{oc}} \qquad \text{(Eq. 2)}$$

Here, the activity coefficients, γ_w and γ_{oc}, represent the incompatibility of the sorbate for the given phase versus a pure liquid of itself while the OC density (ρ_{oc}, kg/L), the molar volume of water (V_w, L/mol), and the molar volume of OC (V_{oc}, L/mol) are constants. If a given chemical has the same affinity for all organic matter, then the K_{oc} value for that chemical should remain constant and depend solely on the chemical's incompatibility with the aqueous phase. For example, the measured log K_{oc} values for pyrene remains relatively constant (4.8 ±0.2 logarithm units, Z = 15) for a suite of sediment/soil samples measured by two different investigators [5, 9].

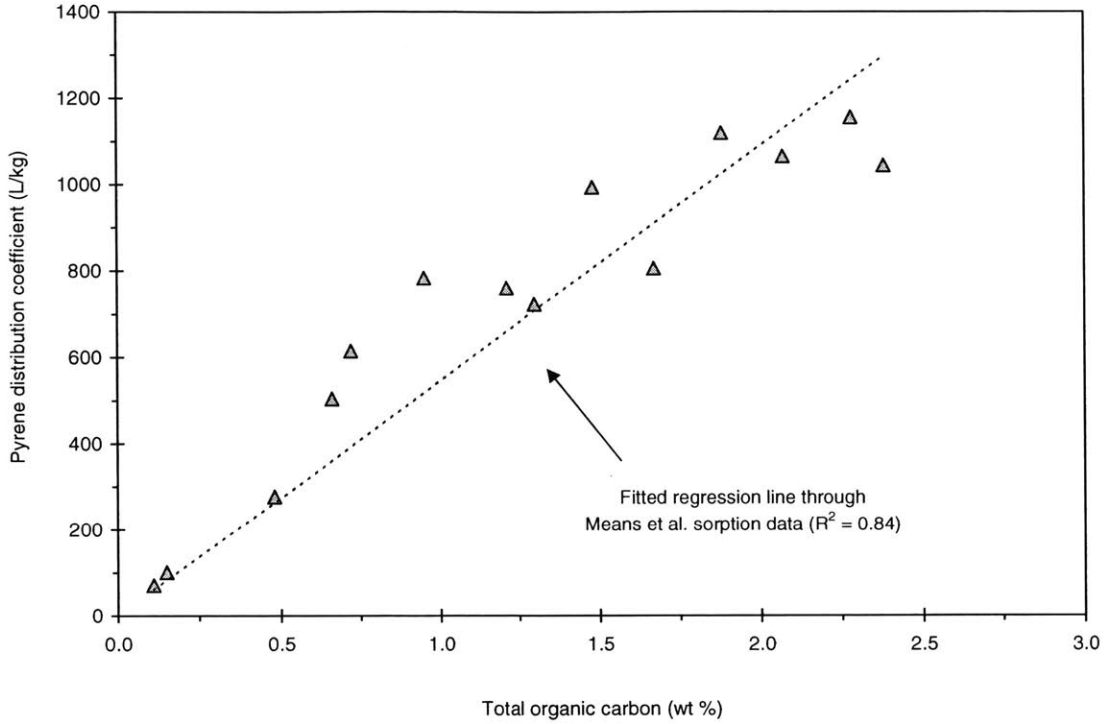

Figure 2: Reported pyrene distribution coefficients (filled triangles; L/kg) by Means *et al.* (1980) Environ. Sci. Technol. and corresponding total organic carbon contents (weight percentage) for a suite of EPA sediment and soil standards with the fitted regression line (forced through zero) and correlation coefficient. Sorption experiments incubated for 1 day.

The simplicity of the $f_{oc} K_{oc}$ model to predict the sorption of hydrophobic organic chemicals based purely on partitioning has influenced a variety of research fields. Oceanographers have developed sediment quality criteria/guidelines to evaluate if coastal sediments are polluted to the extent that benthic organisms are endangered [14, 15]. Biologists have instituted biota-sediment accumulation factors to predict the accumulation of toxic chemicals in marine organisms, assuming that chemicals exist in equilibrium between the lipid content of the biota, the OC content of sediment, and the aqueous phase [16]. The $f_{oc} K_{oc}$ model has also influenced other fields outside oceanography. For example, engineers and hydrologists have incorporated $f_{oc} K_{oc}$ into their models to determine the extent that sorption will retard the transport of chemicals in groundwater systems [17, 18, 19].

Chemists have also constructed empirical formulas to estimate log K_{oc} values from octanol-water partitioning coefficients (log K_{ow}) and the aqueous solubility coefficient ([20] and references therein) to predict how chemicals partition in the environment. However, recent work by Pontolillo and Eganhouse (and later reviewed by Renner) reported the alarming uncertainty in the octanol-water partitioning coefficient and the aqueous solubility coefficient for two hydrophobic chemicals (*p,p′*-dichlorodiphenyldichloroethene (DDE) and *p,p′*-dichlorodiphenyltrichloroethane (DDT)) [21, 22]. This uncertainty will therefore propagate to large uncertainties in calculating log K_{oc} values. An extensive compilation of published DDE and DDT values by Pontolillo and Eganhouse revealed that the aqueous solubility and octanol-water partitioning coefficients varied by 2-4 logarithm units over the past 40 years. Moreover, the reported magnitude for these two coefficients has decreased over time. Pontolillo and Eganhouse attributed the uncertainty in the aqueous solubility and octanol-water partitioning coefficients to (1) multi-level referencing, (2) citation errors, and (3) data errors. For example, they noted that in reported compilation reviews 6-23% of the total aqueous solubility data and 14-26% of the total octanol-water partitioning data were the directly measured values [21]. The remaining data in these compilation reviews consisted primarily of multi-level referencing and redundancy. The authors also noted

that the inclusion of erroneous data artificially lowers the standard deviation and the confidence level of the average reported value for the aqueous solubility and octanol-water partitioning coefficients.

In addition to redundant referencing, Pontolillo and Eganhouse also highlighted the notably bad quality of data in the literature, and they suggested that 95-100% of database literature is plagued with experimental errors [21]. For example, aqueous solubility values are measured at "ambient temperature," which can range from 18-25°C. Additionally, octanol-water partitioning coefficients are measured traditionally with the shake-flask method leaving residue octanol in the aqueous phase, which can then act as a detergent. Moreover, the authors noted a steady trend of computational methods to determine aqueous solubility and partitioning coefficients instead of direct measurements. Although the authors only focused on two hydrophobic chemicals (DDT and DDE), similar uncertainties are expected to occur for the aqueous solubility and octanol-water partitioning coefficients of other organic compound classes, including PAHs. Hence, calculated log K_{oc} values reported in the literature as well as in this thesis will have a certain degree of uncertainty (possibly as large as 2-4 logarithm units) due to propagation of error.

4.3 DIFFERENT CARBONACEOUS SORBENTS

Unfortunately, the underlying assumption of the $f_{oc} K_{oc}$ model – that all organic matter in the environment is the same – is flawed. Degradation and diagenesis are known to alter the elemental composition and structure of organic matter. For example, organic matter settling into sediment beds will degrade into simple biopolymers (carbohydrates and proteins), then condense to complex humic substances, and ultimately convert to kerogen through diagenesis [19, 23]. These processes tend to increase the C/O molar ratio and the C/N molar ratio as the carbon content increases due to polymerization and as polar functional groups weather away [24]. Hence, geologically older organic matter will be more nonpolar and will have a stronger sorption capacity than geologically younger organic matter.

Several researchers have illustrated that geologically older sorbents tend to sorb hydrophobic chemicals more strongly than geologically younger material. For example, Rutherford *et al.* showed that the log K_{oc} for benzene increased as the C/O molar ratio increased from 1.2 to 3.0 [25]. Similar results were observed for Huang and Weber who noted that the log K_{oc} for phenanthrene increased from 4.0 for peat to 5.1 for shale [10] as the C/O molar ratio increased and the aliphatic carbon content decreased (Table 1). For example, they observed that shales had a larger aromatic carbon content (41%) than peats (17%), and that shales contained less carboxyl and aliphatic carbon (59%) than peats (84%) [10]. Further work by Kile *et al.* and Chiou *et al.* suggests that the log K_{oc} value for soils may be less than the corresponding log K_{oc} for sediments [26, 27]. For example, Kile *et al.* reported that the average K_{oc} value for carbon tetrachloride was 60 ±7 on 32 soil samples, whereas the average K_{oc} value on 36 sediment samples was 102 ±11 [26]. To explain this K_{oc} discrepancy (0.3 logarithm units), Chiou *et al.* showed that soils contained more polar functional groups and less aromatic carbon than sediments, which made soils a less favorable partitioning medium than sediment.

In this investigation (Figure 3), single-point log K_{oc} values were calculated from the literature for phenanthrene sorption onto a spectrum of carbonaceous material. It is shown that the log K_{oc} for phenanthrene varied 2 logarithm units from 3.6 to 5.6 for partitioning into cellulose to activated carbon (Figure 3; Note that the octanol-water distribution coefficient is included in the figure as a reference.) Although the log K_{oc} estimated by Karickhoff *et al.* (4.2; dashed bar in Figure 3) can predict phenanthrene sorption into peat, and possibly humic acid or low-grade coal, previous estimations cannot accurately predict phenanthrene sorption to more condensed carbons, like activated carbon, diesel soot, and kerogen.

Similar results were reported by Kleineidam *et al.* for phenanthrene sorption onto a suite of sediment samples and sedimentary rocks with log K_{oc} values ranging from 4.0 to 6.8 (Figure 4). In their work, particles were classified by their lithocomponents, and the thermal maturity of the organic matter was determined with fluorescence. Several types of organic matter were identified, but their data could be divided into three regimes:

Table 1: Reported log K_{oc} values (L/kg) for phenanthrene partitioning into various sorbents along with the C/O molar ratio of the sorbent and the percent carbon type in the sorbent as measured with ^{13}C-NMR spectroscopy (Huang and Weber (1997) Environ. Sci. Technol.)

	log K_{oc} (L/kg) [a]	C/O mole Ratio	^{13}C-NMR Percent Carbon Type		
			Aliphatic[b]	Aromatic	Carboxyl
Chelsea Humic Acid	3.9	1.7	56	22	22
Average Peat (Z = 2)	4.0	1.6	75	17	9
Houghton Much Soil	4.0	1.8	NA	NA	NA
Average Shale (Z = 3)	5.1	NA [c]	59	41	0
Average Kerogen (Z = 3)	5.2	6.1	NA	NA	NA

a: For phenanthrene, single-point log K_{oc} values were calculated with the literature Freundlich coefficient and Freundlich exponent at a dissolved concentration of 1,000 µg/L.

b: The percent "aliphatic carbon" includes both unsubstituted and substituted aliphatic carbon.

c: NA equals "not available"

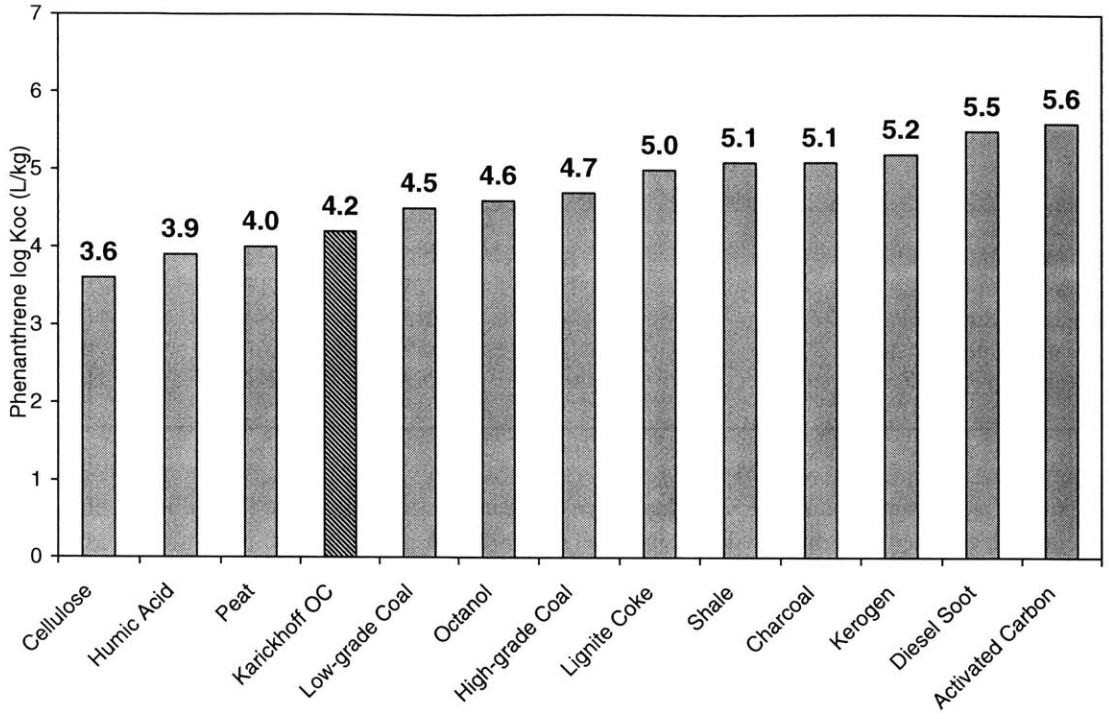

Figure 3: Calculated log K_{oc} values (from the literature) for the partitioning of phenanthrene into a spectrum of carbonaceous materials. If a nonlinear isotherm were reported in the literature, then single-point log K_{oc} values were calculated at the dissolved phenanthrene concentration of 1,000 μg/L to focus on phenanthrene partitioning rather than adsorption. The hashed bar (4.2) represents the expected log K_{oc} value calculated by Karickhoff's using the following Koc/Kow relationship: log K_{oc} = 0.989 log K_{ow} – 0.354. Literature reference: cellulose in LeBoeuf *et al.* (1997) Environ. Sci. Technol.; humic acid, shale, and kerogen in Huang and Weber (1997) Environ. Sci. Technol.; peat, low-grade coal, high-grade coal, coke, charcoal, and activated carbon in Kleineidam *et al.* (2002) Environ. Sci. Technol.; octanol in Schwarzenbach *et al.* (1993) in Environmental Organic Chemistry; and diesel soot in Bucheli and Gustafsson (2002) Environ. Sci. Technol.

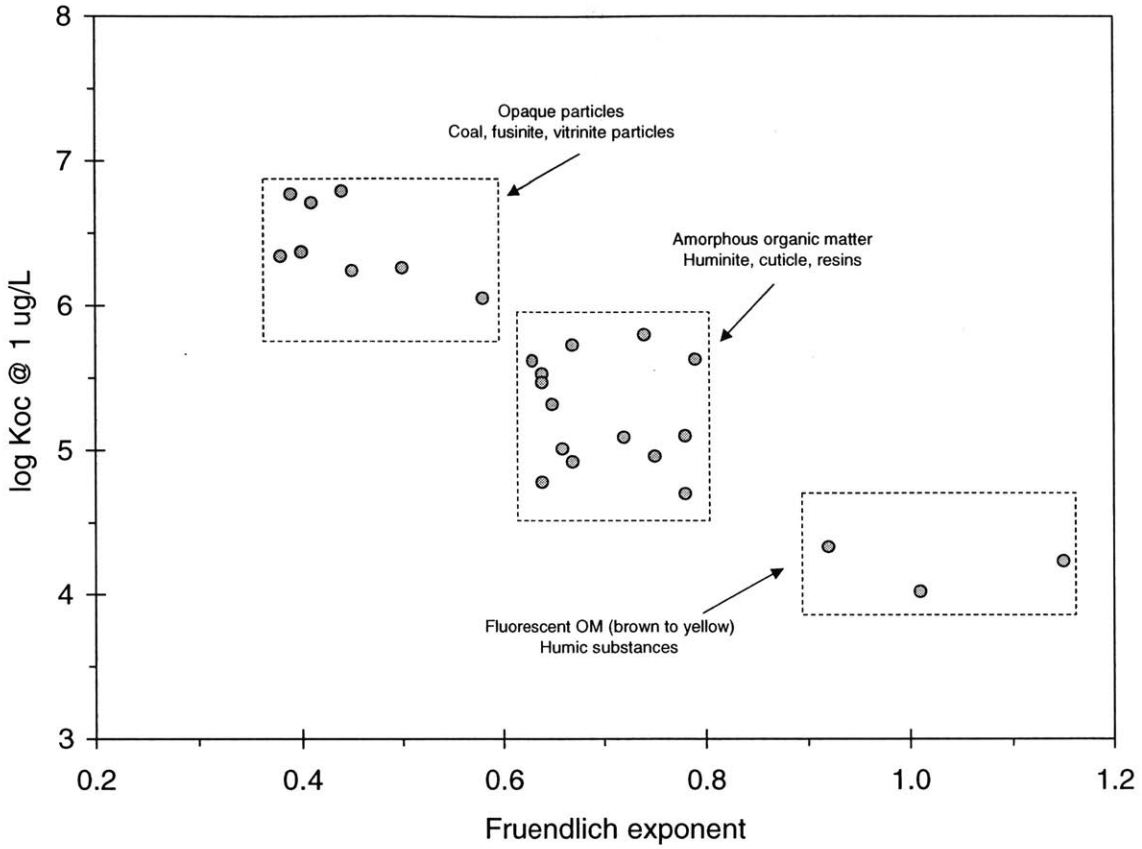

Figure 4: Reported phenanthrene sorption data (filled circles) by Kleineidam *et al.* (1999) Environ. Sci. Technol. plotted here as single-point log K_{oc} values calculated at 1 µg/L versus the Freundlich exponent. Based on the reported maturity of the organic matter, the data is subdivided with three dotted boxes to distinguish three organic carbon facies.

humic substances, amorphous organic matter, and condensed carbon particles (Figure 4). Kleineidam *et al.* observed that phenanthrene sorption onto humic substances (young carbon) displayed linear isotherms (Freundlich exponent ≈ 1) with measured log K_{oc} values equal to Karickhoff's expected log K_{oc} values (4.2). However, sorption onto more condensed, older carbon was nonlinear (Freundlich exponent <1) with measured log K_{oc} values exceeding expected values (Figure 4). Their work suggests that while phenanthrene may partition into the labile OC fraction, adsorption will dominate on more condensed carbon types.

4.4 ADSORPTION AND NONLINEAR ISOTHERMS

The adsorption of hydrophobic chemicals onto condensed carbon (or hard carbon) in sediments and soils was introduced by Grathwohl and Weber *et al.* [24, 28]. Weber *et al.* modified the traditional $f_{oc} K_{oc}$ model by proposing that the overall solid-water distribution coefficient reflected the sum of two mechanisms: absorption into a labile "soft carbon" and adsorption onto a "hard carbon." Since then, a range of dual-sorption models and theories has been proposed to explain the observed nonlinear sorption of hydrophobic chemicals [6, 29, 30, 31, 32]. One common conceptualization of adsorption is a sum of Langmuir isotherms, which is expressed as a Freundlich model where the exponent describes the distribution of adsorption sites (Eq. 3).

$$C_s = x_L K_L C_w + x_F K_F C_w^n \qquad \text{(Eq. 3)}$$

Here, x_L represents the mass fraction of the solid phase exhibiting linear sorption and K_L (L/kg) represents the linear solid-water distribution coefficient. The Freundlich distribution coefficient (K_F, $(\mu g/kg)/(\mu g/L)^n$), the Freundlich exponent (n), and x_F, which represents the mass fraction that exhibits nonlinear sorption, describe the adsorption of hydrophobic chemicals.

The most critical aspect of the dual sorption model is the implication that the overall solid-water distribution coefficient (K_d) is a function of the dissolved concentration. For example, if the isotherm for a hydrophobic chemical sorbing to organic matter is nonlinear (reflecting absorption and adsorption), then a Freundlich

isotherm would be the most economical model (e.g. incorporate the least number of parameters) to describe the overall dependency of the sorbed concentration on the dissolved concentration (Eq. 4a). Here, the Freundlich distribution coefficient (K_F) is a constant and independent of the dissolved concentration. However, if this expression is rewritten in terms of K_d (Eq. 4b), then the new equation shows that K_d is indeed dependent on the dissolved concentration while K_F remains independent.

$$C_s = K_F C_w^n \qquad \text{(Eq. 4a)}$$

$$\frac{C_s}{C_w} = \frac{K_F C_w^n}{C_w}$$

$$\text{or, } K_d = K_F C_w^{n-1} \qquad \text{(Eq. 4b)}$$

Therefore, the value of K_d (or K_{oc} when K_d is normalized) will increase as the dissolved concentration decreases, and K_d values can only be compared at the same unit concentration.

For example, for a set of nonlinear phenanthrene isotherms (Freundlich exponent ranging from 0.55 to 0.89) the single-point log K_{oc} values calculated at 1 μg/L are distinctly greater than the corresponding log K_{oc} values calculated at 1,000 μg/L (Figure 5; [33]). Moreover, the log K_{oc} values at 1 μg/L increase sharply as nonlinearity increases (or the Freundlich exponent decreases) as expressed by the strong correlation coefficient ($R^2 = 0.85$). In other words, as the heterogeneity of adsorption sites increases (Freundlich exponent decreases), more phenanthrene is adsorbed, and the log K_{oc} value increases accordingly. However, at high concentrations (1,000 μg/L) the log K_{oc} values do not change as expressed by a shallow regression slope and low correlation coefficient ($R^2 = 0.25$). The average log K_{oc} value at 1,000 μg/L equals 4.4 ±0.2, which is within error of Karickhoff's expected log K_{oc} for phenanthrene (4.2). These results suggest that at high concentrations, even if a strong adsorbent is present, the dominant sorption mechanism is partitioning assuming all the adsorption sites are now saturated. Xia and Ball also noted that at dissolved concentration greater than 10% solubility, partitioning

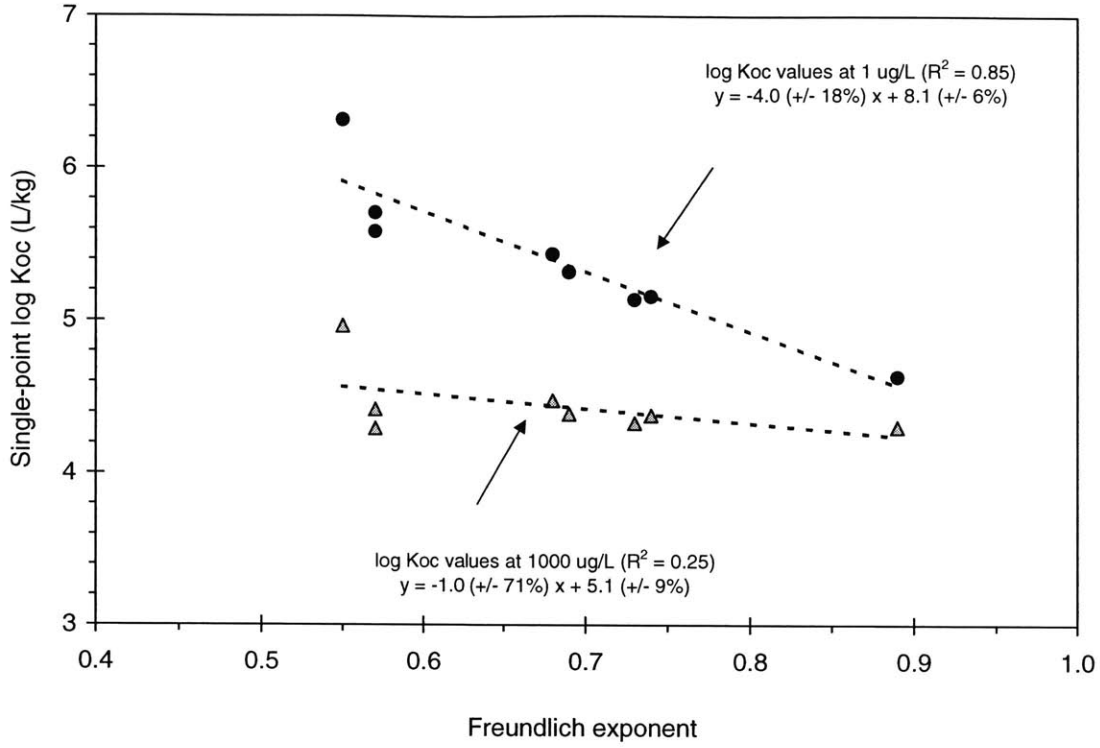

Figure 5: Reported phenanthrene sorption data by Karapanagioti *et al.* (2000) Environ. Sci. Technol. plotted here as single-point log K_{oc} values calculated at 1 µg/L (black circles) and 1,000 µg/L (filled triangles) versus the Freundlich exponent along with the fitted regression lines and correlation coefficients.

will account for more than 80% of the total sorption phenomena (for a group of PAHs and chlorobenzenes compounds) [6].

4.4.1 Hard Carbon versus Soft Carbon. Since natural sediment and soil samples are heterogeneous and contain both absorbents and adsorbents, isotherms reflect this heterogeneity. Recently, LeBoeuf and Weber proposed that "soft" and "hard" carbons were analogous to "rubbery" and "glassy" polymers where diagenesis converts young, expandable, lightly cross-linked, "rubbery" organic matter into a more condensed, highly cross-linked, aromatic, "glassy" organic matter [34, 35]. Chemicals could partition into "rubbery" organic matter because of its fluid, expandable nature; however, because of the condensed nature of "glassy" organic matter, chemicals would adsorb. Further work by Xing *et al.* showed that "glassy" sorbents exhibited a competitive nature in a binary system while "rubbery" sorbents did not, providing more evidence that chemicals are partitioning [36]. (Note that experiments performed by Xing *et al.* [36] and Xing and Pignatello [30] may not be in equilibrium since samples were incubated for only 2 days.) Hence, samples loaded with "rubbery" organic matter would have near linear isotherms (i.e., Freundlich exponent ranging from 0.8 to 1.0) with log K_{oc} values approaching values expected by Karickhoff. In contrast, samples loaded with "glassy" organic matter would have nonlinear isotherms (i.e., Freundlich exponents <0.8) and sorption capacities that exceed Karickhoff's log K_{oc} value [28].

In later work, Weber and Huang argued that while partitioning into soft/rubbery carbon had fast kinetics and could reach equilibrium within days, adsorption onto hard/glassy carbon has slow kinetics and requires a longer time scale to reach an apparent equilibrium due to restricted diffusion [7]. Brusseau *et al.* similarly suggested that the rate-limiting step in sorption was not transport, but intra-organic matter diffusion [37]. They described organic matter as possessing two domains: an instantaneous sorption zone and a rate-limited zone where sorption and desorption are hindered by the "pore" size of organic matter. These "pores," or internal microvoids as described by Xing *et al.*, are located in restricted regions, and over time, these holes becomes more accessible as

solute diffuses into the organic matrix [30]. Therefore, sorption experiments need to incubate longer than 1 day in order to observe adsorption.

To illustrate this change in linearity over time, Weber and Huang observed how the phenanthrene isotherm with EPA15 (sediment standard) would transition from a linear isotherm to a nonlinear isotherm during a 2-week period [7]. Initially, the Freundlich exponent equaled 1 and then decreased to a value of 0.7 over the following 2 weeks. Meanwhile, the Freundlich distribution coefficient increased with the final coefficient being twice as large as the coefficient measured after 1 day ([7, 38]). Interestingly, Karickhoff studied phenanthrene sorption onto the same EPA15 sediment sample and reported a K_{oc} value of 12,000 L/kg after a 1-day incubation [5]. With this information, Karickhoff's isotherm was plotted knowing that the dissolved phenanthrene concentration ranged from 10-50% of the solubility and that isotherms typically contained few data points (Figure 6; [4]). The overlap of Karickhoff's isotherm with the 1-day isotherm by Weber and Huang is remarkable. The plot illustrates how early researchers may have overlooked, or missed, the adsorption of phenanthrene onto sediments and soils when their protocols emphasized partitioning (short incubation times and high dissolved concentrations).

4.4.2 A Black Carbon Adsorbent. New research has suggested that a combustion-derived black carbon (BC), or a "high surface area carbonaceous material," may be responsible for the observed nonlinear isotherms of hydrophobic chemicals in the environment [6, 19, 39, 40, 41, 42] similar to the adsorption of hydrophobic chemicals onto activated carbon [43, 44]. BC is a collective term describing a spectrum of natural and anthropogenic combustion-derived particles, such as: coke, charcoal, wood char, soot, and ash. (As noted in Chapter 1, BC is a collective term representing thermally altered carbonaceous material. The term OC (or the "non-BC fraction") represents the biogenic/diagenetic carbonaceous material. The sum of these two carbon fractions represents the total organic carbon (TOC) content of a sample.) Once emitted into the environment, these particles are disseminated into soils and sediment. Due to their high

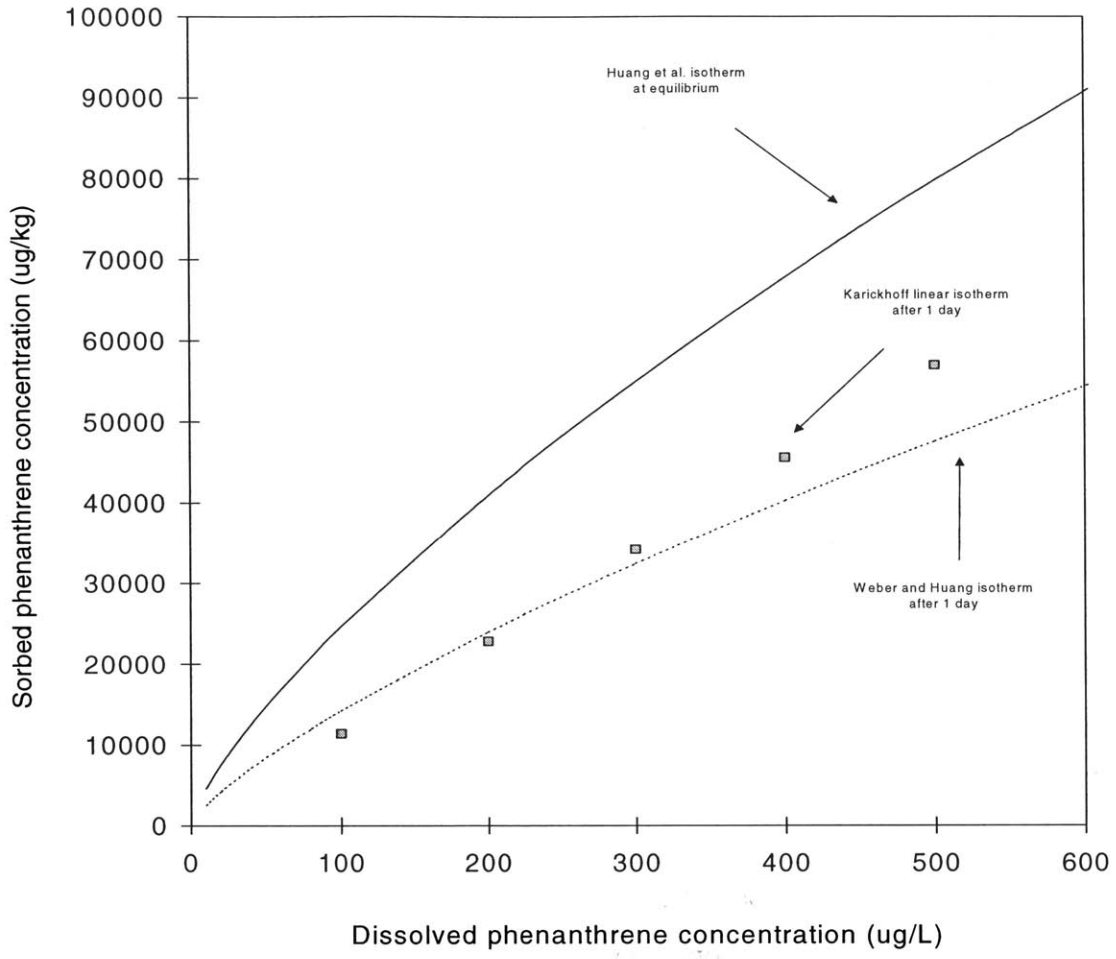

Figure 6: Reported phenanthrene isotherms onto EPA15 sediment standard. The dotted line represents the nonlinear isotherm reported by Weber and Huang (1996) for phenanthrene sorption after 1 day (K_F = 450 (μg/kg)/(μg/L)^n and n = 0.75). The solid line represents the nonlinear isotherm reported by Huang *et al.* (1997) for phenanthrene sorption at an apparent equilibrium (K_F = 854 (μg/kg)/(μg/L)^n and n = 0.73). The filled squares represents the linear isotherm reported by Karickhoff (1981) for phenanthrene sorption after 1 day (Koc = 12,000 l/kg). Linear isotherm constructed knowing the OC fraction of EPA15 (0.95 wt % C) and knowledge that Karickhoff's isotherms ranged from 10-50% of the phenanthrene solubility.

aromatic carbon content and low polar group content (denoted by high C/H and C/O molar ratios), BC particles are exceptionally strong adsorbents in the environment. For example, the logarithm BC-normalized distribution coefficients (K_{BC}, $(\mu g/kg)/(\mu g/\mu L)^n$) for the sorption of pyrene and phenanthrene onto soot (NIST SRM 1650, diesel particulate matter, assuming 77 wt % C) are 5.5 and 6.4, respectively [45]. These log K_{BC} values are more than 1 logarithm unit greater than the corresponding partitioning coefficient into natural organic matter, 4.2 and 4.7, respectively [5].

In an independent investigation here, it was observed in the work by Karapanagioti *et al.* that phenanthrene sorption to coal particles in a Canadian river aquifer accounted for more than 70% (at 10 μg/L) of the total sorption measured in the composite sample (Figure 7; [33]). Similar results were reported by Ghosh *et al.* who observed that coal/wood particles from a Milwaukee sediment accounted for 62% of the sorbed PAH concentration while only constituting 5% of the total mass [46]. Interestingly, when the sorption contributions are summed from all the particles observed by Karapanagioti *et al.*, the calculated isotherm approximated the measured isotherm for the composite sample. For example, the calculated Freundlich exponent and Freundlich coefficient for the sum of the particles equaled 0.63 and 1,400 $(\mu g/kg)/(\mu g/\mu L)^n$, respectively, whereas the corresponding values measured for the sediment sample were 0.65 and 1,100 $(\mu g/kg)/(\mu g/\mu L)^n$ [33]. This calculation supports the contention that the overall log K_d value represents the sum of two sorption mechanisms: adsorption onto BC and absorption into OC.

Adsorption to BC may explain field observations of unusually high sorbed concentrations and high log K_d values for a variety of hydrophobic compounds [42, 47]. For example, surficial marine sediment that surrounded an aluminum smelter plant in Canada contained >30,000 μg $\Sigma PAH/g_{oc}$ [48]. (As a point of reference, previous work by Swartz concluded that sorbed PAH concentrations exceeding the threshold of 10,000 μg $\Sigma PAH/g_{oc}$ can cause extreme adverse effects on the benthic community [49].) Sorbed PAH concentrations then decreased as a function of distance from the smelter plant as did the total carbon content in the sediment. Simpson *et al.* hypothesized that soot, coal dust,

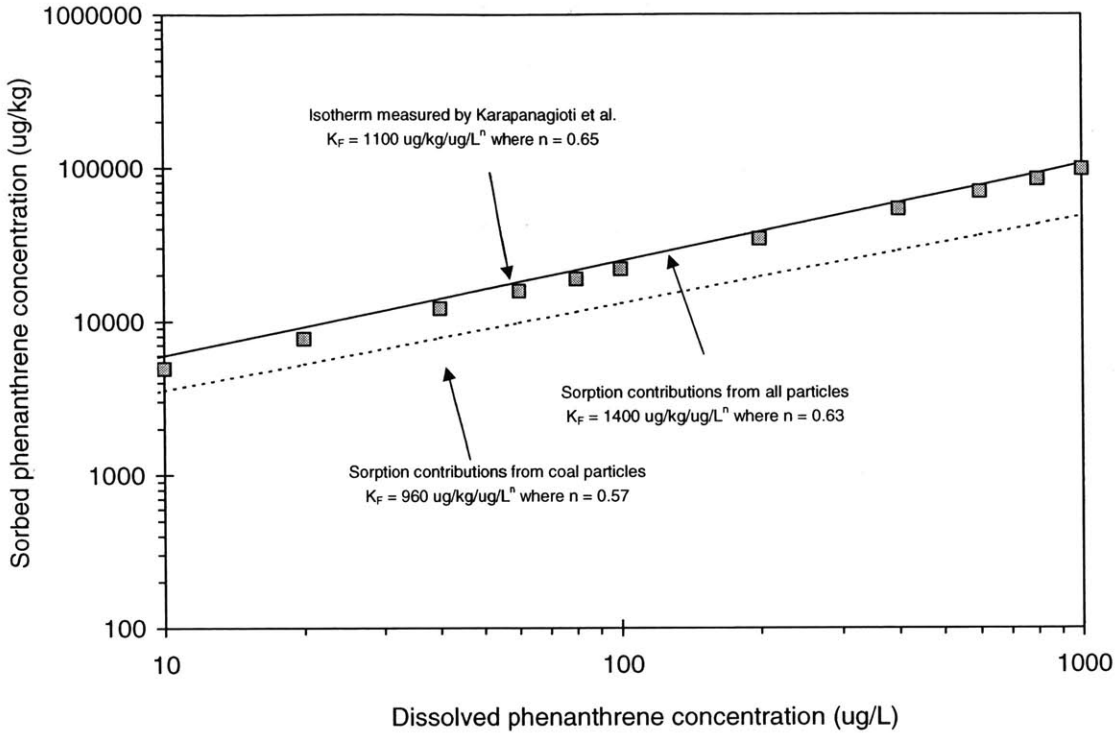

Figure 7: Reported phenanthrene isotherms by Karapanagioti *et al.* (2000) Environ. Sci. Technol. The dotted line represents the calculated isotherm for sorption onto coal particles (K_F = 960 (μg/kg)/(μg/L)^n and n = 0.57). The solid line represents the calculated isotherm for sorption onto all the particles (K_F = 1,400 (μg/kg)/(μg/L)^n and n = 0.63). The filled squares represent the measured isotherm on the composite sample (K_F = 1,100 (μg/kg)/(μg/L)^n and n = 0.65).

and tar balls emitted from the plant and settled in sediment beds near the plant may contribute to the intense sorbed PAH concentration [48]. However, no direct measurements of the BC content in the sediments were made.

Similar conclusions were made by Krauss *et al.* who measured the sorbed concentrations of PAHs and PCBs in Norwegian soils [50, 51]. They observed that for a given log K_{ow} value, the soils were enriched in PAHs relative to PCBs. This enrichment was attributed to the possible presence of BC in the soil, assuming that BC sorbed pyrogenic PAHs more strongly than PCBs. Jonker and Smedes observed the same phenomena between PAHs and PCBs in their lacustrine sediment sample (0-30 cm), but they noted that planar PCBs as well as PAHs and chlorobenzenes were enriched in the sediment relative to nonplanar PCBs [52]. For example, they report for their planar chemicals a K_{oc}/K_{ow} relationship of $\log K_{oc(estimate)} = 1.1 \log K_{ow} + 1.5$ ($R^2 = 0.92$) whereas for their nonplanar chemicals they report $\log K_{oc(estimate)} = 1.0 \log K_{ow} + 0.92$ ($R^2 = 0.95$). Note that log K_{oc} values were not directly measured, but were extrapolated from a methanol/water cosolvent experiment. Hence, for a given log K_{ow} value, the planar compound will sorb more strongly to the sediment than a nonplanar compound based on these reported parameters.

Although many scientists have inferred from their data that the presence of BC in the sediment or soil may explain unusually high sorbed concentrations of PAHs and other hydrophobic compounds [47], no work has been done to directly measure the BC-distribution coefficient for environmental BC. Previous investigators, such as Bucheli and Gustafsson [45] as well as Jonker and Koelmans [53] have made strides in measuring the log K_{BC} for various chemicals onto BC representatives. However, both investigating teams assumed linear BC isotherms and tested PAH sorption onto commercial products, which do not accurately depict BC in the environment. In the following thesis chapters (Chapters 5 and 6), the adsorption of PAHs onto environmental BC samples is explored, and the overall sorption of PAHs is explained with a dual sorption model that includes absorption into labile OC and adsorption onto a combustion-derived BC.

4.5 REFERENCES

1. Lambert, S. M.; Porter, P. E. *Weeds* **1965**, *13,* 185-190.
2. Chiou, C. T.; Peters, L. J.; Freed, V. H. *Science* **1979**, *206,* 831-832.
3. Schwarzenbach, R. P.; Gschwend, P. M.; Imboden, D. M. *Sorption: Solid-Aqueous Solution Exchange* in *Environmental Organic Chemistry*. **1993**, John Wiley & Sons, Inc.: New York. 255-341.
4. Karickhoff, S. W.; Brown, D. S.; Scott, T. A. *Water Res.* **1979**, *13,* 241-248.
5. Karickhoff, S. W. *Chemosphere* **1981**, *10,* 833-846.
6. Xia, G. S.; Ball, W. P. *Environ. Sci. Technol.* **1999**, *33,* 262-269.
7. Weber, W. J.; Huang, W. *Environ. Sci. Technol.* **1996**, *30,* 881-888.
8. Chiou, C. T.; Porter, P. E.; Schmedding, D. W. *Environ. Sci. Technol.* **1983**, *17,* 227-231.
9. Means, J. C.; Wood, S. G.; Hassett, J. J.; Banwart, W. L. *Environ. Sci. Technol.* **1980**, *14,* 1524-1528.
10. Huang, W.; Weber, W. J. *Environ. Sci. Technol.* **1997**, *31,* 2562-2569.
11. Hassett, J. J.; Banwart, W. L.; Wood, S. G.; Means, J. C. *Soil. Sci. Soc. Am. J.* **1981**, *45,* 38-42.
12. Hassett, J. J.; Means, J. C.; Banwart, W. L.; Woods, S. G. *Sorption Properties of Sediments and Energy-Related Pollutants*. **1980**, US Environmental Protection Agency: Washington D.C., EPA-600/603-680-041.
13. Mader, B. T.; Uwe-Goss, K.; Eisenreich, S. J. *Environ. Sci. Technol.* **1997**, *31,* 1079-1086.
14. Shea, D. *Environ. Sci. Technol.* **1988**, *22,* 1256-1261.
15. DiToro, D. M.; Zarba, C. S.; Hansen, D. J.; Berry, W. J.; Swartz, R. C.; Cowan, C. E.; Pavlou, S. P.; Allen, H. E.; Thomas, N. A.; Paquin, P. R. *Environ. Toxicol. Chem.* **1991**, *10,* 1541-1583.
16. Tracey, G. A.; Hansen, D. J. *Arch. Environ. Contam. Toxicol.* **1996**, *30,* 467-475.
17. Schwarzenbach, R. P.; Westall, J. *Environ. Sci. Technol.* **1981**, *15,* 1360-1367.
18. Wu, S. C.; Gschwend, P. M. *Environ. Sci. Technol.* **1986**, *20,* 717-725.
19. Allen-King, R. M.; Grathwohl, P.; Ball, W. P. *Adv. Water Resour.* **2002**, *25,* 985-1016.
20. Gawlik, B. M.; Sotiriou, N.; Feicht, E. A.; Schulte-Hostede, S.; Kettrup, A. *Chemosphere* **1997**, *34,* 2525-2551.
21. Pontolillo, J.; Eganhouse, R. P. *The Search for Reliable Aqueous Solubility and Octanol-Water Partitioning Coefficient Data for Hydrophobic Organic Compounds: DDT and DDE as a Case Study*. **2001**, U.S. Geological Society: Reston, VA. *01-4201*, 1-55.
22. Renner, R. *Environ. Sci Technol.* **2002**, *36,* 411A-413A.
23. Berner, R. A. *Early Diagenesis: A Theoretical Approach*. **1980**, Princeton Universtiy Press: Princeton, NJ. 1-241.
24. Grathwohl, P. *Environ. Sci. Technol.* **1990**, *24,* 1687-1693.

25. Rutherford, D. W.; Chiou, C. T.; Kile, D. E. *Environ. Sci. Technol.* **1992**, *26,* 336-340.
26. Kile, D. E.; Chiou, C. T.; Zhou, H.; Li, H.; Xu, O. *Environ. Sci. Technol.* **1995**, *29,* 1401-1406.
27. Chiou, C. T.; McGroddy, S. E.; Kile, D. E. *Environ. Sci. Technol.* **1998**, *32,* 264-269.
28. Weber, W. J.; McGinley, P. M.; Katz, L. E. *Environ. Sci. Technol.* **1992**, *26,* 1955-1962.
29. Luthy, R. G.; Aiken, G. R.; Brusseau, M. L.; Cunningham, S. D.; Gschwend, P. M.; Pignatello, J. J.; Reinhard, M.; Triana, S. J.; Weber, W.; Westall, J. C. *Environ. Sci. Technol.* **1997**, *31,* 3341-3347.
30. Xing, B.; Pignatello, J. J. *Environ. Sci. Technol.* **1997**, *31,* 792-799.
31. Karapanagioti, H. K.; Childs, J.; Sabatini, D. A. *Environ. Sci. Technol.* **2001**, *35,* 4684-4690.
32. Kleineidam, S.; Schuth, C.; Grathwohl, P. *Environ. Sci. Technol.* **2002**, *36,* 4689-4697.
33. Karapanagioti, H. K.; Kleineidam, S.; Sabatini, D.; Grathwohl, P.; Ligouis, B. *Environ. Sci. Technol.* **2000**, *34,* 406-414.
34. LeBoeuf, E. J.; Weber, W. J. *Environ. Sci. Technol.* **1997**, *31,* 1697-1702.
35. LeBoeuf, E. J.; Weber, W. J. *Environ. Toxicol. Chem.* **1999**, *18,* 1617-1626.
36. Xing, B. S.; Pignatello, J. J.; Gigliotti, B. *Environ. Sci. Technol.* **1996**, *30,* 2432-2440.
37. Brusseau, M. L.; Jessup, R. E.; Rao, P. S. C. *Environ. Sci. Technol.* **1991**, *25,* 134-142.
38. Huang, W.; Young, T. M.; Schlautman, M. A.; Yu, H.; Weber, W. J. *Environ. Sci. Technol.* **1997**, *31,* 1703-1710.
39. Chiou, C. T.; Kile, D. E. *Environ. Sci. Technol.* **1998**, *32,* 338-343.
40. Chiou, C. T.; Kile, D. E.; Rutherford, D. W. *Environ. Sci. Technol.* **2000**, *34,* 1254-1258.
41. Accardi-Dey, A.; Gschwend, P. M. *Environ. Sci. Technol.* **2002**, *36,* 21-29.
42. Lohmann, R.; MacFarlane, J. K.; Gschwend`, P. M. *Environ. Sci Technol.* **submit**.
43. Walters, R. W.; Luthy, R. G. *Environ. Sci. Technol.* **1984**, *18,* 395-403.
44. Crittenden, J. C.; Luft, P.; Hand, D. W.; Oravitz, J. L.; Loper, S. W.; Art, M. *Environ. Sci. Technol.* **1985**, *19,* 1037-1043.
45. Bucheli, T. D.; Gustafsson, Ö. *Environ. Sci. Technol.* **2000**, *34,* 5144-5151.
46. Ghosh, U.; Gillette, S.; Luthy, R. G.; Zare, R. N. *Environ. Sci. Technol.* **2000**, *34,* 1729-1736.
47. Bucheli, T. D.; Gustafsson, Ö. *Environ. Toxicol. Chem.* **2001**, *20,* 1450-1456.
48. Simpson, C. D.; Mosi, A. A.; Cullen, W. R.; Reimer, R. J. *Sci. Total Environ.* **1996**, *181,* 265-278.
49. Swartz, R. C. *Environ. Toxicol. Chem.* **1999**, *18,* 780-787.
50. Krauss, M.; Wilcke, W.; Zech, W. *Environ. Pollut.* **2000**, *110,* 79-88.
51. Krauss, M.; Wilcke, W.; Zech, W. *Environ. Sci. Technol.* **2000**, *34,* 4335-4340.

52. Jonker, M. T. O.; Smedes, F. *Environ. Sci. Technol.* **2000**, *34,* 1620-1626.
53. Jonker, M. T. O.; Koelmans, A. A. *Environ. Sci. Technol.* **2002**, *36,* 3725-3734.

CHAPTER 5: ASSESSING THE COMBINED ROLES OF NATURAL ORGANIC MATTER AND BLACK CARBON AS SORBENTS IN SEDIMENTS

Reproduced with permission from: Accardi-Dey, A.; Gschwend, P. M. *Environ. Sci. Technol.* **2002** *36,* 21-29.

5.1 ABSTRACT

The hypothesis for this work is that two mechanisms, *absorption* into natural organic matter and *adsorption* onto combustion-derived black carbon (BC), act in parallel to bind polycyclic aromatic hydrocarbons (PAHs) to Boston Harbor sediments. To focus on BC-adsorption, the non-BC fraction was removed by combusting near shore sediments at 375°C for 24 hours under air leaving *ca.* 16% of the reduced carbon. The isotherm for pyrene sorption onto the combusted sediment was nonlinear with a Freundlich exponent of 0.62 ±0.12 and a logarithm BC-normalized distribution coefficient ($(\mu g/kg_{BC})/(\mu g/L)^n$) of log 6.25 ±0.14. Pyrene sorption to untreated sediment was estimated reasonably using $K_d = f_{oc}\, 10^{4.7} + f_{BC}\, 10^{6.25}\, C_w^{(0.62-1)}$ where f_{oc} was the non-BC organic carbon content, $10^{4.7}$ was the organic carbon-normalized absorption coefficient for pyrene (L/kg_{oc}), f_{BC} was the BC content, and C_w was the dissolved pyrene concentration (μg/L). C/H/N molar ratios indicated that the environmental BC differed substantially from NIST diesel soot, possibly due to inclusion of larger BC particles from near source atmospheric fallout and urban runoff. The impact of BC on total PAH sorption may explain reports of nonlinear isotherms, K_{oc} values for PAHs that exceed their respective K_{ow} values, and discrepancies in bioavailability between planar and non-planar sorbates.

5.2 INTRODUCTION

Sorption is a key process controlling the fate of organic pollutants in the environment. It can limit the degradation of pollutants as well as influence the rate and extent that bioaccumulation occurs. A quantitative understanding of sorption is necessary to evaluate the hazards that pollutants pose.

Laboratory sorption studies since the late 1970s indicated that nonionic organic compounds partition into the natural organic matter of sediments and soils [1, 2]. This conceptualization yielded a solid-water distribution coefficient (K_d, L/kg_{solid}):

$$K_d = f_{oc} K_{oc} \quad (1)$$

where f_{oc} is the weight fraction of organic carbon (OC) in the solid phase, which serves as a metric of the organic matter content, and K_{oc} is the OC-normalized distribution coefficient for the compound of interest (L/kg_{oc}). (Note that in the OC definition used here, the OC fraction unknowingly contained black carbon.) However, investigators in the early 1990s noted that this linear relationship failed to characterize the equilibrium sorption of nonionic organic compounds in some laboratory studies [3]. To account for these observations, Weber *et al.* hypothesized that organic matter consists of a heterogeneous mix of sorbents, for example "soft" and "hard" carbon. Additional research on other processes influenced by sorption, such as bioremediation and bioaccumulation, suggested that some phenomenon "sequestered" chemicals or limited their accessibility [4, 5, 6, 7, 8]. One explanation for these observations was that a strong sorbent in addition to OC was present in the sediments and soils [9, 10, 11, 12].

Meanwhile, the observed distribution coefficient for polycyclic aromatic hydrocarbons (PAHs) in the field was greater than the K_d value calculated by the $f_{oc} K_{oc}$ model [13, 14, 15, 16, 17, 18, 19]. Researchers recognized that PAHs, derived from pyrogenic sources [20, 21], co-occur in soils and sediments with soot, chars, and other carbonaceous particles, collectively called "black carbon" (BC) in this paper. Gustafsson *et al.* and Gustafsson and Gschwend proposed that the BC fraction in sediments and soils acted like activated carbon and accounted for the high sorption affinities for PAHs [10, 22]. In support of this contention, Bucheli and Gustafsson demonstrated that PAHs

exhibit high distribution coefficients and nonlinear isotherms for sorption onto NIST diesel particulate matter (soot, SRM 1650) [23].

This work proposes that BC and OC act in parallel to sorb organic compounds from the water. (As noted in Chapter 1, BC is a collective term representing thermally altered carbonaceous material. The term OC (or the "non-BC fraction") represents the biogenic/diagenetic carbonaceous material. The sum of these two carbon fractions represents the total organic carbon (TOC) content of a sample.) The BC in sediments would act as an *adsorbent* interacting primarily with organic molecules of planar structure [24], and these adsorbent interactions should be characterized by Freundlich isotherms as reported widely for activated carbons [25, 26, 27] and diesel soot [23]. Simultaneously, the OC would serve as an *absorbent* that operates as described by Chiou *et al.* and Karickhoff [1, 2]. Hence at equilibrium, the sorbed PAH concentration is hypothesized to depend on the dissolved PAH concentration according to:

$$C_s = f_{oc} K_{oc} C_w + f_{BC} K_{BC} C_w^n \quad (2)$$

where C_s is the sorbed concentration ($\mu g/kg_{solid}$), C_w is the truly dissolved concentration ($\mu g/L$), f_{BC} is the weight fraction of BC in the solid phase, K_{BC} is the BC-normalized distribution coefficient ($(\mu g/kg_{BC})/(\mu g/L)^n$), and n is the Freundlich exponent appropriate for each PAH-BC combination of interest. Given this formulation, the overall solid-water distribution coefficient should take the form:

$$K_d = f_{oc} K_{oc} + f_{BC} K_{BC} C_w^{n-1} \quad (3)$$

Observations reported by other investigators appear likely to fit such a model [28, 29, 30, 31, 32].

In this study, the $f_{oc} K_{oc}$ and the $f_{BC} K_{BC} C_w^{n-1}$ contributions to the overall sorption of a representative PAH, pyrene, were assessed, as were the interactions with sediments from Boston Harbor, MA. To this end, pyrene sorption to both untreated sediments and pre-combusted sediments (at 375°C for 24 hours under air [10]) was investigated. The sediments were characterized with respect to both their elemental mole ratios and their f_{oc} and f_{BC} contents. Then, the combusted sediments were used to determine the sorption isotherm (K_{BC} and n) for pyrene interacting with environmental BC as this material

occurs in the Boston Harbor. This work indicated that (1) BC is the dominant sorbent for pyrene at the selected sites, (2) sorption of pyrene onto untreated sediment involves the sum of partitioning into OC plus adsorption onto BC, and (3) the equilibrium distribution coefficient for BC in the Boston Harbor is lower than the corresponding distribution coefficient for NIST diesel soot.

5.3 METHODS

5.3.1 Sediments. Grab samples of surface sediment were collected from littoral sites in Boston Harbor at south Dorchester Bay (SDB) and north Quincy Bay (NQB) near Quincy, MA in December 1999 (Figure 1). Archived subsamples were also gathered from box cores taken in 1990 [16] from sites near Fort Point Channel (FPC) and Spectacle Island (SI; Figure 1). Previous studies [33, 34] showed that these bays and the adjacent Moon Island region are polluted from a waste discharge outlet with PAH concentrations in the sediment exceeding 20,000 ng ΣPAHs/gdw. For each site studied, a 5 g sample was dried (75°C) and coarse grains were manually removed. The remaining sediment was then ground with a mortar and pestle and sieved through a 425 μm aperture, ultimately removing <30% of the sediment by weight. A 450 mg subsample was spread out among eight pre-combusted crucibles, and then was combusted in a Sybron F-A1730 Thermolyne muffle furnace (Dubuque, Iowa) under air for 24 hours at 375°C. (Note that in work presented here the muffle furnace was not pre-heated to 375°C.) This method oxidizes labile organic matter but retains a BC fraction in the sediment [10, 35].

A Perkin Elmer 2400 CHN Elemental Analyzer (Norwalk, CT) was used to determine the carbon weight percent and elemental mole ratios for both the untreated and combusted sediments. Sediment samples were *not* acidified to remove carbonate solids because test samples showed that the carbon added during the acidification method was greater than the amount of BC present in the sediment. (Previous work concluded that the inorganic content was <0.2 ±0.1 wt % C at SDB and <0.4 ±0.2 wt % C at NQB). In the untreated sediment, the total organic carbon (TOC) was assumed to include both the

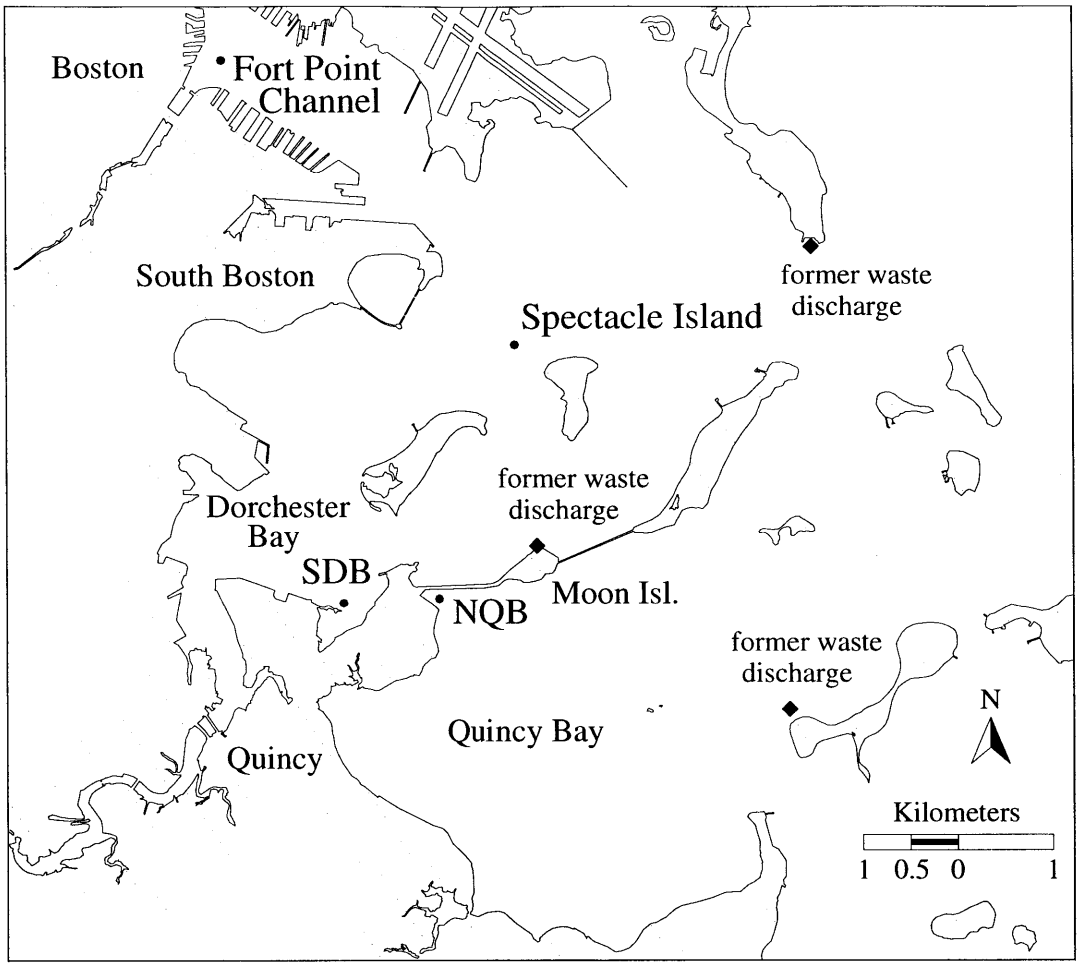

Figure 1: Map of Boston Harbor, MA showing the locations of South Dorchester Bay site (SDB; 42°18.0′ N, 71°1.8′ W) and North Quincy Bay site (NQB; 42°18.1′ N, 71°1.0′ W) along with two other sites previously examined by McGroddy and Farrington [16] and Gustafsson *et al.* [10]: Fort Point Channel (42°21′22″ N, 71°02′41″ W) and Spectacle Island (42°19′46″ N, 70°59′34″ W). The map also shows the approximate locations of former waste discharge outlets (filled diamonds).

OC and BC whereas the carbon in the combusted sediment was operationally defined as the BC fraction. The OC in the untreated sediments was obtained by subtracting the two measured carbon weight percents (OC = TOC – BC). NIST diesel particulate matter (soot, SRM 1650) was also combusted and analyzed on the CHN Elemental Analyzer. The CHN response factors were determined using acetanilide standards (Elemental Microanalysis, Manchester, MA) and were monitored after every six samples to check for reproducibility. The carbon and nitrogen response factors were more stable and reproducible (±0.03% for carbon and ±1% for nitrogen with 1500 μg acetanilide) than the hydrogen response factor (±8%). Elemental weight percents were accepted only when standard acetanilide samples were within ±0.3 weight percent of the known acetanilide values. (Acetanilide carbon ranged from 70.81 ±0.01 to 71.29 ±0.04 wt %, hydrogen ranged from 6.43 ±0.24 to 6.99 ±1.7 wt %, and nitrogen ranged from 10.32 ±0.01 to 10.51 ±0.08.) The carbon signal-to-noise ratio was >4:1 for the combusted samples and >10:1 for untreated samples with a method detection limit of 8.9 ±0.6 μg carbon [36]. (The signal-to-noise ratio corresponds to the number of CHN electronic counts with a sample compared to the number of counts without a sample.) Blanks were run after samples to verify that combustion was complete. All reported CHN errors represent ±1 standard deviation.

5.3.2 PAH Extraction. Approximately 5 g of untreated wet sediment were spiked with deuterated PAH recovery standards: d_{10}-acenaphthene, d_{10}-phenanthrene, d_{14}-p-terphenyl, d_{12}-benz(a)anthracene, and d_{12}-perylene[10]. The sediment was Soxhlet extracted for 24 hours using a 9:1 mixture of CH_2Cl_2:CH_3OH. Anhydrous Na_2SO_4 was used to precipitate residual water in the extract, and activated copper was used to remove elemental sulfur. The extract was concentrated and exchanged into hexane using a Kuderna-Danish apparatus and N_2-blow down techniques. The concentrate was fractionated on a fully activated silica gel column (EM Science, 100-200 mesh, 16:1 height to width). PAH quantification was performed on a JEOL GCmate gas chromatograph-mass spectrometer, equipped with a Hewlett Packard 6890 gas chromatograph. Extracts were injected

splitless and separated on a 30 m x 0.32 mm DB-5 (0.25 μm film thickness) fused-silica capillary column (J&W Scientific, Inc.). The temperature program began with a 20°C/min ramp from 70°C to 180°C, followed by 6°C/min from 180°C to 300°C. The injector and transfer zone temperatures were 280°C, and the MS source temperature was 250°C. Electronic pressure control maintained the He flow rate at 2 mL/min. The response factors, determined daily with a three-point calibration curve, had a variability of ±7%. Procedural blanks were analyzed concurrently with the samples. Blanks were <0.6 pg/μL-injection corresponding to a signal-to-noise ratio >500:1 for the PAHs reported. Using the methodology described above, this laboratory found 81 ±32% (±2σ) of the certified concentrations of several PAHs reported for NIST NY/NJ waterway sediment (SRM 1944) and NIST marine sediment (SRM 1941a).

5.3.3 Sorption. Sorption experiments were conducted in pre-combusted, 100-mL volumetric flasks with untreated or combusted sediment (10 mg to 200 mg) and varying initial concentrations of pyrene (2 μg/L to 21 μg/L, Aldrich Chemical Co., Milwaukee, WI). Each sorption experiment included three flasks: a control flask that contained the initial dissolved pyrene concentration, another control flask that contained only sediment and water (18 mΩ, low-carbon water produced using an Aries Vaponic system, Rockland, MA), and an experimental flask that contained both sediment and dissolved pyrene. All flasks were closed with glass stoppers, covered to avoid the photodegradation of pyrene, and tumbled once every 3 sec for a minimum of 1 month. Losses of dissolved pyrene in control flasks were <5% over the duration of the experiment.

A Perkin Elmer LS50B Luminescence Spectrofluorometer (Buckinghamshire, England) was used to monitor the pyrene in solution in the flasks. Before sampling, the flasks stood overnight undisturbed to allow particles to settle. A Stokes calculation revealed that a particle with a radius of 1 μm will settle to the bottom of a 100 mL volumetric flask within 12 hours (overnight) at T=24°C assuming a density of 2.5 g/cm^3. Aliquots were transferred to a Starna quartz cell (1 cm path length; Atascadero, CA) for

fluorescence analysis at 272.5 nm (excitation wavelength) and were then returned to their respective flasks. The background signals from the control flasks (containing sediment and water) were subtracted from the pyrene signals from the experimental flask. Fluorescence signals were quantified by synchronous scans, which were performed with $\Delta\lambda$ of 100 nm, an entrance slit of 2.5 nm, an exit slit of 5.0 nm, and a scan speed of 240 nm/min [37]. The method detection limit of the spectrofluorometer with these parameters was 0.27 μg pyrene/L (signal-to-noise of 3:1) with a 13% instrumental error [36]. This instrumental error decreased to 4% when pyrene concentrations were >1 μg/L. The experiments were designed to have final dissolved pyrene concentrations on the order of 0.5 μg/L to 10 μg/L because of the limitations of the LS50B Spectrofluorometer. This concentration range was greater than typical ambient concentrations, but it allowed for precise sorption observations with triplicate experiments varying <10%. All reported sorption parameters and errors (representing ±1 standard deviation) were generated using SigmaPlot version 4 (Scientific Graphing Software, SPSS Inc.). Errors were propagated for derived parameters following the equations listed in Harris [38].

5.3.4 Kinetic Experiments. Using SDB sediment, kinetic experiments were performed in a manner similar to the sorption experiments described above. However, tubes were spiked with 1 mM sodium azide (Fluka Chemika, Switzerland) to inhibit microbial growth and activity. Before analyzing these solutions with the spectrofluorometer, the tubes were centrifuged at 1100*g* for 8 min. After analysis, the tubes were returned to the tumbler within 1 hour. Test samples showed no difference in the fluorescence intensity between centrifuging and allowing particles to settle overnight.

5.3.5 Quenching Experiments. Additional experiments were conducted to determine if the OC desorbing from the sediments was affecting the dissolved pyrene fluorescence by inner filter effects or quenching [39, 40, 41]. Supernatants were obtained from a control flask of sediment (either untreated or combusted) desorbing in water (≈100 mL) for >29 days (no pyrene spike). The supernatants were transferred into centrifuge tubes and

centrifuged at 1100*g* for 8 min to remove any remaining particles, and then transferred to clean flasks. Afterwards, the absorbance of these supernatants was measured at 272.4 nm (excitation) and 372.4 nm (emission) wavelengths on a Beckman DU640 Spectrophotometer (Fullerton, CA) in a Uvonic quartz cuvette (1 cm path length; Plainview, NY) with a scan speed of 240 nm/min to investigate inner filter effects. Test samples with 225 ppm hexane in methanol suggested that the error between the measured absorbance and the expected absorbance was <21% at 255 nm. Then, successive 100 μL spikes of pyrene were added to the supernatants and a corresponding flask containing only Aries Vaponic water. Fluorescence intensities between successive spikes in the supernatants and water were compared to determine if fluorescence was quenched by any desorbed OC in the supernatants.

5.3.6 Influence of Pretreatment Temperature. Since the Thermolyne muffle furnace operated with a slow-response thermocouple control (Furnatrol 133, Sybron Corp), variations in the combustion temperature could affect the quantity and quality of BC retained. A typical temperature cycle involved a ramp from 364 ±1°C to 375 ±1°C at 2°C/min for 5 min followed by a cool down at 1°C/min for 10 min. To assess the effect of this temperature variability on sorption, sediments were also combusted in a Fisher Scientific IsoTemp programmable muffle furnace at the Woods Hole Oceanographic Institution (WHOI) at three different temperatures: 365°C, 375°C, and 385°C. The temperature program included a ramp at 15°C/min to 300°C, hold for 5 min, a second ramp at 5°C/min to the designated combustion temperature, and a hold for 24 hours. Sorption experiments were then conducted in triplicate on these sediments to deduce the sensitivity of the results within this temperature range.

5.4 RESULTS AND DISCUSSION

5.4.1 PAH Composition. The composition of PAHs in the sediment suggested that high-temperature combustion was the dominant source of the PAHs deposited at SDB and NQB. For both SDB and NQB, the phenanthrene/Σmethyl-phenanthrenes ratio was 3 and

the fluoranthene/pyrene ratio was 1. The phenanthrene/anthracene ratio was 6 at NQB and 4 at SDB. All these ratios are consistent with a high temperature pyrogenic source, rather than a petrogenic source [20, 21, 42]. In addition, the dimethylphenanthrenes (DMP) distribution, and especially the ratio of 1,7-DMP/2,6-DMP, indicated the predominance of a fossil fuel pyrogenic source as opposed to a wood burning source [43, 44, 45]. In light of the urban surroundings of these bays, such pyrogenic inputs of PAHs are likely derived from atmospheric fallout of BC particles [46], roadway runoff [47], and local combined sewer overflow sites.

5.4.2 CHN Elemental Analysis. The OC weight percent of untreated sediment from SDB was 1.2 ±0.15 wt % (Z = 10) with a C/H/N mole ratio of 1 / 1.4 ±1.1 / 0.062 ±0.017 (Table 1). The untreated sediment from NQB had a substantially larger OC weight percent of 3.1 ±0.64 wt % (Z = 7) but a similar C/H/N mole ratio of 1/ 1.1 ±0.47 / 0.064 ±0.014. After removing the labile OC by thermal oxidation, the BC weight percent in SDB sediment was 0.26 ±0.07 wt % (Z = 12) with a C/H/N mole ratio of 1 / 1.4 ±2.3 / 0.067 ±0.038. The BC weight percent in the NQB sediment was 0.60 ±0.07 wt % (Z = 6) with a C/H/N mole ratio of 1 / 1.3 ±1.0 / 0.059 ±0.016. For comparison, the elemental mole ratio for combusted NIST diesel soot (SRM 1650) was 1 / 0.091 ±0.069 / 0.017 ± 0.0011 (Z = 4). (The nitrogen residue was 0.02 ±0.01 wt % N (Z = 16) in the combusted SDB sediment and 0.04 ±0.01 wt % N (Z = 6) in the combusted NQB sediment. Based on the nitrogen residue, charring was probably absent in these samples. However, the similarities between the C/H/N molar ratios for the untreated and combusted sediments cannot be ignored and suggests that charring may have occurred.)

The BC weight percents for SDB and NQB were similar to those reported previously for two other stations in Boston Harbor: 0.66 ±0.08% at FPC (7-9 cm) and 0.27 ±0.04% at SI (0-2 cm) [48]. However, the BC weight percents contributed a larger fraction of the total sedimentary reduced carbon (BC/TOC) at SDB and NQB than either FPC or SI. For example, these observations showed that at SDB and NQB, 16 to 18% of

Table 1: Weight percent carbon (mean ±1 σ) and molar ratios (mean ±1 σ) for Boston Harbor sediments (untreated and combusted samples) and combusted NIST diesel particulate matter (SRM 1650)

Sample	C wt %	C/H Ratio	C/N Ratio
SDB Untreated Sediment (OC + BC)	1.5 ±0.13	0.7 ±0.3	16 ±1
SDB Combusted Sediment (BC)	0.26 ±0.07	0.7 ±0.07	15 ±4
NQB Untreated Sediment (OC + BC)	3.7 ±0.64	0.9 ±0.3	16 ±2
NQB Combusted Sediment (BC)	0.60 ±0.07	0.8 ±0.1	17 ±2
NIST Combusted (BC)	86 ±1.6 [a]	11 ±1	60 ±3

a: Carbon weight percent for NIST diesel particulate matter equals grams of elemental carbon per grams of combusted diesel matter times 100.

the total carbon was BC as opposed to 9 to 13% at the other Boston Harbor sites examined by Gustafsson and Gschwend [48]. The higher BC/TOC ratios in the southern part of Boston Harbor may indicate that post-depositional processes affected BC less than OC in these littoral sediments, since BC is known as a recalcitrant material [49]. Recently, Middelburg *et al.* investigated the post-depositional affects on BC in a 140 kyr old turbidite from the northwestern African margin. After 10-20 kyr of exposure to oxic pelagic conditions, only 36% of the BC was degraded in the turbidite (comparing the BC content in the upper oxidized section with the lower reduced section) [50]. Based on these findings, weathering and post-depositional processes probably did not affect the BC characteristics in Boston Harbor since the sediment was only a few decades old.

The C/H and C/N ratios in the combusted sediments from SDB and NQB (Table 1) suggested that the BC deposited at these sites was not exclusively composed of the submicron soot particles typified by NIST diesel soot. Such submicron soot particles, which have a C/H mole ratio near 10 and C/N near 60 (Table 1; [51, 52, 53, 54]), are likely transported farther offshore before settling out of the atmosphere [55]. For example, Windsor and Hites estimated that the submicron soot particles generated in the Boston Metropolitan area had a residence time of 4 days and were transported an average over 1000 km offshore before settling [46]. Conversely, larger (*ca.* 10 μm) BC particles would settle near their source and would accumulate in Boston Harbor from roadway runoff and sewer overflows. (Note that Boston Harbor sediments may include soot particles transported by long-range aeolian transport from inland sites. However, as noted in Chapter 3, the 375°C thermal method oxidizes these soot particles during the pretreatment, and hence, the elemental analysis of BC particles in the combusted sediments reflects only the isolated char particles.)

Rockne *et al.* also showed that C/H mole ratios varied among BC particles [54]. They observed that while submicron soot particles generated in a flame had C/H ratios of 7.1 ±0.4, the 10 μm BC particles collected from marine vessels and buses had C/H ratios of 0.72 ±0.04 and 1.1 ±0.06, respectively. Thus, the C/H data from combusted sediments (C/H ratios ranging from 0.4 to 1.5, Table 1) indicated that BC at SDB and NQB may not

be entirely composed of submicron soot, but rather a collection of larger combustion-derived BC particles. Furthermore, the similar C/H mole ratios for the combusted sediment and the BC particles reported by Rockne *et al.* suggest that the thermal oxidation method did not affect the surface chemistry of the BC in the sediment. Since BC forms at high temperatures (>1000°C) in the absence of oxygen, exposure to 375°C for 24 hours in the presence of oxygen may have minimal surface effects, but further work is necessary to confirm this assumption. (See Appendix A5.1 on work comparing the sorption of pyrene to SDB combusted sediment in acidified and non-acidified solutions to investigate if iron oxides formed during the combustion pre-treatment affected the distribution coefficient.)

The measured C/N molar ratios for combusted sediments at SDB and NQB (C/N ratios ranging from 14 to 18, Table 1) suggest that the BC included more nitrogenous functionality than typically represented in chemical models of soot. Although it should be noted that the C/N ratios reported here were not corrected for the inorganic nitrogen potentially present in the sediment [56], or the possible charring of nitrogen-containing proteins. Nonetheless such soot models conceptualize soot as a super-PAH with occasional oxygen functional groups and alkyl chains [57] – nitrogen is not included in these models. If soot forms from the radical condensation of hydrocarbons [58, 59, 60], then nitrogenous radicals, such as NO_x species also produced during combustion, could also condense with these radical hydrocarbons. Roadway tunnel studies of diesel and gasoline exhaust reported nitro-PAHs compounds in both the solid and gas phase [61, 62]. In addition, Kozin *et al.* also measured heterocyclic PAH in sediments of lakes and rivers [63]. Hence, environmental BC might exhibit some nitrogen-derived functionality that could affect the sorption of H-bonding sorbates.

5.4.3 Sorption Method Checks. Kinetic experiments showed that the dissolved pyrene concentrations approached equilibrium with a half-life on the order of hours for the untreated SDB sediment (triangles; Figure 2). Interestingly, the combusted sediment from the same site approached equilibrium more slowly with a half-life of approximately

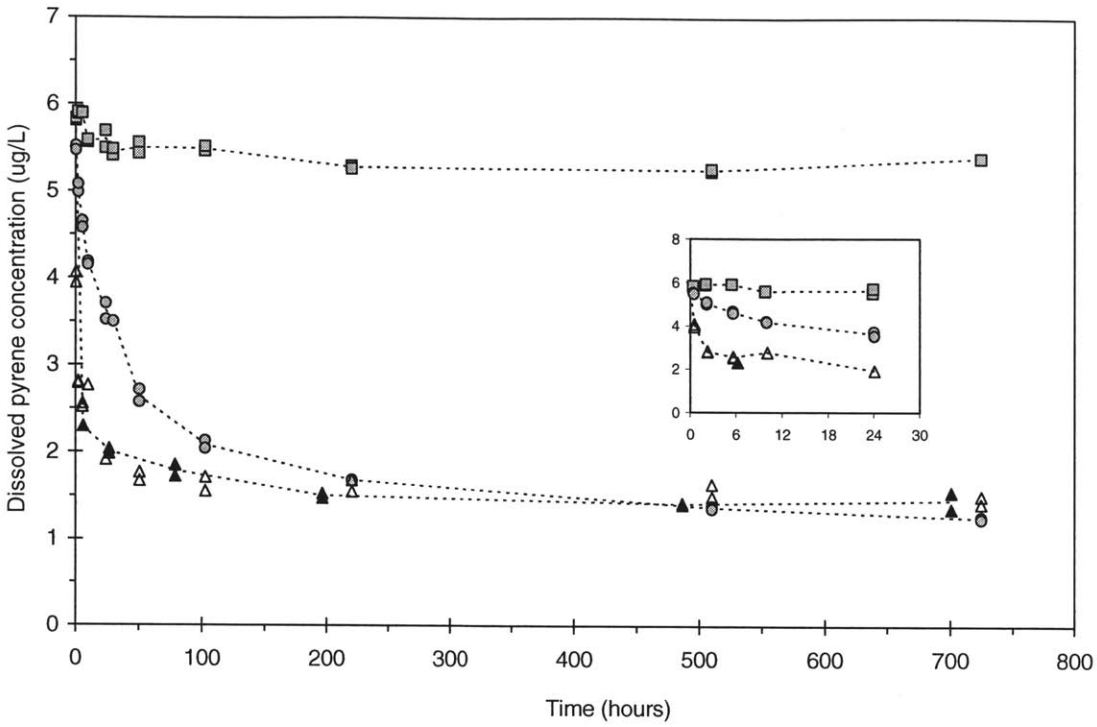

Figure 2: Kinetics experiment showing the loss of dissolved pyrene (μg/L) over time (hours) with (a) no sediment present (filled squares), (b) 40.0 mg of SDB combusted sediments added to 0.049 L of solution (filled circles), and (c) replicate experiments using 40.0 mg of SDB untreated sediment added to both 0.049 L of solution (open triangles) and 0.050 L of solution (black filled triangles). Each point is the average of four fluorescence measurements. The error associated with the dissolved pyrene concentrations in the control flask was ±4% and increased to ±8 to ±12% in the experimental flasks. The inserted graph shows an expanded view of the first 24 hours for the same kinetic data (same axes as larger graph).

1 day (circles). To insure that pyrene reached equilibrium in the sorption experiments, they were conducted for over a month.

Within the sensitivity limits of the spectrofluorometer, pyrene fluorescence in the experimental supernatants were not affected by dissolved organic carbon (DOC). The absorbance values for the supernatants from untreated and combusted sediments were <0.011 at 272.4 nm and were <0.004 at 372.4 nm reflecting transmission >97% at the two wavelengths (Figure 3). These absorbance values imply that inner filter effects did not affect fluorescence. In addition, successive spikes of pyrene gave statistically indistinguishable incremental increases in fluorescence for the control solution, the supernatant from untreated sediment (Figure 4a), and the supernatant from combusted sediment (Figure 4b). The absence of inner filter effects and quenching in the experiments was probably due to the low concentration of desorbed organic matter in the samples. Given an OC fraction at SDB of 0.012, the maximum concentration of carbon that could desorb from 50 mg of untreated sediment was $6x10^{-6}$ kg_{DOC}/L. These low DOC concentrations would not sorb a significant fraction of the dissolved pyrene (<15%) assuming a pyrene-DOC distribution coefficient near $3x10^4$ L/kg_{DOC} [64, 65, 66].

5.4.4 Pyrene Sorption. With fluorescence, the loss of 20-90% of the dissolved pyrene was observed due to sorption in experiments using both untreated and combusted sediments from SDB and NQB (representative fluorescence scans presented in Figure 5). The fraction of dissolved pyrene remaining in the water (f_w) after equilibrating with various sediments yielded a single sediment-water distribution coefficient (K_d, L/kg_{sed}) via:

$$K_d = \frac{(1-f_w)}{f_w r_{sw}} \tag{4}$$

where r_{sw} is the ratio of sediment-to-water (kg_{sed}/L). Pyrene sorption for both the untreated and combusted sediments exhibited an average log K_d of 3.50 ±0.20 for SDB (Figure 6a and Table 2) and an average log K_d of 3.72 ±0.17 for NQB (Figure 6b and Table 2). (See Appendix A5.2 for pyrene mass balance and an independent measurement

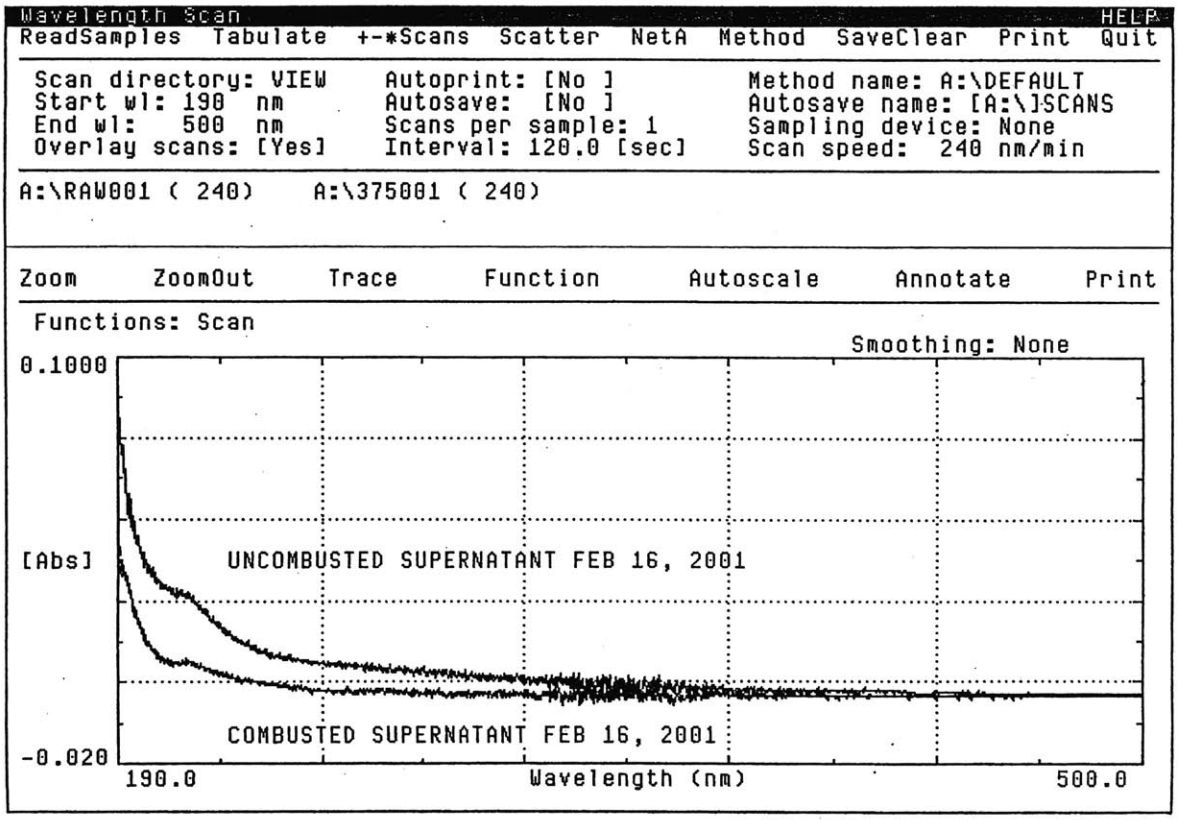

Figure 3: Spectrophotometer scans (absorbance vs. wavelength) of supernatants from 59.9 mg untreated sediment (top scan) and 40.7 mg combusted sediment (bottom scan) each desorbing in water (≈100 mL) for >29 days (no pyrene spike added). Scans corrected for background water signal and have <27% error.

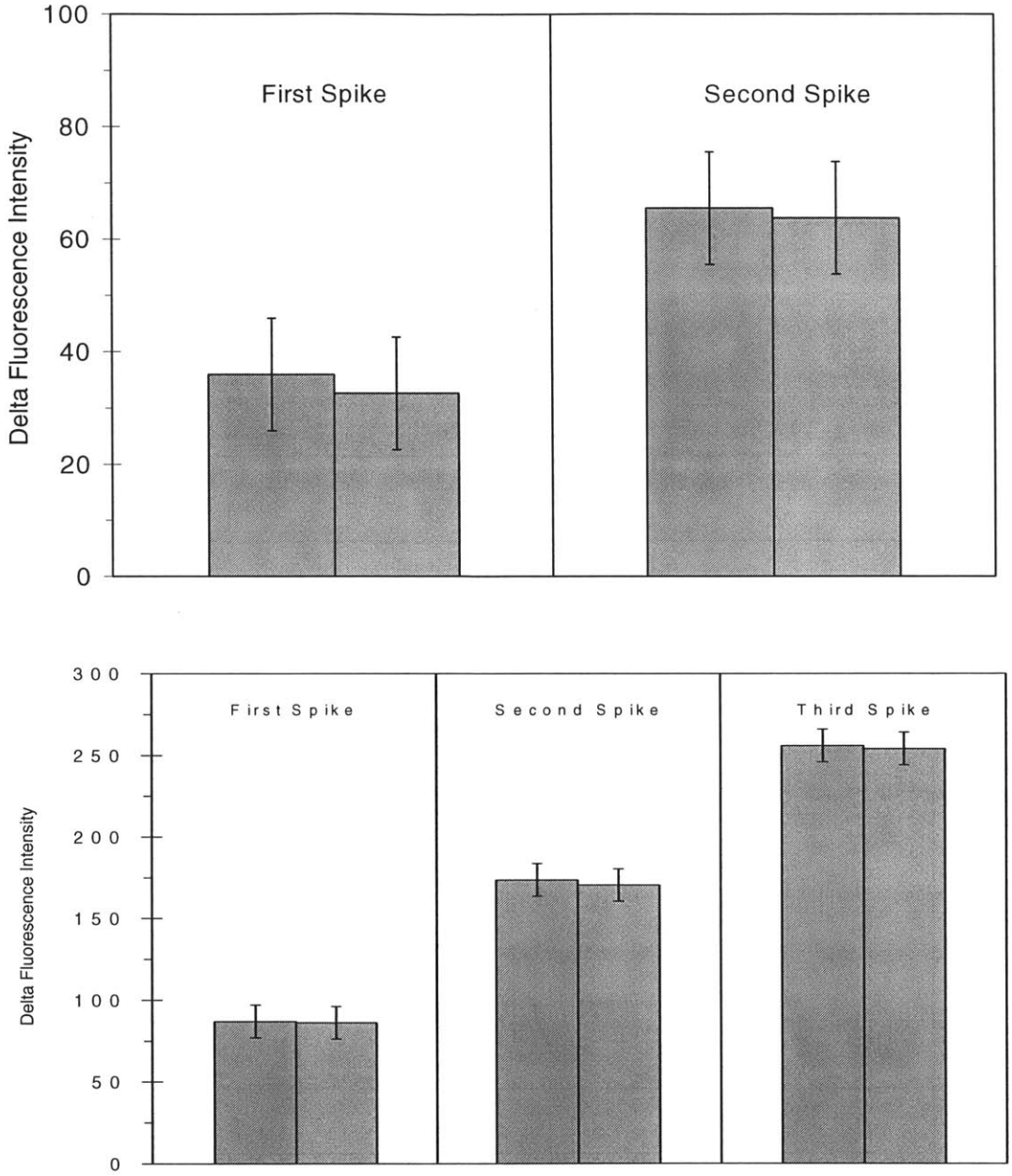

Figure 4: No quenching was observed with successive pyrene spikes (measured as delta fluorescence intensity) in supernatants from untreated and combusted sediments each desorbing in water (≈100 mL) for >29 days compared to control solution (no sediment desorbing). Intensity differences resulting from spiking corrected for background signal and have <10% error. (a) Two successive pyrene spikes (≈35 intensity units) to a control solution (hashed bars) and supernatant (solid bars) from untreated sediment (59.9 mg). (b) Three successive pyrene spikes (≈85 intensity units) to a control solution (hashed bars) and supernatant (solid bars) from combusted sediment (40.7 mg).

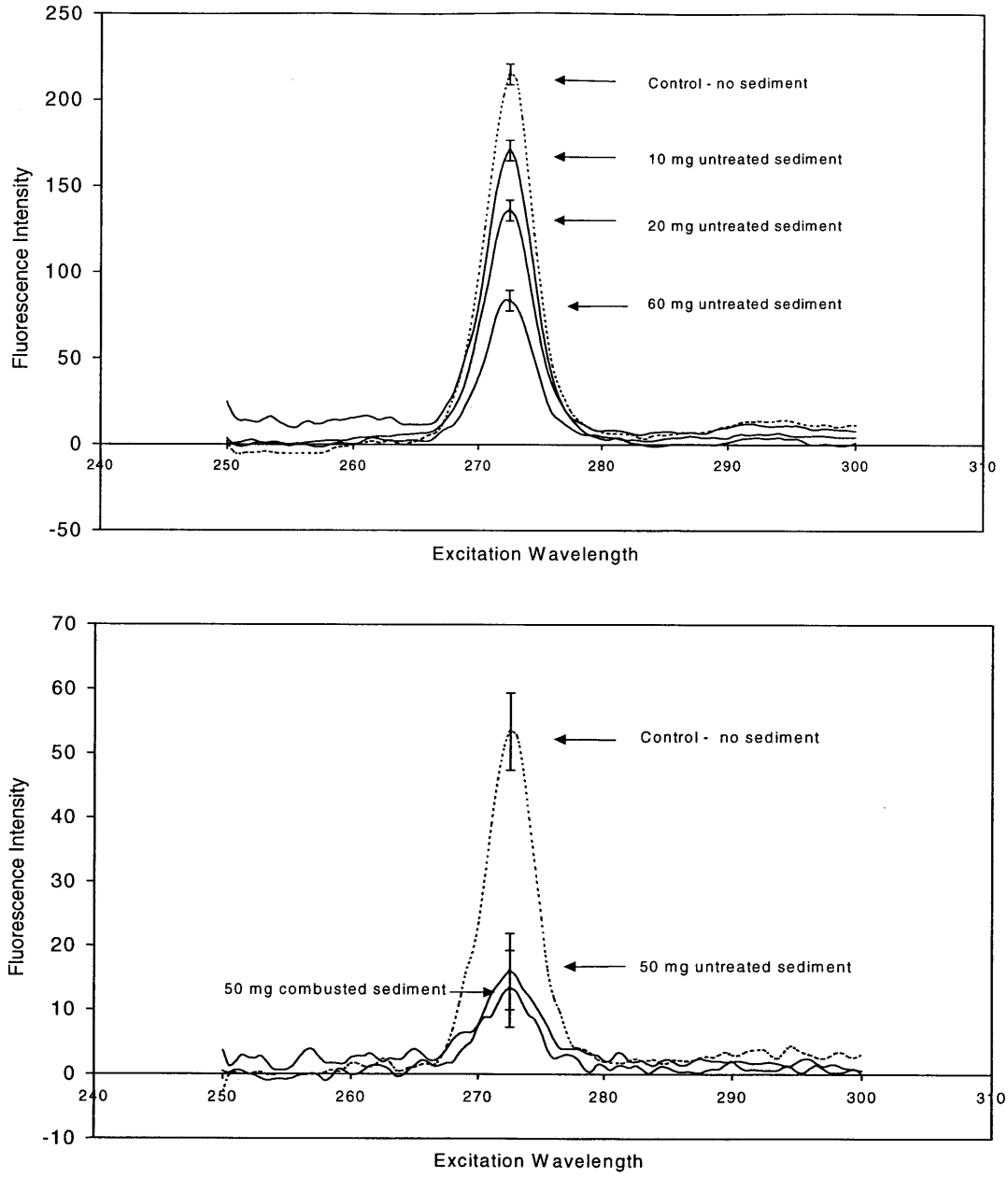

Figure 5: Fluorescence scans (intensity vs. excitation wavelength) showing the observed loss of dissolved pyrene due to sorption onto untreated and combusted SDB sediments after >38 days. Scans corrected for background signal and have a propagated error of 6%. (a) The dotted line represents the control experiment with no sediment (intensity corresponds to 9.23 µg pyrene/L). The three solid lines and corresponding labels represent experiments with varying amounts of untreated sediment: 10 mg sediment (20.4% loss of pyrene), 20 mg sediment (43.6% loss of pyrene), and 60 mg sediment (67.4% loss of pyrene). (b) The dotted line represents the control experiment with no sediment (intensity corresponds to 2.13 µg pyrene/L). The two solid lines and corresponding labels represent experiments with varying amounts of sediment: 50 mg untreated sediment (76.1% loss of pyrene) and 50 mg combusted sediment (82.2% loss of pyrene).

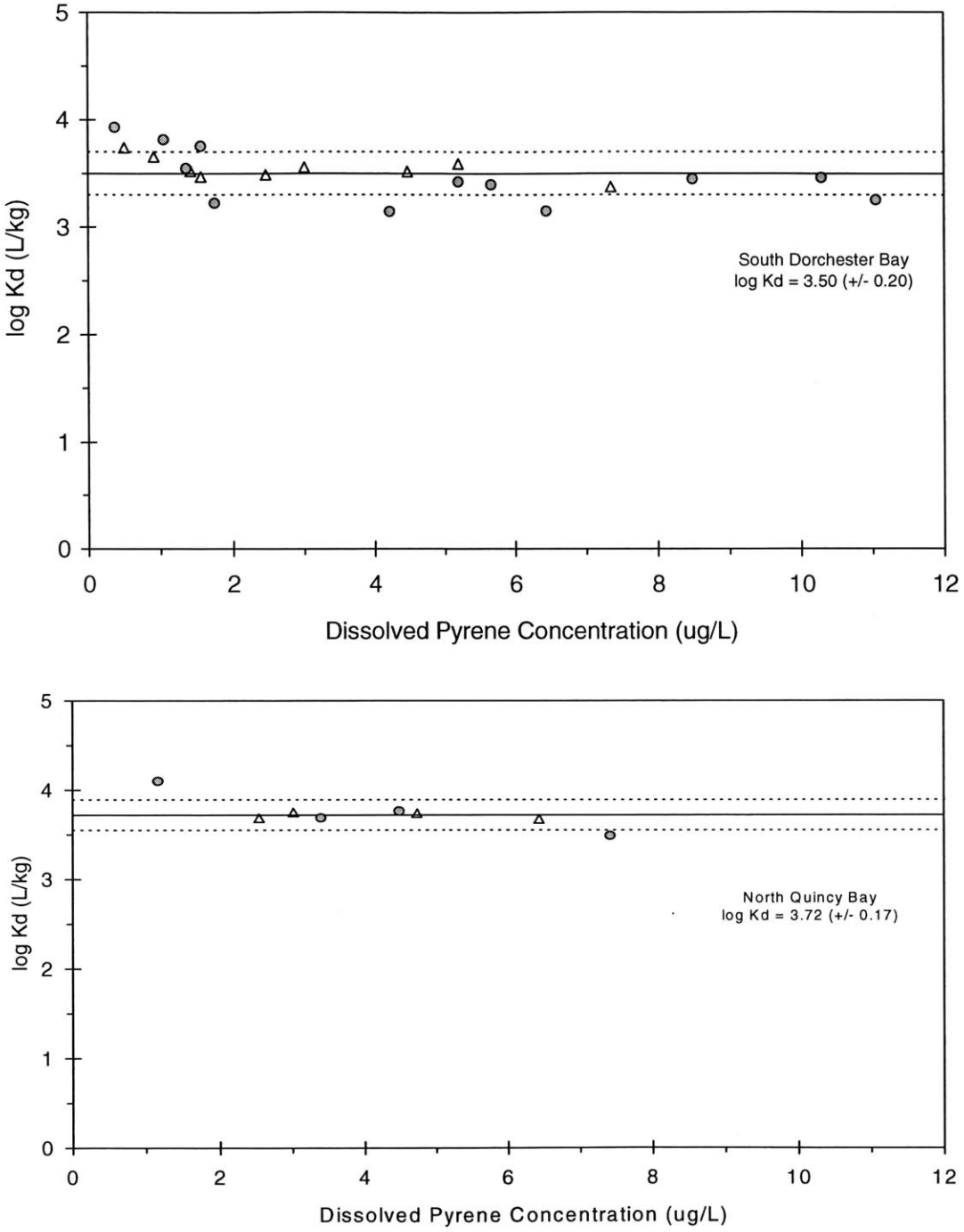

Figure 6: The dependence of the sediment-water distribution coefficients (log K_d, L/kg_{sed}) on dissolved pyrene concentrations (μg/L) for Boston Harbor sediments. (a) Distribution coefficients for untreated (open triangles) and combusted (filled circles) sediments from SDB with a mean log K_d of 3.50 ±0.20. (b) Distribution coefficients for untreated (open triangles) and combusted (filled circles) sediments from NQB with a mean log K_d of 3.72 ±0.17. Data corresponds to experimental results listed in Table 2

Table 2: Summary of sorption experiments (corresponding to Figures 3a and 3b) [a]

Sorbent (mg)	Volume (L)	Initial Conc (µg /L)	Percent Loss of Pyrene	Log K_d (L/kg)
Untreated Sediment – South Dorchester Bay				
11.4	0.106	9.23	20.4	3.37
20.0	0.105	9.88	43.0	3.60
20.0	0.104	9.88	38.3	3.51
20.0	0.105	9.88	32.2	3.40
20.1	0.101	9.23	43.6	3.59
39.3	0.050	4.15	78.1	3.65
40.0	0.050	5.25	70.3	3.47
40.0	0.049	5.25	73.0	3.52
56.2	0.094	2.15	76.7	3.74
60.7	0.106	9.23	67.4	3.56
101.4	0.090	21.1	78.8	3.52
199.0	0.081	21.1	88.3	3.49
Combusted Sediment – South Dorchester Bay				
10.1	0.106	13.1	21.5	3.46
20.1	0.103	13.1	35.2	3.45
40.0	0.049	5.25	74.1	3.55
40.5	0.049	4.15	57.8	3.22
46.2	0.092	21.1	47.5	3.25
51.0	0.101	4.50	76.7	3.81
52.0	0.092	2.15	82.8	3.93
59.6	0.104	13.1	60.3	3.42
96.1	0.088	21.1	73.1	3.40
102.2	0.100	15.7	58.9	3.15
195.5	0.100	15.7	73.1	3.14
199.1	0.090	21.1	92.6	3.75
Untreated Sediment – North Quincy Bay				
11.0	0.106	9.60	32.9	3.68
19.7	0.105	9.60	50.7	3.74
41.0	0.105	9.60	68.6	3.75
59.9	0.104	9.60	73.6	3.69
Combusted Sediment – North Quincy Bay				
10.1	0.106	9.60	22.5	3.48
20.5	0.104	9.60	53.4	3.76
39.8	0.106	9.60	64.6	3.69
60.2	0.104	9.60	87.9	4.10

a: The error associated with the sorbent mass and volume was less than ±1%. Initial dissolved concentrations had an error of ±4%. The percent loss of pyrene and the distribution coefficient had a compounded error of ±13%, which includes reproducibility error, instrumental error, and experimental error with the oven.

of the distribution coefficient using chemical extractions.) In general, the data were slightly above average at concentrations lower than 2 μg/L and slightly below average at concentrations greater than 8 μg/L. Statistically, the slope for the untreated SDB sediment in Figure 6a was –0.03 ±0.01 with a R^2 of 0.62, and the slope for the combusted SDB sediment in Figure 6a was –0.04 ±0.02 with a R^2 of 0.52. These values were likely different from zero suggesting that the distribution coefficient is dependent on the dissolved pyrene concentrations.

5.4.5 Influence of Combustion Temperature. Experiments involving SDB sediment combusted in a programmable oven at WHOI showed that pyrene sorption was sensitive to the pretreatment combustion temperature. Over the range of temperatures tested, the log K_d values decreased from 3.42 ±0.05 for the 365°C combusted sediment to 3.14 ±0.08 for the 385°C combusted sediment (Table 3). CHN analysis of these sediments showed that the BC weight percents also decreased from 0.22 ±0.03 in the 365°C combusted sediment to 0.15 ±0.03 in for the 385°C combusted sediment. In other words, the distribution coefficient decreased by a factor of 2 with increasing pretreatment temperatures, which corresponded to a 30% decline in the surviving f_{BC}.

These results indicated two caveats to the sorption data. First, because the Thermolyne muffle furnace operated with a slow-response thermocouple control, experimental imprecision was introduced when preparing the combusted sediments. Although the carbon weight percent was tested after most burns, the assumption that the BC fraction in all the combusted sediment was uniform may not hold. Therefore, the log K_d values reported have ≤0.2 logarithm units of error associated with imprecision in the combustion temperature. Secondly, based on the 365°C, 375°C, and 385°C data (Table 3), the lower carbon weight percents and lower log K_d values for the sediment combusted at WHOI indicate that the cycling of the MIT oven may have caused the effective combustion temperature to be <375°C.

Table 3: Summary of sorption experiments [a] and BC weight percents (mean ±1σ) for South Dorchester Bay sediment combusted at WHOI

Sorbent (mg)	Volume (L)	Initial Conc (μg/L)	Percent Loss of Pyrene	Log K_d (L/kg)	BC wt %
		365°C Combusted Sediment at WHOI			
20.0	0.105	9.88	31.7	3.38	0.22 ±0.03
20.0	0.105	9.88	31.8	3.39	
20.0	0.104	9.88	36.9	3.48	
		375°C Combusted Sediment at WHOI			
20.0	0.107	9.88	18.2	3.08	0.18 ±0.04
20.0	0.105	9.88	41.8	3.58	
20.0	0.103	9.88	30.1	3.34	
		385°C Combusted Sediment at WHOI			
20.0	0.106	9.88	20.3	3.13	0.15 ±0.03
20.0	0.105	9.88	18.2	3.07	
20.0	0.105	9.88	24.2	3.22	

a: The error associated with the sorbent mass and volume was less than ±1%. Initial dissolved concentrations had an error of ±4%. The percent loss of pyrene and the distribution coefficient had a compounded error of ±13%, which includes reproducibility error, instrumental error, and experimental error with the oven.

5.4.6 Sorption to OC Fraction. The similar distribution coefficients for pyrene sorption onto untreated and combusted sediments (Figure 6) demonstrated the strong contribution of BC to the overall sorption of pyrene in the original sediments. The PAH composition data and the f_{BC} values support the contention that combustion-derived solids have accumulated in these sediments. These results have several implications regarding BC as a sorbent in coastal environments.

The absorption model (Eq. 1), which ascribes that all hydrophobic compounds will partition into natural organic matter [1, 2], underestimated the extent of pyrene sorption at the selected sites. With a log K_{oc} for pyrene of 4.7 [2, 67], the expected log K_d value was 2.87 ±0.06 for SDB and was 3.27 ±0.08 for NQB. These values were significantly less than the observed values for the untreated sediments (Figures 7; dotted line). One argument for this discrepancy was that the chosen literature value for log K_{oc} was too low. The most renowned K_{oc}-K_{ow} correlation for PAHs was reported by Karickhoff in 1981 (log K_{oc} = 0.989 log K_{ow} – 0.346; [2]). The log K_{oc} for pyrene using this equation is 4.7 with a log K_{ow} of 5.1. However, several K_{oc}-K_{ow} correlations for PAHs exist in the literature. Gawlik *et al.* compiled most of the reported K_{oc}-K_{ow} correlations, and using these equations, the log K_{oc} for pyrene ranged from 5.0 to 3.9 with an average log K_{oc} of 4.7 ±0.3 using a log K_{ow} of 5.1 [67]. Not only does the log K_{oc} vary from one K_{oc}-K_{ow} correlation to the next, which contributes to the uncertainty in this value, but the calculated log K_{oc} also includes the propagated error from the uncertainty in the log K_{ow} value [68, 69]. Hence, the log K_{oc} value for pyrene is approximately 4.7.

Another argument was that the log K_{oc} for pyrene in this particular organic matter was anomalously high compared to most literature values. With an OC fraction of 0.012 and an average log K_d of 3.54 for the untreated SDB sediment, the calculated log K_{oc} is approximately 5.5. Likewise, the log K_{oc} value calculated for untreated NQB sediment was 5.2 (3.1 wt % OC and an average log K_d of 3.71). Both of these log K_{oc} values are similar to reported values by Chiou *et al.* [70]. However, a log K_{oc} value of ≈5.3 is greater than the pyrene log K_{ow} of 5.1, and K_{oc} values that exceed their K_{ow} values are suspicious since natural organic matter is slightly hydrophilic.

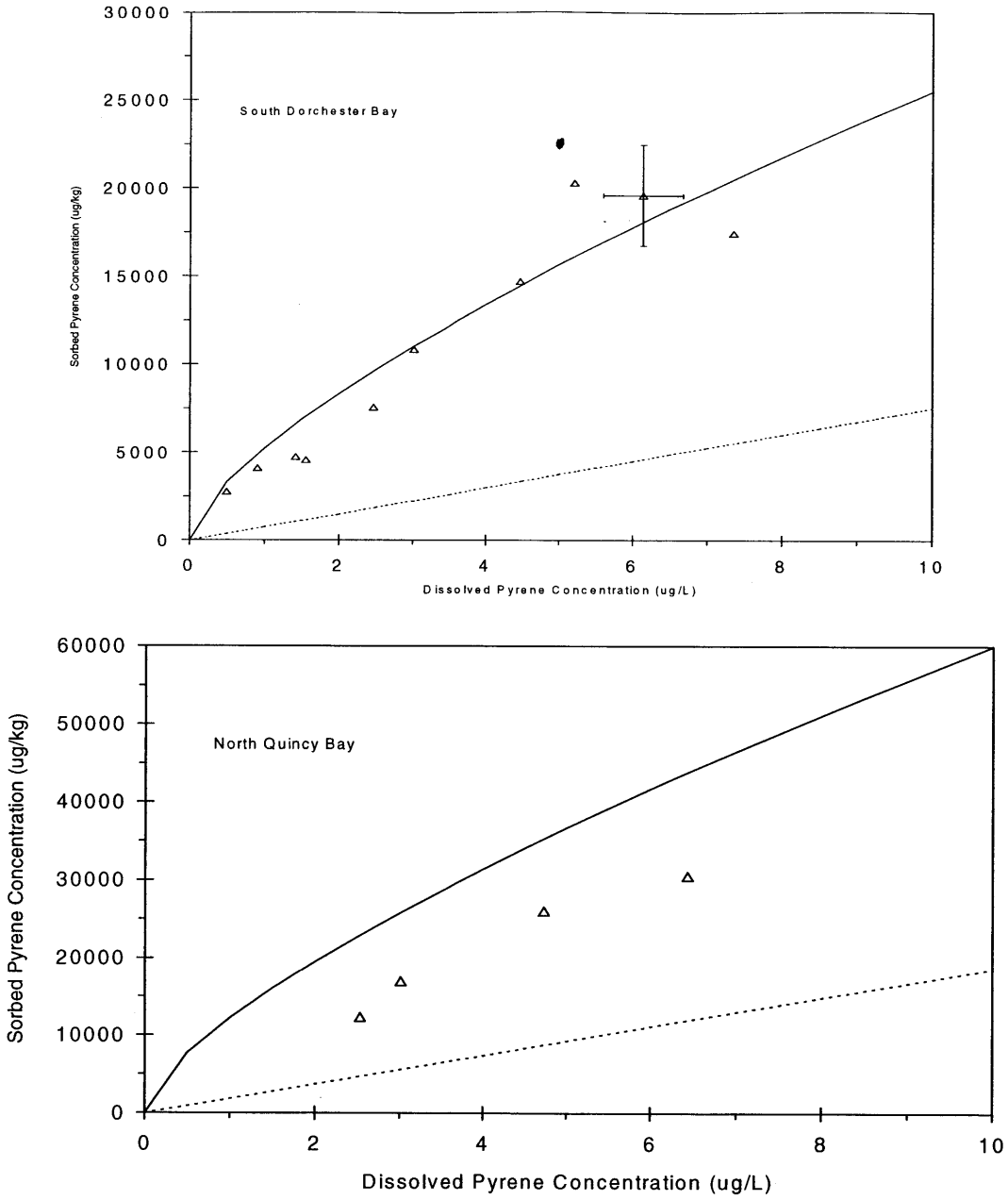

Figure 7: Sorbed pyrene concentration ($\mu g/kg_{sed}$) vs. dissolved pyrene concentration ($\mu g/L$) deduced from (a) SDB untreated sediments (open triangles) and (b) NQB untreated sediments (open triangles). The error associated with the dissolved pyrene concentration was ±8%, which propagated to ±15% error for the sorbed concentration. The error bars for one SDB experiment performed in triplicate are noted in panel (a). Also shown are (i) the expected sorbed concentrations from $C_s = f_{oc} K_{oc} C_w$ (dashed line) and (ii) the model predicted sorbed concentrations from $f_{oc} K_{oc} C_w + f_{BC} K_{BC} C_w^n$ (solid line) where f_{oc} is the OC content, $K_{oc}(\text{pyrene}) = 10^{4.7}$, f_{BC} is the BC content, $K_{BC}(\text{pyrene}) = 10^{6.25 \pm 0.14}$, and n is 0.62 ±0.12.

Although petroleum in the sediments can contribute to a larger K_{oc} value, analysis of extracted PAHs suggested that high-temperature pyrolysis was the dominant source of PAHs at SDB and NQB. For example, the phenanthrene/Σmethyl-phenanthrenes ratio was 3 at both sites (other ratios discussed above). In addition, the fraction of extractable lipid from SDB sediments was 0.002 (personal communication from G. Ewald) corresponding to a K_d value of only 250 L/kg assuming that the distribution coefficient for octanol applies. Therefore, the lipid/oil fraction alone cannot account for the large K_d values of 3500 L/kg observed at SDB. Likewise, the fraction of extractable lipid at NQB was 0.01, which only accounts for 24% of the observed K_d value (5200 L/kg). Another sorbent, like BC, must be present in the sediment to account for the observed K_d values and the corresponding large K_{oc} values [13, 14, 15, 16, 17, 18, 19].

5.4.7 Sorption to BC Fraction. To accommodate additional sorption to BC, Gustafsson *et al.* suggested a model that described the observed distribution coefficient as a sum of two linear isotherms involving the OC fraction and the BC fraction [10]:

$$K_d = f_{oc} K_{oc} + f_{BC} K_{BC} \quad (5)$$

This model assumed that the distribution coefficient for pyrene (K_d) is independent of the dissolved concentration; however the untreated and combusted sediment data suggested that K_d is dependent on sorbate levels (Figure 6). To assess whether the data suggested a dependency on the dissolved concentration, the correlation coefficients were examined for different linear and nonlinear models. Although correlation coefficients cannot prove linearity, they should increase from a linear model to a Langmuir model or a Freundlich model because the number of fitting parameters is increasing in the models from one to two. For example, for the untreated-sediment data, the R^2 value was 0.88 assuming a linear model; this correlation increased to 0.91 for the Langmuir model, and continued to increase to 0.95 for the Freundlich model. In this sense, the nonlinear Freundlich model fit the data better than a linear model. For the combusted sediment, the R^2 value was 0.72 for the linear model, decreased to 0.50 for the Langmuir model, and then increased again

to 0.70 for the Freundlich model. This situation implied that correlation coefficients alone cannot distinguish between a linear or nonlinear model for the combusted sediment.

To determine if the sorption to the combusted sediment was linear, the Freundlich exponent was examined to disprove the linear scenario (i.e., $n \pm 1\sigma \neq 1$). A Freundlich exponent of $n = 0.62 \pm 0.12$ (Figure 8) was calculated, implying that sorption to the combusted sediment was nonlinear. This nonlinearity may not be surprising since sorption isotherms to activated carbon are widely reported as nonlinear [25, 26, 27]. Furthermore, Bucheli and Gustafsson reported a Freundlich exponent of 0.67 for sorption of pyrene onto NIST diesel soot [23]. Likewise, work by Ghosh *et al.* using a microprobe laser desorption technique to examine coal dust in Milwaukee Harbor sediments showed that PAHs resided on the external surfaces of this carbonaceous material [71]. These observations suggest that adsorption of PAHs onto BC in the combusted sediments may have a similar adsorption mechanism, and not all surface sites may exhibit equal affinities for pyrene.

Although pyrene is adsorbing to the BC fraction, it is simultaneously partitioning into the thermally labile organic matter. To incorporate both of these sorption mechanisms, Eq. 5 was modified to yield:

$$K_d = f_{oc} K_{oc} + f_{BC} K_{BC} C_w^{n-1} \quad (3)$$

where the logarithm BC-normalized distribution coefficient ($\log K_{BC}$) is 6.25 ± 0.14 based on normalizing the best-fit Freundlich $\log K_d$ value of 3.67 ± 0.08 ($Z = 13$; Figure 8) to the measured BC fraction in SDB combusted sediment. This new model (or Eq. 2, re-written in terms of the sorbed concentration) was tested to predict the pyrene sorption to untreated SDB sediment. Good agreement was found between the observed and predicted sorbed pyrene concentrations (Figure 7a) using the parameters derived from the combusted sediment experiments ($n = 0.62$ and $\log K_{BC} = 6.25$), a literature value for $\log K_{oc}$ (4.7), and the measured f_{oc} and f_{BC} values for SDB. Since BC was a significant sorbent at this site (Figure 6a) – contributing to about 80% of the overall distribution coefficient – an isotherm through the SDB untreated sediment was also nonlinear ($n = 0.82 \pm 0.07$; Figure 7a) reflecting the presence of this BC fraction. Although BC was the

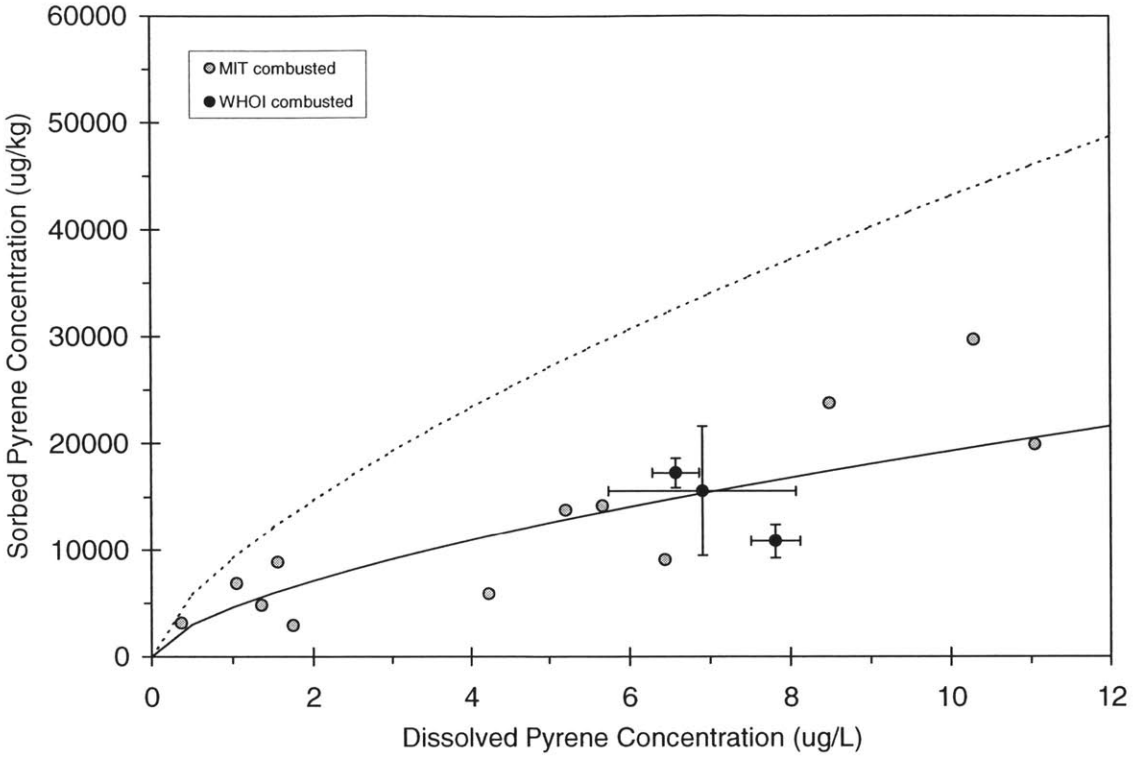

Figure 8: Sorbed pyrene concentration ($\mu g/kg_{sed}$) vs. dissolved pyrene concentration ($\mu g/L$) deduced for SDB sediment combusted with the MIT muffle furnace (filled circles) and the WHOI programmable oven (black filled circles). The error associated with the dissolved pyrene concentration was ±12%, which propagated to ±22% error for the sorbed concentration. The error bars are noted for experiments performed in triplicate and correspond to the WHOI sorption data in Table 3. Also shown are (i) the predicted sorbed concentrations (solid line) for the best-fit Freundlich isotherm through the data with the parameters $K_d(\text{pyrene}) = 10^{3.67 \pm 0.08}$ (which implies that $K_{BC} = 10^{6.25 \pm 0.14}$ with a $f_{BC} = 0.0026 \pm 0.0007$) and $n = 0.62 \pm 0.12$, and (ii) the sorbed pyrene concentration (dashed line) assuming that the BC at SDB sorbed like the diesel soot investigated by Bucheli and Gustafsson (2000) Environ. Sci. Technol. with a $K_{BC} = 10^{6.55}$ and $n = 0.67$.

dominant sorbent at SDB, the OC fraction was still an important sorbent and contributed to about 20% of the overall K_d value (3500 L/kg) for dissolved pyrene concentrations ranging from <1 μg/L to 8 μg/L. Nonetheless, sorption to BC may explain many reported cases of nonlinear sorption isotherms as well as cases where the log K_{oc} value exceeds the log K_{ow} value.

5.4.8 Sorption to NIST Soot. The data for SDB combusted sediment fell well below the Freundlich isotherm derived by Bucheli and Gustafsson (Figure 8; [23]). This difference chiefly resulted from the larger distribution coefficient for NIST diesel soot (log $K_{NIST\ BC}$ = 6.55) than the environmental BC (log K_{BC} = 6.25 ±0.14). The lower distribution coefficient for the combusted sediment, along with the C/H/N data, indicated that the near shore BC was not dominated by diesel soot. (Note that Boston Harbor sediments may include soot particles transported by long-range aeolian transport from inland sites. However, as noted in Chapter 3, the 375°C thermal method oxidizes these soot particles during the pretreatment, and hence, the BC-normalized distribution coefficient (defined on a mass basis) reflects pyrene adsorption to the isolated char particles.) If the near shore sites contain disproportionately more of the larger BC particles, then near shore BC would have less surface area than submicron NIST diesel soot settling offshore. Consequently, lower K_{BC} values are expected on a BC-normalized mass basis. Moreover, environmental BC in the Boston Harbor is likely a combination of carbonaceous solids, conceivably each sorbing compounds, like pyrene, with different strengths. For example, carbon black from tire wear may be a major contributor to environmental BC where street runoff is important [72], but this graphite-like BC may not be a strong sorbent. Kim *et al.* predicted that the distribution coefficient for carbon black was 1.1 to 4.4% of the distribution coefficient for activated carbon (K_{ac}, L/kg_{ac}; [73]), and it is proposed that the K_{BC} value approximates the K_{ac} value [22]. Hence, due to variations in specific surface areas and surface chemistries, various BC types may exhibit significantly different distribution coefficients.

5.4.9 Application of New Sorption Model (Eq. 3) at Other Boston Harbor Sites. Based on the elemental analysis of the combusted sediments at SDB and NQB and the proximity of these sites, the environmental BC at both sites may be similar (Table 1). The model (Eq. 3) was then tested to predict the distribution coefficient for pyrene sorption to NQB sediments using the measured f_{oc} and f_{BC} values for NQB, a literature log K_{oc} value (4.7), and the Freundlich exponent (0.62) and log K_{BC} value (6.25) from SDB. Although the predicted distribution coefficients were 0.1 to 0.3 logarithm units above the measured values, they were within error for three of the four comparisons (Table 4). The largest overestimation of the distribution coefficient was at the lowest dissolved concentration (2.53 μg/L) where the predicted log K_d of 3.96 ±0.14 exceeded the observed log K_d of 3.69 ±0.05. Another explanation for the overestimation of log K_d values at NQB may be due to the incorporation of an inorganic carbon fraction in the TOC value or the presence of charring. A correction for the inorganic content (0.4 ±0.2 wt %) then yielded predicted log K_d values that overestimated the measured log K_d values by <0.2 logarithm units at all the points.

Although extrapolation of the BC parameters from SDB to NQB may be reasonable, it is unclear how these parameters apply to other sites in the Greater Boston Harbor and at lower pyrene concentrations (10 ng/L to 100 ng/L). McGroddy and Farrington reported log K_d values (derived from dissolved-PAH and sorbed-PAH concentrations in cores from Boston Harbor) that were unexpectedly high [16]. In this study, the measured BC weight percents at FPC (15-17 cm depth) and SI (16-18cm depth) were 0.84 ±0.05% and 0.40 ±0.12%, respectively. Both of these subsections were deep enough in the core, so bioturbation and pore water flushing did not affect PAH equilibrium with the sediment. At FPC, the sorbed and dissolved pyrene data indicated a log K_d of 4.32 ±0.15 with a dissolved pyrene concentrations near 0.4 μg/L (Table 4; [74]). This value measured under field conditions compared very well to a predicted log K_d of 4.39 ±0.18 using Eq. 3. Likewise, at SI with a dissolved pyrene concentration of 0.06 μg/L, the model predicted a log K_d value of 4.34 ±0.18, which was within error of the observed log K_d value of 4.55 ±0.15 (Table 4). The agreement between the predicted

Table 4: Measured versus predicted distribution coefficients (L/kg; mean ± 1σ) at given dissolved pyrene concentrations (μg/L) for North Quincy Bay untreated sediment, McGroddy Fort Point Channel sediment (15-17 cm), and McGroddy Spectacle Island sediment (16-18 cm).

Dissolved Pyrene [a]	Measured log K_d [a]	Predicted log K_d [b]
	North Quincy Bay sediment	
6.44	3.68 ±0.05	3.83 ±0.14
4.73	3.74 ±0.05	3.87 ±0.14
3.02	3.75 ±0.05	3.93 ±0.14
2.53	3.69 ±0.05	3.96 ±0.14
	Fort Point Channel sediment	
0.4	4.32 ±0.15	4.39 ±0.18
	Spectacle Island sediment	
0.06	4.55 ±0.15	4.34 ±0.18

a: Measured dissolved pyrene concentrations (μg/L) and measured distribution coefficients (log K_d, units of L/kg) for the untreated sediment at North Quincy Bay (NQB) are the same data as Table 2, and the data for Fort Point Channel and Spectacle Island are from McGroddy (1993).

b: Predicted distribution coefficient (log K_d, units of L/kg) with the new model (Eq. 3) assuming that log K_{oc} = 4.7, log K_{BC} = 6.25 ±0.14, and n = 0.62 ±0.12.

and measured distribution coefficients suggests: (1) similar BC matrices occur around Boston Harbor and (2) the approach used is reasonable for predicting log K_d values at environmental concentrations.

5.4.10 Implications. The results from this work have several implications concerning the importance of BC as a sorbent in soils and sediments. First, the sorption of other PAH-like compounds onto BC may explain reported nonlinear isotherms [28, 29, 30, 31, 32] and unexpectedly high K_{oc} values [75]. Second, since BC is ubiquitous in the environment and was disseminated over geological time [52], a large percentage of the aromatic content observed with ^{13}C-NMR [70] in the soil and sediment organic matter may be due to the presence of BC. Therefore, this work supports the institution of a new procedure to quantify the BC fraction and to identify the various BC components (i.e. char, fly ash, and soot) in natural solids before they are tested as sorbents. This new procedure would also apply to atmospheric particles, which are known to contain BC (often referred to as elemental carbon (EC) in atmospheric literature [76, 77]).

In addition, BC in sediments and soils will especially affect the desorption rates of planar organic compounds like PAHs, and conceivably co-planar PCB congeners, pesticide derivatives like *p,p′*-dichlorodiphenyldichloroethene (DDE), and polychlorinated dibenzodioxins and furans. Based on the observed sorption kinetics and equilibrium constants, the equilibration time in aquatic environments having a low BC-to-water ratio could approach months [78]. Lastly, the data suggest that very different bioaccumulation and biodegradation behaviors should be expected for sediments that contain (1) a significant BC fraction versus sediments that do not, and (2) BC-sorbed compounds like PAHs. The BC fraction in SDB and NQB sediments would lower the chemical availability of PAHs by 4 to 6 times that expected from $f_{oc} K_{oc}$ alone, and this difference is similar to the "discrepancy" in Biota-Sediment Accumulation Factors reported widely between PCBs and PAHs [79].

5.5 ACKNOWLEDGMENTS

This work was supported by NSF Grant No. BES-9800485 and project number RC-70 of the MIT Sea Grant College Program under a federal grant number NA86RG0074 from the National Sea Grant College Program, National Oceanic and Atmospheric Administration, US Department of Commerce. Thanks to Goran Ewald, John MacFarlane, and John Farrington for sediment collection; John MacFarlane, Jed Goldstone, and Christopher Swartz for assistance in the lab; and Ana Lima for assistance in combusting sediments at WHOI. Additional thanks to Tim Eglinton, Chris Reddy, Jean Whelan, Richard Bopp, and Greg Noonan for guidance and helpful discussions.

5.6 REFERENCES

1. Chiou, C. T.; Peters, L. J.; Freed, V. H. *Science* **1979**, *206,* 831-832.
2. Karickhoff, S. W. *Chemosphere* **1981**, *10,* 833-846.
3. Weber, W. J.; McGinley, P. M.; Katz, L. E. *Environ. Sci. Technol.* **1992**, *26,* 1955-1962.
4. Steinberg, S. M.; Pignatello, J. J.; Sawhney, B. I. *Environ. Sci. Technol.* **1987**, *21,* 1201-1208.
5. Scribner, S. L.; Benzing, T. R.; Sun, S.; Boyd, S. A. *J. Environ. Qual.* **1992**, *21,* 115-120.
6. Keil, R. G.; Montlucon, D. B.; Prahl, F. G.; Hedges, J. L. *Nature* **1994**, *370,* 549-552.
7. Tang, J.; Garcia, R.; Holden, K. M. L.; Mitchell, S. C.; Pis, J. J. *Environ. Sci. Technol.* **1998**, *32,* 3586-3590.
8. Alexander, M. *Environ. Sci. Technol.* **2000**, *34,* 4259-4265.
9. Grathwohl, P. *Environ. Sci. Technol.* **1990**, *24,* 1687-1693.
10. Gustafsson, Ö.; Haghseta, F.; Chan, C.; MacFarlane, J.; Gschwend, P. M. *Environ. Sci. Technol.* **1997**, *31,* 203-209.
11. Luthy, R. G.; Aiken, G. R.; Brusseau, M. L.; Cunningham, S. D.; Gschwend, P. M.; Pignatello, J. J.; Reinhard, M.; Triana, S. J.; Weber, W.; Westall, J. C. *Environ. Sci. Technol.* **1997**, *31,* 3341-3347.
12. Lamoureux, E. M.; Brownawell, B. J. *Environ. Toxicol. Chem.* **1999**, *18,* 1733-1741.
13. Prahl, F. G.; Carpenter, R. *Geochim. Cosmochim. Acta* **1983**, *47,* 1013-1023.
14. Socha, S. B.; Carpenter, R. *Geochim. Cosmochim. Acta* **1987**, *51,* 1273-1284.
15. Readman, J. W.; Mantoura, R. F. C.; Rhead, M. M. *Sci. Total Environ.* **1987**, *66,* 73-94.
16. McGroddy, S. E.; Farrington, J. W. *Environ. Sci. Technol.* **1995**, *29,* 1542-1550.

17. Simpson, C. D.; Mosi, A. A.; Cullen, W. R.; Reimer, R. J. *Sci. Total Environ.* **1996**, *181,* 265-278.
18. Zhou, J. L.; Fileman, T. W.; Evans, S.; Donkin, P.; Readman, J. W.; Mantoura, R. F. C.; Rowland, S. *Sci. Total Environ.* **1999**, *244,* 305-321.
19. Jonker, M. T. O.; Smedes, F. *Environ. Sci. Technol.* **2000**, *34,* 1620-1626.
20. Youngblood, W. W.; Blumer, M. *Geochim. Cosmochim. Acta* **1975**, *39,* 1303-1314.
21. Gschwend, P. M.; Hites, R. A. *Geochim. Cosmochim. Acta* **1981**, *43,* 2359-2367.
22. Gustafsson, Ö.; Gschwend, P. M. *Soot as a strong partition medium of polycyclic aromatic hydrocarbons in aquatic systems* in *Molecular Markers in Environmental Geochemistry*. R. P. Eganhouse. **1997**, ACS Symposium Series: Washington DC. *671,* 365-381.
23. Bucheli, T. D.; Gustafsson, Ö. *Environ. Sci. Technol.* **2000**, *34,* 5144-5151.
24. Kubicki, J. D.; Apitz, S. E. *Org. Geochem.* **1999**, *30,* 911-927.
25. Crittenden, J. C.; Luft, P.; Hand, D. W.; Oravitz, J. L.; Loper, S. W.; Art, M. *Environ. Sci. Technol.* **1985**, *19,* 1037-1043.
26. Blum, D. J. W.; Suffet, I. H.; Duguet, J. P. *Water Res.* **1994**, *28,* 687-699.
27. Karanfil, T.; Kilduff, J. E. *Environ. Sci. Technol.* **1999**, *33,* 3217-3224.
28. Chiou, C. T.; Kile, D. E. *Environ. Sci. Technol.* **1998**, *32,* 338-343.
29. Xia, G. S.; Ball, W. P. *Environ. Sci. Technol.* **1999**, *33,* 262-269.
30. Kleineidam, S.; Rugner, H.; Ligouis, B.; Grathwohl, P. *Environ. Sci. Technol.* **1999**, *33,* 1637-1644.
31. Karapanagioti, H. K.; Kleineidam, S.; Sabatini, D.; Grathwohl, P.; Ligouis, B. *Environ. Sci. Technol.* **2000**, *34,* 406-414.
32. Xia, G. S.; Pignatello, J. J. *Environ. Sci. Technol.* **2001**, *35,* 84-94.
33. Shiaris, M. P.; Jambard-Sweet, D. *Mar. Pollut. Bull.* **1986**, *17,* 469-472.
34. Gardner, G. R.; Pruell, R. J. *Mar. Environ. Res.* **1989**, *28,* 393-397.
35. Gustafsson, Ö.; Bucheli, T. D.; Kukulska, Z.; Anderson, M.; Largeau, C.; Rouzaud, J. N.; Reddy, C. M.; Eglinton, T. E. *Global Biogeochem. Cy.* **2001**, *15,* 881-890.
36. Glaser, J. A.; Foerst, D. L.; McKee, G. D.; Quave, S. A.; Budde, W. L. *Environ. Sci Technol.* **1981**, *15,* 1426-1435.
37. Eiroa, A. A.; Blanco, V.; Mahia, P. L.; Lorenzo, S. M.; Rodriguez, D. P. *Analyst* **1998**, *123,* 2113-2117.
38. Harris, D. C. *Quantitative Chemical Analysis*. **1995**, WH Freeman and Company: New York.
39. Gauthier, T. D.; Shane, E. C.; Guerin, W. F.; Seltz, W. R.; Grant, C. L. *Environ. Sci. Technol.* **1986**, *20,* 1162-1166.
40. Backhus, D. A.; Gschwend, P. M. *Environ. Sci. Technol.* **1990**, *24,* 1214-1222.
41. Auger, R. L.; Jacobson, A. M.; Domach, M. M. *Environ. Sci. Technol.* **1995**, *29,* 1273-1278.
42. Budzinski, H.; Jones, I.; Bellocq, J.; Pierard, C.; Garrigues, P. *Marine Chem.* **1997**, *58,* 85-97.

43. Garrigues, P.; Parlanti, E.; Radk, M.; Bellocq, J.; Willsch, H.; Ewald, M. *J. Chromatogr.* **1987**, *395,* 217-228.
44. Benner, B. A.; Gordon, G. E.; Wise, S. A. *Environ. Sci. Technol.* **1989**, *23,* 1269-1278.
45. Benner, B. A.; Wise, S. A.; Currie, L. A.; Klouda, G. A.; Klinedinst, D. B.; Zweidinger, R. B.; Stevens, R. K.; Lewis, C. W. *Environ. Sci. Technol.* **1995**, *29,* 2382-2389.
46. Windsor, J. G.; Hites, R. A. *Geochim. Cosmochim. Acta* **1979**, *43,* 27-33.
47. Miguel, A. H.; Kirchstetter, T. W.; Harley, R. A. *Environ. Sci. Technol.* **1998**, *32,* 450-455.
48. Gustafsson, Ö.; Gschwend, P. M. *Geochim. Cosmochim. Acta* **1998**, *62,* 465-472.
49. Schmidt, M. W. I.; Noack, A. G. *Global Biogeochem. Cy.* **2000**, *14,* 777-793.
50. Middelburg, J. J.; Nieuwenhuize, J.; Breugel, P. V. *Mar. Chem.* **1999**, *65,* 245-252.
51. Medalia, A. I.; Rivin, D. *Carbon* **1982**, *20,* 481-492.
52. Goldberg, E. D. *Black Carbon in the Environment: Properties and Distribution.* **1985**, A Wiley-Interscience Publication, John Wiley & Sons: New York. 1-198.
53. Kuhlbusch, T. A. J.; Crutzen, P. J. *Global Biogeochem. Cy.* **1995**, *9,* 491-501.
54. Rockne, K. J.; Taghon, G. L.; Kosson, D. S. *Chemosphere* **2000**, *41,* 1125-1135.
55. Sumam, D. O.; Kulbusch, T. A. J.; Lim, B. *Marine sediments: A reservoir for black carbon and their use as spacial and temporal records of combustion* in *Sediment Records of Biomass Burning and Global Change.* J. S. Clark. **1994**, NATO ASI Series: *51,* 271-293.
56. Ruttenberg, K. C.; Goni, M. A. *Mar. Geol.* **1997**, *139,* 123-145.
57. Akhter, M. S.; Chughtal, A. R.; Smith, D. M. *Appl. Spectrosc.* **1985**, *39,* 143-153.
58. Harris, S. J.; Weine, A. M. *Combust. Sci. Technol.* **1983**, *31,* 155-167.
59. Lahaye, J. *Polym. Degrad. Stabil.* **1990**, *30,* 111-121.
60. Frenklach, M. *On surface growth mechanism of soot particles* in *Twenty-sixth Symposium (International) on Combustion.* **1996**, The Combustion Institute: Pittsburgh. 2285-2293.
61. Handa, T.; Yamauchi, T.; Sawai, K.; Yamamura, T.; Koseki, Y.; Ishii, T. *Environ. Sci. Technol.* **1984**, *18,* 895-902.
62. Dimashki, M.; Harrad, S.; Harrsion, R. M. *Atmos. Environ.* **2000**, *34,* 2459-2469.
63. Kozin, I. S.; Larsen, O. F. A.; Voogt, P. d.; Gooijer, C.; Velthorst, N. H. *Anal. Chim. Acta* **1997**, *354,* 181-187.
64. Chin, Y.; Gschwend, P. M. *Environ. Sci. Technol.* **1992**, *26,* 1621-1626.
65. MacDonald, B. C.; Lvin, S. J.; Patterson, H. *Anal. Chim. Acta* **1997**, *338,* 155-162.
66. Mitra, S.; Dickhut, R. M. *Environ. Toxicol. Chem.* **1999**, *18,* 1144-1148.
67. Gawlik, B. M.; Sotiriou, N.; Feicht, E. A.; Schulte-Hostede, S.; Kettrup, A. *Chemosphere* **1997**, *34,* 2525-2551.
68. Pontolillo, J.; Eganhouse, R. P. *The Search for Reliable Aqueous Solubility and Octanol-Water Partitioning Coefficient Data for Hydrophobic Organic*

Compounds: DDT and DDE as a Case Study. **2001**, U.S. Geological Society: Reston, VA. *01-4201*, 1-55.
69. Renner, R. *Environ. Sci Technol.* **2002**, *36,* 411A-413A.
70. Chiou, C. T.; McGroddy, S. E.; Kile, D. E. *Environ. Sci. Technol.* **1998**, *32,* 264-269.
71. Ghosh, U.; Gillette, S.; Luthy, R. G.; Zare, R. N. *Environ. Sci. Technol.* **2000**, *34,* 1729-1736.
72. Reddy, C. M.; Quinn, J. G. *Environ. Sci. Technol.* **1997**, *31,* 2847-2853.
73. Kim, J. Y.; Park, J. K.; Edil, T. B. *J. Environ. Eng.* **1997**, *123,* 827-835.
74. McGroddy, S. E. *Ph.D Thesis: Sediment-Pore Water Partitioning of PAHs and PCBs in Boston Harbor, Massachusetts*. **1993**, University of Massachusetts at Boston: Boston. 1-255.
75. Bucheli, T. D.; Gustafsson, Ö. *Environ. Toxicol. Chem.* **2001**, *20,* 1450-1456.
76. Hildemann, L. M.; Markowski, G. R.; Cass, G. R. *Environ. Sci. Technol.* **1991**, *25,* 744-759.
77. Venkataraman, C.; Friedlander, S. K. *Environ. Sci. Technol.* **1994**, *28,* 563-572.
78. Wu, S. C.; Gschwend, P. M. *Environ. Sci. Technol.* **1986**, *20,* 717-725.
79. Tracey, G. A.; Hansen, D. J. *Arch. Environ. Contam. Toxicol.* **1996**, *30,* 467-475.

CHAPTER 6: RE-INTERPRETING LITERATURE SORPTION DATA CONSIDERING BOTH ABSORPTION INTO ORGANIC CARBON AND ADSORPTION ONTO BLACK CARBON

6.1 ABSTRACT

This work hypothesized that the sorption of polycyclic aromatic hydrocarbons (PAHs) to natural sediments and soils should consider both *absorption* into a biogenic/diagenetic organic carbon (OC) fraction and *adsorption* onto a combustion-derived, black carbon (BC) fraction. Here, two sets of literature data were re-evaluated to illustrate that an OC absorbent and a BC adsorbent together can: (1) account for sediment-pore water distribution coefficients observed in the field that are greater than predicted by a simple $f_{oc} K_{oc}$ partitioning model, and (2) explain a group of nonlinear phenanthrene isotherms observed in the laboratory with a single value for the BC-normalized distribution coefficient ($\log K_{BC} = 6.1 \pm 0.04$) and a Freundlich exponent ($n \approx 0.6$ if $\log K_{oc} = 4.0$) that is strongly dependent on the K_{oc} value selected.

6.2 INTRODUCTION

Current research has demonstrated that sediments contain at least two reduced carbon fractions: (1) a biogenic/diagenetic organic carbon (OC) fraction and (2) a combustion-derived, black carbon (BC) fraction [1, 2, 3, 4, 5, 6, 7]. Both of these carbon fractions can act as sorbents of hydrophobic organic compounds, such as polycyclic aromatic hydrocarbons (PAHs). Thus, it is hypothesized that PAH sorption in sediments and soils and the associated solid-water distribution coefficient (K_d, $L/kg_{sediment}$) must consider both an OC *absorbent* and a BC *adsorbent* acting in parallel [6]:

$$K_d = f_{oc} K_{oc} + f_{BC} K_{BC} C_w^{n-1} \quad (1)$$

Here, the absorption term is the product of the OC fraction (f_{oc}, $kg_{oc}/kg_{sediment}$) and the OC-normalized distribution coefficient (K_{oc}, L/kg_{oc}). The adsorption term is the product of the BC fraction (f_{BC}, $kg_{BC}/kg_{sediment}$), the BC-normalized distribution coefficient (K_{BC}, $(\mu g/kg_{BC})/(\mu g/L)^n$), and a function of the dissolved concentration (C_w, $\mu g/L$) where *n* is the Freundlich exponent that describes the distribution of adsorption sites on BC. Because the OC fraction (f_{oc}) has traditionally reflected the sum of OC and BC [8, 9], it should be noted that, in this paper, the f_{oc} parameter includes only the OC absorbent, and is calculated as the difference between the total organic carbon (TOC) content in the solid phase and the BC fraction.

This combined sorption model (Eq. 1) is mathematically similar to other models reported in the literature that describe sorption as a combination of absorption into "soft carbon" and adsorption onto "hard carbon" [10, 11, 12]. In these models, the OC absorption term is expressed as a linear model with low sorption enthalpies, noncompetitive exchange, and rapid kinetics. Meanwhile, the nonlinear component of sorption is assigned to adsorption onto a non-OC fraction. Although a multi-parameter model that apportions nonlinearity to both the OC and BC terms [13] is plausible and more versatile, a model with fewer adjustable parameters is more economical. Therefore, this work sought to ascertain whether reported nonlinear PAH sorption could be understood by considering only a three-parameter model in which all nonlinear interactions are proportional to the presence of BC.

The combined model can account for many of the shortcomings present in the traditional $f_{oc} K_{oc}$ model [8, 9, 14, 15]. Unlike a simple partitioning scheme, the new model is tunable in accord with the presence of more than one reduced carbon fraction in sediments and soils exhibiting distinct chemical affinities. This alternative sorption approach now enables us to explain observations of widely varying K_{oc} values for single sorbates interacting with diverse organic matter [16, 17, 18] and observations of deduced K_{oc} values that exceeded their corresponding K_{ow} values [19, 20, 21, 22].

To assess the effectiveness of the combined sorption model (Eq. 1), two sets of literature observations were re-interpreted. These data sets include: (1) field observations by McGroddy and Farrington, who measured log K_d values for PAHs in cores that were greater than those predicted by the $f_{oc} K_{oc}$ model [19, 20] and (2) laboratory observations by Huang *et al.* [17], who found a group of nonlinear phenanthrene isotherms for diverse sediments and soils used in earlier efforts to establish the $f_{oc} K_{oc}$ model. These recently reported log K_d values and this group of nonlinear isotherms could be explained by considering both an OC absorbent and a BC adsorbent. Subsequent investigation implies that three sorbate parameters (K_{oc}, K_{BC}, and n) and two measured sorbent factors (f_{oc} and f_{BC}) are needed to estimate sorption for any natural solid/PAH combination of interest.

6.3 METHODS

6.3.1 Sample Site: Boston Harbor. In 1990, investigators from the University of Massachusetts at Boston [20] and Massachusetts Institute of Technology [23] retrieved three box cores from Boston Harbor at: (1) Fort Point Channel (FPC) from the Inner Harbor, (2) Spectacle Island (SI) from the Northwest Harbor, and (3) Peddocks Island (PI) from the Southeast Harbor (see Chapter 5; Figure 1). In general, the Inner Harbor is the most polluted area in Boston Harbor mainly because of local combined sewer overflow sites and effluent discharge from former primary treatment plants [24, 25]. The Southeast Harbor is the least polluted area because of its distance from the urban center. Sewage discharge (>150 tons of solids per day in 1990 [26]) had severely affected the benthic communities in the harbor and limited bioturbation in the sediment to <1 cm at

Figure 1: Depth profile (cm) of log K_d values (L/kg) for pyrene at (a) Fort Point Channel (FPC), (b) Spectacle Island (SI), and (c) Peddocks Island (PI). Each panel includes the log K_d values predicted by $K_d = f_{oc} K_{oc}$ (filled circles; assuming log $K_{oc} = 4.7$), the log K_d value observed by McGroddy (1993; open squares), and the log K_d value calculated by the model $K_d = f_{oc} K_{oc} + f_{BC} K_{BC} C_w^{n-1}$ (filled triangles; eq 1 assuming log $K_{oc} = 4.7$, log $K_{BC} = 6.25$, and $n = 0.62$). The dotted lines at 1 cm (FPC) and 10 cm (SI and PI) mark the approximate depth of bioturbation.

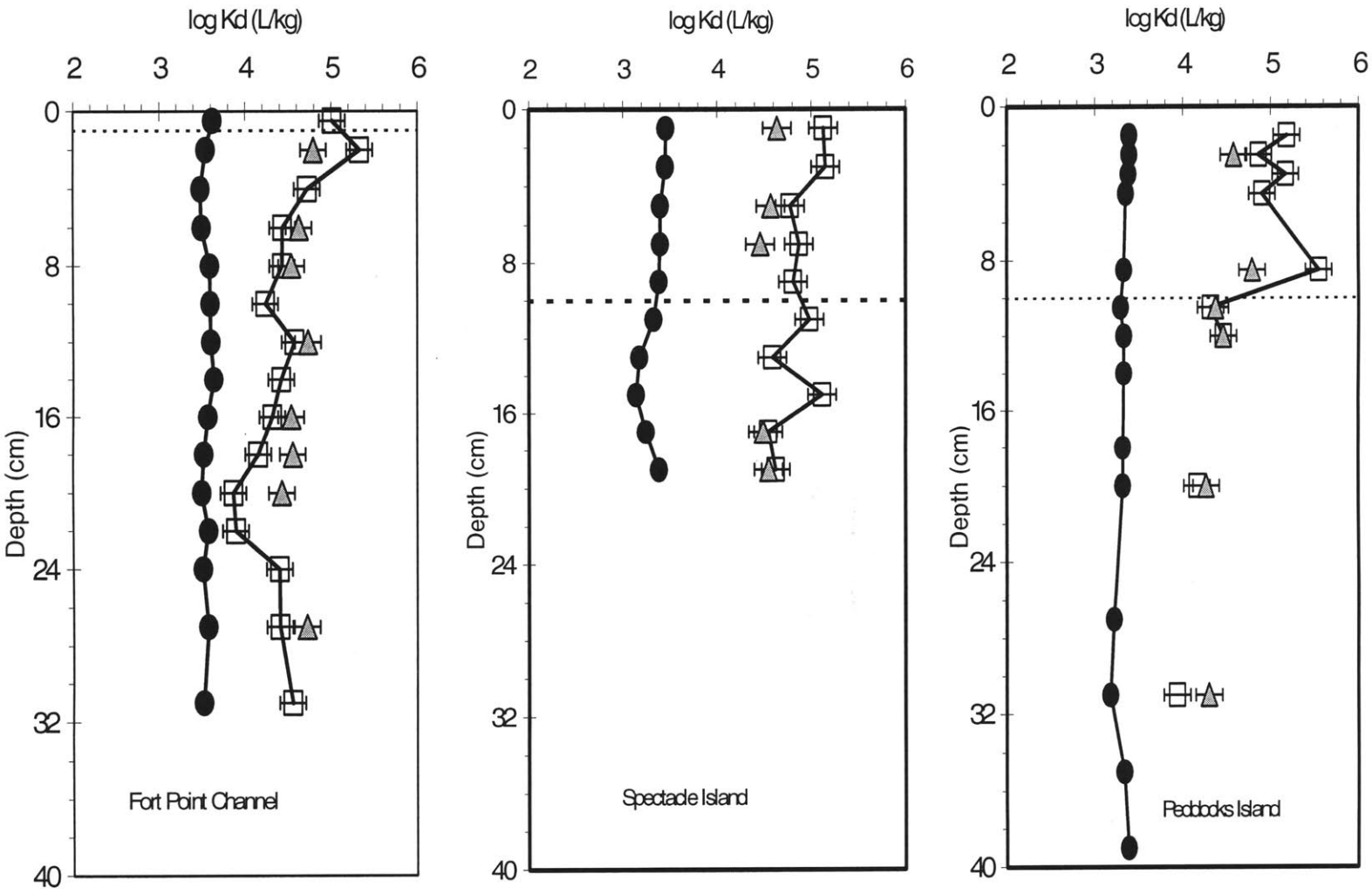
log Kd (L/kg)
2
3
4
5
6
0
8
16
24
32
40
Depth (cm)
Fort Point Channel
log Kd (L/kg)
Spectacle Island
log Kd (L/kg)
Peddocks Island

FPC and <10 cm at SI and PI [27, 28]. Sediments and pore waters from the retrieved box cores were analyzed for percent TOC, pore water organic colloidal concentrations, pore water PAHs, and sediment-sorbed PAHs [19, 23]. With a sedimentation rate of mm/yr in the Inner and Northwest Harbors, core horizons below the depth of bioturbation reflect deposits that are years to decades old [19] allowing protracted times for sorptive equilibration.

6.3.2 Sample Site: U.S. EPA Survey. Sediment and soil samples were collected in the late 1970s in collaboration with the U.S. Environmental Protection Agency (EPA) to investigate the sorption of several organic compounds [29]. Most of the samples were located in the watersheds of the Missouri, Mississippi, Illinois, Wabash, and Ohio Rivers and were chosen on the basis of their depositional characteristics and proximity to potential energy-generating facilities [15, 29]. Recently, Huang *et al.* used these archived sediments and soils to remeasure phenanthrene sorption over wide concentration ranges with extended incubation times [17]. In brief, they measured final dissolved phenanthrene concentrations (between 1-1000 μg/L) after 14-28 days of incubation with the EPA sorbents in solutions containing 0.005 M $CaCl_2$ and 100 mg/L $NaHCO_3$. The final sorbed concentrations were then back-calculated by Huang *et al.* assuming no other losses of phenanthrene.

6.3.3 BC Determinations. BC contents from archived EPA survey samples and Boston Harbor sediments were determined by us as described previously [1]. The dry EPA samples were powders and used as received. The frozen Boston Harbor samples were dried overnight at 80°C, ground with a mortar and pestle, and sieved to remove coarse mineral grains >425 μm. Less than 50 mg of each sample was spread in pre-combusted crucibles, covered with pre-combusted aluminum foil, and combusted under air for 24 hours at 371-372°C in a Sybron F-A1730 Thermolyne muffle furnace (Dubuque, IA).

A Perkin Elmer 2400 CHN elemental analyzer (Norwalk, CT) was then used to measure the BC fractions in the combusted samples. A 15-mg subsample of combusted

sediment was wetted with 100 μL of low-carbon water (Aries Vaponic, Rockland, MA) in silver capsules and then acidified *in situ* with 100 μL sulfurous acid (Fischer Scientific, Fairlawn, NJ, 6% assay) to remove the inorganic carbon fraction. Once the sediment had dried, the silver capsules were wrapped in tin capsules to catalyze the oxidation reaction in the CHN analyzer. The elemental weight percents were accepted only when standard acetanilide samples were within ±0.3 wt % of the known acetanilide values (71.09 wt % C). The carbon blank for the CHN analysis was 14.9 ±0.9 μg of carbon (Z = 13). The signal-to-noise ratio was >3:1 for most of the combusted samples. In three EPA samples, this ratio was 2:1 (Z = 6). Instrumental blanks were run after each sample to verify that previous samples were completely combusted. The OC fraction was then estimated by subtracting the measured BC weight percent from the originally reported TOC content (OC = TOC – BC). Reported TOC values for the EPA samples were verified by independent measurements of the TOC content in three samples. All reported weight percents represent the mean ±1 standard deviation.

6.3.4 Phenanthrene Sorption onto Boston Harbor Sediments. Phenanthrene sorption onto BC in sediments from south Dorchester Bay in Boston Harbor [6] was measured to compare with best-fit log K_{BC} values deduced from the Huang *et al.* data set. Combusted sediments (40-80 mg) were mixed with ≈100 mL of low-carbon water containing phenanthrene at 3.62 μg/L or 8.54 μg/L using methods described previously [6]. After 28 days of tumbling, a Perkin Elmer LS50B Luminescence Spectrofluorometer (Buckinghamshire, England) was used to measure dissolved phenanthrene concentrations remaining in test and control solutions. Synchronous scans were performed with $\Delta\lambda$ of 100 nm, an entrance slit of 5.0 nm, an exit slit of 7.0 nm, and a scan speed of 240 nm/min. The background scans from the control flasks (containing sediment and water) were subtracted from their corresponding experimental flasks to quantify the phenanthrene fluorescence signal at 248.6 nm (excitation wavelength). Fluorescence quenching in the experimental flasks was determined to be negligible. Individual K_d

values were then calculated from the fraction of phenanthrene remaining in the test solutions, and these values were normalized to the BC fraction in the sediment.

6.4 DATA ANALYSIS

For the reported Boston Harbor PAH data, pore water and sediment-sorbed concentrations were corrected for losses during analysis using reported recoveries [19]. All pore water concentrations were further corrected for the fraction of PAHs bound to colloids. For this correction, measured $K_{colloid}$ values for pyrene were used [19, 23], whereas $K_{colloid}$ values for other PAHs were estimated from $\log K_{colloid} = 1.02 \log K_{ow} - 0.53$ [30]. Note that the calculated $\log K_{colloid}$ values contain additional error due to the uncertainty in the $\log K_{ow}$ value [31, 32]. For the McGroddy data examined here, field $\log K_d$ values for pyrene were calculated using the combined sorption model (Eq. 1), the measured BC and OC fractions, and measured pore water concentrations. The following values were assumed for the calculations in this work: a $\log K_{oc}$ value of 4.7 [33], a $\log K_{BC}$ value of 6.25 ±0.14, and an n value of 0.62 ±0.12 for pyrene [6]. Distribution coefficients were adjusted with a Setschenow factor, $10^{(0.3/M)(0.5\ M)}$, to accommodate for 0.5 M salt, but no temperature adjustments were made. The reported $\log K_{oc}$ value of 4.7 might overestimate the "true" K_{oc} value because early investigators did not consider adsorption onto BC. However, at field concentrations considered here (ng/L), the $f_{oc} K_{oc}$ term contributes <26% of the sum K_d values, and minor adjustments of the K_{oc} value will not substantially affect the estimates.

Next, SigmaPlot (version 4.0, Scientific Graphing Software, Inc.) was utilized along with the measured BC and OC fractions for each core section to extract optimal K_{BC} values for 17 other PAHs from the McGroddy data. All reported K_{BC} values derived from SigmaPlot had a coefficient of variation between 15 and 50% (13 non-bioturbated, sediment layers from FPC, SI, and PI). In this analysis, K_{oc} values for individual PAHs were calculated from the K_{oc}-K_{ow} relationship: $\log K_{oc} = 0.989 \log K_{ow} - 0.346$ [9]. Note that the calculated $\log K_{oc}$ values contain additional error due to the uncertainty in the $\log K_{ow}$ value [31, 32]. Because of past experimental protocols (high sorbate concentrations

and short incubation) that emphasized absorption [12, 18], reported K_{oc} values are not believed to be grossly overestimated. For example, in the pyrene sorption experiment by Means *et al.* (C_w = 100-1000 μg/L with EPA 4 [15]), absorption accounted for 76-88% of the total sorption phenomena. Likewise, in the phenanthrene experiment by Karickhoff *et al.* (C_w = 100-500 μg/L with EPA 4 [14]), the $f_{oc} K_{oc}$ term accounted for 54-69% of the overall sorption.

For the reported phenanthrene data, each isotherm was fit using SigmaPlot and the measured BC and OC fractions to extract K_{BC} and n values (Z=12). The phenanthrene log K_{oc} value was fixed at 4.0 for these optimizations in accordance with previous measurements by Karickhoff using the same EPA samples [9]. All errors in the K_{BC} and n values deduced from SigmaPlot are reported in terms of coefficients of variation. For completeness, each isotherm was also fit with the combined sorption model and three adjustable parameters: K_{oc}, K_{BC}, and n. However, because the $f_{oc} K_{oc}$ term does not significantly contribute to the overall sorption value at equilibrium for much of the concentration range examined, SigmaPlot reported a negative value for the K_{oc} term for most of the isotherms with 31-310% error (Appendix A6.1). Thus, no conclusions could be made on the "true" K_{oc} value. Note that for EPA 22, the OC fraction was estimated using this work's own measured TOC value of 2.6 wt % carbon since a BC/TOC ratio of 96% was unreasonable when considering the TOC value of 1.6 wt % carbon reported by Huang *et al.* [17].

In the second approach, MATLAB (version 6.1.0.450 R12.1, The MathWorks, Inc., Natick, MA) was used to solve simultaneously for single values of K_{BC} and n for phenanthrene sorption to eleven EPA samples using the Levenberg-Marquardt nonlinear least-squares function. For this optimization, a suite of likely K_{oc} values was investigated (3.7-4.3; [33]). Errors were minimized between the predicted and observed values of the logarithm of the dissolved concentration (μg/L) to have equal weighting of low and high dissolved concentrations. All reported MATLAB errors represent ±1 standard deviation. All isotherms were fit using sorbed concentrations in μg/g and dissolved concentrations in μg/L to be consistent with the original work by Huang *et al.* [17]. However, K_{BC}

values and K_d values were converted to units of $(\mu g/kg_{BC})/(\mu g/L)^n$ and L/kg, respectively, for comparison with previously reported literature results.

6.5 RESULTS AND DISCUSSION

6.5.1 Re-interpreting PAH Sorption to Boston Harbor Sediment in the Environment.

To evaluate the combined sorption model, the unusually large K_d values observed for Boston Harbor sediments needed to be explained. McGroddy and Farrington previously reported that sorbed PAH concentrations observed in Boston Harbor sediments were much greater than predicted by the $f_{oc} K_{oc}$ model using measured pore water concentrations [20]. For example, the "observed" log K_d values for pyrene at FPC, SI, and PI (Figure 1, open squares) were approximately 1 logarithm unit greater than the "$f_{oc} K_{oc}$-based" log K_d values (Figure 1, filled circles). (Note that all log K_d values for Figure 1 are reported in Appendix A6.2.) Although petroleum in the sediments can contribute to large distribution coefficients, the extractable lipid contents in the sediments at FPC, SI, and PI did not indicate any excessive presence of oils (0.7 ±0.3% at FPC, 0.4 ±0.1% at SI, and 0.3 ±0.1% at PI; [19]).

McGroddy and Farrington suggested that the presence of BC in the sediments could explain this discrepancy for PAHs. They proposed that a certain percentage of PAHs was occluded within BC particles and was unavailable for equilibrium partitioning [20]. Due to the urban surroundings of Boston Harbor, the BC particles that accumulated in these near shore sites were likely derived from atmospheric fallout [34], roadway runoff [35], and local combined sewer overflow sites [36]. Recent sedimentary flux estimations by Gustafsson and Gschwend [2] suggest that Boston Harbor receives approximately 10^6 kg of BC annually. The analysis of core sections studied by McGroddy and Farrington showed that the measured BC weight percents ($kg_{BC}/kg_{sediment}$) were 0.7-1.2 wt % in FPC, 0.3-0.4 wt % in SI, and approximately 0.2 wt % in PI (Table 1). With the total nitrogen content in the untreated sediments <0.5 wt % N and the nitrogen residue in the combusted sediment <0.05 wt % N for the three cores (data not

Table 1: Measured BC weight percents (mean ± 1σ), reported TOC (BC + OC) weight percents, and BC/TOC ratios for McGroddy and Farrington (1995) Environ. Sci. Technol. Boston Harbor, MA cores.

Sample	BC wt %	TOC wt %	BC * 100 / TOC
Fort Point Channel			
1-3 cm	0.70 ±0.14	4.92	14
5-7 cm	0.84 ±0.09	4.40	19
7-9 cm [a]	0.66 ±0.08	5.47	12
11-13 cm	1.2 ±0.13	5.65	22
15-17 cm	0.84 ±0.05	5.19	16
17-19 cm	0.86 ±0.09	4.67	18
19-21 cm	0.67 ±0.07	4.39	15
25-29 cm	0.96 ±0.12	5.23	18
Spectacle Island			
0-2 cm [a]	0.27 ±0.04	4.06	7
4-6 cm	0.29 ±0.07	3.54	8
6-8 cm	0.26 0.05	3.53	7
16-18 cm	0.40 ±0.12	2.48	16
18-20 cm	0.44 ±0.16	3.43	13
Peddocks Island			
2-3 cm	0.21 ±0.04	3.46	6
7-8 cm	0.18 ±0.02	3.24	6
10-11 cm	0.22 ±0.03	2.78	8
13-15 cm	0.24 ±0.02	3.01	8
19-21 cm	0.18 ±0.01	2.97	6
29-33 cm	0.23 ±0.01	2.16	11

a: Literature value for BC wt % measured previously in the laboratory with the same method (Gustafsson et al. (1997) Environ. Sci. Technol.)

shown), charring of nitrogen- containing organic macromolecules probably did not affect the measured BC content in these samples.

Previous studies have shown that pyrene sorption to Boston Harbor sediments is approximated well when simultaneous absorption into an OC fraction and adsorption onto a BC fraction is considered [6]. Likewise, for the McGroddy core sections examined here, the "Eq. 1-based" log K_d values (Figure 1, filled triangles) are a much better approximations of the observed data than the values obtained by the traditional f_{oc} K_{oc} approach. In general, the combined sorption model underpredicted the observed log K_d values in the upper core sections by 0.4 ±0.2 logarithm units (Z = 6). The discrepancy in the upper cores of SI and PI is suspected to attribute to pore water flushing and bioturbation. PI and SI had substantial infaunal abundance [37, 38], and measurements of naturally occurring ^{222}Rn activity suggested that mixing and irrigation were present at both sites. Pore water flushing (either by wave mixing, bioturbation, or gas production) penetrated to 9 cm at SI (10^{-7} sec^{-1}) to 12 cm at PI (10^{-6} sec^{-1}) [27]. In addition, excess ^{232}Th activity was also detected at both PI and SI down to 10 cm, implying a bioturbation flux of 1.2 x 10^{-5} cm^2/sec at PI and 6.3 x 10^{-6} cm^2/sec at SI [27]. The corresponding bioturbation flux at FPC was less intense at 2.0 x 10^{-7} cm^2/sec for depths of <1 cm [28], but this flux might contribute to the log K_d discrepancies observed in surficial sediment at FPC. In light of the observation that the combined sorption model consistently underestimated the observed log K_d values in the bioturbated portions of these cores, it is suspected that dissolved PAH concentrations do not reflect sorption equilibrium in the upper sections of these cores.

Recent reports suggest that PAH sorption is a combination of both fast and slow sorption [18, 39, 40, 41]. For example, Weber and Huang showed that – for the same sediments and soils used by Means *et al.* [15] and Karickhoff [9] – the ratio of sorbed-to-dissolved phenanthrene concentrations ($C_s/C_w^n = K_F$ in units of $(\mu g/g)/(\mu g/L)^n$) increased continuously over a 2-week study [40]. In some instances, the C_s/C_w^n ratio after 1 day was 58-82% of the C_s/C_w^n ratio attained after 2 weeks. Recent work by Accardi-Dey and Gschwend also showed that the adsorption of pyrene onto combusted sediments in the

laboratory took several days to reach an apparent equilibrium [6]. If PAH desorption rates from BC are limited by the surface detachment process, then these rates can be estimated as the ratio of the observed sorptive rate to the BC distribution coefficient. Consequently, when processes such as bioturbation deplete pore water sorbate concentrations in the field, desorption and re-equilibration of PAHs may take weeks to months. Thus, PAH sorption at SI and PI might occur on the same time scale as (or possibly on a longer time scale than) pore water irrigation and bed mixing [27].

The combined sorption model also tended to overestimate the observed K_d values in deeper non-bioturbated horizons by 0.3 ±0.2 logarithm units (Z = 10), especially at FPC. For example, the model does not explain the dip in the observed log K_d values at FPC between 18 and 22 cm corresponding chronologically to the late-1970s. This dip might reflect changes in the sorptive strength of the BC in these horizons (e.g., due to changing fuel usage in response to the oil embargo). Alternatively, this dip in observed log K_d values may represent the presence of petroleum hydrocarbons in the sediment and coating the BC particles. Hence, PAH absorption into the petroleum would be the dominant sorption mechanism in these sediment horizons, resulting in the observed log K_d values approximately equal to the f_{oc} K_{oc}-predicted log K_d value. Another explanation for the elevated field K_d values may also be due to an overcorrection for colloid-bound PAHs. Nonetheless, tuning to measured values of f_{oc} and f_{BC} and using estimates of K_{oc}, K_{BC}, and *n* for pyrene allowed reasonable *a priori* estimates of field K_d values for PAHs.

6.5.1.1 Extracting *in situ* log K_{BC} values for PAHs. Similarly to pyrene, other PAHs in Boston Harbor sediments were observed to exhibit K_d values that were much greater than predicted by a simple partitioning scheme [19]. If PAH sorption is the sum of absorption into the OC fraction and adsorption onto the BC fraction, then the underestimated sorption was due to PAH adsorption onto BC. If this assumption is true, then best-fit K_{BC} values can be "extracted" for other PAHs from the remaining adsorption data using the combined sorption model and the measured BC fractions (for non-bioturbated layers).

Since it is not known how the Freundlich exponent changes for the various PAHs and BC in the environment, a K_{BC} value was calculated for each case of n = 0.6, 0.7, and 0.8 (Table 2; [19]). This exponent range is supported by recent reports of Freundlich exponents varying from 0.6 to 0.8 for activated carbon [42], black carbon [6, 43], sediments, and soil [10, 18, 40] for a range of organic chemicals. In general, the extracted K_{BC} values varied by less than ±0.3 logarithm units in this range. The coefficient of variation on the K_{BC} values (ranging from 15-50%) increased for each PAH as the Freundlich exponent increased from 0.6 to 0.8 implying that lower Freundlich exponents yielded a better fit to the data. The SigmaPlot-derived log K_{BC} values compared well with other reported values for the sorption of PAHs onto NIST diesel particulate matter (SRM 1650; [43]) and combusted Boston Harbor sediment [6] (Table 2).

These K_{BC} values derived from *in situ* concentrations and conditions need to be regarded with caution, however, because the field data may reflect other environmental factors in addition to sorption. For example, colloids might have a stronger effect on the dissolved concentration of HMW PAHs than predicted [23, 30, 44]; thus, the field K_d values for these compounds might actually be higher than reported. Sorption competition, arising because PAHs in the environment occur as mixtures, can also have a pronounced affect on the K_d values. As favorable adsorption sites become occupied, the adsorbed concentration of other competing PAHs decreases [11]. In this case, the field data might reflect K_d values that are lower than would be expected for single-compound testing. Furthermore, anaerobic degradation of LMW PAHs by sulfate reducers can potentially increase the apparent distribution coefficients by lowering the dissolved PAH concentration [45, 46] if this removal mechanism is faster than desorptive replacement. Finally, the BC matrix might change with sediment depth, reflecting a change in BC source over time and thus affecting the adsorption capacity and log K_{BC} values.

With these caveats in mind, the data fitting showed larger BC distribution coefficients for more hydrophobic PAHs – where log K_{ow} is used as a metric of hydrophobicity (Figure 2). Although a linear dependency between octanol-water

Table 2: Log K_{BC} values $((\mu g/kg_{BC})/(\mu g/L)^n)$ at given Freundlich exponents (n) for the BC fraction measured from McGroddy (1993) non-bioturbated samples for 17 co-occurring PAHs in Boston Harbor, MA (0.5 molar salinity and temperature of ≈15°C).

ID [a]	PAH	log K_{ow} [b]	SigmaPlot derived log K_{BC}						Z^d	log K_{BC} [e]
			n = 0.6	%CV [c]	n = 0.7	%CV	n = 0.8	%CV		
1	Naphthalene	3.3	5.1	21	5.2	24	5.4	26	5	5.2
2	Acenaphthene	4.0	5.4	24	5.6	26	5.9	27	6	
3	Acenaphthylene	4.1	4.8	30	5.0	30	5.3	30	4	
4	Fluorene	4.2	6.0	33	6.2	39	6.4	46	7	5.3
5	Phenanthrene	4.5	6.3	24	6.4	27	6.5	30	14	5.7, 5.6
6	Anthracene	4.5	6.1	27	6.3	31	6.5	35	11	
7	1-Methylphenanthrene	5.0	6.2	34	6.4	41	6.6	49	9	
8	Fluoranthene	5.1	6.7	15	6.9	15	7.1	15	14	
9	Pyrene	5.1	6.2	25	6.3	28	6.4	32	13	6.6, 6.3
10	1-Methylpyrene	5.7	6.1	21	6.3	26	6.4	32	12	
11	Chrysene	5.7	6.8	36	7.0	38	7.1	39	8	
12	Benz[*a*]anthracene	5.8	6.9	38	7.1	40	7.3	41	9	
13	Benzo[*b*]fluoranthene	5.9	6.0	15	6.2	18	6.3	20	4	
14	Benzo[*k*]fluoranthene	6.0	6.8	1.5	7.0	1.5	7.2	5	2	
15	Benzo[*a*]pyrene	6.2	6.9	18	7.2	20	7.4	21	10	
16	Benzo[*e*]pyrene	6.3	6.9	25	7.1	27	7.3	29	10	
17	Dibenz[*a,h*]anthracene	6.8	6.8	43	7.1	46	7.4	50	8	

a: ID number for individual PAH corresponding to Figure 2.
b: Note that log K_{ow} values are used only as a metric of hydrophobicity
c: %CV represents the coefficient of variation as a percentage for each Freundlich exponent.
d: Population size from McGroddy (1993) data set.
e: Literature values for BC-normalized distribution coefficients (Buccheli and Gustafsson (2000), Accardi-Dey and Gschwend (2002), and this study).

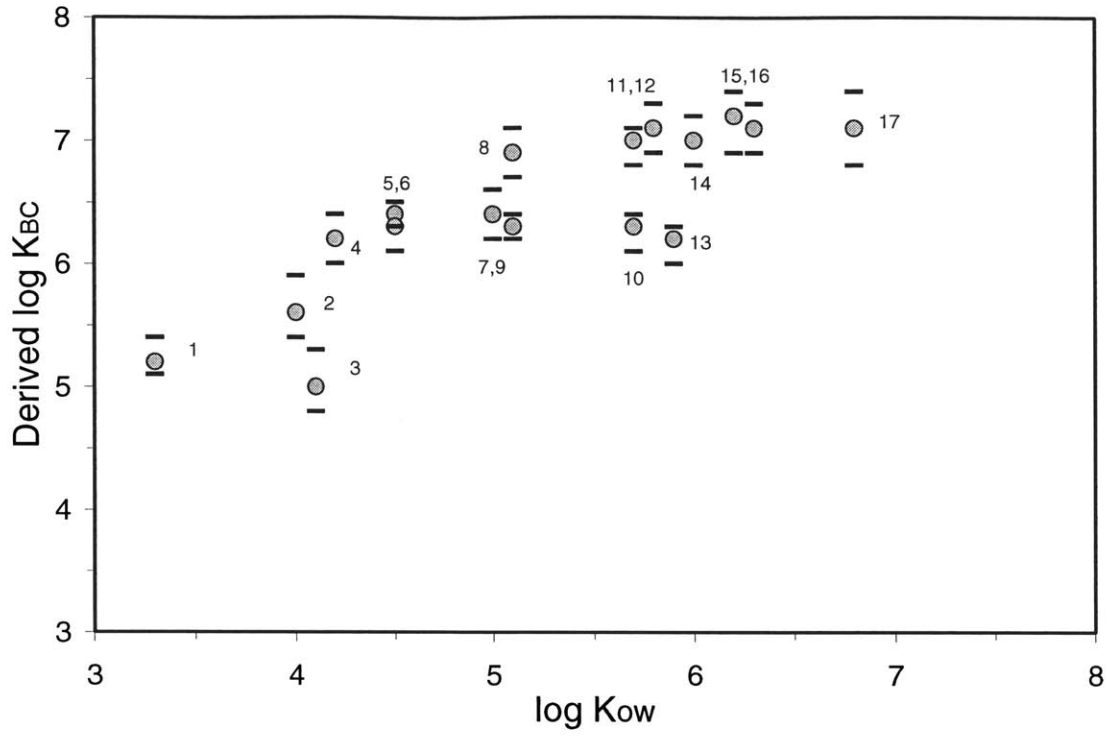

Figure 2: Derived log K_{BC} values ($(\mu g/kg_{BC})/(\mu g/L)^n$) from the McGroddy (1993) field data versus log K_{ow} ($L_{octanol}/L_{water}$) used here only as a metric of PAH hydrophobicity. Filled circles represent the best-fit log K_{BC} values for non-bioturbated sediment layers from all three cores (N = 13) when the Freundlich exponent (n) is fixed at 0.7 and assuming that $K_{BC} = K_d - f_{oc} K_{oc} / (f_{BC} C_w^{n-1})$. Tabs above and below the filled circle show the variability in log K_{BC} when $n = 0.8$ (tabs above circles) and $n = 0.6$ (tabs below circles). ID numbers for the PAHs are listed in Table 2.

partitioning and BC adsorption is not implied, the increasing trend for log K_{BC} values is expected because larger, more hydrophobic PAHs are less compatible with water. However, it is worth noting that this trend in hydrophobicity does not exclude the possibility of an occlusion mechanism – assuming that "occluded" means "chemically extractable" but not "water-exchangeable." If McGroddy extracted both the sorbed and occluded PAHs from the BC in the sediment, then, for a given PAH, there would be a larger K_{BC} value in the SigmaPlot analysis of the McGroddy data than in laboratory spiking experiments that do not involve any chemical extractions. Previous work in the laboratory with pyrene and native Boston Harbor sediment suggest that the log K_{BC} value for spiked pyrene is approximately 6.3 ±0.1 [6], which compares very well with the estimate SigmaPlot-estimated log K_{BC} value of 6.2-6.4 for pyrene (Table 2). Therefore, reversible adsorption onto the BC fraction as represented by spiked compounds (as opposed to PAH occlusion) explains much of the reported high log K_d values observed in these sediments and others.

6.5.2 Re-Interpreting PAH Sorption to EPA Samples in the Laboratory. To continue the assessment of the hypothesis that PAH sorption reflects both OC absorption and BC adsorption, this work attempted to explain nonlinear phenanthrene sorption onto EPA sediments and soils using the model and single values of K_{BC} and n. To explain the nonlinear isotherms observed by Huang *et al.*, the BC fractions in all of the EPA samples were first measured. BC weight percents ranged from 0.03 ±0.01 to 1.6 ±0.02 among the 12 samples (Table 3). The two soil samples (i.e., EPA 14 and EPA 20) were among the lowest values both exhibiting a BC weight percent of 0.03 ±0.01, but an insufficient amount of data exists to determine whether soils usually contain a lower BC content than sediments. These observations, combined with previous measurements [2, 6], suggest that BC often contributes up to 20% of the TOC (Tables 1 and 3). Higher BC/TOC ratios (such as 65% BC/TOC for EPA 22) are uncommon, but they have been reported for surface sediments of the North Sea and in estuaries of The Netherlands [3].

Table 3: Measured BC weight percents (mean ± 1σ), reported TOC weight percents (BC + OC; mean ± 1σ), and BC/TOC ratios for Huang *et al.* (1997) EPA sediments and soils along with best-fit log K_{BC} values ($(\mu g/kg_{BC})/(\mu g/L)^n$) and Freundlich exponents (*n*) for phenanthrene.

Sample	BC wt %	TOC wt %	BC*100 /TOC	SigmaPlot derived Values [a]			
				log K_{BC}	%CV [d]	*n*	%CV [d]
EPA 4 (river sediment, ND)	0.11 ±0.01	2.28 ±0.05	5	6.0	3.8	0.61	2.9
EPA 5 (river sediment, ND)	0.05±0.01	2.07 ±0.14	2	6.4	3.3	0.60	2.6
EPA 13 (river sediment, WV)	0.15 ±0.01	4.50 ±0.10	3	6.3	2.9	0.62	2.2
EPA 14 (soil, WV)	0.03 ±0.01 [b]	0.446 ±0.031	7	5.6	1.2	0.79	5.4
EPA 15 (river sediment, IN)	0.20 ±0.08	1.24 ±0.09	16	5.6	2.5	0.63	1.8
EPA 18 (river sediment, KY)	0.05 ±0.02	0.543 ±0.030, 0.64 ±0.05 [c]	9, 8 [c]	5.9	2.7	0.64	1.9
EPA 20 (soil, IL)	0.03 ±0.01 [b]	1.18 ±0.03	3	6.3	4.2	0.59	3.4
EPA 21 (river sediment, IL)	0.34 ±0.08	2.36 ±0.16	14	5.9	1.6	0.63	1.2
EPA 22 (river sediment, IL)	1.6 ±0.22	1.65 ±0.06, 2.6 ±0.27 [c]	96, 62 [c]	4.5	0.5	0.85	0.2
EPA 23 (lake sediment, IL)	0.09 ±0.01	2.57 ±0.08	4	6.3	3.3	0.61	2.6
EPA 26 (river sediment, IL)	0.05 ±0.01	1.50 ±0.01	3	6.2	2.9	0.65	2.0
EPA B2 (stream sediment, GA)	0.03 ±0.01 [b]	1.07 ±0.03, 1.49 ±0.29 [c]	3, 2 [c]	6.3	5.0	0.56	4.5

a: SigmaPlot derived values assuming a phenanthrene log K_{oc} value of 4.0.
b: Signal-to-noise ratio was 2:1 with Z = 6.
c: Independent measurements of TOC wt % (mean ± 1σ) by this laboratory and corresponding BC/TOC*100 ratios
d: % CV represents the coefficient of variation as a percentage.

No correlation between BC and TOC existed within the EPA data set ($R^2 = 0.08$, Z=12), indicating that the measurements were not affected by charring or other artifacts. Low correlation coefficients between BC and TOC have also been observed for coastal sediments in the New England region ($R^2 = 0.25$, Z = 15; [2]). These results contradict recent claims that the thermal oxidation method creates BC from the incomplete combustion of organic matter [5]. Instead, reported linear correlation between BC and TOC might reflect similar depositional conditions encouraging accumulation of both types of carbon at the same loci rather than analytical error [3, 5].

SigmaPlot was used with the combined sorption model to extract the best-fit *n* and log K_{BC} parameters for *each* isotherm generated by Huang *et al.* [17]. The average of the twelve log K_{BC} values for phenanthrene was 5.9 ±0.5 (Z = 12; Table 3) and the average *n* value was 0.65 ±0.08 (Z = 12). The average log K_{BC} value approximated the reported value of 5.7 for the sorption of phenanthrene onto NIST diesel particulate matter [43]. It also compared reasonably well with the measured log K_{BC} value, which ranged from 5.3-5.9 (Z = 4) for the sorption of phenanthrene onto combusted sediments from Boston Harbor (Table 4; representative fluorescence scan shown in Figure 3). However, the average SigmaPlot *n* value (0.65 ±0.08 (Z = 12)) did not compare well with the *n* values (0.87-1.00) reported by Bucheli *et al.* in the same NIST experiment [43], and an insufficient amount of data existed in this laboratory to construct an isotherm for comparison.

A closer inspection of the twelve SigmaPlot log K_{BC} values reveals a 2-logarithm-unit range of values from 4.5 to 6.4 (Table 3; Figure 4). Unlike the previous discussion that focused on Boston Harbor sediments, the EPA samples considered here represent a diverse suite of sites and might include BC from a variety of sources (e.g., engine-derived soot, incinerator fly ash, chars from biomass burns, and carbon black from tire wear). Each source might produce a BC adsorbent with a different affinity for PAHs. Contributions from diverse surface chemistry (considering crystalline graphite versus oxygen moiety substituted activated carbons) and surface area might account for the range of log K_{BC} values observed. However, it is suspicious that EPA 22 – with the

Table 4: Measured phenanthrene sorption (mean ±1σ) to combusted sediment (Boston Harbor, MA) in the laboratory.

Sediment [a] (mg)	Volume [a] (L)	Initial Concentration (μg/L)	Final Concentration (μg/L)	Measured K_d (L/kg)	Estimated log K_{BC} [b] $(\mu g/kg)/(\mu g/L)^n$
40.6	0.102	3.62 ±0.14	2.97 ±0.14	550 ±170	5.5 – 5.6
41.6	0.104	8.54 ±0.34	7.77 ±0.33	250 ±160	5.3 – 5.4
79.8	0.103	3.62 ±0.14	1.96 ±0.12	1100 ±130	5.8 – 5.9
80.2	0.105	8.54 ±0.34	6.38 ±0.29	450 ±100	5.5 – 5.7

a: Error in sediment mass and volume is <1%.
b: BC-normalized distribution coefficient (log K_{BC}) assuming that $K_{BC} = K_d/f_{BC}/(C_{final}^{n-1})$ where f_{BC} = 0.002 ±0.0002 wt % for n = 0.6 and n = 0.8.

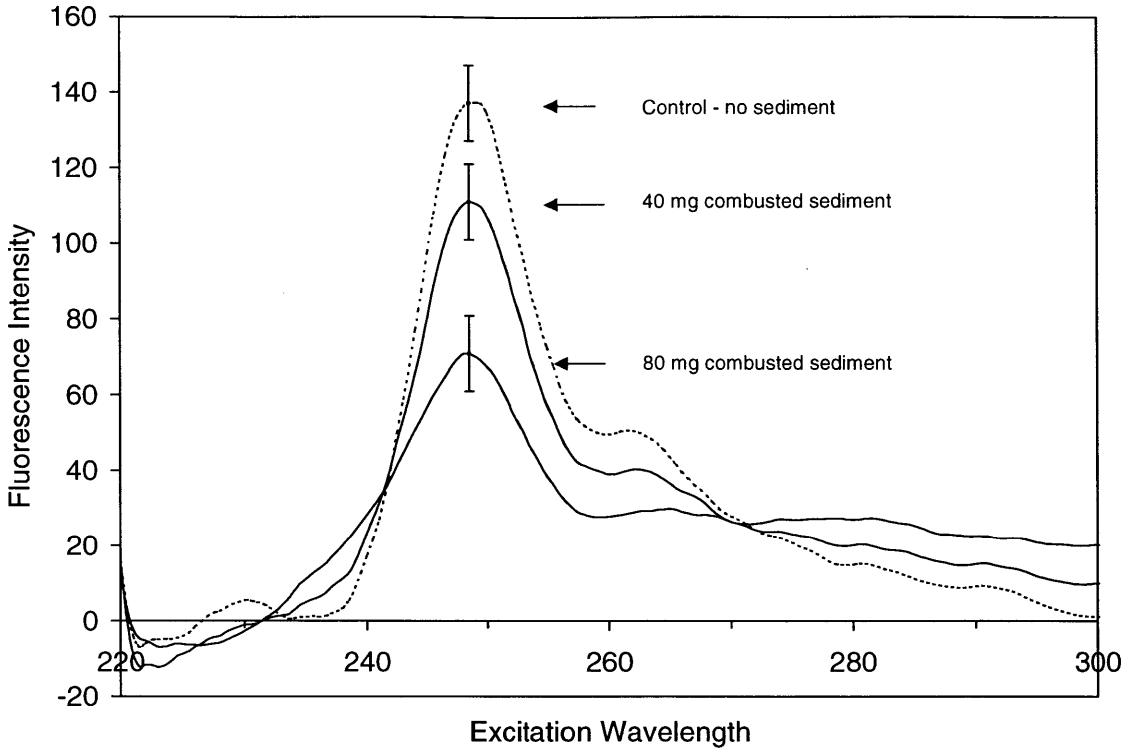

Figure 3: Fluorescence scans (intensity vs. excitation wavelength) showing the observed loss of dissolved phenanthrene due to sorption onto combusted SDB sediments after >28 days. Scans corrected for background signal and have a propagated error of 8%. The dotted line represents the control experiment with no sediment (intensity corresponds to 8.54 μg phenanthrene/L). The two solid lines and corresponding labels represent experiments with varying amounts of uncombusted sediment: 40 mg sediment (9.02% loss of phenanthrene) and 80 mg sediment (25.3% loss of phenanthrene).

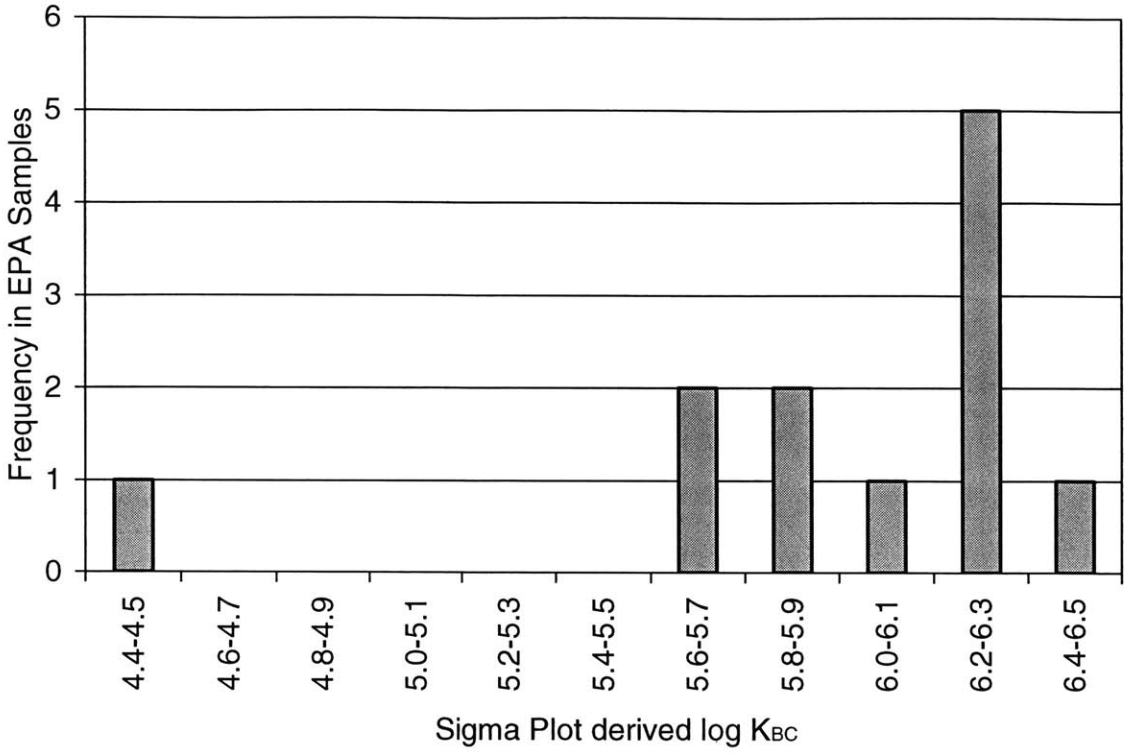

Figure 4: Histogram of the phenanthrene log K_{BC} values $((\mu g/kg_{BC})/(\mu g/L)^n)$ extracted from isotherms for EPA sediments and soils reported by Huang *et al.* (1997) Environ. Sci. Technol. using C_s (μg/g) = f_{oc} K_{oc} C_w (μg/L) + f_{BC} K_{BC} C_w (μg/L)^n and assuming log K_{oc} = 4.0. Log K_{BC} values correspond to values listed in Table 3.

highest BC weight percent – had the lowest log K_{BC} value. An alternative explanation for the low distribution coefficient for EPA 22 might be that the incubation period chosen by Huang *et al.* was not long enough for this particular sample because of the large BC fraction. Thus, equilibrium might not have been established, so that the BC distribution coefficient was underestimated.

In addition to examining these twelve log K_{BC} values separately, all of the isotherms were fit collectively using the combined sorption model. To this end, MATLAB was used to solve simultaneously for the best-fit log K_{BC} and n values for the eleven EPA isotherms with a fixed log K_{oc} value of 4.0. EPA 22 was not included in this fit because of its unusual BC/TOC ratio and low log K_{BC} value. The MATLAB optimization yielded a single, best-fit log K_{BC} value for phenanthrene of 6.1 ±0.04 and an n value of 0.55 ±0.03 with an R^2 of 0.95. Remarkably, when BC adsorption and OC absorption were considered together, single values for log K_{BC} and n could explain the phenanthrene sorption onto this diverse array of sediments and soils. In addition, the model's parameters for phenanthrene sorption compared well with an independent sorption experiment performed by Karapanagioti *et al.* who examined the sorption of phenanthrene in synthetic groundwater onto a soil subsample (0.5-0.25 mm grain size, nonmagnetic) dominated by isolated coal particles [18]. In their work, the best-fit Freundlich exponent was 0.55 ±0.02 with a log K_{BC} value of 6.3-6.4 at 1 μg/L (assuming that all of the carbon (1.60 wt % C) is attributed to the coal particles).

In this optimization, the log K_{BC} value was affected only slightly by the choice of log K_{oc} value, whereas the n value was extremely sensitive to log K_{oc}. Since the Freundlich exponent (n) reflects the curvature of the isotherm, the n value decreased to compensate for the higher log K_{oc} values. For example, as the log K_{oc} values for phenanthrene were adjusted from 3.7 to 4.3 [33], the best-fit n value decreased from 0.66 to 0.27 whereas the log K_{BC} value remained virtually the same, decreasing slightly from 6.1 to 6.0 (Table 5). The constancy of the log K_{BC} term throughout this fitting suggests that, at low dissolved concentration where adsorption dominates [12, 18], only one BC distribution coefficient can reasonably fit all of these isotherms. Furthermore, these

Table 5. Best-fit log K_{BC} value ((μg/kg)/(μg/L)^n) and Freundlich exponent (n) for phenanthrene sorption simultaneously to eleven EPA sediment and soil standards (exclude EPA 22) reported by Huang *et al.* (1997) Environ. Sci. Technol. assuming a range of log K_{oc} values (L/kg).

Assumed log K_{oc}	MATLAB-derived			
	log K_{BC}	%CV [a]	n	%CV [a]
3.7	6.09	10	0.66	4.1
3.8	6.09	10	0.63	4.4
3.9	6.09	9.8	0.60	4.8
4.0	6.08	9.6	0.55	5.4
4.1	6.07	9.7	0.49	7.0
4.2	6.07	11	0.40	11
4.3	6.06	15	0.27	27

a: %CV represents the coefficient of variation as a percentage.

results suggest that observed nonlinear isotherms are dominated by BC adsorption, and therefore minor manipulations in the nonlinear/linear nature of the OC fraction will have minor implications on the predicted log K_d values for low phenanthrene concentrations.

All eleven EPA isotherms were reconstructed using the combined sorption model with a log K_{oc} value of 4.0, a log K_{BC} value of 6.1 and an *n* value of 0.55. These model isotherms were then compared to the observed isotherms reported by Huang *et al.* [17]. The model estimated the observed, sorbed concentration well at high dissolved concentrations (>10 μg/L); however, at lower concentrations (<10 μg/L), the model either overestimated or underestimated the observed, sorbed concentrations. The equal scattering of data above and below the observed isotherms is expected though because of the modeling optimization scheme. For simplicity, only three representative isotherms are shown in Figure 5 – one that is overestimated, one that is underestimated, and one that is predicted well. (Note that all remaining isotherms are shown in Appendix A6.3.) In general, the combined sorption model was able to predict the K_d values observed by Huang *et al.* within a factor of 3. To illustrate this approximation differently, a compilation of data along all eleven isotherms was made for the predicted log K_d values (Eq. 1) versus observed log K_d values [17] at three different dissolved concentrations (2 μg/L, 20 μg/L, and 400 μg/L; Figure 6). As noted above, the data are more scattered at the lower concentrations (2 μg/L, filled circles) than the higher concentrations (400 μg/L, filled squares). The difference between the predicted log K_d values at 2 μg/L and the one-to-one line was 0.3 ±0.4 logarithm units, whereas the difference at 400 μg/L was only 0.1 ±0.2 logarithm units. No correlation was noticed between the BC fraction of the samples and the accuracy of these estimates. Hence, the model and best-fit parameters allow for reasonable estimates of phenanthrene sorption to a diverse set of sediments and soils.

This work suggests that the simple OC absorption model does not capture all the sorption phenomena influencing PAHs in natural solids that contain BC, especially at ambient concentrations. It is expected that similar behaviors will especially apply to the planar congeners in other important hydrophobic compound classes (e.g., PCBs,

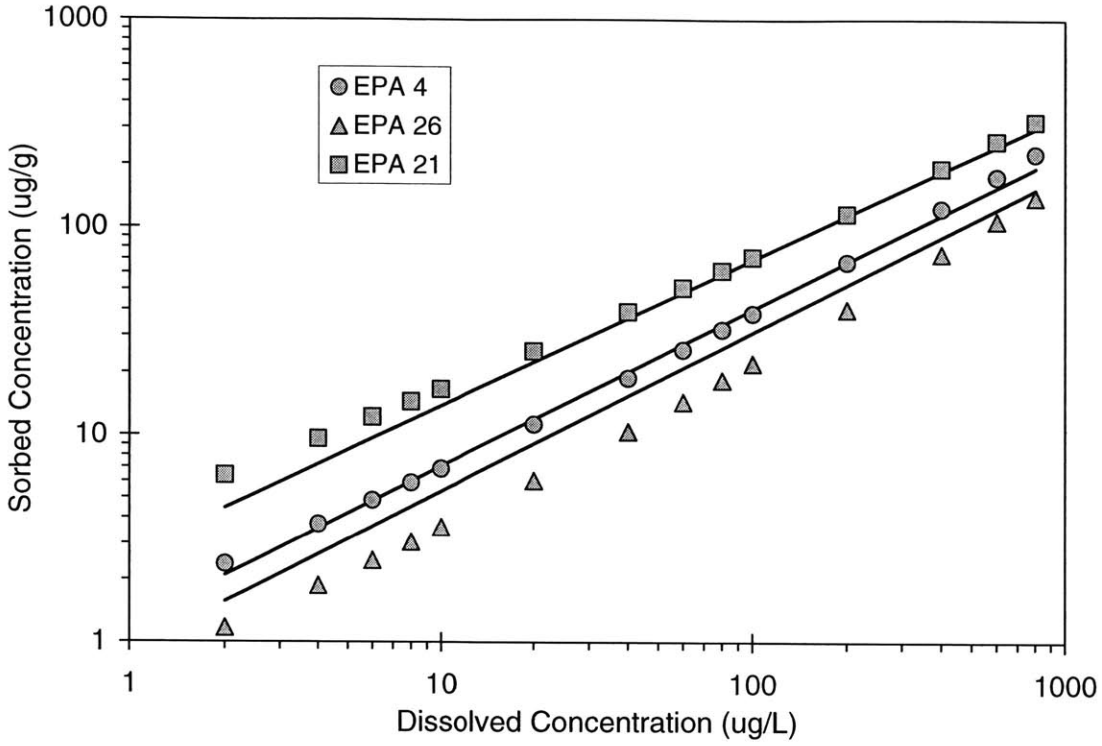

Figure 5: Comparison of observed phenanthrene isotherms (solid line; C_s (μg/g) = K_d C_w (μg/L)^n) from Huang *et al.* (1997) Environ. Sci. Technol. and model isotherms (filled symbols; C_s (μg/g) = f_{oc} K_{oc} C_w (μg/L) + f_{BC} K_{BC} C_w (μg/L)^n assuming log K_{oc} = 4.0, log K_{BC} = 6.1, and n = 0.55) for three representative EPA samples (EPA 4, 26, and 21). For the sorbed concentration (μg/g), the propagated error was approximately 20% for the observed isotherm by Huang *et al.* (1997) Environ. Sci. Technol. and 50% for the model isotherm. Samples correspond to data listed in Table 3.

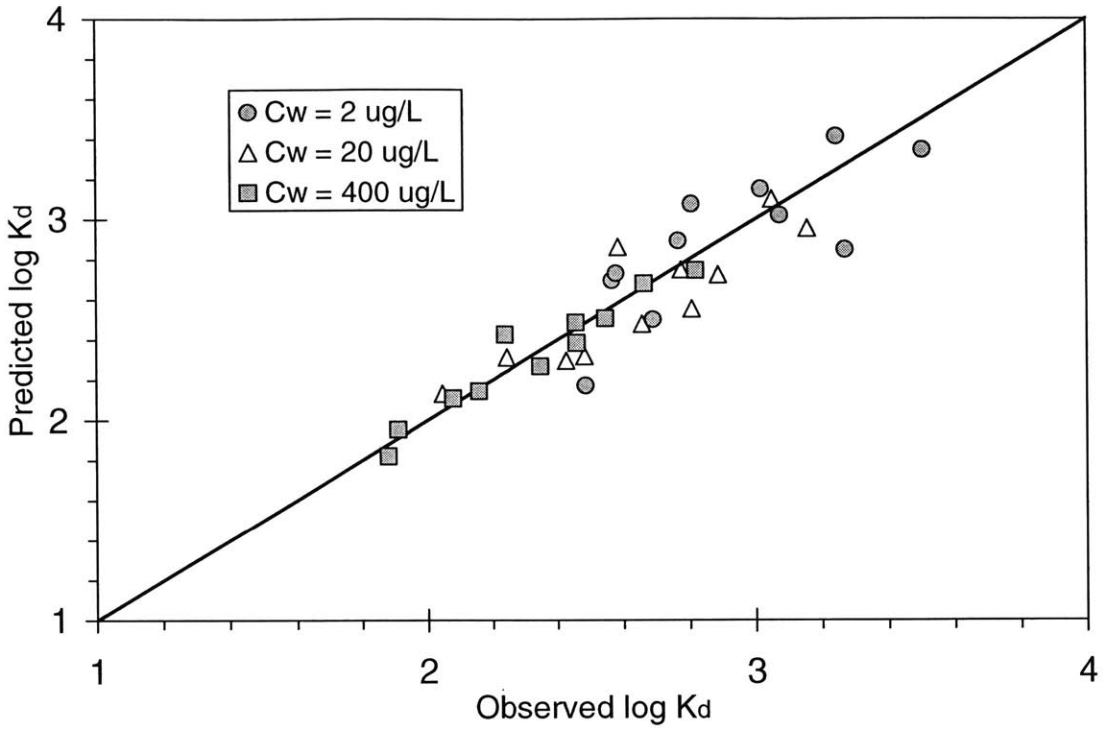

Figure 6: Log K_d values (L/kg) predicted from eq 1 ($K_d = f_{oc} K_{oc} + f_{BC} K_{BC} C_w^{n-1}$ assuming log $K_{oc} = 4.0$, log $K_{BC} = 6.1$, and $n = 0.55$) versus the log K_d values (L/kg) observed by Huang *et al.* (1997) Environ. Sci. Technol. at the dissolved concentrations (C_w) of 2 µg/L (filled circles), 20 µg/L (open triangles), and 400 µg/L (filled squares) along eleven isotherms. The approximate errors for all the data are ±0.2 log units for the predicted log K_d value (y-axis) and ±0.1 log units for the observed log K_d value (x-axis). The solid line marks the one-to-one line.

chlorinated dioxins, and *p,p'*-dichlorodiphenyldichloroethene (DDE) [22]) where BC is the dominant sorbent. Therefore, remediation programs and risk-management teams need to consider the implication of both a BC adsorbent and an OC absorbent in sediments and soils. These BC sorptive interactions might explain the limited desorption [47] and limited bioavailability of PAHs in the environment [48, 49, 50, 51].

6.6 ACKNOWLEDGMENTS

This work was supported by NSF Grant No. BES-9800485. The project, number RC-70, was also funded (in part) by the MIT Sea Grant College Program under a federal grant number NA86RG0074 from the National Sea Grant College Program, National Oceanic and Atmospheric Administration, U.S. Department of Commerce. Thanks to Wayne Banwart, Suresh Rao, and Ryan Hultgren for locating and donating the EPA samples and John Farrington, Tim Eglinton, and Chris Reddy for locating and donating the McGroddy cores. Special thanks go to John MacFarlane of MIT for his continuous support in the lab, Dave Glover of WHOI for help on the MATLAB modeling, and Richard Bopp for his useful discussions on this project.

6.7 REFERENCES

1. Gustafsson, Ö.; Haghseta, F.; Chan, C.; MacFarlane, J.; Gschwend, P. M. *Environ. Sci. Technol.* **1997**, *31,* 203-209.
2. Gustafsson, Ö.; Gschwend, P. M. *Geochim. Cosmochim. Acta* **1998**, *62,* 465-472.
3. Middelburg, J. J.; Nieuwenhuize, J.; Breugel, P. V. *Mar. Chem.* **1999**, *65,* 245-252.
4. Zhou, J. L.; Fileman, T. W.; Evans, S.; Donkin, P.; Readman, J. W.; Mantoura, R. F. C.; Rowland, S. *Sci. Total Environ.* **1999**, *244,* 305-321.
5. Gelinas, Y.; Prentice, K. M.; Baldock, J. A.; Hedges, J. I. *Environ. Sci. Technol.* **2001**, *35,* 3519-3525.
6. Accardi-Dey, A.; Gschwend, P. M. *Environ. Sci. Technol.* **2002**, *36,* 21-29.
7. Mitra, S.; Bianchi, T. S.; McKee, B. A.; Sutula, M. *Environ. Sci. Technol.* **2002**, *36,* 2296-2302.
8. Chiou, C. T.; Peters, L. J.; Freed, V. H. *Science* **1979**, *206,* 831-832.
9. Karickhoff, S. W. *Chemosphere* **1981**, *10,* 833-846.

10. Weber, W. J.; McGinley, P. M.; Katz, L. E. *Environ. Sci. Technol.* **1992**, *26,* 1955-1962.
11. Xing, B. S.; Pignatello, J. J.; Gigliotti, B. *Environ. Sci. Technol.* **1996**, *30,* 2432-2440.
12. Xia, G. S.; Ball, W. P. *Environ. Sci. Technol.* **1999**, *33,* 262-269.
13. Laor, Y.; Rebhun, M. *Environ. Sci. Technol.* **2002**, *36,* 955 - 961.
14. Karickhoff, S. W.; Brown, D. S.; Scott, T. A. *Water Res.* **1979**, *13,* 241-248.
15. Means, J. C.; Wood, S. G.; Hassett, J. J.; Banwart, W. L. *Environ. Sci. Technol.* **1980**, *14,* 1524-1528.
16. Grathwohl, P. *Environ. Sci. Technol.* **1990**, *24,* 1687-1693.
17. Huang, W.; Young, T. M.; Schlautman, M. A.; Yu, H.; Weber, W. J. *Environ. Sci. Technol.* **1997**, *31,* 1703-1710.
18. Karapanagioti, H. K.; Kleineidam, S.; Sabatini, D.; Grathwohl, P.; Ligouis, B. *Environ. Sci. Technol.* **2000**, *34,* 406-414.
19. McGroddy, S. E. *Ph.D Thesis: Sediment-Pore Water Partitioning of PAHs and PCBs in Boston Harbor, Massachusetts.* **1993**, University of Massachusetts at Boston: Boston. 1-255.
20. McGroddy, S. E.; Farrington, J. W. *Environ. Sci. Technol.* **1995**, *29,* 1542-1550.
21. Chiou, C. T.; McGroddy, S. E.; Kile, D. E. *Environ. Sci. Technol.* **1998**, *32,* 264-269.
22. Bucheli, T. D.; Gustafsson, Ö. *Environ. Toxicol. Chem.* **2001**, *20,* 1450-1456.
23. Chin, Y.; Gschwend, P. M. *Environ. Sci. Technol.* **1992**, *26,* 1621-1626.
24. Shiaris, M. P.; Jambard-Sweet, D. *Mar. Pollut. Bull.* **1986**, *17,* 469-472.
25. Eganhouse, R. P.; Sherblom, P. M. *Mar. Environ. Res.* **2000**, *51,* 51-74.
26. Rex, A. C. *The State of Boston Harbor 1997-1998: Beyond the Boston Harbor Project.* **2000**, Massachusetts Water Resources Authority: Charlestown. 1-24.
27. Wong, C. S. *M.S. Thesis: Assessing the Flux of Organic Pollutants from the Sediments of Boston Harbor.* **1992**, Massachusetts Institute of Technology: Cambridge. 1-138.
28. Stolzenbach, K. D.; Adams, E. E. *Exchange of contaminants between the sediments and the water column* in *Contaminated Sediments in Boston Harbor.* **1998**, Marine Center for Coastal Processes, MIT Sea Grant Program: Cambridge. 45-74.
29. Hassett, J. J.; Means, J. C.; Banwart, W. L.; Woods, S. G. *Sorption Properties of Sediments and Energy-Related Pollutants.* **1980**, US Environmental Protection Agency: Washington D.C., EPA-600/603-680-041.
30. Mitra, S.; Dickhut, R. M. *Environ. Toxicol. Chem.* **1999**, *18,* 1144-1148.
31. Pontolillo, J.; Eganhouse, R. P. *The Search for Reliable Aqueous Solubility and Octanol-Water Partitioning Coefficient Data for Hydrophobic Organic Compounds: DDT and DDE as a Case Study.* **2001**, U.S. Geological Society: Reston, VA. *01-4201,* 1-55.
32. Renner, R. *Environ. Sci Technol.* **2002**, *36,* 411A-413A.
33. Gawlik, B. M.; Sotiriou, N.; Feicht, E. A.; Schulte-Hostede, S.; Kettrup, A. *Chemosphere* **1997**, *34,* 2525-2551.

34. Windsor, J. G.; Hites, R. A. *Geochim. Cosmochim. Acta* **1979**, *43,* 27-33.
35. Miguel, A. H.; Kirchstetter, T. W.; Harley, R. A. *Environ. Sci. Technol.* **1998**, *32,* 450-455.
36. Lefkovitz, L.; Dahlen, D.; Hunt, C.; Ellis, B. *1998 CSO Sediment Study Synthesis Report.* **2000**, Massachusetts Water Resource Authority: Charlestown. 1-54.
37. Gallagher, E. D.; Keay, K. E. *Organism-Sediment-Contaminant Interactions in Boston Harbor* in *Contaminated Sediments in Boston Harbor.* K. D. Stolzenback; E. E. Adams. **1998**, Marine Center for Coastal Processes, MIT Sea Grant Program: Cambridge. 89-132.
38. Leo, W. S.; Alber, M.; Connor, M. S.; Keay, K. E.; Rex, A. C. *Contaminated Sediments in Boston Harbor.* **1994**, Massachusetts Water Resource Authority: Boston. 1-53.
39. Pignatello, J. J.; Xing, B. S. *Environ. Sci. Technol.* **1996**, *30,* 1-11.
40. Weber, W. J.; Huang, W. *Environ. Sci. Technol.* **1996**, *30,* 881-888.
41. Hulscher, T. E. M. T.; Vrind, B. A.; Heuvel, H. V. d.; Velde, L. E. V. d.; Noort, P. C. M. V.; Beurskens, J. E. M.; Govers, H. A. J. *Environ. Sci. Technol.* **1999**, *33,* 126-132.
42. Crittenden, J. C.; Luft, P.; Hand, D. W.; Oravitz, J. L.; Loper, S. W.; Art, M. *Environ. Sci. Technol.* **1985**, *19,* 1037-1043.
43. Bucheli, T. D.; Gustafsson, Ö. *Environ. Sci. Technol.* **2000**, *34,* 5144-5151.
44. Masiello, C. A.; Druffel, E. R. M. *Science* **1998**, *280,* 1911-1913.
45. Coates, J. D.; Woodward, J.; Allen, J.; Philp, P.; Lovley, D. R. *Appl. Environ. Microb.* **1997**, *63,* 3589-3593.
46. Hayes, L. A.; Nevin, K. P.; Lovley, D. R. *Org. Geochem.* **1999**, *30,* 937-945.
47. Lamoureux, E. M.; Brownawell, B. J. *Environ. Toxicol. Chem.* **1999**, *18,* 1733-1741.
48. Tracey, G. A.; Hansen, D. J. *Arch. Environ. Contam. Toxicol.* **1996**, *30,* 467-475.
49. Tang, J.; Garcia, R.; Holden, K. M. L.; Mitchell, S. C.; Pis, J. J. *Environ. Sci. Technol.* **1998**, *32,* 3586-3590.
50. Alexander, M. *Environ. Sci. Technol.* **2000**, *34,* 4259-4265.
51. Krauss, M.; Wilcke, W.; Zech, W. *Environ. Pollut.* **2000**, *110,* 79-88.

CHAPTER 7: CONCLUSIONS

7.1 SUMMARY OF THESIS

The thesis work presented here explores black carbon (BC) in marine sediments. Experiments were conducted to (1) re-examine a method designed to isolate and quantify BC in sediment samples, and (2) investigate the sorptive properties of BC for polycyclic aromatic hydrocarbons (PAHs), pollutants emitted into marine ecosystems. BC is operationally defined here as thermally altered carbonaceous material and is subdivided into two regimes: soot (sub-micron particles formed from the gaseous condensation of radical hydrocarbons) and char (micro-size fragments of unburnt material; Ch. 2, Fig. 1). Teragrams of BC particles (estimates ranging from 1,000 Tg/yr [1] to 10 Tg/yr [2]; Tg = 10^{12} grams) are emitted into the environment (from land to atmosphere) mainly by biomass burning and fossil fuel combustion [3]. While larger char particles will settle out of the atmosphere close to the BC source, soot is widely dispersed by long-range aeolian transport (Ch. 2, Fig 2). Eventually, these BC particles will settle into sediment beds and contribute a certain percentage of the measured total carbon. For example, BC measurements suggest that BC typically accounts for 15-25% of the total organic carbon content in sediments from the New England coast [4], the Southern Ocean and Northeastern Pacific Ocean [5], as well as the North Sea and Black Sea [6]. Similar BC/TOC ratios were reported in this thesis for sediment samples from the Boston Harbor (16-18%; Ch. 5, Tbl. 1); however, a wider BC/TOC range was measured for a suite of EPA sediments and soils (3-62%; Ch. 6, Tbl. 3) and for horizons in sediment cores from the Boston Harbor (7-22%, Ch. 6, Tbl 1).

Many BC methods are reported in the literature that use various optical, thermal, and chemical techniques to remove organic carbon (OC) from a sample and quantify the BC content [7]. However, reported BC values may vary more than a factor of 10 among these various methods due to incomplete removal of OC, the creation of a BC artifact, or the loss/oxidation of BC particles (Ch. 2, Fig. 3 & 4). After reviewing the advantages and disadvantages of various methods (Ch. 2, Tbl. 4), the 375°C thermal oxidation

method (375°C combustion for 24 hours under air [8, 9]) was selected as the best method to oxidize labile OC and to isolate combustion-derived BC. However, critics of the 375°C method argue that the pretreatment is flawed because either OC will char and create a bias in the BC measurement [10], or BC particles can potentially be oxidized, thus underestimating the true BC content [11]. To address these concerns, experiments were designed and were tested to investigate the potential charring of organic matter and the loss of BC during the 375°C pretreatment.

By combusting sediment samples mixed with natural compounds like cellulose, bovine serum albumin, and phytoplankton material, charring was constrained to samples containing a high total nitrogen (TN) content (Ch. 3, Fig. 3; Ch. 3, Tbl. 1). Further studies with proteins revealed that while nitrogen functional groups are susceptible to oxidation (Ch. 3, Tbl. 2), the physical packaging of proteins may restrict oxygen accessibility and cause charring. The charring of protein was reduced by a factor 3 by physically grinding the particle diameter from 125 μm to <38 μm (Ch. 3, Fig. 5), and charring of proteins was virtually eliminated by dispersing the compound among sediment grains. Since oxygen accessibility appears to be the key factor in determining what material can survive the 375°C method, BC particles are also susceptible to the pretreatment if oxygen becomes more accessible to the carbon surface (Ch. 3, Fig. 7 & 9). An extensive study on carbon oxidation was then conducted to determine at what temperature half of the added BC (or OC) was oxidized after a 24-hour pretreatment. A model (Ch. 3, Eq. 2) was applied to use this carbon oxidation information (in the form of Boltzmann sigmoidal functions, Eq. 1) to estimate the total OC content and the total BC content in sediment samples (Ch. 3, Fig. 14-17). Between the 375°C method and the proposed model, the BC content was reasonably estimated in the sediment samples tested and accounted for 15-30% of the TOC (Ch. 3, Tbl. 4).

Meanwhile, BC has been proposed to act as an adsorbent in sediment beds and may account for the high sorption affinities of PAHs [4, 12, 13, 14]. Historically, sorption of hydrophobic chemicals, like PAHs, was explained with a partitioning model where the solid-water distribution coefficient (K_d, units L/kg) was dependent on the

fraction of organic carbon (f_{oc}) in the sediment and a known, OC-normalized distribution coefficient (K_{oc}, L/kg_{oc}; Ch. 4, Eq. 2 & Fig. 2) [15, 16]. Based on the f_{oc} K_{oc} model, sorbates would display linear isotherms, would exhibit reversible exchanges, and would not compete with other hydrophobic sorbates. However, this partitioning model failed to fit the equilibrium sorption of organic compounds in some laboratory experiments (Ch. 4, Fig. 4 & 5) [17, 18, 19] and could not explain the strong sorption of PAHs to sediments in the field (Ch. 6, Fig. 1) [20, 21, 22, 23, 24, 25]. To account for these observations, Weber *et al.* hypothesized that organic matter contained a heterogeneous mix of sorbents, for example, "hard" and "soft" carbons [17] (Ch. 4, Fig. 3 & 6). Moreover, they suggested that organic compounds would partition into the "soft" carbon and adsorb onto the "hard" carbon.

Here, the sorption of PAHs in sediments and soils is hypothesized as the sum of absorption into a labile, biogenic OC fraction and adsorption onto a combustion-derived BC fraction (Ch.1 for definitions of terms; Ch. 5, Eq. 2 & 3). This combined sorption model is mathematically similar to other models reported in the literature that describe sorption as a combination of adsorption and absorption mechanisms [26, 27]. To characterize the adsorption of pyrene, a representative PAH, to an environmental BC matrix, an isotherm was constructed with 375°C combusted, Boston Harbor sediment to measure the BC-normalized distribution coefficient (K_{BC}, units $(\mu g/kg)/(\mu g/L)^n$) and the Freundlich exponent (n; Ch. 5, Fig. 5 & 7). Although the 375°C method underestimates the total BC fraction, the measured K_{BC} value is still acceptable since the value is determined on a mass basis. Nonetheless, the fraction of BC that survived a 375°C thermal pretreatment accounted for >80% of the total pyrene sorption in this Boston Harbor sediment. Moreover, the pyrene isotherm for untreated sediment was characterized well as the sum of OC absorption and BC adsorption. Finally, the measured log K_{BC} for pyrene on environmental BC (6.3 ±0.2) was less than the measured value for sorption onto NIST 1650 soot (6.6 [28]), indicating that different BC particles have different sorption affinities.

To assess the effectiveness of our combined sorption model, two sets of literature data were re-interpreted. These data sets include (1) field observations by McGroddy and Farrington, who measured log K_d values for PAHs in cores that were greater than those predicted by the f_{oc} K_{oc} model [23, 29] (Ch. 6, Fig 1), and (2) laboratory observations by Huang *et al.* [30], who found a group of nonlinear phenanthrene isotherms for diverse sediments and soils used in earlier efforts to establish the f_{oc} K_{oc} model (Ch. 6, Fig. 5). In the McGroddy cores below the zone of bioturbation, the log K_d values calculated from the combined sorption model were in general a much better approximation of the observed data than the values obtained with the f_{oc} K_{oc} model. Meanwhile, the discrepancy in the upper cores of Spectacle Island and Peddocks Island was attributed to disequilibrium due to pore-water flushing and bioturbation [31, 32, 33, 34]. For the Huang *et al.* data, when BC adsorption and OC absorption were considered together single values (model derived) for log K_{BC} (6.1 ±0.04) and n (0.55 ±0.03) could explain the phenanthrene sorption onto a diverse array of sediments and soils. In general, the combined sorption model was able to predict the observed K_d values within a factor of 3.

This thesis work estimated the BC content in marine sediment and investigated the implication of BC for the sorption of PAHs in sediments. Between the 375°C method and the Eq. 2-based model in Chapter 3, the BC content was reasonably estimated in sediment samples tested. In addition, sorption studies revealed that BC in the dominant sorbent in the samples tested and accounted for the nonlinear isotherms observed for PAHs.

7.2 IMPLICATIONS OF THESIS WORK

7.2.1 PAH Sorption and Bioavailability. The presence of BC in marine sediments has several implications for the sorption of PAHs in sediments. First, the adsorption of PAHs onto BC may explain reports of nonlinear isotherms [18, 19, 27] and observed PAH log K_{oc} values that exceed their corresponding log K_{ow} value [29, 35] (note the uncertainty in the log K_{ow} value [36, 37]). In addition, BC interactions might explain limited desorption [38]. Strong sorptive interactions with BC might also account for the limited

bioavailability of PAHs in the environment [39]. For example, by accounting for the BC fraction in SDB and FPC (samples sites tested in Ch. 5 & 6), the chemical availability of pyrene decreases by a factor of 10 compared to the f_{oc} K_{oc} alone. This limited availability may begin to explain the observed discrepancies between PAH-biota sediment accumulation factors and other chemicals [39]. Similar sorption behavior is also expected to apply to other planar congeners from important hydrophobic classes, such as: PCBs, chlorinated-dioxins, and *p,p'*-dichlorodiphenyldichloroethene (DDE) [40, 41] where BC is the dominant sorbent.

7.2.2 Implications of BC to the Carbon Cycle, Interpretation of Paleorecords and World Health Issues. A reliable BC method, possibly based on the 375°C thermal method, is necessary to provide an accurate estimate of the global BC cycle. Kuhlbusch attempted to provide quantitative constraints on the BC cycle in 1998 [42], and several researchers since the 1980s have attempted to estimate the BC flux from the land to the atmosphere [1, 43, 44, 45, 46]. However, since each research group defines BC differently and measures BC emission factors differently, an array of fluxes and reservoirs are reported in the literature. The universal application of one BC method, like the 375°C thermal method, may assist in estimating BC fluxes and reservoirs and help in the understanding of the global BC cycle.

For example, based on BC weight percentages and BC/TOC ratios measured in this thesis, BC reservoirs and BC sedimentary fluxes can be reasonably estimated. For example, if the total carbon reservoir in surface sediments (1m) equals 150 Pg (10^{15} grams) of carbon [47] and if the BC/TOC ratio for surface sediments is estimated as 15-30% globally (Ch. 5 & 6), then the BC reservoir in surface sediment is 23-45 Pg BC. Reasonable estimates are also possible on the BC reservoir in soils. A BC analysis of EPA 14 and EPA 20 (soil standards from Ch. 6, Tbl. 3) suggests that BC accounts for 3-7% of the TOC in soils. If the total carbon reservoir of soil is approximately 1,500 Pg of carbon [47], then the BC reservoir is 50-100 Pg. However, taking into account that the 375°C method may only account for 20% of the total BC content, the BC reservoir for

temperate soils could be as high as 400 Pg of BC, which is 10 times greater than the BC reservoir in surface sediments. In addition, Gustafsson and Gschwend calculated that the BC sedimentary flux in New England coastal sediments was approximately 100 μg BC/cm^2/yr [4]. However, if the 375°C method isolates only 20% of the total BC content in sediments (Ch.3, Fig. 7), then the revised BC sedimentary flux to coastal sediments equals 500 μg BC/cm^2/yr.

An improved understanding of the global BC cycle could significantly alter our perspective on the global carbon cycle, have implications for the interpretation of paleoclimate records, and impact the debate on world health issues. To begin, BC particles may act as an important sink of anthropogenic carbon dioxide (CO_2). For example, if combustion reactions were complete, then all burning carbon would be converted to CO_2 and emitted into the atmosphere. However, since combustion reactions are usually incomplete, a certain percentage (depending on the material) of the burning carbon converts to BC. Thus, carbon is moved from a labile, short-term OC reservoir to a recalcitrant, long-term BC reservoir [44]. Kuhlbusch and Crutzen have also proposed that if burning carbon is converted to BC instead of CO_2, then BC formation is responsible for a net release of oxygen to the environment [44]. Thus, an accurate BC method will allow for a more accurate interpretation of paleorecords in regards to the amount of carbon sequestered and the amount of oxygen released on a global time scale. Moreover, accurate BC measurements will result in more accurate measurements on the amount of OC preserved in a paleorecord. Similar to BC formation, OC preservation is also responsible for the net release of oxygen to the environment [48].

Airborne BC particles containing PAHs [49] will also have implications on world health issues [50, 51, 52], especially in third world and developing nations that have few restrictions on air pollution. For example, two-thirds of the electrical power in India (as of 1999) is generated by coal combustion, which produces 40-45% ash compared to American coal-burning plants that produce 3-9% ash [53]. Moreover, Cooke *et al.* and Streets *et al.* proposed that one-quarter of the global anthropogenic BC might originate from China from the burning of coal and biofuels [54, 55]. As the amount of coal

combustion varies seasonally, the concentration of PAHs extracted from aerosols containing BC particles were observed to vary accordingly [56, 57, 58]. For example, Guo *et al.* observed that the PAH concentration in aerosols of China was 10 times higher in the winter than in the summer [58]. Furthermore, Parks *et al.* noted that PAHs concentrations in aerosols from South Korea correlated well with fuel consumption [56].

7.3 FUTURE WORK

Several future experiments can be designed to continue the work presented in this thesis. Although the 375°C method isolates only a fraction of the total BC content, the greater challenge is handling problematic matrices (i.e. organic crystals and N-containing compounds) that have a potential of charring. Physically grinding a sample to <38 μm size particle may reduce charring in some problematic matrices by increasing oxygen accessibility. However, as observed in the bovine serum albumin experiments (Ch. 3, Fig. 5), physically grinding a sample does not always eliminate charring. In these cases, a chemical pretreatment may be necessary to break up macromolecules in order to increase oxygen accessibility.

A proposed chemical pretreatment would involve two steps: a hydrochloric acid (HCl) digestion to remove amorphous iron hydroxides and amorphous volatile sulfides [59] and a trifluoroacetic acid (TFA) digestion to digest organic matter [10] (Figure 1). Preliminary experimentation suggests that this pretreatment will substantially minimize charring in problematic samples; however, the method has not undergone vigorous testing and has many attached caveats. To minimize the possible loss of BC particles from multiple manipulations, samples were not centrifuged, and supernatants were not discharged in-between steps; instead the reagents (HCl and TFA) were allowed to evaporate inside a fume hood. Consequently, the treated sediments cemented on the bottom of the reaction vial. This crust of sediment has to be broken before subsequent steps can be executed. Another caveat to this pretreatment is that preliminary work has indicated that melanoidin will form after the TFA digestion. If a large quantify of melanoidin were formed, then charring will be enhanced during the subsequent thermal

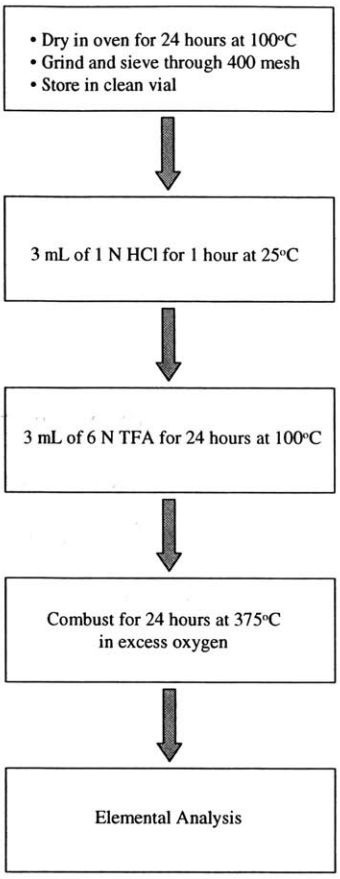

Figure 1: Schematic of proposed BC method where 30 mg of sediment (dried and ground) is treated with hydrochloric acid (HCl) to remove authigenic minerals and trifluoroacetic acid (TFA) to remove proteins. BC is then operationally defined as the carbon remaining after a 375°C thermal oxidation treatment and measured with an elemental analyzer.

oxidation. Future work should focus on developing ways to avoid the formation of melanoidin while minimizing the loss of BC particles. Other future work should focus on testing this chemical protocol on environmental samples and adjusting the pretreatment to handle various problematic matrices. For example, ammonium oxalate/oxalic acid can also remove amorphous iron oxyhydroxides (0.2 M for 2 hours at 25°C); titanium (II)-citrate-EDTA bicarbonate can remove crystalline iron oxyhydroxides (0.05 M for 2 hours at 25°C); and nitric acid can remove crystalline sulfides (16 N for 2 hours at 25°C) [59].

If a suitable wet chemistry method cannot be established, or if charring is unavoidable, then a correction factor needs to be researched and tested. For example, a method developed by Birch and Cary uses thermal oxidation to remove OC but continually monitors charring by measuring the transmission of a 670 nm diode laser beam through the sample on a filter [60]. A correction factor for charring could then evolve from modeling the blackening of a filter versus temperature. Other correction factors or models may evolve from the phytoplankton thermograms in Chapter 3; however future work is needed to determine how (or if) the shape of the phytoplankton thermogram changes when more (or different) phytoplankton material is added.

More sorption experiments are also necessary to understand the fate of PAHs in the environment. Experiments should focus on constructing isotherms for PAHs other than pyrene and phenanthrene to calculate the respective values for log K_{BC} and the Freundlich exponent. These experiments should also investigate how the isotherms change for PAH adsorption onto different BC particles as they exist in the environment (i.e. BC originating from fossil fuel burning or biomass burning). In addition, since the K_{BC} value reflects adsorption, future work should investigate competition between PAHs and other planar compounds, as well as competition between PAHs and organic matter. Competition should affect the adsorption of PAHs onto BC since activated carbon (a BC representative) is known to display competitive sorption behavior [61, 62, 63]. For the sorption experiments discussed above, if the BC particles are isolated with the 375°C thermal method, then additional experiments should be conducted to determine if the thermal pretreatment affects the adsorptive characteristics of the BC. Lastly, field

experiments should be setup to observe directly the adsorption of PAH onto BC. For example, deuterated PAHs can be injected into pore waters, and after an equilibration period, PAHs can be extracted from the sediment sample. The presence of deuterated PAHs in the BC fraction would separate the native PAHs fraction from the spiked fraction.

In summary, BC is a strong PAH adsorbent and may accounts for a significant percentage of the TOC content in marine sediments. A clear understanding of how much BC is present in sediment, and how strongly BC adsorb, will assist in understanding the fate of PAHs in the environment.

7.4 REFERENCES

1. Seiler, W.; Crutzen, P. J. *Climatic Change* **1980**, *2,* 207-247.
2. Sumam, D. O.; Kulbusch, T. A. J.; Lim, B. *Marine sediments: A reservoir for black carbon and their use as spacial and temporal records of combustion* in *Sediment Records of Biomass Burning and Global Change.* J. S. Clark. **1994**, NATO ASI Series: *51*, 271-293.
3. Goldberg, E. D. *Black Carbon in the Environment: Properties and Distribution.* **1985**, A Wiley-Interscience Publication, John Wiley & Sons: New York. 1-198.
4. Gustafsson, Ö.; Gschwend, P. M. *Geochim. Cosmochim. Acta* **1998**, *62,* 465-472.
5. Masiello, C. A.; Druffel, E. R. M. *Science* **1998**, *280,* 1911-1913.
6. Middelburg, J. J.; Nieuwenhuize, J.; Breugel, P. V. *Mar. Chem.* **1999**, *65,* 245-252.
7. Currie, L. A.; Benner, B. A.; Kessler, J. D.; Klinedinst, D. B.; Klouda, G. A.; Marolf, J. V.; Slater, J. F.; Wise, S. A.; Cachier, H.; Cary, R.; Chow, J. C.; Watson, J.; Druffel, E. R. M.; Masiello, C. A.; Eglinton, T. I.; Pearson, A.; Reddy, C. M.; Gustafsson, O.; Quinn, J. G.; Hartmann, P. C.; Hedges, J. I.; Prentice, K. M.; Kirchstetter, T. W.; Novakov, T.; Puxbaum, H.; Schmid, H. *J. Res. Natl. Inst. Stan.* **2002**, *107,* 279-298.
8. Gustafsson, Ö.; Haghseta, F.; Chan, C.; MacFarlane, J.; Gschwend, P. M. *Environ. Sci. Technol.* **1997**, *31,* 203-209.
9. Gustafsson, Ö.; Bucheli, T. D.; Kukulska, Z.; Anderson, M.; Largeau, C.; Rouzaud, J. N.; Reddy, C. M.; Eglinton, T. E. *Global Biogeochem. Cy.* **2001**, *15,* 881-890.
10. Gelinas, Y.; Prentice, K. M.; Baldock, J. A.; Hedges, J. I. *Environ. Sci. Technol.* **2001**, *35,* 3519-3525.
11. Nguyen, T. H.; Brown, R. A.; Ball, W. P. *Org. Geochem.* ***submitted.***

12. Gustafsson, Ö.; Gschwend, P. M. *Soot as a strong partition medium of polycyclic aromatic hydrocarbons in aquatic systems* in *Molecular Markers in Environmental Geochemistry*. R. P. Eganhouse. **1997**, ACS Symposium Series: Washington DC. *671*, 365-381.
13. Chiou, C. T.; Kile, D. E. *Environ. Sci. Technol.* **1998**, *32,* 338-343.
14. Chiou, C. T.; Kile, D. E.; Rutherford, D. W. *Environ. Sci. Technol.* **2000**, *34,* 1254-1258.
15. Chiou, C. T.; Peters, L. J.; Freed, V. H. *Science* **1979**, *206,* 831-832.
16. Karickhoff, S. W.; Brown, D. S.; Scott, T. A. *Water Res.* **1979**, *13,* 241-248.
17. Weber, W. J.; McGinley, P. M.; Katz, L. E. *Environ. Sci. Technol.* **1992**, *26,* 1955-1962.
18. Kleineidam, S.; Rugner, H.; Ligouis, B.; Grathwohl, P. *Environ. Sci. Technol.* **1999**, *33,* 1637-1644.
19. Karapanagioti, H. K.; Kleineidam, S.; Sabatini, D.; Grathwohl, P.; Ligouis, B. *Environ. Sci. Technol.* **2000**, *34,* 406-414.
20. Prahl, F. G.; Carpenter, R. *Geochim. Cosmochim. Acta* **1983**, *47,* 1013-1023.
21. Socha, S. B.; Carpenter, R. *Geochim. Cosmochim. Acta* **1987**, *51,* 1273-1284.
22. Readman, J. W.; Mantoura, R. F. C.; Rhead, M. M. *Sci. Total Environ.* **1987**, *66,* 73-94.
23. McGroddy, S. E.; Farrington, J. W. *Environ. Sci. Technol.* **1995**, *29,* 1542-1550.
24. Simpson, C. D.; Mosi, A. A.; Cullen, W. R.; Reimer, R. J. *Sci. Total Environ.* **1996**, *181,* 265-278.
25. Zhou, J. L.; Fileman, T. W.; Evans, S.; Donkin, P.; Readman, J. W.; Mantoura, R. F. C.; Rowland, S. *Sci. Total Environ.* **1999**, *244,* 305-321.
26. Xing, B. S.; Pignatello, J. J.; Gigliotti, B. *Environ. Sci. Technol.* **1996**, *30,* 2432-2440.
27. Xia, G. S.; Ball, W. P. *Environ. Sci. Technol.* **1999**, *33,* 262-269.
28. Bucheli, T. D.; Gustafsson, Ö. *Environ. Sci. Technol.* **2000**, *34,* 5144-5151.
29. McGroddy, S. E. *Ph.D Thesis: Sediment-Pore Water Partitioning of PAHs and PCBs in Boston Harbor, Massachusetts*. **1993**, University of Massachusetts at Boston: Boston. 1-255.
30. Huang, W.; Young, T. M.; Schlautman, M. A.; Yu, H.; Weber, W. J. *Environ. Sci. Technol.* **1997**, *31,* 1703-1710.
31. Wong, C. S. *M.S. Thesis: Assessing the Flux of Organic Pollutants from the Sediments of Boston Harbor*. **1992**, Massachusetts Institute of Technology: Cambridge. 1-138.
32. Stolzenbach, K. D.; Adams, E. E. *Exchange of contaminants between the sediments and the water column* in *Contaminated Sediments in Boston Harbor*. **1998**, Marine Center for Coastal Processes, MIT Sea Grant Program: Cambridge. 45-74.
33. Gallagher, E. D.; Keay, K. E. *Organism-Sediment-Contaminant Interactions in Boston Harbor* in *Contaminated Sediments in Boston Harbor*. K. D. Stolzenback; E. E. Adams. **1998**, Marine Center for Coastal Processes, MIT Sea Grant Program: Cambridge. 89-132.

34. Leo, W. S.; Alber, M.; Connor, M. S.; Keay, K. E.; Rex, A. C. *Contaminated Sediments in Boston Harbor.* **1994**, Massachusetts Water Resource Authority: Boston. 1-53.
35. Jonker, M. T. O.; Smedes, F. *Environ. Sci. Technol.* **2000**, *34,* 1620-1626.
36. Pontolillo, J.; Eganhouse, R. P. *The Search for Reliable Aqueous Solubility and Octanol-Water Partitioning Coefficient Data for Hydrophobic Organic Compounds: DDT and DDE as a Case Study.* **2001**, U.S. Geological Society: Reston, VA. *01-4201,* 1-55.
37. Renner, R. *Environ. Sci Technol.* **2002**, *36,* 411A-413A.
38. Lamoureux, E. M.; Brownawell, B. J. *Environ. Toxicol. Chem.* **1999**, *18,* 1733-1741.
39. Tracey, G. A.; Hansen, D. J. *Arch. Environ. Contam. Toxicol.* **1996**, *30,* 467-475.
40. Bucheli, T. D.; Gustafsson, Ö. *Environ. Toxicol. Chem.* **2001**, *20,* 1450-1456.
41. Lohmann, R.; MacFarlane, J. K.; Gschwend`, P. M. *Environ. Sci Technol.* **submit**.
42. Kuhlbusch, T. A. J. *Science* **1998**, *280,* 1903-1904.
43. Crutzen, P. J.; Andreae, M. O. *Science* **1990**, *250,* 1669-1678.
44. Kuhlbusch, T. A. J.; Crutzen, P. J. *Global Biogeochem. Cy.* **1995**, *9,* 491-501.
45. Cooke, W. F.; Wilson, J. N. *J. Geophys. Res.* **1996**, *101,* 19395-19409.
46. Liousse, C.; Penner, J. E.; Chuang, C.; Walton, J. J.; Eddleman, H.; Cachier, H. *J. Geophys. Res.* **1996**, *101,* 19411-19432.
47. Masters, G. M. *Chapter 8: Global Atmospheric Change* in *Introduction to Environmental Engineering and Science.* B. Stenquist; M. Horton; A. M. Longobardo. **1991**, Prentice Hall: Upper Saddle River, NJ. 453-554.
48. Berner, R. A.; Canfield, D. E. *Am. Jour. Sci.* **1989**, *289,* 333-361.
49. Venkataraman, C.; Friedlander, S. K. *Environ. Sci. Technol.* **1994**, *28,* 563-572.
50. Dockery, D. W.; Arden, P. C.; Xu, X. P.; Spengler, J. D.; Ware, J. H.; Fay, B. C.; Apenzier, F. E. *New Engl. J. Med.* **1993**, *329,* 1753.
51. Larsen, J. C.; Larsen, P. B. *Chemical Carcinogens* in *Air Pollution and Health.* R. E. Hester; R. M. Harrison. **1998**, The Royal Society of Chemistry: Cambridge, UK. 33-56.
52. Hsiao, W. L. W.; Mo, Z. Y.; Fang, M.; Shi, X. M.; Wang, F. *Mutat. Res.-Gen. Tox. En.* **2000**, *471,* 45-55.
53. Singh, V.; Bretz, E. A. *IEEE Spectrum* **1999**, *36,* 48-56.
54. Cooke, W. F.; Liousse, C.; Cachier, H. *J. Geophys. Res.* **1999**, *104,* 22137-22162.
55. Streets, D. G.; Gupta, S.; Waldhoff, S. T.; Wang, M. Q.; Bond, T. C.; Yiyum, B. *Atmos. Environ.* **2001**, *35,* 4281-4296.
56. Parks, S. S.; Kim, Y. J.; Kang, C. H. *Atmos. Environ.* **2002**, *36,* 2917-2924.
57. Fernandes, M. B.; Bricks, L. S. R.; Moreira, J. C.; Cardoso, J. N. *Chemosphere* **2002**, *47,* 417-425.
58. Guo, Z. G.; Sheng, L. F.; Feng, J. L.; Fang, F. *Atmos. Environ.* **2003**, *37,* 1825-1834.
59. Keon, N. E.; Swartz, C. H.; Brabander, D. J.; Harvey, C.; Hemond, H. F. *Environ. Sci Technol.* **2001**, *35,* 2778-2784.

60. Birch, M. E.; Cary, R. A. *Aerosol Sci. Tech.* **1996**, *25,* 221-241.
61. Crittenden, J. C.; Luft, P.; Hand, D. W.; Oravitz, J. L.; Loper, S. W.; Art, M. *Environ. Sci. Technol.* **1985**, *19,* 1037-1043.
62. Blum, D. J. W.; Suffet, I. H.; Duguet, J. P. *Water Res.* **1994**, *28,* 687-699.
63. Karanfil, T.; Kilduff, J. E. *Environ. Sci. Technol.* **1999**, *33,* 3217-3224.

APPENDIX A3.1: PERKIN ELMER CHN ANALYZER

The Perkin Elmer 2400 CHN Elemental Analyzer (Series 1, Serial #130960; Norwalk, CT) determines the carbon, hydrogen, and nitrogen content of an organic matrix by combusting samples in a pure oxygen environment at high temperatures and then measures the resultant combustion gases using a thermal conductivity detector.

A3.1.1. CHN OPERATION

Before analysis on the CHN Analyzer, organic samples are encapsulated in tin capsules (Catalog #D1034, 8 x 5 mm; Elemental Microanalysis Limited, Manchester, MA) and weighed using a CAHN/Ventron Automatic Electrobalance (Model #5725 C-25; CAHN Instrumentation, Cerritos, CA). The mass in each capsule varies such that the total carbon content does not exceed 3,500 μg C (samples usually contain <1,500 μg C as recommended by Perkin Elmer). The CAHN Electrobalance is tared daily with two 10.000 mg weights (Model #7033-3, Class 3 Weight; Troemner Inc., Philadelphia, PA). The electrobalance is within an acceptable range if the sum of the two weights equal 19.998 ±0.002 mg (0.01% error). Propagation of error from the capsule tare weight to the final weight yields a mass error for each sample of ±0.003 mg. If prior acidification of the organic sample is necessary in order to remove inorganic carbon, the samples were weighed in silver capsules (Catalog #D2009, 8 x 5 mm; Elemental Microanalysis Limited), wetted with 50 μL low-carbon water (Aries Vaponics, Rockland, MA), acidified with 50 μL sulfurous acid (6% Assay; Fisher Scientific, Fair Lawn, NJ), dried overnight at room temperature, and then wrapped further in the tin capsules before the analysis. Tin is essential to the CHN operation because this metal catalyzes the combustion reaction by producing a vigorous exothermic reaction in the presence of oxygen in the combustion tube.

Samples are manually inserted into the CHN injector, and then automatically pushed into a "waiting area" when the port is opened by a pneumatic piston (Air Grade D; BOC Group Inc., Murray Hill, NJ; 50 psi). Once the system is purged with helium (Ultra High Purity Grade 5.0; 20 psi), oxygen (Grade 4.7; 20 psi) fills the combustion

tube before the sample is dropped into the combustion zone. The CHN instrument is programmed to allow a one-second-oxygen boost before a static combustion interval of 15 seconds at 925°C, and then the combustion reaction is completed with another one-second-oxygen boost. Note for difficult samples, the instrument is re-programmed to allow a four-second-oxygen boost prior to a 20-second static combustion followed by two more two-second-oxygen boost. This sequence has been tested to oxidize completely samples of anthracite coal and metallurgical coke. In conjunction with the oxygen-rich environment, the reagents of the combustion tube (nickel/chromium oxide, silver tungstate on magnesium oxide, and silver vandate at 925°C) and the reduction tube (copper granules and copper oxide at 640°C) aid in the oxidation of carbon, hydrogen, and nitrogen to carbon dioxide, water, and nitrogen (N_2) gases, respectively.
These resultant gases are then carried into a mixing zone by a helium carrier gas and are pressurized to 6.488 mm/Hg with a fill time set between 23-25 seconds. The gases are homogenized at constant pressure and constant temperature (82.6° C) in the mixing chamber. As the mixing zone depressurizes, the gases separate by employing a frontal chromatography technique that uses selective retention of the gases to produce a steady-state stepwise signal. Each gas is then detected by thermal conductivity in the detector oven (82.6° C) and is reported in terms of dimensionless counts.

A3.1.2. DAILY SYSTEM CHECKS

Before operating the CHN analyzer, the system is purged daily with helium for 200 seconds and then the oxygen lines are purged for 20 seconds. A leak test is performed daily to check the injector assembly for jammed capsules or damaged o-ring seal. For proper operation of the CHN, the injector must form a complete seal. If the seal is compromised, the instrument will have an infinite fill time during sample runs. The leak test occurs in two phases: first the mixing zone is pressurized with helium at approximately 760 mm/Hg for 4 minutes, and then the combustion zone is pressurized at approximately 788 mm/Hg for 4 minutes. Each leak test passes if the decrease in

pressure is <1 mm/Hg. If either leak test fails, then the auto injector must be opened and inspected.

Machine blanks are run daily as part of the set up and run continuously throughout the day to avoid carry over from one sample to the next. Typical carbon machine blanks range from 25-35 counts, or 1.6-2.3 μg C (assuming a maximum carbon conversion factor of 15.2 counts/μg C) while typical nitrogen machine blanks range from 35-40 counts, or 6.7-7.7 μg N (assuming a maximum nitrogen conversion factor of 5.2 counts/μg N). Hydrogen blanks are the least stable and can range from >1000 to almost 100 counts, which corresponds to approximately 30 μg H. The highest hydrogen blanks usually occur after maintenance and slowly decrease over time as water vapor is flushed out of the system. A tin capsule blank tends to affect the carbon signal the most and increases the carbon blank to 50-60 counts, or 3.3-3.9 μg C. At a minimum, the carbon signal from a sample must exceed 100-120 counts (6.6-7.9 μg C) for an acceptable signal-to-noise ratio of 2:1 and nitrogen signals must exceed 70-80 counts (13.5-15.4 μg N).

A3.1.3. CALIBRATION AND K-FACTORS

The CHN instrument operates using a single-point calibration scheme, which works by programming the instrument to recognize the most intense detector signal and assigning a conversion factor (counts/μg), or a "K-factor," to that signal. Typical K-factors for carbon, hydrogen, and nitrogen are 14-15 counts/μg C, 30-40 counts/μg H, and 4-5 counts/μg N. The system then assumes a constant conversion factor for all other signals. Accurate K-factors are established with 1.5-2.0 mg of acetanilide standard in a tin capsule (C_8H_9NO, 71.09 wt % C, 6.71 wt % H, 10.36 wt % N; Catalog #B2000; Elemental Microanalysis Limited). After the K-factors are established, the precision of the CHN instrument is checked with acetanilide as a sample. Weight percentages are then calculated by dividing the difference of the sample counts and the blank by the corresponding K-factor (to determine the mass in terms of micrograms) and then dividing by the mass of the sample (to calculate the weight percentage). The instrument is

operating within an acceptable range if the measured weight percents are ±0.3 wt % of the accepted values.

K-factors will vary day to day and throughout the day; therefore, the CHN Analyzer needs to be calibrated continuously while operating (every 8-12 runs). However, the reproducibility of the K-factors at any given time is usually *less than* 0.10 count/μg, or <1% (except for hydrogen K-factor, which is vary up to 5%). In general, the K-factors tend to decrease over time (i.e. less counts detected per μg) as the reagents in the combustion tube are consumed and the vial receptacle in the combustion tube fills with tin oxide residue. An example of yearly trends in K-factors for carbon and nitrogen (June 2001 to July 2002) is illustrated in Figure 1. Line reference #1 (Figures 1a and 1b) marks the installment of a new combustion tube and reduction tube causing an increase in both the carbon and nitrogen K-factors by 70-80%. Line references #2 and #3 mark the replacement of the reduction tube, vial receptacle, and filter disks while using the same combustion tube. Both the carbon and nitrogen K-factor values increase approximately 40% after this maintenance.

To check the extrapolation of the K-factors, acetanilide was tested as a sample over a range of signals (<100-2000 μg acetanilide corresponding to <70-1,420 μg C, <7-130 μg H, and <10-210 μg N; figure A2) from April 2001 to August 2002 (population size = 135). Acetanilide weight percents for carbon, hydrogen, and nitrogen fell well within the accepted range for sample masses of >400-2000 μg with observed weight percentages averaging 71.04 ±0.17 wt % C, 6.73 ±0.42 wt % H, and 10.36 ±0.08 wt % N (population size = 129). Unlike carbon and nitrogen weight percentages that erred <1% (±1 σ) from their accepted values, the percent error in the hydrogen weight percents was 6.2%. The large hydrogen error reflects the unstable hydrogen blank due to water vapor, which affects the hydrogen K-factor and the resultant weight percents.

Although acceptable weight percents were observed for carbon, hydrogen, and nitrogen over 80% of the mass range tested, less acceptable values were observed for acetanilide masses <400 μg (Figure 2). For example, average weight percents for smaller mass samples were 69.58 ±1.0 wt % C, 6.42 ±1.2 wt % H, and 9.83 ±0.23 wt % N

(population size = 6). These values relative to their accepted weight percents correspond to a 1.5% error for carbon, 19% error for hydrogen, and 2.4% error for nitrogen. Upon closer inspection of these samples, it was noticed that the calculated weight percents were highly dependent on accurate measurements of the total acetanilide mass. For example, the CHN reported 70.33 wt % C for a sample weighing 242 ±3 μg; however, a back-calculation of the expected mass using the expected carbon weight percentage (71.09 wt % C) yielded 239 μg, which is within the error of the CAHN Electrobalance. Hence, while the K-factors may be applicable over the entire range of acetanilide masses, only acceptable weight percents for 80% of the mass range can be shown because of limitations in the analytical balance.

A3.1.4. INTERCALIBRATION

In addition to calibrating the CHN to an acetanilide standard, the instrument was also successfully intercalibrated with a benzoic acid standard and two sediment standards from NIST (Gaithersburg, MD). Benzoic acid (C_7H_6O; Elemental Microanalysis Limited) presents an interesting test for the CHN because this standard has no nitrogen. The measured weight percents (population size = 3) for benzoic acid were 68.86 ±0.08 wt % C, 5.00 ±0.15 wt % H, and 0.00 ±0.02 wt % N compared to the accepted values of 68.85 wt % C, 4.95 wt % H, and 0.00 wt % N (Table 1). This standard shows the integrity of the CHN frontal chromatography method of separation and detection. Not only does the instrument detect no nitrogen (relative to the blank) but also the CHN can simultaneously measure a large carbon signal followed by a small hydrogen signal. Furthermore, the ability of the CHN to measure no nitrogen implies that detectable, reproducible nitrogen signals with a signal-to-noise ratio of 1:1 are in fact real and different from no signal. For example, this work is confident in reporting reproducible weight percents of 0.01-0.02 wt % N (signal-to-noise of 1:1) for combusted sediment from Boston Harbor.

Table 1: Comparison of measured and accepted weight percents for benzoic acid standard

WT % C	WT % H	WT % N
Measured Values for Benzoic Acid		
68.94	4.88	0.00
68.85	4.95	<0.00
68.79	5.15	<0.00
Accepted Values for Benzoic Acid		
68.85	4.95	0.00

The method of detecting total organic carbon (TOC) in sediments was also tested against two NIST sediment standards: NY/NJ Waterway Sediment (SRM 1944) and Marine Organic Sediment (SRM 1941a). Before analysis, the inorganic carbon was removed from the sediments following the procedure described above. The average weight percents (population size = 4) for SRM 1944 were: 4.89 ±0.27 wt % C, 0.51 ±0.06 wt % H, and 0.24 ±0.02 wt % N. The average weight percents (population size = 4) for SRM 1941a were: 4.73 ±0.16 wt % C, 1.11 ±0.17 wt % H, and 0.33 ±0.01 wt % N. Unfortunately, NIST only supplies reference values for the TOC content of these sediments (4.4 ±0.3 wt % TOC for SRM 1944 and 4.8 ±1.3 wt % TOC for SRM 1941a). The CHN measured the TOC very well for SRM 1941a underestimating the TOC by 0.07 wt % but well within the reported error. The analysis for SRM 1944 was also within the reported error, but the instrument overestimated the TOC by 0.49 wt %. These tests show the validity of the method and instrument, and gives credence to any future analyses.

APPENDIX A3.2: MATLAB CODE FOR BOLTZMANN SIGMOIDAL OC/BC MODEL

File 1

```
% AmyMarie Accardi-Dey, FITTING THERMOGRAMS, March 2003
%
% MODEL_THERMO a function file to evaluate thermogram data set.
%
% Use Sigma-Plot parameters and Boltzmann Sigmoidal equation to
% determine the fraction of carbon remaining at a given temperature for
% (1) small BC particles, (2) large BC particles, and (3) humic acid
% material.  Use these calculated fractions and the measured carbon
% weight percent for Boston Harbor sediment to determine the weight
% percents for (1) small BC particles,  (2) large BC particles, and
% (3) humic acid material

% Equation to fit: (Carbon measured at a given temperature) = fraction
% (humic acid carbon) + fraction (large BC).
%
% carbon = measured carbon content (weight percent)
% "fraction" is a matrix of fractions remaining at a given temperature
% p(1) = humic acid content
% p(2) = large BC content

function difference=model_thermo_fit(g,ig,initial_guess);

    %%%%%%%%%%%%%%%%%%%%%%%%%%%%%%%%%%%%%%%%%%%%%%%%%%%%%%%%%%%%%%%%
    %Data Listed Below is the same as what is in Appendix A3.7
    %%%%%%%%%%%%%%%%%%%%%%%%%%%%%%%%%%%%%%%%%%%%%%%%%%%%%%%%%%%%%%%%

%Boston Harbor
Temp=[25 100 150 200 250 300 320 350 365 375 385 400];Temp=Temp';
y=[1.48 1.48 1.42 1.08 0.57 0.47 0.37 0.21 0.16 0.13 0.11 0.08];y=y';

%Mass Bay data
Temp=[25 115 200 220 240 260 280 300 325 350 375 400];Temp=Temp';
y=[.11 .12 .09 .07 .06 .05 .05 .03 .03 .02 .01 0];y=y';

%Boston Blue Clay
Temp=[25 175 220 240 260 280 325 350 375 400];Temp=Temp';
y=[.52 .43  .29 .21 .20 .15 .10 .07 .06 .04];y=y';

%Wilkinson Basin
Temp=[25 175 200 220 240 260 280 300 325 350 375 400];Temp=Temp';
y=[2.28 2.03 1.79 1.46 1.16 0.98 0.85 0.74 0.51 0.37 0.21 0.14];y=y';

%Chemically Extracted Boston Harbor
Temp=[25 175 220 240 260 280 300 325 350 375 400];Temp=Temp';
y=[.63 .51 .38 .32 .30 .27 .23 .19 .18 .13 .10];y=y';

    %%%%%%%%%%%%%%%%%%%%%%%%%%%%%%%%%%%%%%%%%%%%%%%%%%%%%%%%%%%%%%%%
```

```
rowTemp = size(Temp,1);
rowCarbon = size(y,1);

% create a matrix to contain all the fractions of carbon remaining
% column 1: humic acid
% column 2: large BC particles

fraction= zeros(rowTemp,2);
i = 1;

for i=1:rowTemp
 %first humic, second large black carbon
 fraction(i,1) = (1-.00998)/(1+exp((239-Temp(i,1))/-23.2))+.00998;
 fraction(i,2) = (1.006+.4129)/(1+exp((370.7-Temp(i,1))/-62.73))-.4129;
 i=i+1;
end

carbon=g(1).*fraction(:,1)+g(2).*fraction(:,2);

%make a smooth line for plotting
rowTemp = size(Temp,1);
rowCarbon = size(y,1);

% create a matrix to contain all the fractions of carbon remaining
% column 1: humic acid
% column 2: large BC particles

Temp_plot=[25:1:400];Temp_plot=Temp_plot';
rowTemp = size(Temp_plot,1);

fraction= zeros(rowTemp,2);
i = 1;

for i=1:rowTemp
 fraction(i,1) = .9706/(1+exp((237.9-Temp_plot(i,1))/-24.58));
 fraction(i,2) = .9884/(1+exp((330.5-Temp_plot(i,1))/-44.28));
 i=i+1;
end

carbon_plot=g(1).*fraction(:,1)+g(2).*fraction(:,2);

figure(1);plot(Temp,y,'bo',Temp_plot,carbon_plot,'g-');
xlabel('data');
ylabel('prediction');
r=corrcoef(y,carbon);
text(.4,.65,['R^2 = ',num2str(r(2,1)^2)],'units','normalized');
text(.4,.25,['humics = ',num2str(g(1)),],'units','normalized');
text(.4,.20,['L BC = ',num2str(g(2)),],'units','normalized');

pause(.001)

difference=y-carbon;
```

File 2

```
%Least Squares data fitting
%Written by Peter Oates

%PCG = pre-conjugated gradient was used

disp(' ')
disp('   Pick method to minimize the Least Squares function:')
disp('')
disp('          Medium-Scale:   1) Gauss-Newton')
disp('                          2) Levenberg-Marquardt')
disp('          Large-Scale:    3) PCG')
disp(' ')
disp('                          0) Quit')
disp(' ')

method = input('Select a method number: ');

if method~=3&method~=0
 disp('')
 disp('    Choose any of the following line search methods:')
 disp('')
 disp('           1) Mixed Polynomial Interpolation')
 disp('           2) Cubic Interpolation')
 disp('')

 l = input('Select a line search number: ');
 if l==2,
  OPTIONS=optimset('LineSearch','cubicpoly');
 end
end

bounds=0;
if method==3
 disp('Set bounds in the optimization m-file)')
 bounds = input('With Bounds? 1 = yes, 0 = no: ');
end
disp('running...')


    %%%%%%%%%%%%%%%%%%%%%%%%%%%%%%%%%%%%%%%%%%%%%%%%%%%%%%%%%%%%%%%%

%this changes depending on the sample
%to be passed to the function: a k1 k2 alpha_r

initial_guess=[.5 .5 ];

%PCG bounds
low_b=[0   0   0 ];
up_b=[inf   inf inf];

if bounds==1
```

```
 low = low_b ;
 up = up_b;
end

ig=initial_guess'; %makes the change in paramters normalized

%Gauss-Newton
if method == 1
 %be sure to have this all on one line
 options =
optimset('LevenbergMarquardt','off','Largescale','off','MaxIter',400,'T
olFun',10e-5,'MaxFunEvals',4000,'TolX',10e-
5,'Display','iter','ShowStatusWindow','iterplus');

[g,resnorm,residual,exitflag,output,lambda,jacobian]=lsqnonlin('model_t
hermo_fit',ig,[],[],options,initial_guess);

end

%Levenberg-Marquardt
if method ==2
 %be sure to have this all on one line
  options =
optimset('LevenbergMarquardt','on','Largescale','off','MaxIter',400,'Di
splay','iter','ShowStatusWindow','iterplus','TolFun',2e-
4,'MaxFunEvals',4000,'TolX',2e-6,'Diffmaxchange',1e-
1,'Diffminchange',1e-11);

[g,resnorm,residual,exitflag,output,lambda,jacobian]=lsqnonlin('model_t
hermo_fit',ig,[],[],options,initial_guess);

end

%PCG
if method==3
 %be sure to have this all on one line
 options =
optimset('LevenbergMarquardt','off','Diagnostics','on','Largescale','on
','MaxIter',400,'TolFun',10e-10,'MaxFunEvals',33600,'TolX',10e-
10,'Display','iter','PrecondBandWidth',0,'TolPCG',0.01);

 if bounds==1

[g,resnorm,residual,exitflag,output,lambda,jacobian]=lsqnonlin('model_t
hermo_fit',ig,low,up,options,initial_guess);

 else

[g,resnorm,residual,exitflag,output,lambda,jacobian]=lsqnonlin('model_t
hermo_fit',ig,[],[],options,initial_guess);
 end
end

%%%%%%%%%%%%%%%%%%%%%%%%%%%%%%%%%%%%%%%%%%%%%%%%%%%%%%%%%%%%%%%%%%%%%%%
```

```
%Fitting Statistics
%%%%%%%%%%%%%%%%%%%%%%%%%%%%%%%%%%%%%%%%%%%%%%%%%%%%%%%%%%%%%%%%%%%%%%%

[ci,varb,corrb,varinf] = nlparci(g,residual,jacobian);

disp('Parameters')
a=g(1)
b=g(2)

%Variance
var_a=varb(1,1);
var_b=varb(2,2);

disp('STD')
std_a=sqrt(var_a);
std_b=sqrt(var_b);
STD=[std_a std_b]

%Coeffecient of Variation
CV_a=std_a/(g(1));
CV_b=std_b/(g(2));
CV=[CV_a CV_b ]
```

APPENDIX A3.3: ELEMENTAL ANALYSIS OF COMBUSTED SAMPLES BASED ON SIZE

Table 1: Carbon and nitrogen elemental analysis (reported as weight percent; mean ±1 standard deviation) for mixtures of sodium citrate or bovine serum albumin with Boston Harbor sediment based on size both before and after a 375°C combustion. [a]

Sample (TOC wt % and TN wt %)	Combusted Crystals C wt %	Combusted Crystals N wt %	Dissolved & Combust C wt %	Dissolved & Combust N wt %
Sodium Citrate 60 mesh 3.7 wt % TOC, 0.08 wt % TN	0.97 ±0.04	0.02 ±0.01	0.15 ±0.05	0.00 ±0.00
Sodium Citrate 100 mesh 3.8 wt % TOC, 0.08 wt % TN	0.65 ±0.04	0.02 ±0.01	0.14 ±0.02	0.00 ±0.00
Sodium Citrate >200 mesh 3.2 wt % TOC, 0.07 wt % TN	0.43 ±0.01	0.01 ±0.00	0.11 ±0.04	0.00 ±0.00
Sodium Citrate 200 mesh 4.9 wt % TOC, 0.09 wt % TN	0.25 ±0.05	0.02 ±0.01	0.12 ±0.01	0.01 ±0.01
Sodium Citrate 270 mesh 5.0 wt % TOC, 0.08 wt % TN	0.19 ±0.04	0.01 ±0.01	0.14 ±0.01	0.00 ±0.00
Sodium Citrate 400 mesh 4.6 wt % TOC, 0.07 wt % TN	0.17 [b]	0.01	0.15 ±0.02	0.01 ±0.01
Sodium Citrate >400 mesh 4.4 wt % TOC, 0.07 wt % TN	0.12 ±0.01	0.00 ±0.00	0.13 ±0.01	0.00 ±0.00
Bovine serum albumin 120 mesh 5.1 wt % TOC, 1.3 wt % TN	0.63 ±0.13	0.32 ±0.08	0.16 ±0.01	0.05 ±0.00
Bovine serum albumin 200 mesh 11 wt % TOC, 3.0 wt % TN	0.65 ±0.11	0.34 ±0.06	0.14 ±0.00	0.06 ±0.00
Bovine serum albumin 270 mesh 7.5 wt % TOC, 2.0 wt % TN	0.58 ±0.03	0.31 ±0.02	0.11 ±0.01	0.02 ±0.01
Bovine serum albumin 400 mesh 8.1 wt % TOC, 2.2 wt % TN	0.44 ±0.01	0.23 ±0.01	0.13 ±0.00	0.03 ±0.00
Bovine serum albumin >400 mesh 6.8 wt % TOC, 1.9 wt % TN	0.34 ±0.03	0.16 ±0.02	0.15 ±0.01	0.03 ±0.01

a: Column 1 provides the particle size (mesh size that particles were retained on) for the added compound, and the measured total organic carbon (TOC wt %) and total nitrogen (TN wt %) contents (approximately 5% error on TOC and TN values) of the uncombusted sample. Column 2 provides the carbon and nitrogen contents for the crystal/sediment mixtures after being combusted at 375°C for 24 hours under air. Column 3 provides the carbon and nitrogen content for samples that were first dissolved, dried at room temperature, and then combusted at 375°C for 24 hours under air.

b: Population size equals one.

APPENDIX A3.4: CARBON DATA FOR BC AND HUMIC ACID THERMOGRAMS

Table 1: Thermogram data including temperature of 24-hour combustion under air, measured weight percentage of carbon (mean ±1 standard deviation), and the calculated percent carbon remaining and percent carbon burn-off for black carbon (NIST SRM 1650) with sediment, black carbon (NIST SRM 1650) on glass beads, and Aldrich humic acid on glass beads.

Temp (°C)	C wt %	Error (±1 σ)	Percent Remain	Percent Burn-off
	BLACK CARBON WITH SEDIMENT			
25	2.34	0.19	100	0
250	1.94	0.15	83	17
300	1.53	0.16	65	35
320	1.31	0.12	56	44
360	0.95	0.02	41	59
375	0.51	0.05	22	78
380	0.53	0.04	23	77
400	0.35	0.02	15	85
	BLACK CARBON ON BEADS			
25	0.61	0.03	100	0
200	0.45	0.08	74	26
250	0.36	0.05	59	41
300	0.22	0.05	36	64
320	0.10	0.02	16	84
340	0.08	0.03	13	87
360	0.05	0.03	8	92
380	0.02	0.00	3	97
	HUMIC ACID ON BEADS			
25	1.07	0.00	100	0
100	1.02	0.03	95	5
125	1.00	0.01	93	7
150	0.99	0.04	93	7
175	1.01	0.02	94	6
200	0.87	0.02	81	19
225	0.62	0.00	58	42
250	0.41	0.02	38	62
275	0.19	0.00	18	82
350	0.01	0.00	1	99

APPENDIX A3.5: CARBON DATA FOR EXTRACTED MARINE ORGANIC THERMOGRAM

Table 1: Thermogram data including temperature of 24-hour combustion under air, measured carbon weight percent (mean ±1 standard deviation) for extracted Boston Harbor sediment, calculated carbon weight percentage for non-extracted Boston Harbor sediment, the calculated marine organic matter content (difference between extracted from non-extracted weight percentages), and the calculated percent carbon remaining.

Temp (°C)	Measured C wt % Extracted	Calculated C wt % Non-extracted	Marine OM C wt %	Percent Remaining
25	0.63 ±0.03	1.42	0.79	100
175	0.51 ±0.00	1.33	0.82	100
220	0.38 ±0.02	1.06	0.68	86
240	0.32 ±0.02	0.85	0.53	67
260	0.30 ±0.02	0.65	0.35	44
280	0.27 ±0.01	0.49	0.22	28
300	0.23 ±0.02	0.38	0.15	19
325	0.19 ±0.01	0.28	0.09	11
350	0.18 ±0.00	0.20	0.02	3
375	0.13 ±0.00	0.13	0	0
400	0.10 ±0.00	0.08	0	0

APPENDIX A3.6: CARBON AND NITROGEN DATA FOR PHYTOPLANKTON THERMOGRAM

Table 1: Thermogram data including temperature of 24-hour combustion under air, measured weight percentage of carbon and nitrogen (mean ±1 standard deviation), the calculated percent carbon or nitrogen remaining phytoplankton material on glass beads.

Temp (°C)	C wt %	Error (±1 σ)	Percent C Remain	N wt %	Error (±1 σ)	Percent N Remain
			PHYTOPLANKTON ON BEADS			
25	2.01	0.05	100	0.36	0.02	100
100	1.55	0.10	77	0.29	0.02	81
125	1.59	0.02	79	0.3	0.00	83
175	1.43	0.06	71	0.26	0.01	72
200	1.11	0.01	55	0.23	0.00	64
225	0.71	0.03	35	0.17	0.01	47
250	0.43	0.01	21	0.12	0.00	33
275	0.36	0.02	18	0.10	0.00	28
340	0.39	0.01	19	0.08	0.01	22
350	0.27	0.01	13	0.07	0.01	19
360	0.08	0.01	4	0.02	0.01	6
375	0.01	0.00	0	0.00	0.00	0

APPENDIX A3.7: CARBON DATA FOR SEDIMENT THERMOGRAMS

Table 1: Thermogram data including temperature of 24-hour combustion under air, measured weight percentage of carbon (mean ±1 standard deviation), and the calculated percent carbon remaining for sediment samples.

Temp (°C)	C wt %	Error (±1 σ)	Percent C Remain
	BOSTON HARBOR SEDIMENT		
25	1.48	0.10	100
100	1.48	0.07	100
150	1.42	0.02	96
200	1.08	0.14	73
250	0.57	0.07	39
300	0.47	0.04	32
320	0.37	0.03	25
350	0.21	0.02	14
365	0.16	0.05	11
375	0.13	0.02	9
385	0.11	0.00	7
400	0.08	0.01	5
	BOSTON BLUE CLAY SEDIMENT		
25	0.52	0.05	100
175	0.43	0.02	83
200	0.23	0.01	44
220	0.29	0.05	56
240	0.21	0.01	40
260	0.20	0.03	38
280	0.15	0.01	29
325	0.10	0.01	19
350	0.07	0.01	13
375	0.06	0.01	12
400	0.04	0.01	8
	MASSACHUSETTS BAY SEDIMENT		
25	0.11	0.01	100
115	0.12	0.02	100
200	0.09	0.01	82
220	0.07	0.00	64
240	0.06	0.01	55
260	0.05	0.00	45
280	0.05	0.00	45
300	0.03	0.01	27
325	0.03	0.00	27
350	0.02	0.00	18
375	0.01	0.00	9
400	0.00	0.01	0
	WILKINSON BASIN SEDIMENT		
25	2.28	0.03	100
175	2.03	0.01	89
200	1.79	0.00	79
220	1.46	0.01	64
240	1.16	0.01	51
260	0.98	0.00	43
280	0.85	0.00	37
300	0.74	0.00	32
325	0.51	0.02	22
350	0.37	0.00	16
375	0.21	0.00	9
400	0.14	0.00	6

APPENDIX A5.1: POSSIBLE EFFECTS OF IRON OXIDES ON OBSERVED log K_d VALUES

A5.1.1 INTRODUCTION

Similar to iron oxides occluding organic matter and hindering sorption [1], iron oxides formed during the thermal oxidation method (375°C for 24 hours in air [2]) may occlude BC and lower the observed distribution coefficient (log K_d, L/kg) in combusted sediment samples. Here, the sorption of pyrene onto combusted south Dorchester Bay (SDB) sediments is compared in acidified and non-acidified solutions. If iron oxides were present in the combusted sediment, then the distribution coefficient in the acidified samples would be higher than the distribution coefficient in the non-acidified samples assuming that the acid dissolved the oxides and made the occluded BC more accessible to pyrene sorption.

A5.1.2 METHOD

The pyrene sorption experiments were performed as described in Chapter 5 where the loss of dissolved pyrene due to sorption onto combusted sediment was monitored with fluorescence. Two sorption experiments were run in parallel: one series had an initial dissolved pyrene concentration of 7.79 μg/L and was acidified with HCl (Aldrich Chemical Co., WI) to a pH = 1.5. The second series had an initial dissolved pyrene concentration of 8.39 μg/L and was not acidified (pH = 6.0). For both series, approximately 20 mg of combusted SDB sediment (1.2 ±0.15 wt % OC and 0.16 ±0.03 wt % BC) was added to ≈100 mL of solution (either acidified or non-acidified) and tumbled for 21 days. The loss of 26-46% of the dissolved pyrene was observed due to sorption, and single-point distribution coefficients were calculated from the fraction of pyrene remaining in the dissolved phase. All error represents the mean ±1 standard deviation.

As noted in Chapter 5, additional experiments were conducted with the supernatants obtained from combusted sediment desorbing in water (acidified and non-acidified) to determine if desorbed OC was quenching fluorescence. In addition, the

dissolved OC (DOC) concentration in these supernatants was measured on a Shimadzu Scientific Instrument Total Organic Carbon Analyzer (TOC 5000; Columbia, MD) and compared to the DOC concentration in a water blank. The TOC Analyzer was calibrated with dilutions of a 50 ppm potassium phthalate standard (2-24 ppm C), and operated with a normal-total carbon catalyst at maximum range. Before an analysis, each sample was acidified with phosphoric acid and was purged for 4 min with N_2 gas to remove inorganic carbon. The detection limit of the TOC Analyzer was 0.6 ±0.1 ppm C assuming a signal-to-noise ratio of 3:1 with a water blank of 0.2 ±0.04 ppm C (N = 4). All reported DOC measurements represent the mean ±1 standard deviation (or 15% error).

A5.1.3 RESULTS AND DISCUSSION

A5.1.3.1 Fluorescence Quenching Check. The same level of DOC (signal-to-noise <2:1) was measured in the supernatants obtained from combusted sediment desorbing in acidified and non-acidified solutions indicating that the HCl stock solution did not add carbon to the system. The DOC concentration in the supernatant from the acidified sample was 0.3 ±0.05 ppm C and in the non-acidified sample was 0.4 ±0.06 ppm C. Both supernatants had DOC levels that were below the detection limit of the TOC Analyzer and statistically the same (±2 σ) as the water blank (0.2 ±0.04 ppm C). Calculations reveal that 99% of the dissolved pyrene would remain in the water despite the 0.4 ppm DOC levels (assuming a distribution coefficient of $3x10^4$ L/kg_{DOC} [3, 4]). This calculation suggests that quenching would not affect the fluorescence measurements.

To double-check the quenching prediction, the supernatants were spiked successively with pyrene, and the delta fluorescence intensities were compared to a blank. Statistically indistinguishable incremental increases were observed in fluorescence for the control solution of water, the supernatant from combusted sediment in an acidified solution, and the supernatant from combusted sediment in a non-acidified solution. For example, two successive pyrene spikes in a water blank increased the fluorescence intensity by 33 ±1 units and then another 27 ±1 units. Similarly, the fluorescence intensity for both supernatants increased 34 ±1 units and then 27 ±1 units

for the same two pyrene spikes. These results suggest that fluorescence quenching was not occurring in these samples.

A5.1.3.2 Distribution Coefficients in Acidified and Non-acidified Solutions. For the non-acidified experiments, approximately 68.4 ±2.1% (N = 3) of the dissolved pyrene remained in the water. On the contrary, the percentage of pyrene remaining in the water for the acidified samples was 55.7 ±1.7% (N = 3; Table A1). The more pronounced pyrene sorption in the acidified samples (larger percentage of dissolved pyrene lost) may suggest that the iron oxides formed during the thermal pretreatment were dissolved in the acid, which made the occluded BC more accessible for pyrene sorption. However, since sorption to combusted SDB sediment, or the distribution coefficient (log K_d, L/kg), is dependent on the dissolved concentration [5], one cannot rely solely on the percentage of pyrene lost to conclude if sorption was affected by the presence of iron oxides.

Then, the average BC-normalized distribution coefficient (log K_{BC}, $(\mu g/kg)/(\mu g/L)^n$) was compared for the two sets of experiments. The K_{BC} values were calculated from the K_d values:

$$K_{BC} = \frac{K_d}{f_{BC} C_w^{\,n-1}} \qquad \text{(A1)}$$

where f_{BC} is the BC fraction in the combusted sediment, C_w is the dissolved pyrene concentration (μg/L), and n is the Freundlich exponent assumed to equal 0.62 for pyrene [5]. The average log $K_{BC\text{-non acid}}$ value in the non-acidified solution was 6.46 ±0.22 (N = 3), which compared well to the previously reported log K_{BC} value of 6.3 using the same method [5]. For the acidified solutions, an average log $K_{BC\text{-acid}}$ of 6.66 ±0.10 (N = 3) was measured, which is slightly higher than log $K_{BC\text{-non acid}}$ value by 0.2 logarithm units but within experimental error. Hence, based on the observed distribution coefficients no conclusion can be made on whether iron oxides (formed during the thermal pretreatment) occluded BC and caused a decrease pyrene sorption.

Table 1: Summary of pyrene sorption onto combusted sediment from south Dorchester Bay in acidified and non-acidified solutions

Sorbent (mg)	Volume (L)	Initial Conc (μg/L)	Percent Loss of Pyrene	Log K_{BC} ($\mu g/kg/\mu g/L^n$)
		Sorption in non-acidified solutions		
20.2	0.104	8.39	25.6	6.35 ±0.08
20.2	0.104	8.39	32.6	6.48 ±0.08
19.9	0.104	8.39	36.5	6.55 ±0.08
		Sorption in acidified solutions		
20.2	0.104	7.79	45.0	6.66 ±0.08
19.5	0.104	7.79	42.0	6.63 ±0.08
19.7	0.105	7.79	46.0	6.69 ±0.08

a: The error associated with the sorbent mass and volume was less than ±1%. Initial dissolved concentrations had an error of ±4%. The percent loss of pyrene had a compounded error of ±13%, which includes instrumental error and experimental error.

A5.1.4 REFERENCES

1. Holmen, B. A.; Gschwend, P. M. *Environ. Sci. Technol.* **1997** *31,* 105-113.
2. Gustafsson, Ö.; Haghseta, F.; Chan, C.; MacFarlane, J.; Gschwend, P. M. *Environ. Sci. Tech.* **1997** *31,* 203-209.
3. MacDonald, B. C.; Lvin, S. J.; Patterson, H. *Anal. Chim. Acta.* **1997** *338,* 155-162.
4. Mitra, S.; Dickhut, R. M. *Environ. Toxicol. Chem.* **1999** *18,* 1144-1148.
5. Accardi-Dey, A.; Gschwend, P. M. *Environ. Sci. Tech.* **2002** *36,* 21-29.

APPENDIX A5.2: MASS BALANCE FOR PYRENE SORPTION EXPERIMENT

A5.2.1 INTRODUCTION

The distribution coefficient for pyrene (log K_d, L/kg) was previously measured with fluorescence and calculated via the dissolved pyrene fraction remaining in the water. Here, the pyrene mass balance is confirmed by chemically extracting the dissolved and sorbed pyrene in two representative experiments, and then independently determining the distribution coefficient as the ratio of the sorbed concentration (μg/kg) to the dissolved concentration (μg/L). The log K_d values calculated by chemical extraction were within experimental error of the values previously calculated with fluorescence.

A5.2.2 METHOD

A5.2.2.1 Pyrene sorption. The pyrene sorption experiments were performed as described in Chapter 5 – in brief, 20.2 mg of combusted SDB sediment (1.2 wt % ±0.15 wt % OC and 0.16 ±0.03 wt % BC) was added to 0.104 L of solution spiked with 8.39 μg/L of pyrene and tumbled for 21 days.

A5.2.2.2 Pyrene Mass Balance. Pyrene was chemically extracted from four flasks: a control flask with pyrene (no sediment), another control flask with low-carbon water (no pyrene spike, no sediment), and two experimental flasks containing dissolved pyrene in equilibrium between sediment and water phases. Each flask was spiked with 1.5 μg of m-terphenyl as an internal standard, and then the two phases were separated by centrifuging for 7 min at 1,250*g*. The supernatants were transferred into glass separatory funnels, and the dissolved pyrene was extracted three times with dichloromethane (DCM; 2-8 mL/extraction). Meanwhile, the wet sediments remaining in the centrifuge tubes were spiked with 0.5 μg d_{10}-pyrene as an internal standard for the solid phase, and the sorbed pyrene was extracted with 9:1 DCM:methanol (30-40 mL) for 24 hours. Note that the original flasks were also rinsed with DCM to collect the remaining solids coating the glassware, and this solvent was combined with the solvent in the centrifuge tubes. The solids were then filtered out (Whatman GFF, Series 934-AH) of the DCM:methonal

solvent with a hand vacuum pump. Anhydrous Na_2SO_4 was used to precipitate residual water in the dissolved and sorbed pyrene extracts, and then the extracts were concentrated and exchanged into hexane using N_2-blow down techniques.

Pyrene quantification was performed on a JEOL GCmate gas chromatograph-mass spectrometer, equipped with a Hewlett Packard 6890 gas chromatograph. Extracts were injected splitless and separated on a 30 m x 0.32 mm DB-5 (0.25 μm film thickness) fused-silica capillary column (J&W Scientific, Inc.). The temperature program began with a 20°C/min ramp from 70°C to 180°C, followed by 6°C/min from 180°C to 300°C. The injector and transfer zone temperatures were 280°C, and the MS source temperature was 250°C. Electronic pressure control maintained the He flow rate at 2 mL/min. The response factors, determined daily with a three-point calibration curve, had a variability of ±7%. The pyrene concentration in a procedural blank was <1 pg/μL-injection corresponding to a signal-to-noise ratio >90:1 for the PAHs reported. With this methodology, 57-85% of the m-terphenyl and 66% of the d_{10}-pyrene were recovered (all extracts were corrected for recovery losses). All reported values represent the mean ±1 standard deviation (or 20% error).

A5.2.3 RESULTS AND DISCUSSION

For the control flask containing only a pyrene spike (no sediment), 0.65 ±0.13 μg of pyrene was chemically extracted, corresponding to a dissolved pyrene concentration of approximately 6.3 ±1.3 μg/L (Table 1). This concentration was lower than the previously determined pyrene concentration of 8.39 ±0.5 μg/L using fluorescence (Perkin Elmer LS50B Luminescence Spectrofluorometer) for the same solution. While the discrepancy between the two concentrations may reflect losses of pyrene during the extraction, the difference more likely reflects an intercalibration error between the two instruments.

The total mass of pyrene (dissolved + sorbed) extracted from the two experimental flasks were within error of the total pyrene mass extracted from the control (Table 1). In the first system (S1), 0.15 ±0.03 μg of pyrene was chemically extracted from the solid phase, and 0.54 ±0.11 μg pyrene from the water phase – thus equaling 0.69

±0.11 μg pyrene total, or a mass balance of 106%. Similarly, 0.18 ±0.04 μg of pyrene was measured in the solid phase, and 0.57 ±0.11 μg pyrene in the water phase for a mass balance of 115%, or 0.75 ±0.12 μg pyrene total in the second system (S2; Table 1).

The chemically extracted dissolved and sorbed pyrene concentrations were then used to calculate the log K_d value for each system. Since both experiments had the same initial conditions, similar distribution coefficients would be expected. In the first system, the distribution coefficient was 1430 ±400 L/kg, or a log K_d = 3.16 ±0.11 (S1; Table 1), which compared well to the log K_d value previously determined by fluorescence (3.24 ±0.04) for the same experiment. In the second system (S2), the distribution coefficient was 1630 ±455, or a log K_d = 3.21 ±0.11, which is statistically the same as the distribution coefficient calculated in the first flask (3.16 ±0.11), but lower than the log K_d value calculated previously by fluorescence (3.40 ±0.04).

Table 1: Pyrene mass balance (mean ±1 σ) and calculations of a distribution coefficient (log K_d, L/kg) for pyrene.

Sample [a]	Solids (mg)	Volume (L)	Dissolved Pyrene (μg)	Sorbed Pyrene (μg)	log K_d
Control	NA [b]	0.104	0.65 ±0.13	N/A	NA
S1	20.2	0.104	0.54 ±0.11	0.15 ±0.03	3.16 ±0.11
S2	20.2	0.104	0.57 ±0.11	0.18 ±0.04	3.21 ±0.11

a: Samples correspond to pyrene sorption experiments noted in Appendix A5.1, Table 1 (Sorption in non-acidified solution)

b: NA = not applicable

APPENDIX A6.1: BEST FIT PARAMETERS FOR PHENANTHRENE ISOTHERMS

Table 1. Best-fit K_{oc} value (L/kg), K_{BC} value ((μg/kg)/(μg/L)^n), and Freundlich exponent (n) with corresponding error (presented as a positive percentage) for each phenanthrene isotherm reported by Huang *et al.*

Sample	K_{oc}	% Error	K_{BC}	% Error	n	% Error
EPA B2	-187	44	1990×10^3	0.10	0.735	0.13
EPA 4	187	35	1130×10^3	0.08	0.753	0.09
EPA 5	-193	46	2870×10^3	0.09	0.734	0.11
EPA 13	63.5	49	2070×10^3	0.03	0.741	0.04
EPA 14	1870	31	522×10^3	1.4	0.861	0.40
EPA 15	-21.9	310	426×10^3	0.06	0.734	0.07
EPA 18	-611	36	758×10^3	0.20	0.749	0.23
EPA 20	126	90	2140×10^3	0.14	0.749	0.16
EPA 21	-94.6	69	804×10^3	0.03	0.736	0.05
EPA 22	-1103	51	40.0×10^3	0.84	0.891	0.16
EPA 23	54.5	96	1890×10^3	0.05	0.736	0.01
EPA 26	-153	95	1840×10^3	0.17	0.766	0.16

APPENDIX A6.2: PYRENE SORPTION IN THE McGRODDY CORES

Table 1. Pyrene sorption to sediments at Fort Point Channel, Spectacle Island, and Peddocks Island: Estimated truly dissolved pyrene concentration (ng/L), measured sorbed pyrene concentration (μg/kg), measured log K_d values (L/kg), log K_d values (L/kg) predicted with the $f_{oc} K_{oc}$ model, and log K_d values (L/kg) predicted with the combined sorption model (data corresponds to Chapter 6: Figure 1 and Table 1).

Sample Depth (cm)	Dissolved Pyrene [a]	Sorbed Pyrene [b]	log K_d [c] Measured	log K_d [d] ($f_{oc} K_{oc}$)	log K_d [e] ($f_{oc} K_{oc} + f_{BC} K_{BC} C_w^{n-1}$)
Fort Point Channel					
0-1	28	2880	5.01	3.47	NA [f]
1-3	41	8810	5.33	3.39	4.64
3-5	83	4370	4.72	3.33	NA
5-7	190	5150	4.43	3.34	4.48
7-9	190	5170	4.43	3.44	4.39
9-11	410	7080	4.24	3.45	NA
11-13	280	10,400	4.58	3.45	4.58
13-15	530	14,100	4.42	3.49	NA
15-17	360	7370	4.32	3.42	4.39
17-19	330	4620	4.15	3.37	4.40
19-21	390	2860	3.86	3.34	4.28
21-23	330	2570	3.89	3.42	NA
23-25	190	4750	4.40	3.36	NA
25-29	150	3820	4.40	3.42	4.57
29-33	120	4340	4.55	3.37	NA
Spectacle Island					
0-2	8.8	1190	5.13	3.31	4.49
2-4	7.7	1090	5.15	3.30	NA
4-6	16	960	4.78	3.25	4.42
6-8	25	1860	4.87	3.25	4.31
8-10	26	1670	4.81	3.24	NA
10-12	22	2130	4.98	3.18	NA
12-14	50	1950	4.59	3.03	NA
14-16	26	3440	5.12	2.99	NA
16-18	59	2090	4.55	3.09	4.34
18-20	55	2330	4.62	3.24	4.40
Peddocks Island					
1-2	3.7	570	5.18	3.24	NA
2-3	6.5	475	4.86	3.24	4.43
3-4	3.5	518	5.17	3.23	NA
4-5	7.9	632	4.90	3.20	NA
8-9	1.5	520	5.55	3.18	4.64
10-11	28	569	4.31	3.14	4.22
11-13	18	511	4.46	3.18	4.31
13-15		570		3.18	NA
17-19		550		3.17	NA
19-21	32	475	4.17	3.17	4.12
25-29		423		3.07	NA
29-33	46	395	3.94	3.03	4.15
33-35		661		3.19	NA
37-41		510		3.22	NA

a: The truly dissolved pyrene concentration (PW_{true}) was estimated as the measured dissolved pyrene concentration ($PW_{measured}$) reported by McGroddy (Chapter 6, reference [19]) times the unbound colloidal fraction: $PW_{true} = PW_{measured}/(1+ R_{colloid} K_{colloid})$ where $R_{colloid}$ is the measured colloid concentration (kg $_{colloid}$/L; Chapter 6, reference [19]) and $K_{colloid}$ is the estimated colloidal-normalized distribution coefficient (L/kg $_{colloid}$; Chapter 6, reference [23]).

b: The sorbed pyrene concentration was measured by McGroddy (Chapter 6, reference [19]).

c: The measured log K_d values equal the logarithm of the ratio of sorbed pyrene concentration (μg/kg) to dissolved pyrene concentration (μg/L).

d: The log K_d values predicted from the $f_{oc} K_{oc}$ model assuming a log $K_{oc} = 4.7$ for pyrene and were adjusted for salt content. The f_{oc} fraction equals the total organic carbon (OC + BC) reported in Chapter 6, Table 1.

e: The log K_d values predicted from the $f_{oc} K_{oc} + f_{BC} K_{BC} C_w^{n-1}$ model assuming a log $K_{oc} = 4.7$, a log $K_{BC} = 6.25$, and a Freundlich exponent (n) = 0.62 for pyrene and were adjusted for salt content. The f_{oc} fraction equals the non-BC fraction (OC = TOC – BC) in the combined sorption model. All OC and BC contents are reported in Chapter 6, Table 1.

f: Not applicable (NA)

APPENDIX A6.3: PREDICTED AND OBSERVED PHENANTHRENE ISOTHERMS ON EPA SEDIMENTS AND SOILS

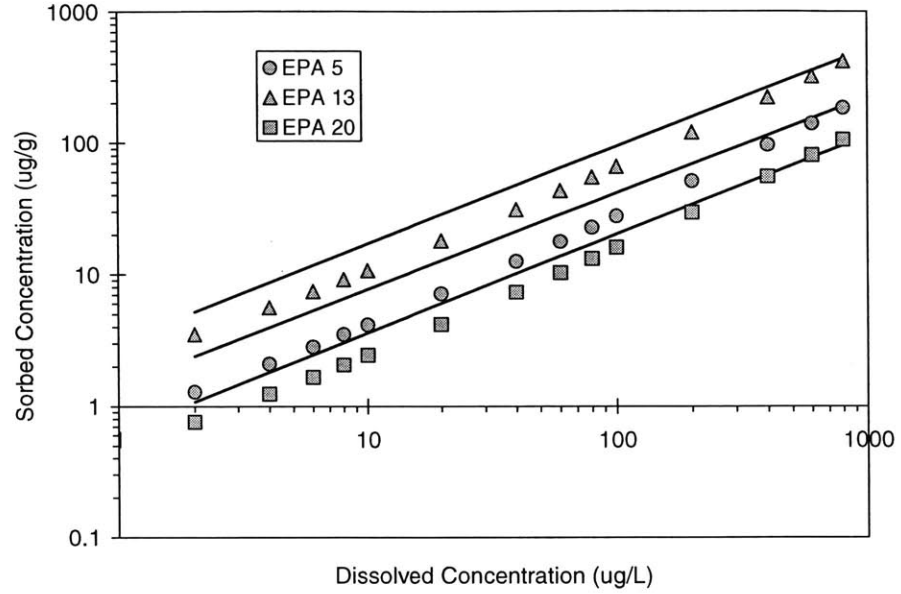

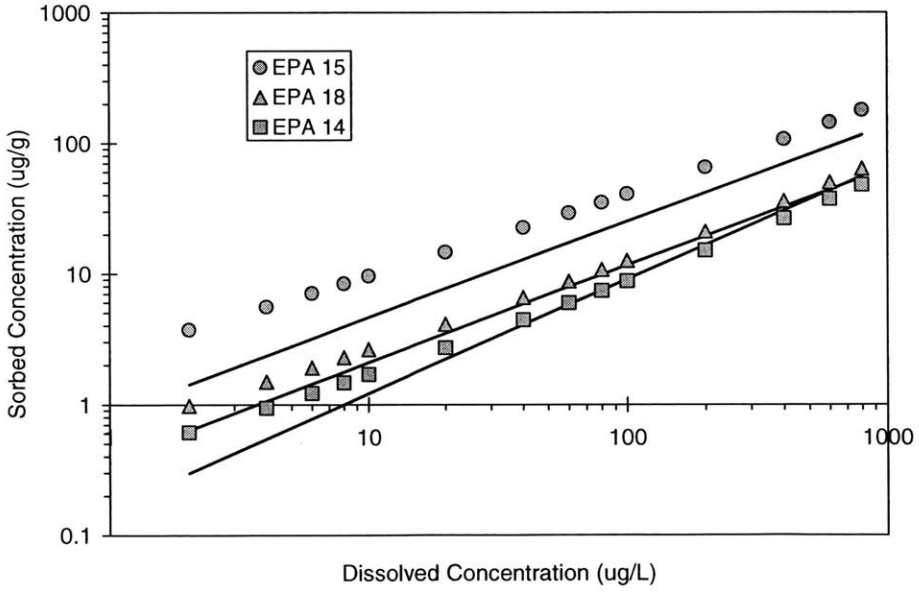

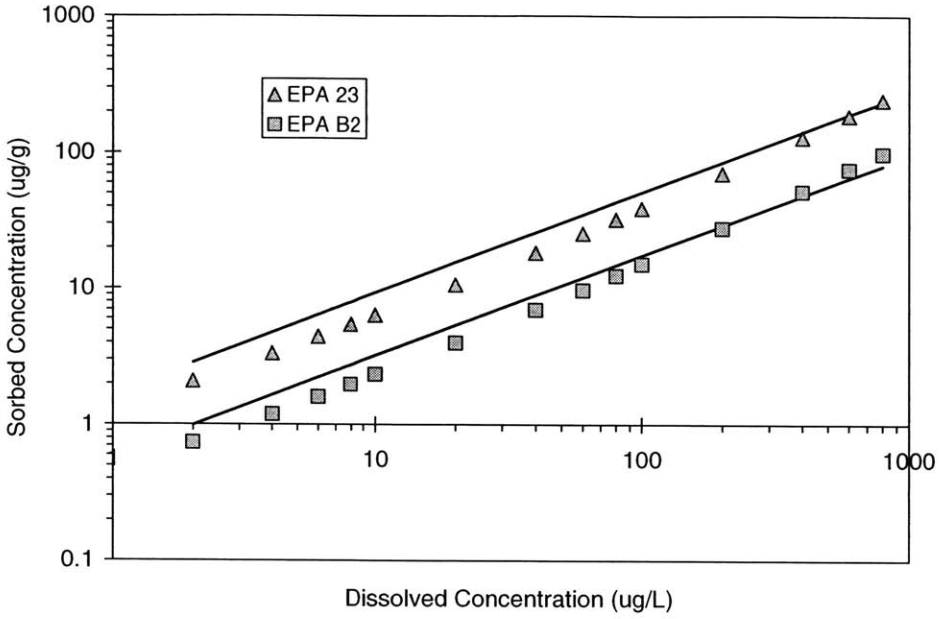

Figure 1: Comparison of observed phenanthrene isotherms (solid line; C_s (μg/g) = K_d C_w (μg/L)^n) from Huang *et al.* (1997) Environ. Sci. Technol. and model isotherms (filled symbols; C_s (μg/g) = f_{oc} K_{oc} C_w (μg/L) + f_{BC} K_{BC} C_w (μg/L)^n assuming log K_{oc} = 4.0, log K_{BC} = 6.1, and n = 0.55) for eight EPA samples. For the sorbed concentration (μg/g), the propagated error was approximately 20% for the observed isotherm by Huang *et al.* (1997) Environ. Sci. Technol. and 50% for the model isotherm. Samples correspond to data listed in Table 3 of Chapter 6.

"I feel like the man who was tarred and feathered and ridden out of town on a rail. To the man who asked him how he liked it, he said, 'if it wasn't for the honor of the thing, I'd rather walk.'"

- Abraham Lincoln, responding to the question on how he liked being President